REGULATORY MECHANISMS OF FASTING

Philip M. M. Ruppert

Propositions

1. Despite its potent lipid-lowering effects, ANGPTL4 is not a suitable therapeutic target for the treatment of dyslipidemia.
   (this thesis)

2. Conservation of function is distinct from conservation of mechanism (this thesis).

3. The stark induction of βOHB during fasting signifies its importance as an energy metabolite during this physiological state.

4. Speculation is a dangerous ingredient in the scientific process.

5. Abstract thinking and capacity to untangle complex issues are key to do science, but counterproductive to scientific writing.

6. The public resistance to wearing masks is a sad testament to the fact that people care only about themselves.

7. To engage in public discussions the layman is better served with tools to query facts than by public outreach by scientists.

Propositions belonging to the PhD thesis entitled:

"Regulatory mechanisms of fasting"

Philip M. M. Ruppert

Wageningen, December 18th, 2020

REGULATORY MECHANISMS OF FASTING

Philip M. M. Ruppert

Thesis committee

Promotor

Prof. Dr Sander Kersten
Professor in Nutrition, Metabolism and Genomics
Chair Division of Human Nutrition & Health
Wageningen University & Research

Other members

Prof. Dr Patrick C.N. Rensen - Leiden University Medical Center
Prof. Dr Jaap Keijer - Wageningen University & Research
Dr Maaike H. Oosterveer - University Medical Center Groningen
Dr Aldo Grefhorst - Amsterdam UMC

This research was conducted under the auspices of the Graduate School VLAG (Advanced studies in Food Technology, Agrobiotechnology, Nutrition and Health Sciences).

REGULATORY MECHANISMS OF FASTING

Philip M. M. Ruppert

Thesis

submitted in fulfilment of the requirements for the degree of doctor
at Wageningen University
by the authority of the Rector Magnificus
Prof. Dr A.P.J. Mol,
in the presence of the
Thesis Committee appointed by the Academic Board
to be defended in public
on Friday December 18, 2020
at 11 a.m. in the Aula.

Philip M. M. Ruppert

Regulatory mechanisms of fasting
238 pages

PhD thesis, Wageningen University, Wageningen, NL (2020)
With references, with summary in English

ISBN: 978-94-6395-472-3
DOI: 10.18174/527117

Tell me and I forget, teach me and I remember,
involve me and I learn

Chinese proverb by Xunzi

Contents

Chapter 1

General Introduction

Contents

Fasting as a metabolic state

The fasted state refers to a distinct metabolic state that maintains homeostasis of an organism in the absence of food, relying solely on stored energy. This distinguishes it from the fed state, where the organism maintains vital chemical energy levels (ATP) and obtains building blocks for structural components from ingested nutrients directly. Feeding and fasting habits are rhythmically aligned to the 24-hour day-night cycle on earth and dictated by food and water availability, activity and temperature (seasonality). Nowadays, humans typically consume 3 to 5 meals and experience one over-night fasting bout per day, while many animal species display interesting and more extreme feeding-fasting behaviors. For instance, hummingbirds and shrews are known to require almost constant feeding, while some python species require food only twice a year. Defined as absorptive (fed) and post-absorptive (fasted) state, both states need to occur in sequence yet are mutually exclusive. The switch from food to stored energy as primary fuel source therefore requires distinct and evolutionarily conserved organ and cellular activities that drive adequate physiological, morphological and behavioral adaptations to ensure survival [1].

Health benefits of fasting

Over the years a wealth of pre-clinical and clinical studies have examined the salutary effects of various fasting regimens [2]–[7]. Most of these studies used an intermittent fasting (IF) design, in which either the daily over-night fasting window was extended, or volunteers engaged in complete fasting for one or more days on a weekly or monthly basis. Time-restricted feeding (TRF) protocols define daily eating windows of 6-12 hours, while in alternate-day fasting (ADF) protocols study subjects undergo fasts of up to 48 hours alternated with days of normal eating behavior. Periodic fasting (PF) protocols ascribe fasting periods of several days per week or month, on a reoccurring basis. One example is the 5:2 protocol, in which subjects fast for 2 days a week.

In preclinical studies, IF protocols were shown to extend life span, reduce body weight, mitigate inflammation, improve glucose homeostasis and insulin sensitivity, and delay the onset of disease in experimental models for diabetes, cardiovascular disease, neurological disease and cancer [2]–[7]. In humans, these protocols normalize HbA1c and glucose levels, improve insulin sensitivity and blood lipid parameters, reduce blood pressure and also induce weight loss, yet evidence for disease mitigation and life-span extension is currently lacking [8], [9]. Inasmuch as fasting reduces caloric intake, it is not surprising that there is

striking overlap in the salutary effects of the various fasting regimens and caloric restriction (CR). It is widely accepted that daily CR – inducing weight loss – extends life-span and leads to similar improvements in above mentioned health parameters in animal models [10], [11]. Human studies on CR corroborate improvements in cardiometabolic health parameters [12], [13]. Long-term studies on rhesus monkeys at the University of Wisconsin and the National Institute of Aging support the health and longevity benefits of CR, and suggest that the life-extension effect may be translatable to humans [14]–[16]. The over-arching question is whether the health promoting effects of fasting are inherent to the fasting metabolism and therefore facilitated by reduced meal timing or are driven by weight loss due to caloric intake below maintenance levels. This question has important clinical implications, as long-term adherence to CR is low, and reductions in body weight are partly driven by undesirable loss of fat-free mass [17]–[19].

The clear overlap in weight reduction and health promoting effects of the various fasting protocols and CR suggest that the degree of weight loss is a potential determinant. Studies that incorporated CR and ADF or PF groups mostly report comparable weight loss [8]. In one ADF study where weight loss was different between the ADF and CR group, the improvements in blood lipid parameters positively correlated with the degree of weight loss [20]. Of note, in the same study, another ADF intervention group that was kept in energy balance did not show improvements in metabolic health parameters, cumulatively suggesting that improvements in ADF and PF interventions may depend on (the degree of) weight loss.

A recent metanalysis also documented significant weight loss in most TRF trials [9]. However, Moon *et al.* uncovered that weight loss was only observed in diseased and obese subjects undergoing TRF. A recent clinical trial indeed supports the notion that time-restriction may facilitate a caloric deficit in obese subjects [19]. By contrast, in healthy individuals, the meta-analysis reports improvements in metabolic parameters in the absence of weight loss, suggesting that timing of food intake can modulate health. In particular early dinner TRF was shown to improve insulin sensitivity, blood pressure and oxidative stress in the absence of weight loss [21] and bolstered rhythmicity of circadian genes in PBMCs [22]. These observations suggest that the mechanisms leading to improvements in health parameters may ultimately be different between study populations. For healthy subjects the improvements in health parameters may potentially be explained by the notion that food intake as an environmental cue influences the circadian rhythm. Misalignment between the circadian clock and metabolic processes, as for example observed in shift workers, promotes the risk for type 2 diabetes and cardiovascular disease [23], [24].

Cumulatively, further studies are required to delineate how long and how often one has to fast to elicit favorable changes and what the underlying mechanisms are that drive improvements in diseased and healthy populations. Therefore, it is of high interest to understand the transcriptional and translational regulatory mechanisms that govern the transition from the fed state to the fasted state.

Key metabolic organs

Key metabolic organs to understand feeding-fasting cycles are the liver, muscle tissue, adipose tissue and the brain.

The liver is the central nutrient processing and distributing organ in the body. It plays a critical role in carbohydrate metabolism by breaking down glucose to produce ATP via glycolysis. In the fed state, the liver converts part of the glucose into glycogen via glycogenesis. When tissues are in demand of glucose during fasting conditions, the stored glycogen can in turn be broken down via glycogenolysis to release glucose into the blood. Under prolonged fasting, the liver utilizes non-carbohydrate precursors to synthesize glucose via a process called gluconeogenesis in order to generate glucose for vital organs such as the brain. The liver also plays a central role in lipid metabolism. It produces bile acids required for the digestion of dietary triglycerides and the subsequent uptake of fatty acids. Furthermore, the liver can take up fatty acids from the circulation, convert them into triglycerides, and repackage them into very low-density lipoproteins (VLDLs). The VLDLs provide fuel to several tissues including the heart and skeletal muscle. The liver generates ATP for its own needs via glycolysis and oxidative phosphorylation using glucose and fatty acids.

The central role of the adipose tissue is the storage of fatty acids as triglycerides within lipid droplets. During lipolysis, the adipose tissue releases stored triglycerides back into the circulation as free fatty acids. This supplies other tissues with fuel for oxidative phosphorylation or the synthesis of structural lipids. The adipose tissue can generate ATP via glycolysis and oxidative phosphorylation using glucose and fatty acids.

Skeletal muscle tissue provides the capacity for locomotion and has the highest ATP requirement per tissue in the human body. To meet this requirement, skeletal muscle tissue can utilize all energy substrates to generate ATP. The type of fuel used depends on the intensity of the muscle activity, with glucose being the major sources during high-intensity exercise and fatty acids during moderate to low intensity exercise. Although the muscle is able to store glycogen, it cannot contribute to circulating glucose levels due to the absence

of glucose 6-phosphatase. Once taken up into muscle, glucose is reserved for locomotion activities.

The brain is the center of intellectual and nervous activity, yet neuronal cells have no capacity to synthesize and thus store glycogen or triglycerides [25]. Additionally, to what extent neurons metabolize fatty acids remains unclear. Alongside other non-neuronal cell types, neurons express the machinery to transport and metabolize fatty acids and recent studies suggests that at least medium-chain triglycerides may be metabolized [26], [27]. However, brain fatty acid pools do not always reflect plasma fatty acid pools, which supports the alternative hypothesis that the blood-brain barrier acts as a metabolic barrier for fatty acids [28], [29]. At least the latter scenario may call for a constant glucose supply to neurons in order to maintain their function. This is supported by the observation that glucose uptake into brain tissues is in fact mediated by insulin-insensitive GLUT1 and GLUT3 transporters [30], [31].

Fed-state physiology

The fed state commences with the ingestion of a meal. After digestion in the gastrointestinal tract, glucose and amino acids are absorbed in the small intestine and pass through enterocytes into the blood circulation via the portal vein. Free fatty acids (FFA) are absorbed, re-esterified intro triglycerides (TG) and packaged into chylomicrons, and then transported to the circulation via the lymph. In response to rising glucose levels, β-cells in the pancreas release the hormone insulin. Insulin is a key hormone that signals the 'fed' state due to its numerous central functions in nutrient uptake and storage. It triggers the uptake of glucose into liver, adipose and muscle tissue, and its utilization to produce ATP via glycolysis. Furthermore, glucose is stored in the liver and muscle in the form of glycogen (glycogenesis) while the opposing pathway, glycogenolysis, is inhibited. In the liver and adipose tissue, excess glucose can also be converted to FFA via de novo lipogenesis. The liver secretes FFA in the form of TG packed into very-low density lipoproteins. The oxidation of FFA for ATP is generally low in most tissues when Insulin levels are high. Thus, in the fed state, the adipose tissue remains the principal tissue for the uptake and storage of FFA in the form of TG inside its characteristic lipid droplets. Lastly, the brain, as mentioned, constantly metabolizes glucose and possibly certain FFA species. Conversely, amino acids (AA) are mostly used for anabolic processes throughout the body when Insulin levels are high. The flow of fuel in the fed state is depicted in Figure 1.

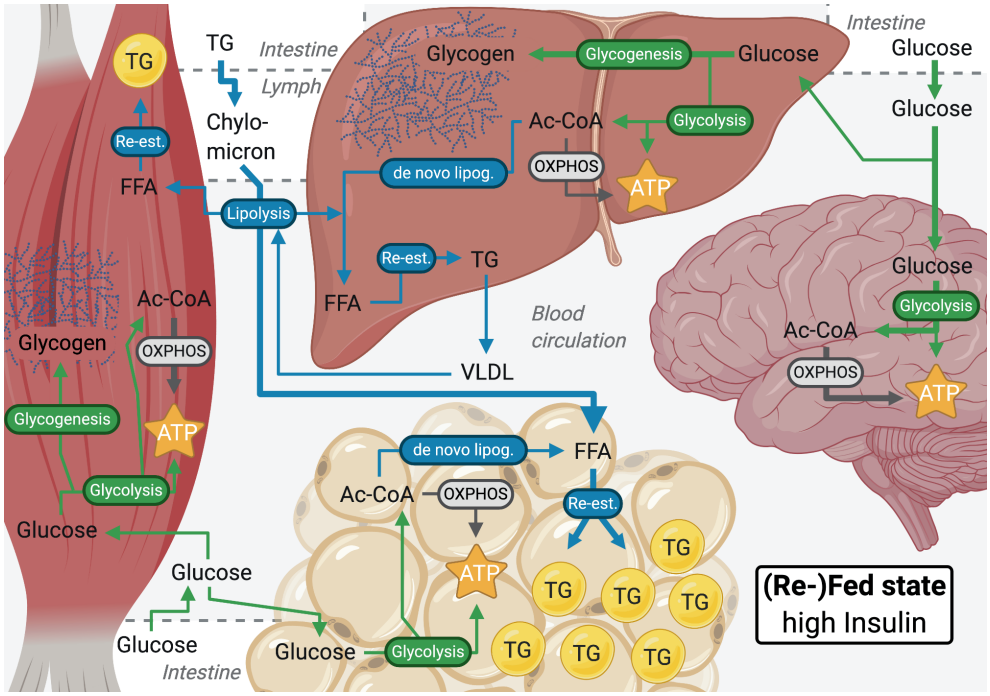

Figure 1: Simplified overview of Fed state fuel flows. After ingestion of a meal, glucose enters the circulation directly from the intestine. Fatty acids are re-esterified into triglycerides (TG), which enter the circulation via the lymph inside chylomicrons. Under high insulin levels, in particular glucose is utilized for glycogenesis in liver and skeletal muscle as well as ATP production in liver, skeletal muscle, brain and adipose tissue. In addition, excess glucose can be stored as TG in lipid droplets via de novo lipogenesis. Chylomicrons supply liver, skeletal muscle and adipose tissue with FFA. The liver contributes to circulating plasma TG levels by repackaging chylomicron-derived free fatty acids (FFA) into very low density lipoproteins (VLDL). Under high insulin levels, FFA are mostly stored as TG in adipose tissue lipid droplets. Amino acids (AA) are mostly used for anabolic processes under high insulin conditions (not depicted).

Transition to fasted physiology – Phase I

The body transitions from the fed to the fasted state when the last meal is fully digested and absorbed. Two main phases can be distinguished in this transition [32], [33].

In the first phase, hours after the meal, plasma glucose levels are no longer maintained from ingested carbohydrates. It becomes the body's prime priority to maintain adequate glucose levels, in particular to supply the brain and CNS with energy substrates. Lowering of blood glucose levels reduces the release of insulin while simultaneously increasing the release of glucagon by the pancreas' alpha cells. The drop in plasma insulin may occur quicker than the rise in glucagon [34]. Glucagon is the key hormone of the fasted state, as it directly stimulates the replenishment of plasma glucose levels. For one, the hormonal switch from insulin to glucagon promotes hepatic glycogenolysis, leading to the breakdown of glycogen that was stored during the fed state. In addition, gluconeogenic activity increases [35]. By repeatedly probing forearm muscles in fasting men, Felig and Pozefsky documented an increase in protein catabolism in the initial days of the fast, causing a net increase in plasma amino acid levels [36]–[38]. Corroborated by recent studies, in particular BCAA levels increase and possibly support hepatic ketogenesis (see following chapter) [39]–[42]. Interestingly, not all amino acids increase in abundance in plasma. In what has been coined the glucose-alanine or Cahill cycle, amino acids released via catabolic processes feed into the de novo synthesis of alanine via transamination of liver glucose-derived pyruvate. Alanine, a potent gluconeogenic amino acid, is secreted and shuttled back to the liver for hepatic gluconeogenesis at very high rates, effectively reducing its plasma levels [43], [44].

Cumulatively, these observations illustrate that hepatic glycogenolysis and gluconeogenesis are augmented and jointly maintain blood glucose levels. Together with other gluconeogenic substrates like lactate, amino acids are readily liberated upon fasting to maintain blood glucose levels. The extensive efforts to maintain glucose levels at the expense of muscle mass are reflective of high basal requirements for glucose.

Transition to the fasted physiology – Phase II

While it is currently unknown precisely how much muscle mass is lost in the initial hours of a fast, its uncontrolled catabolism for the maintenance of blood glucose levels is expected to impede with the long-term survival of the fasting individual [32], [45]. Hence with the extension of the fast from several hours into days, a second vital priority has to be the preservation of muscle mass. Indeed, in this second phase , net plasma amino acid levels and urinary nitrogen excretion decrease in fasting individuals [39]–[42], [46]. Alongside declining plasma alanine levels, also alanine turnover declines, as determined by a recent NMR tracer study by Shulman comparing 60h vs 12h fasted subjects [47]. In addition, the average liver of an adult human can only hold approximately 0.2 kg of glycogen, which depending on the level of physical activity can last between 12 to 24 hours. Tracer studies attest to a gradual increase in the relative contribution of hepatic gluconeogenesis to blood glucose levels [47]–[50]. Cahill and colleagues speculated that when hepatic glycogen reserves are depleted, gluconeogenesis alone cannot maintain blood glucose levels. Indeed total glucose production declines after 1 day of fasting [47]–[49], in line with reducing plasma glucose levels (Figure 3A) [34], [39], [46], [51] and declining glucose clearance by tissues such as muscle [52], [53]. Together these observations suggest that the body reduces its dependence on glucose as the primary source of fuel when fasting beyond 24h.

One hallmark of this phase is the increasing reliance on β-oxidation to provide ATP. Alongside a hormonal switch from insulin to glucagon, many other plasma hormone levels change. Stress-hormones such as cortisol and epinephrine begin to rise [40], [54], [55], while Leptin and T_3 levels decline (Figure 3B) [34], [40], [41], [46], [56]. Cumulatively these hormonal changes contribute to increased adipose tissue lipolysis. Free fatty acid and glycerol levels increase after 24h of fasting, and continue to rise until approx. day 3 [34], [46], [51]. Simultaneously, lipid turnover increases and plasma triglyceride levels start to decline [57]. The respiratory quotient (RQ) approaches 0.7, indicating that β-oxidation becomes the primary source of ATP in the liver, skeletal and heart muscle [53], [58]. TG accumulation has been observed in tissues, for example in liver and muscle tissue [34], [48], driven by the elevated plasma NEFA levels and concomitant tissue fatty acid uptake.

Another hallmark of the second phase is the induction of ketogenesis, resulting in the formation of the ketone bodies acetoacetate (AcAc) and β-hydroxybutyrate (βOHB). Despite the switch to β-oxidation, a basal rate of gluconeogenesis is still maintained to supply for instance red blood cells with glucose [47], [49]. The main substrates for gluconeogenesis at this stage are glycerol, co-released from the hydrolysis of triglycerides in adipose tissue and hepatic TCA cycle intermediates such as oxaloacetate formed from lactate or amino acid-derived pyruvate. Diverting oxaloacetate towards gluconeogenesis results in reduction of TCA cycle activity in the liver [47]. In turn, acetyl-CoA molecules

accumulate and “spill-over” into ketogenesis [59]. Two or 3 molecules of acetyl-CoA condense into AcAc or βOHB respectively, which are released into the circulation as an alternative energy substrate next to fatty acids. Reaching levels of up to 8 mM cumulatively, AcAc and βOHB are increasingly oxidized in peripheral tissues via ketolysis, most prominently by the brain. In 1967, Owen *et al.* catheterized the internal jugular bulb and the carotid artery of fasting individuals and measured significant levels of ketone bodies going in but not going out of the brain. They reported that after several weeks of fasting, the brain derives up to 2/3rd of its energy requirements from the oxidation of ketone bodies [60], [61]. This study laid the foundation for the notion that the formation ketone bodies is a vital evolutionary mechanism to provide an alternative fuel source to glucose that may spare amino acids and thereby increase chances for survival during prolonged fasts [32], [61]. The preferential use of ketone bodies by the brain during the fasted state has since been further quantified and visualized with PET scans [62], [63]. In addition, elevation of fasting βOHB levels via infusion lowers uptake of glucose into forearm muscle and whole body glucose oxidation [64]. Figure 2 depicts fuel flows during the fasted state. Figure 3 provides a longitudinal overview of typical plasma parameters during the feeding-fasting transition in humans. Typical minimum and maximum values are summarized in Table 1.

The maximal duration of the fast depends on the quantity of endogenous energy stores when the fast starts. It is estimated that a 70 kg man with 15 kg of adipose tissue (140.000 kcal) could a survive a 70-90 day fast, based on a basal energy expenditure of 1800 kcal/day [45]. Owen estimated that if the human body would not switch to fatty acids but instead continues to mobilize amino acids for gluconeogenesis, a 70 kg man would only be able to fast for 23-34 days [61]. The switch to fatty acids and ketones as fuel sources thus provides a huge fitness advantage when food is scarce. For an obese man with 140 kg body weight and 80 kg of adipose tissue, the above calculation extrapolates to 14 months of estimated survival. In the 1960’s and 70’s two studies were performed that confirmed this estimation by successfully fasting obese individuals for 249 resp. 382 days providing only water and electrolytes [65], [66].

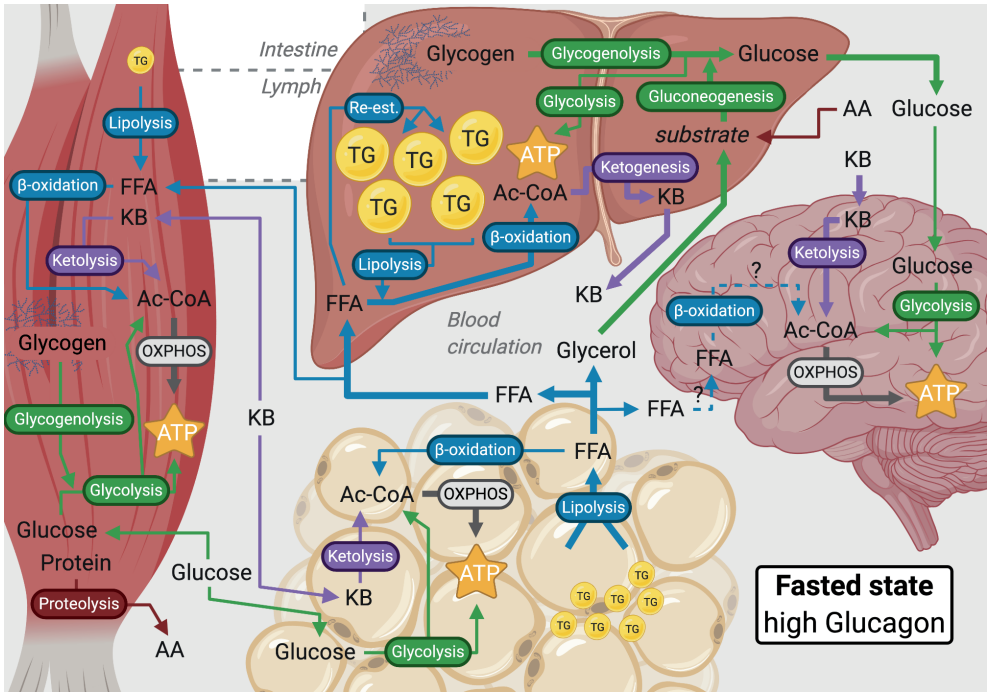

Figure 2: Simplified overview of Fasted state fuel flows. In the initial phase of the fast glycogenolysis and amino acid driven gluconeogenesis (Cahill cycle) are utilized to maintain blood glucose levels. With the depletion of hepatic glycogen stores hepatic glucose production declines after about 24h. High glucagon and low leptin levels promote lipolysis and switch to fatty acids and ketone bodies to supply extrahepatic tissues with a source for ATP. Continued gluconeogenic activity depletes the TCA cycle intermediate Oxaloacetate, which causes a buildup of acetyl-CoA in hepatic mitochondria. These acetyl-CoA molecules condense to ketone bodies Acetoacetate and beta-hydroxybutyrate and are avidly oxidized in extrahepatic tissues.

Table 1: Typical human plasma parameters in fed and fasted state [34], [40], [45]–[47], [51], [54]–[58], [66]–[72], [74]–[79].

Substrate	Fed	Fasted
Glucose (mM)	5.0 – 8.0	2.0 – 4.5
NEFA (mM)	0.4 – 0.8	0.8 – 2.0
TG (mM)	1.5 – 2.4	0.3 – 1.1
Ketone bodies (mM)	< 0.1	0.5 – 7.0

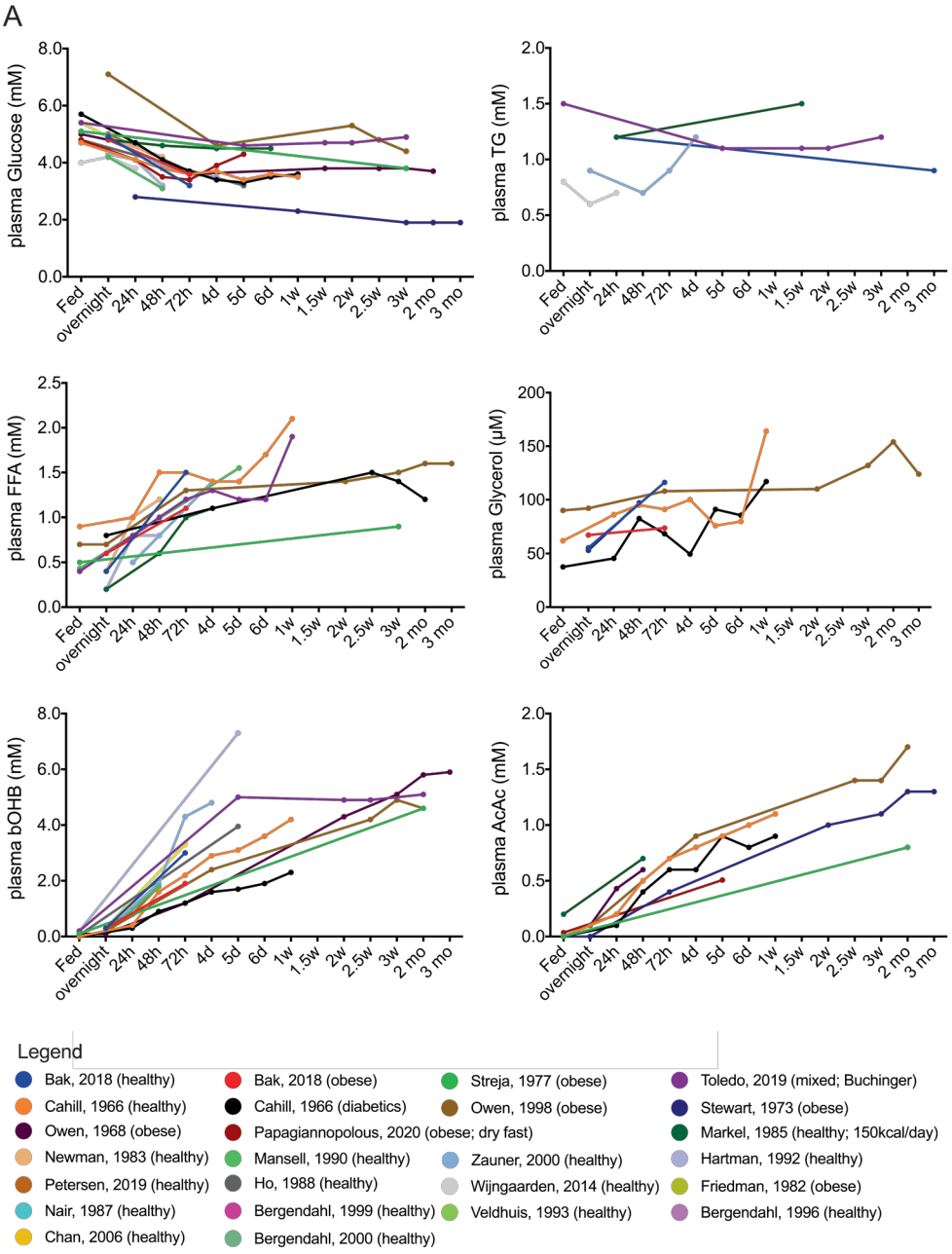
A
plasma Glucose (mM)
plasma TG (mM)
plasma FFA (mM)
plasma Glycerol (µM)
plasma bOHB (mM)
plasma AcAc (mM)
Fed
overnight
24h
48h
72h
4d
5d
6d
1w
1.5w
2w
2.5w
3w
2 mo
3 mo
Legend
Bak, 2018 (healthy)
Cahill, 1966 (healthy)
Owen, 1968 (obese)
Newman, 1983 (healthy)
Petersen, 2019 (healthy)
Nair, 1987 (healthy)
Chan, 2006 (healthy)
Bak, 2018 (obese)
Cahill, 1966 (diabetics)
Papagiannopolous, 2020 (obese; dry fast)
Mansell, 1990 (healthy)
Ho, 1988 (healthy)
Bergendahl, 1999 (healthy)
Bergendahl, 2000 (healthy)
Streja, 1977 (obese)
Owen, 1998 (obese)
Zauner, 2000 (healthy)
Wijngaarden, 2014 (healthy)
Veldhuis, 1993 (healthy)
Toledo, 2019 (mixed; Buchinger)
Stewart, 1973 (obese)
Markel, 1985 (healthy; 150kcal/day)
Hartman, 1992 (healthy)
Friedman, 1982 (obese)
Bergendahl, 1996 (healthy)

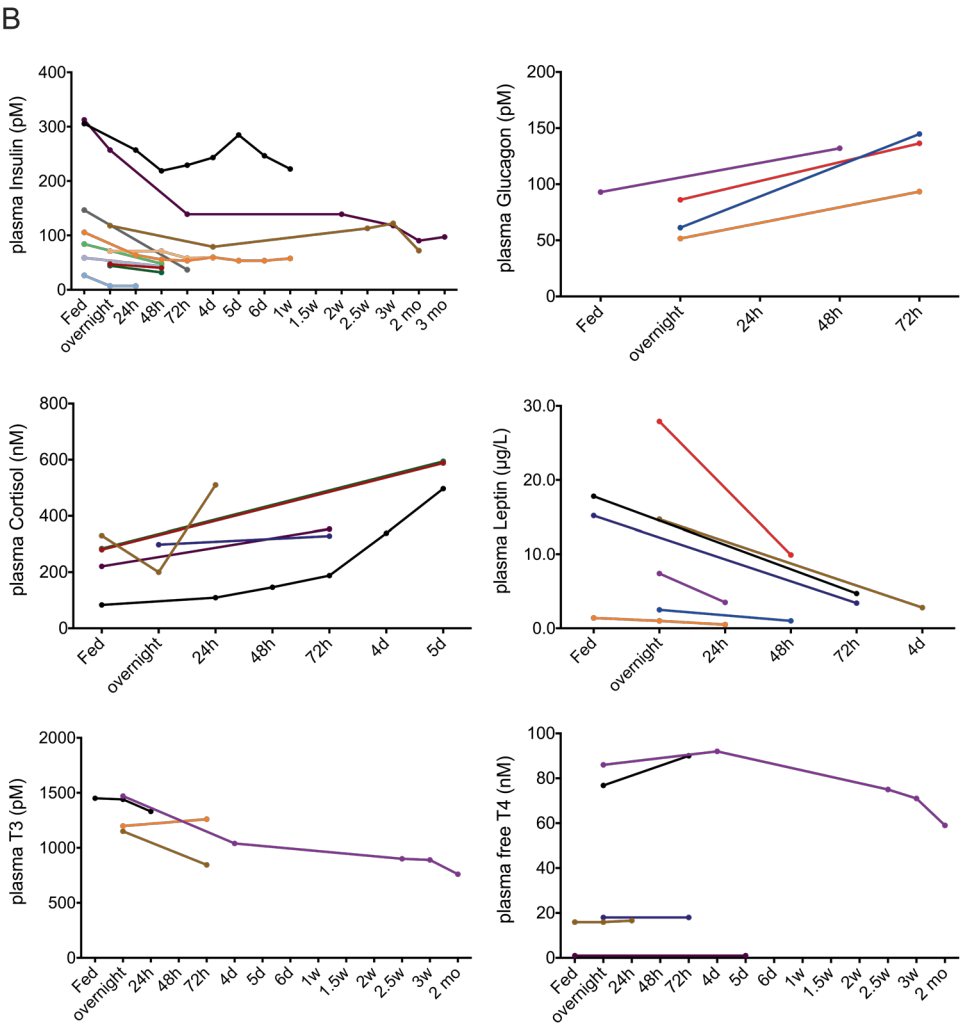

Figure 3: Changes in plasma parameters from fed state to various fasting-durations. A) Development of plasma levels of Glucose, TG, FFA, Glycerol and ketone bodies βOHB and AcAc after feeding and various durations of fasting. Glucose and TG progressively decline, while FFA, glycerol and ketone bodies increase. B) Plasma levels of the hormones Insulin, Glucagon, Cortisol, Leptin, T3 and T4. Insulin, Leptin and T3 decline, while Glucagon and Cortisol increase. T4 is not impacted by fasting. C) Color legend for plotted studies [34], [40], [46], [47], [51], [54]–[58], [60], [66]–[77] Depicted are mean values only. Overnight reflects a 8-12h fast. Abbreviations: h hours, d days, w weeks, mo months.

Transcriptional regulation of hepatic gene expression during feeding-fasting cycles by the transcription factor PPARα

Underlying the drastic changes seen in plasma parameters and the switch in fuel utilization during feeding–fasting cycles are multiple mechanisms working hand in hand to regulate required enzymes and pathways that facilitate the required adaptations. One such level of control is the regulation of gene expression via transcription factors. Transcription factors are proteins that are capable of selective binding to recognition sites on the DNA. Subsequently, they recruit transcriptional co-activators or co-repressors, including polymerases, to alter expression of target genes. More than 30 families of transcription factors have been identified in humans so far [80]. One transcription factor that allows the liver to fulfill its imperative role in the feeding–fasting transition is the peroxisome proliferator-activated receptor alpha (PPARα) [81].

PPARα belongs to the family of peroxisome proliferator-activated receptors (PPAR) that include PPARγ and PPARδ. While their expression profile discriminates them, PPARs share a common mode of action. As nutrient-sensitive nuclear receptors, PPARs are activated via ligand-binding of fatty acids and fatty acid derivatives. Upon activation, PPARs translocate to the nucleus where they heterodimerize with retinoid X receptor (RXR), another nuclear receptor. Subsequently, this complex binds to specific PPAR response elements (PPRE) in the promoter region of target genes, which allows the recruitment of the transcriptional machinery and thus the regulation of expression [81], [82].

Animal experiments were immensely conducive to our understanding of the role of this transcription factor during fasting. When subjected to fasting, mice deficient in PPARα present with dramatically altered plasma and liver parameters. Plasma levels of long chain acyl-carnitines and free fatty acids are increased during fasting compared to wild-type mice. Hepatic levels of these metabolites, including triglycerides, are also increased. On the other hand, short chain acyl-carnitines, glucose and β-hydroxybutyrate levels in the plasma are significantly reduced [81]. Already 20 years ago, these observations lead several research groups to classify PPARα as a critical regulator of hepatic lipid metabolism. Dysfunctional or absent PPARα signaling impairs the uptake and oxidation of fatty acids, preventing acetyl-CoA formation and entry into the ketogenesis pathway. Free fatty acids instead are re-esterified into triglycerides, leading to a fatty liver. Reduced blood glucose levels is likely the result of augmented peripheral utilization to offset the lack of ketone bodies [83]–[86].

Transcriptomic studies have revealed that the metabolic changes mentioned above are rooted in altered expression of numerous genes involved in fatty acid uptake (e.g. *Cd36*), fatty acid activation (e.g. *Fatp2*, *Fatp4*), fatty acid binding (e.g. *Fabp2*, *Fabp4*), fatty acid storage (e.g. *Dgat1*, *Plin*s), as well as peroxisomal fatty acid oxidation (e.g. Acox1),

mitochondrial β-oxidation (e.g. *Cpt1*, *Cpt2*, *Acad*s), and ketogenesis (e.g. *Acat1*, *Hmgcs2*, *Bdh1*). Also, a limited number of genes involved in gluconeogenesis (e.g. *Pcx*, *Gpd1*, *Gpd2*) and glycogenesis (*Gys2*) are regulated by PPARα. The catalogue of genes and pathways currently known to be under control of PPARα has led to its designation as the "master regulator of hepatic lipid metabolism" [81]. Importantly, the transcriptional regulatory function of mouse PPARα seems to be largely conserved in humans [82].

However, evidence abounds that PPARα is not the sole regulator of hepatic glucose and lipid metabolism. In particular, the transcription factor Cyclic AMP-responsive element-binding protein 3 Like 3 (CREB3L3) has been shown to regulate several aspects of glucose and lipid metabolism [87], [88]. It is highly expressed in the liver [89], is also induced during fasting [90] and may physically interact and/or cooperate with PPARα to regulate target genes [91], [92] such as *Hmgcs2* [93]. **Chapter 2** further characterized the interrelationship between PPARα and CREB3L3 in regulating hepatic gene expression. To this end, whole hepatic gene expression of PPARα$^{-/-}$, CREB3L3$^{-/-}$ and double knockout mice subjected to fasting and ketogenic diet feeding was investigated. Depending on nutritional status both transcription factors showed great plasticity in the degree of synergism and co-dependence in regulating gene expression of target genes.

Post-translational regulation of LPL by ANGPTL4 controls triglyceride uptake into adipose tissue during feeding-fasting cycles

Changes in gene expression, as for example mediated by PPARα, ultimately impact physiological parameters via alteration in enzyme abundances and activities. However, transcriptional regulation is often not the most important, arguably because translational or post-translational mechanisms allow for a speedier fine-tuning of enzymes and pathways in specific physiological states. The relevance of translational or post-translational mechanisms during fasting is exemplified by the lack of a transcriptional signature for the lipolysis pathway in adipose tissue of fasting mice [94], yet the release of fatty acids from adipose tissue is a key process during fasting. One protein that increases in abundance during the fasted state and regulates the flow of triglycerides via a post-translational mechanism is Angiopoietin-like 4 (ANGPTL4) [95], [96].

20 years ago, *Angptl4* was identified as a PPARα and PPARγ target gene with a potential role during fasting [97], [98]. Originally named as fasting-induced adipose factor (FIAF), genetic studies in mice subsequently illustrated the importance of ANGPTL4 in the regulation of plasma triglyceride levels. Overexpression of *Angptl4* and injection of recombinant ANGPTL4 resulted in an increase in plasma TG levels, while knockout of *Angptl4* and administration of anti-ANGPTL4 antibodies reduced plasma TG levels in mice [99]–[102]. Mechanistically, ANGPTL4 was shown to inhibit lipoprotein lipase (LPL) activity, *in vitro* [99] and later *in vivo* [100], [103].

LPL belongs to a family of lipases that are generally involved in hydrolysis reactions of triglycerides for digestion, uptake or oxidation. Secreted from various cell types including adipose tissue, skeletal and heart muscle, LPL locates on the endothelial surface and hydrolyses VLDL and chylomicron particles to accommodate the tissue specific requirements for fatty acids [104], [105]. The pivotal role of LPL in this process is illustrated by human genetic studies. LPL gain-of-function mutation carriers present with lower plasma triglyceride levels while LPL loss-of-function mutation carriers suffer from familial chylomicronemia syndrome (FCS), a condition marked by hypertriglyceridemia [106], [107]. Notably, plasma triglyceride levels are an independent risk factor for coronary artery disease [108].

The activity of LPL is tightly regulated in a tissue-specific manner in response to physiological stimuli such as fasting, physical activity, and cold exposure to account for tissue-specific requirements for fuel [96]. Research over the past decade has shown that ANGPTL4 inhibits lipoprotein lipase activity by unfolding its catalytic domain [109], and that this regulation may occur in a cell-type specific fashion along the secretory route either intracellularly [110], in the subendothelial space [111], [112], or on the endothelial surface

[102]. Several mice studies addressed the specific role of ANGPTL4 in the context of fasting. Kroupa *et al.* found that *Angptl4* expression is highly sensitive to fasting and inversely correlated to LPL activity. This correlation was lost in knockout animals [113]. Induction of *Angptl4* peaks after only 2h of food withdrawal and is rapidly downregulated upon refeeding [95]. Furthermore, in whole body ANGPTL4-knockout animals, radiolabeled intralipid and chylomicron injection shows increased TG clearance exclusively in adipose tissues during fasting [95]. This finding is corroborated by studies in transgenic ANGPTL4 mice, which display reduced in TG clearance in the fasted but not in the fed state [114]. Cumulatively, these studies support the notion that ANGPTL4 functions locally to divert TG away from the adipose tissue in the fasted state. It can be argued that this action promotes the utilization of TG-derived fatty acids by non-adipose tissues and ultimately supports the release of fatty acids from adipose tissue (futile cycle) and the whole-body shift to fatty acid utilization.

Since most data on the physiological role of ANGPTL4 stems from mice studies, **Chapter 3** of this thesis, was designed to confirm its role in human adipose tissue. After 24h of fasting, ANGPTL4 levels in human adipose tissue were determined alongside LPL activity. **Chapter 4** further explores the intracellular degradation pathway of LPL by ANGPTL4 in mouse adipocytes. Members of the proprotein convertase subtilisin/kexin (PCSK) protein family have been implicated in the ANGPTL4-LPL pathway by prior research. Lastly, **Chapter 5**, addresses potential safety concerns that emerged from mouse experiments in which the suitability of ANGPTL4 as a potential target for the treatment of dyslipidemia had been investigated. This study employed a more modest approach of whole-body inactivation of ANGPTL4 than the original complete knockout and studied these mice after high-fat feeding and fasting.

β-hydroxybutyrate as a novel fasting-associated signaling molecule

Fasting and caloric restriction-type interventions elicit a myriad of health benefits and are expected to provide clinical benefit for prevention and treatment of metabolic disorders including obesity and diabetes (see “Health benefits of fasting”) [6]. The two main ketone bodies, β-hydroxybutyrate (βOHB) and acetoacetate (AcAc) serve as sensitive biomarkers as they increase in abundance from around 100 µM in the fed state to up to 7 mM after several days of fasting [32], [115].

In addition to serving as a substrate for ATP synthesis, research in the recent years unveiled that βOHB may serve as a direct signaling molecule, potentially mediating some of the

beneficial health effects of fasting [6], [59], [116]–[125]. βOHB was shown to be a ligand for G-protein coupled receptors GPR41 and GPR109A regulating *in vitro* adipocyte lipolysis [126] and sympathetic activity [127]. Via the GPR109A signaling cascade βOHB was also exerting anti-inflammatory effects in macrophages, primary hypothalamic and RPE cells after LPS stimulation [128]–[132]. Additionally, anti-inflammatory GPR109A-independent effects have been documented via the reduction of NLRP3 inflammasome activation in monocytes [133], hepatocytes [134] and neutrophils, mitigating NLRP3 mediated diseases such as gout [135]. Yet, reports of βOHB inducing gene expression of pro-inflammatory mediators as well as promoting growth of tumor cells i*n vivo* and *in vitro* indicate that βOHB's effect may not always be beneficial [136]–[139].

Mice studies, *in vitro* and enzymatic assays provided evidence that βOHB may also exert some of its effects by regulating gene expression via epigenetic mechanisms. The first report was by Shimazu *et al.*, correlating increased acetylation of histone H3 lysine residues 9 and 14 by βOHB to protection against oxidative stress in kidney via the induction of *FOXO3a*, *catalase* and *MnSOD* [140]. While subsequent studies in neonatal hepatocytes, brain microvascular endothelial cells and NB2a neuronal cells suggested conservation of this mechanism in other cell types [141], [142], subsequent studies refuted βOHB as a potent HDAC inhibitor [137], [143]. Instead studies in hepatocytes, cortical neurons, myotubes and endothelial cells identified and confirmed that βOHB may serve itself as a novel, transcriptionally-activating histone modification. In the absence of changes in H3K9/14 levels, lysine β-hydroxybutyrylation was found in proximity to fasting-relevant hepatic pathways including amino acid catabolism, circadian rhythm and PPAR signaling [143], regulating BDNF expression [144] or hexokinase 2 [137].

Chapter 6 further characterizes the capacity of βOHB to regulate gene expression and thereby serve as a direct signaling molecule during fasting. Primary mouse adipocytes, macrophages, myotubes and hepatocytes with physiological concentrations of βOHB for 6h and assessed gene expression via RNA-seq.

Outline of this thesis

Fasting, i.e. the abstinence from food intake, elicits a multi-organ response that maintains the physiological homeostasis of an organism despite a constant requirement for energy. An intricate network of evolutionarily conserved transcriptional, translational and post-translational regulatory mechanisms underlie this adaptive response and provide the basis for the survival of every fasting bout. In recent years, numerous studies have been

conducted to study the potential health benefits of caloric restriction, time-restricted eating and intermittent fasting. **The goal of this thesis was to characterize a number of transcriptional and translational regulatory mechanisms relevant to fasting**. Their uncovering and understanding in the context of basic animal and human physiology is expected to provide new avenues for clinical mitigation of metabolic diseases.

Chapter 1 is an introductory chapter. Firstly, it summarizes the purported health benefits of the various forms of fasting. Secondly, it highlights the key metabolic organs that participate in the transition from the fed to the fasted state and the metabolic adaptations that occurs in this process. In **Chapter 2** of this thesis, the interrelationship of the transcription factors PPARα and CREB3L3 in regulating the adaptive response of the liver to feeding-fasting cycles was characterized. The results indicate great plasticity in the degree of synergism and co-dependence between both transcription factors that was dependent on nutritional status. **Chapter 3** of this thesis describes a 24h fasting study in human volunteers to investigate the mechanistic control of LPL and thereby triglyceride clearance. Our results indicate that ANGPTL4 levels in human adipose tissue are increased by fasting, likely via increased plasma cortisol and free fatty acids, and decreased plasma insulin, resulting in decreased LPL activity. **Chapter 4** examines the mechanism of action of ANGPTL4 in mouse adipocytes. It is shown that ANGPTL4 promotes the intracellular degradation of LPL by members of the proprotein convertase subtilisin/kexin (PCSK) protein family. This regulation was feeding-fasting dependent. In **Chapter 5**, the mechanisms underlying the adverse effect of whole-body inactivation of ANGPTL4 are studied using Angptl4-hypomorphic and Angptl4 -/- mice. It was found that whole body inactivation of ANGPTL4 is not suitable as a clinical strategy for dyslipidemia. **Chapter 6** explores whether the ketone body β-hydroxybutyrate (βOHB) influences differentiation *in vitro* and regulates genes expression in several primary cell types. Previous research indicated that βOHB may be a fasting-specific signaling molecule. RNA sequencing of various primary cells after 6h treatment revealed minimal effects of βOHB on gene expression, questioning βOHB's signaling role. **Chapter 7** is a general discussion of the major outcomes of the previous chapters, recommendations for future studies and a final conclusion.

References

[1] S. M. Secor and H. V. Carey, “Integrative physiology of fasting,” Compr. Physiol., vol. 6, no. 2, pp. 773–825, 2016.

[2] A. Nencioni, I. Caffa, S. Cortellino, and V. D. Longo, “Fasting and cancer: molecular mechanisms and clinical application.,” Nat. Rev. Cancer, vol. 18, no. 11, pp. 707–719, Nov. 2018.

[3] V. D. Longo and M. P. Mattson, “Fasting: Molecular mechanisms and clinical applications,” Cell Metab., vol. 19, no. 2, pp. 181–192, Feb. 2014.

[4] M. P. Mattson, V. D. Longo, and M. Harvie, “Impact of Intermittent Fasting on Health and Disease Processes,” Ageing Res. Rev., vol. 39, pp. 46–58, Oct. 2016.

[5] V. D. Longo and S. Panda, “Fasting, Circadian Rhythms, and Time-Restricted Feeding in Healthy Lifespan,” Cell Metab., vol. 23, no. 6, pp. 1048–1059, Jun. 2016.

[6] A. Di Francesco, C. Di Germanio, M. Bernier, and R. de Cabo, “A time to fast.,” Science, vol. 362, no. 6416, pp. 770–775, Nov. 2018.

[7] R. De Cabo and M. P. Mattson, “Effects of intermittent fasting on health, aging, and disease,” New England Journal of Medicine, vol. 381, no. 26. Massachussetts Medical Society, pp. 2541–2551, 26-Dec-2019.

[8] K. Liu, B. Liu, and L. K. Heilbronn, “Intermittent fasting: what questions should we be asking?,” Physiol. Behav., vol. 218, p. 112827, Feb. 2020.

[9] S. Moon et al., “Beneficial effects of time-restricted eating on metabolic diseases: A systemic review and meta- analysis,” Nutrients, vol. 12, no. 5. MDPI AG, 01-May-2020.

[10] J. R. Speakman and S. E. Mitchell, “Caloric restriction,” Mol. Aspects Med., vol. 32, no. 3, pp. 159–221, 2011.

[11] W. R. Swindell, Dietary restriction in rats and mice: A meta-analysis and review of the evidence for genotype-dependent effects on lifespan, vol. 11, no. 2. 2012, pp. 254–270.

[12] E. Ravussin et al., “A 2-year randomized controlled trial of human caloric restriction: Feasibility and effects on predictors of health span and longevity,” Journals Gerontol. - Ser. A Biol. Sci. Med. Sci., vol. 70, no. 9, pp. 1097–1104, 2015.

[13] D. Omodei and L. Fontana, “Calorie restriction and prevention of age-associated chronic disease,” FEBS Letters, vol. 585, no. 11. No longer published by Elsevier, pp. 1537–1542, 06-Jun-2011.

[14] R. J. Colman et al., “Caloric restriction delays disease onset and mortality in rhesus monkeys,” Science (80-.)., vol. 325, no. 5937, pp. 201–204, Jul. 2009.

[15] J. A. Mattison et al., “Impact of caloric restriction on health and survival in rhesus monkeys from the NIA study,” Nature, vol. 489, no. 7415, pp. 318–321, Sep. 2012.

[16] J. A. Mattison et al., “Caloric restriction improves health and survival of rhesus monkeys,” Nat. Commun., vol. 8, Jan. 2017.

[17] E. A. M. H. Moreira, M. Most, J. Howard, and E. Ravussin, “Dietary adherence to long-term controlled feeding in a calorie-restriction study in overweight men and women,” Nutr. Clin. Pract., vol. 26, no. 3, pp. 309–315, Jun. 2011.

[18] K. A. Gudzune et al., “Efficacy of commercial weight-loss programs: An updated systematic review,” Annals of Internal Medicine, vol. 162, no. 7. American College of Physicians, pp. 501–512, 07-Apr-2015.

[19] L. S. Chow et al., “Time-Restricted Eating Effects on Body Composition and Metabolic Measures in Humans with Overweight: A Feasibility Study,” Obesity, vol. 00, no. 00, pp. 1–10, 2020.

[20] A. T. Hutchison et al., “Effects of Intermittent Versus Continuous Energy Intakes on Insulin Sensitivity and Metabolic Risk in Women with Overweight,” Obesity, vol. 27, no. 1, pp. 50–58, Jan. 2019.

[21] E. F. Sutton, R. Beyl, K. S. Early, W. T. Cefalu, E. Ravussin, and C. M. Peterson, “Early Time-Restricted Feeding

Improves Insulin Sensitivity, Blood Pressure, and Oxidative Stress Even without Weight Loss in Men with Prediabetes," Cell Metab., vol. 27, no. 6, pp. 1212-1221.e3, Jun. 2018.

[22] H. Jamshed, R. A. Beyl, D. L. D. Manna, E. S. Yang, E. Ravussin, and C. M. Peterson, "Early time-restricted feeding improves 24-hour glucose levels and affects markers of the circadian clock, aging, and autophagy in humans," Nutrients, vol. 11, no. 6, Jun. 2019.

[23] J. Wefers et al., "Circadian misalignment induces fatty acid metabolism gene profiles and compromises insulin sensitivity in human skeletal muscle," Proc. Natl. Acad. Sci. U. S. A., vol. 115, no. 30, Jul. 2018.

[24] L. Pickel and H.-K. Sung, "Feeding Rhythms and the Circadian Regulation of Metabolism," Front. Nutr., vol. 7, Apr. 2020.

[25] C. N. Barber and D. M. Raben, "Lipid Metabolism Crosstalk in the Brain: Glia and Neurons," Front. Cell. Neurosci., vol. 13, p. 212, May 2019.

[26] P. Chatterjee et al., "Potential of coconut oil and medium chain triglycerides in the prevention and treatment of Alzheimer's disease," Mech. Ageing Dev., p. 111209, Jan. 2020.

[27] Q. Xu et al., "Medium-chain triglycerides improved cognition and lipid metabolomics in mild to moderate Alzheimer's disease patients with APOE4(-/-): A double-blind, randomized, placebo-controlled crossover trial," Clin. Nutr., pp. S0261-5614(19)33104–8, Oct. 2019.

[28] E. J. Murphy, "The blood–brain barrier and protein-mediated fatty acid uptake: role of the blood–brain barrier as a metabolic barrier: An Editorial Comment for 'The blood-brain barrier fatty acid transport protein 1 (FATP1/SLC27A1) supplies docosahexaenoic acid to the b," J. Neurochem., vol. 141, no. 3, pp. 324–329, 2017.

[29] S. M. Gray, R. I. Meijer, and E. J. Barrett, "Insulin regulates brain function, but how does it get there?," Diabetes, vol. 63, no. 12, pp. 3992–3997, 2014.

[30] E. R. Seaquist, G. S. Damberg, I. Tkac, and R. Gruetter, "The Effect of Insulin on in Vivo Cerebral Glucose Concentrations and Rates of Glucose Transport/Metabolism in Humans," Diabetes, vol. 50, no. 10, pp. 2203–2209, 2001.

[31] S. G. Hasselbalch et al., "No effect of insulin on glucose blood-brain barrier transport and cerebral metabolism in humans," Diabetes, vol. 48, no. 10, pp. 1915–1921, 1999.

[32] G. F. Cahill, "Fuel Metabolism in Starvation," Annu. Rev. Nutr., vol. 26, no. 1, pp. 1–22, 2006.

[33] E. Marliss, E. Marliss, O. E. Owen, and G. F. Cahill, "Blood Glucose and Gluconeogenesis in Fasting Man," Arch. Intern. Med., vol. 123, no. 3, pp. 293–298, Mar. 1969.

[34] A. M. Bak et al., "Prolonged fasting-induced metabolic signatures in human skeletal muscle of lean and obese men," PLoS One, vol. 13, no. 9, pp. 1–19, 2018.

[35] A. J. Garber, P. H. Menzel, G. Boden, and O. E. Owen, "Hepatic ketogenesis and gluconeogenesis in humans," J. Clin. Invest., vol. 54, no. 4, pp. 981–989, 1974.

[36] T. Pozefsky, R. G. Tancredi, R. T. Moxley, J. Dupre, and J. D. Tobin, "Effects of Brief Starvation on Muscle Amino Acid Metabolism in Nonobese Man."

[37] P. Felig, O. E. Owen, J. Wahren, and G. F. Cahill, "Amino acid metabolism during prolonged starvation.," J. Clin. Invest., vol. 48, no. 3, pp. 584–94, Mar. 1969.

[38] P. Felig, T. Pozefsk, E. Marlis, and G. F. Cahill, "Alanine: Key Role in Gluconeogenesis," Science (80-.)., vol. 167, no. 3920, pp. 1003 LP – 1004, Feb. 1970.

[39] T. Teruya, R. Chaleckis, J. Takada, M. Yanagida, and H. Kondoh, "Diverse metabolic reactions activated during 58-hr fasting are revealed by non-targeted metabolomic analysis of human blood," Sci. Rep., vol. 9, no. 1, p. 854, Dec. 2019.

[40] K. S. Nair, P. D. Woolf, S. L. Welle, and D. E. Matthews, "Leucine, glucose, and energy metabolism after 3 days of fasting in healthy human subjects.," Am. J. Clin. Nutr., vol. 46, no. 4, pp. 557–62, Oct. 1987.

[41] M. L. Steinhauser et al., “The circulating metabolome of human starvation,” JCI insight, vol. 3, no. 16, Aug. 2018.

[42] P. She et al., “Disruption of BCATm in Mice Leads to Increased Energy Expenditure Associated with the Activation of a Futile Protein Turnover Cycle,” Cell Metab., vol. 6, no. 3, pp. 181–194, Sep. 2007.

[43] T. Sarabhai and M. Roden, “Hungry for your alanine: When liver depends on muscle proteolysis,” Journal of Clinical Investigation, vol. 129, no. 11. American Society for Clinical Investigation, pp. 4563–4566, 01-Nov-2019.

[44] P. Felig, “AMINO ACID METABOLISM IN MAN,” 1975.

[45] L. M. Sherwood, E. E. Parris, and G. F. Cahill, “Starvation in Man,” N. Engl. J. Med., vol. 282, no. 12, pp. 668–675, Mar. 1970.

[46] O. E. Owen, K. J. Smalley, D. A. D’Alessio, M. A. Mozzoli, and E. K. Dawson, “Protein, fat, and carbohydrate requirements during starvation: Anaplerosis and cataplerosis,” Am. J. Clin. Nutr., vol. 68, no. 1, pp. 12–34, 1998.

[47] K. F. Petersen, S. Dufour, G. W. Cline, and G. I. Shulman, “Regulation of hepatic mitochondrial oxidation by glucose-alanine cycling during starvation in humans,” J. Clin. Invest., vol. 129, no. 11, pp. 4671–4675, Nov. 2019.

[48] J. D. Browning, J. Baxter, S. Satapati, and S. C. Burgess, “The effect of short-term fasting on liver and skeletal muscle lipid, glucose, and energy metabolism in healthy women and men,” J. Lipid Res., vol. 53, no. 3, pp. 577–586, Mar. 2012.

[49] D. L. Rothman, I. Magnusson, L. D. Katz, R. G. Shulman, and G. I. Shulman, “Quantitation of hepatic glycogenolysis and gluconeogenesis in fasting humans with 13C NMR,” Science (80-.)., vol. 254, no. 5031, pp. 573–576, 1991.

[50] B. R. Landau, J. Wahren, V. Chandramouli, W. C. Schumann, K. Ekberg, and S. C. Kalhan, “Contributions of gluconeogenesis to glucose production in the fasted state,” J. Clin. Invest., vol. 98, no. 2, pp. 378–385, 1996.

[51] G. F. Cahill et al., “Hormone-fuel interrelationships during fasting.,” J. Clin. Invest., vol. 45, no. 11, pp. 1751–1769, 1966.

[52] J. Gjedsted et al., “Effects of a 3-day fast on regional lipid and glucose metabolism in human skeletal muscle and adipose tissue,” Acta Physiol., vol. 191, no. 3, pp. 205–216, Nov. 2007.

[53] B. C. Bergman, M.-A. Cornier, T. J. Horton, and D. H. Bessesen, “Effects of fasting on insulin action and glucose kinetics in lean and obese men and women,” Am J Physiol Endocrinol Metab, vol. 293, pp. 1103–1111, 2007.

[54] C. Zauner et al., “Resting energy expenditure in short-term starvation is increased as a result of an increase in serum norepinephrine,” Am. J. Clin. Nutr., vol. 71, no. 6, pp. 1511–1515, 2000.

[55] I. E. Papagiannopoulos-Vatopaidinos, M. Papagiannopoulou, and V. Sideris, “Dry Fasting Physiology: Responses to Hypovolemia and Hypertonicity,” Complement. Med. Res., 2020.

[56] J. L. Chan, J. E. Mietus, P. M. Raciti, A. L. Goldberger, and C. S. Mantzoros, “Short-term fasting-induced autonomic activation and changes in catecholamine levels are not mediated by changes in leptin levels in healthy humans,” Clin. Endocrinol. (Oxf)., vol. 66, no. 1, pp. 49–57, 2007.

[57] D. A. Streja, E. B. Marliss, and G. Steiner, “The effects of prolonged fasting on plasma triglyceride kinetics in man,” Metabolism, vol. 26, no. 5, pp. 505–516, 1977.

[58] M. A. Wijngaarden et al., “Regulation of skeletal muscle energy/nutrient-sensing pathways during metabolic adaptation to fasting in healthy humans,” Am. J. Physiol. Metab., vol. 307, no. 10, pp. E885–E895, Nov. 2014.

[59] P. Puchalska and P. A. Crawford, “Multi-dimensional Roles of Ketone Bodies in Fuel Metabolism, Signaling, and Therapeutics,” Cell Metab., vol. 25, no. 2, pp. 262–284, 2017.

[60] O. E. Owen, A. P. Morgan, H. G. Kemp, J. M. Sullivan, M. G. Herrera, and G. F. Cahill, “Brain metabolism during fasting.,” J. Clin. Invest., vol. 46, no. 10, pp. 1589–1595, 1967.

[61] O. E. Owen, “Mini-Series : Paths to Discovery Ketone Bodies as a Fuel for the Brain during Starvation,” Liver, vol. 33, no. 4, pp. 246–251, 2005.

[62] S. G. Hasselbalch, G. M. Knudsen, J. Jakobsen, L. P. Hageman, S. Holm, and O. B. Paulson, “Brain metabolism during short-term starvation in humans,” J. Cereb. Blood Flow Metab., vol. 14, no. 1, pp. 125–131, 1994.

[63] C. Redies et al., “Generalized decrease in brain glucose metabolism during fasting in humans studied by PET,” Am. J. Physiol. - Endocrinol. Metab., vol. 256, no. 6, pp. 0–5, 1989.

[64] J. Webber, E. Simpson, H. Parken, and I. A. Macdonald, “Metabolic effects of acute hyperketonaemia in man before and during an hyperinsulinaemic euglycaemic clamp,” Clin. Sci., vol. 86, no. 6, pp. 677–687, Jun. 1994.

[65] T. J. Thomson, J. Runcie, and V. Miller, “Treatment of obesity by total fasting for up to 249 days.,” Lancet, vol. 288, no. 7471, pp. 992–996, 1966.

[66] W. K. Stewart and L. W. Fleming, “Features of a successful therapeutic fast of 382 days’ duration,” Postgrad. Med. J., vol. 49, no. 569, pp. 203–209, 1973.

[67] F. Wilhelmi de Toledo, F. Grundler, A. Bergouignan, S. Drinda, and A. Michalsen, “Safety, health improvement and well-being during a 4 to 21-day fasting period in an observational study including 1422 subjects,” PLoS One, vol. 14, no. 1, p. e0209353, Jan. 2019.

[68] A. Markel, J. G. Brook, and M. Aviram, “Increased plasma triglycerides, cholesterol and apolipoprotein E during prolonged fasting in normal subjects,” Postgrad. Med. J., vol. 61, no. 715, pp. 395–400, 1985.

[69] W. P. Newman and R. G. Brodows, “Insulin action during acute starvation: Evidence for selective insulin resistance in normal man,” Metabolism, vol. 32, no. 6, pp. 590–596, 1983.

[70] P. I. Mansell and I. A. Macdonald, “The effect of starvation on insulin-induced glucose disposal and thermogenesis in humans,” Metabolism, vol. 39, no. 5, pp. 502–510, 1990.

[71] L. Hartman et al., “Augmented growth hormone (GH) secretory burst frequency and amplitude mediate enhanced GH secretion during a two-day fast in normal men.,” J. Clin. Endocrinol. Metab., vol. 74, no. 4, pp. 757–65, Apr. 1992.

[72] K. Y. Ho et al., “Fasting enhances growth hormone secretion and amplifies the complex rhythms of growth hormone secretion in man,” J. Clin. Invest., vol. 81, no. 4, pp. 968–975, 1988.

[73] C. I. Friedman, J. M. Falko, S. T. Patel, M. H. Kim, H. A. I. Newman, and H. Barrows, “Serum lipoprotein responses during active and stable weight reduction in reproductive obese females,” J. Clin. Endocrinol. Metab., vol. 55, no. 2, pp. 258–262, 1982.

[74] M. Bergendahl, W. S. Evans, C. Pastor, A. Patel, A. Iranmanesh, and J. D. Veldhuis, “Short-term fasting suppresses leptin and (conversely) activates disorderly growth hormone secretion in midluteal phase women - A clinical research center study,” J. Clin. Endocrinol. Metab., vol. 84, no. 3, pp. 883–894, 1999.

[75] J. D. Veldhuis, A. Iranmanesh, W. S. Evans, G. Lizarralde, M. O. Thorner, and M. L. Vance, “Amplitude suppression of the pulsatile mode of immunoradiometric luteinizing hormone release in fasting-induced hypoandrogenemia in normal men.,” J. Clin. Endocrinol. Metab., vol. 76, no. 3, pp. 587–93, Mar. 1993.

[76] M. Bergendahl, M. L. Vance, A. Iranmanesh, M. O. Thorner, and J. D. Veldhuis, “Fasting as a metabolic stress paradigm selectively amplifies cortisol secretory burst mass and delays the time of maximal nyctohemeral cortisol concentrations in healthy men.,” J. Clin. Endocrinol. Metab., vol. 81, no. 2, pp. 692–9, Feb. 1996.

[77] M. Bergendahl, A. Iranmanesh, W. S. Evans, and J. D. Veldhuis, “Short-term fasting selectively suppresses leptin pulse mass and 24-hour rhythmic leptin release in healthy midluteal phase women without disturbing leptin pulse frequency or its entropy control (pattern orderliness),” J. Clin. Endocrinol. Metab., vol. 85, no. 1, pp. 207–213, 2000.

[78] J. S. Cohn, J. R. McNamara, and E. J. Schaefer, “Lipoprotein cholesterol concentrations in the plasma of human subjects as measured in the fed and fasted states,” Clin. Chem., vol. 34, no. 12, pp. 2456–2459, 1988.

[79] O. E. Owen, P. Felig, A. P. Morgan, J. Wahren, and G. F. Cahill, “Liver and kidney metabolism during

prolonged starvation.," J. Clin. Invest., vol. 48, no. 3, pp. 574–583, 1969.

[80] S. A. Lambert et al., "The Human Transcription Factors," Cell, vol. 172, no. 4. Cell Press, pp. 650–665, 08-Feb-2018.

[81] S. Kersten, "Integrated physiology and systems biology of PPARα," Mol. Metab., vol. 3, no. 4, pp. 354–371, Jul. 2014.

[82] S. Kersten and R. Stienstra, "The role and regulation of the peroxisome proliferator activated receptor alpha in human liver," Biochimie, vol. 136, pp. 75–84, 2017.

[83] T. Hashimoto, W. S. Cook, C. Qi, A. V. Yeldandi, J. K. Reddy, and M. S. Rao, "Defect in peroxisome proliferator-activated receptor α-inducible fatty acid oxidation determines the severity of hepatic steatosis in response to fasting," J. Biol. Chem., vol. 275, no. 37, pp. 28918–28928, Sep. 2000.

[84] S. Kersten, J. Seydoux, J. M. Peters, F. J. Gonzalez, B. Desvergne, and W. Wahli, "Peroxisome proliferator-activated receptor α mediates the adaptive response to fasting," J. Clin. Invest., vol. 103, no. 11, pp. 1489–1498, 1999.

[85] T. C. Leone, C. J. Weinheimer, and D. P. Kelly, "A critical role for the peroxisome proliferator-activated receptor α (PPARα) in the cellular fasting response: The PPARα-null mouse as a model of fatty acid oxidation disorders," Proc. Natl. Acad. Sci. U. S. A., vol. 96, no. 13, pp. 7473–7478, Jun. 1999.

[86] M. C. Sugden, K. Bulmer, G. F. Gibbons, B. L. Knight, and M. J. Holness, "Peroxisome-proliferator-activated receptor-α (PPARα) deficiency leads to dysregulation of hepatic lipid and carbohydrate metabolism by fatty acids and insulin," Biochem. J., vol. 364, no. 2, pp. 361–368, Jun. 2002.

[87] A. H. Lee, "The role of CREB-H transcription factor in triglyceride metabolism," Curr. Opin. Lipidol., vol. 23, no. 2, pp. 141–146, Apr. 2012.

[88] Y. Nakagawa and H. Shimano, "CREBH regulates systemic glucose and lipid metabolism," Int. J. Mol. Sci., vol. 19, no. 5, pp. 1–15, 2018.

[89] J. H. Lee et al., "The transcription factor cyclic AMP-responsive element-binding protein H regulates triglyceride metabolism," Nat. Med., vol. 17, no. 7, pp. 812–815, Jul. 2011.

[90] H. Danno et al., "The liver-enriched transcription factor CREBH is nutritionally regulated and activated by fatty acids and PPARα," Biochem. Biophys. Res. Commun., vol. 391, no. 2, pp. 1222–1227, Jan. 2010.

[91] H. Kim et al., "Liver-enriched transcription factor CREBH interacts with peroxisome proliferator-activated receptor α to regulate metabolic hormone FGF21," Endocrinology, vol. 155, no. 3, pp. 769–782, Mar. 2014.

[92] H. Kim, R. Mendez, X. Chen, D. Fang, and K. Zhang, "Lysine Acetylation of CREBH Regulates Fasting-Induced Hepatic Lipid Metabolism.," Mol. Cell. Biol., vol. 35, no. 24, pp. 4121–34, Dec. 2015.

[93] Y. Nakagawa et al., "CREB3L3 controls fatty acid oxidation and ketogenesis in synergy with PPARα," Sci. Rep., vol. 6, no. 1, p. 39182, Dec. 2016.

[94] M. Schupp et al., "Metabolite and transcriptome analysis during fasting suggest a role for the p53-Ddit4 axis in major metabolic tissues," BMC Genomics, vol. 14, no. 1, p. 758, Nov. 2013.

[95] E. M. Cushing, X. Chi, K. L. Sylvers, S. K. Shetty, M. J. Potthoff, and B. S. J. Davies, "Angiopoietin-like 4 directs uptake of dietary fat away from adipose during fasting.," Mol. Metab., vol. 6, no. 8, pp. 809–818, 2017.

[96] S. Kersten, "Physiological regulation of lipoprotein lipase," Biochim. Biophys. Acta - Mol. Cell Biol. Lipids, vol. 1841, no. 7, pp. 919–933, 2014.

[97] S. Kersten et al., "Characterization of the fasting-induced adipose factor FIAF, a novel peroxisome proliferator-activated receptor target gene.," J. Biol. Chem., vol. 275, no. 37, pp. 28488–93, Sep. 2000.

[98] J. C. Yoon et al., "Peroxisome Proliferator-Activated Receptor gamma Target Gene Encoding a Novel Angiopoietin-Related Protein Associated with Adipose Differentiation," Mol. Cell. Biol., vol. 20, no. 14, pp. 5343–5349, Jul. 2000.

[99] K. Yoshida, T. Shimizugawa, M. Ono, and H. Furukawa, "Angiopoietin-like protein 4 is a potent

hyperlipidemia-inducing factor in mice and inhibitor of lipoprotein lipase," J. Lipid Res., vol. 43, no. 11, pp. 1770–1772, Nov. 2002.

[100] A. Köster et al., "Transgenic angiopoietin-like (Angptl)4 overexpression and targeted disruption of Angptl4 and Angptl3: Regulation of triglyceride metabolism," Endocrinology, vol. 146, no. 11, pp. 4943–4950, 2005.

[101] S. Mandard et al., "The fasting-induced adipose factor/angiopoietin-like protein 4 is physically associated with lipoproteins and governs plasma lipid levels and adiposity," J. Biol. Chem., vol. 281, no. 2, pp. 934–944, Jan. 2006.

[102] U. Desai et al., "Lipid-lowering effects of anti-angiopoietin-like 4 antibody recapitulate the lipid phenotype found in angiopoietin-like 4 knockout mice," Proc. Natl. Acad. Sci. U. S. A., vol. 104, no. 28, pp. 11766–11771, Jul. 2007.

[103] X. Yu et al., "Inhibition of cardiac lipoprotein utilization by transgenic overexpression of Angptl4 in the heart," Proc. Natl. Acad. Sci. U. S. A., vol. 102, no. 5, pp. 1767–1772, Feb. 2005.

[104] J. R. Mead, S. A. Irvine, and D. P. Ramji, "Lipoprotein lipase: Structure, function, regulation, and role in disease," J. Mol. Med., vol. 80, no. 12, pp. 753–769, 2002.

[105] S. G. Young and R. Zechner, "Biochemistry and pathophysiology of intravascular and intracellular lipolysis," Genes Dev., vol. 27, no. 5, pp. 459–484, Mar. 2013.

[106] G. Ranganathan et al., "The lipoprotein lipase (LPL) S447X gain of function variant involves increased mRNA translation," Atherosclerosis, vol. 221, no. 1, pp. 143–147, Mar. 2012.

[107] P. Benlian, J. L. De Gennes, L. Foubert, H. Zhang, S. E. Gagné, and M. Hayden, "Premature Atherosclerosis in Patients with Familial Chylomicronemia Caused by Mutations in the Lipoprotein Lipase Gene," N. Engl. J. Med., vol. 335, no. 12, pp. 848–854, Sep. 1996.

[108] P. B. Sandesara, S. S. Virani, S. Fazio, and M. D. Shapiro, "The Forgotten Lipids: Triglycerides, Remnant Cholesterol, and Atherosclerotic Cardiovascular Disease Risk," Endocr. Rev., vol. 40, no. 2, pp. 537–557, Apr. 2019.

[109] S. Mysling et al., "The angiopoietin-like protein ANGPTL4 catalyzes unfolding of the hydrolase domain in lipoprotein lipase and the endothelial membrane protein GPIHBP1 counteracts this unfolding," Elife, vol. 5, no. 45, pp. 1–23, Dec. 2016.

[110] W. Dijk, A. P. Beigneux, M. Larsson, A. Bensadoun, S. G. Young, and S. Kersten, "Angiopoietin-like 4 (ANGPTL4) promotes intracellular degradation of lipoprotein lipase in adipocytes.," J. Lipid Res., vol. 7, no. 11, pp. 956–963, 2016.

[111] E. Makoveichuk et al., "Inactivation of lipoprotein lipase occurs on the surface of THP-1 macrophages where oligomers of angiopoietin-like protein 4 are formed," Biochem. Biophys. Res. Commun., vol. 425, no. 2, pp. 138–143, Aug. 2012.

[112] E. Makoveichuk, E. Vorrsjö, T. Olivecrona, and G. Olivecrona, "Inactivation of lipoprotein lipase in 3T3-L1 adipocytes by angiopoietin-like protein 4 requires that both proteins have reached the cell surface," Biochem. Biophys. Res. Commun., vol. 441, no. 4, pp. 941–946, Nov. 2013.

[113] O. Kroupa et al., "Linking nutritional regulation of Angptl4, Gpihbp1, and Lmf1 to lipoprotein lipase activity in rodent adipose tissue.," BMC Physiol., vol. 12, p. 13, 2012.

[114] L. Lichtenstein et al., "Angptl4 Upregulates Cholesterol Synthesis in Liver via Inhibition of LPL- and HL-Dependent Hepatic Cholesterol Uptake," Arterioscler. Thromb. Vasc. Biol., vol. 27, no. 11, pp. 2420–2427, Nov. 2007.

[115] Wildenhoff KE, Johansen JP, K. H, Yde H, and Sorensen NS, "Diurnal variations in the concentrations of blood acetoacetate and 3-hydroxybutyrate.," Acta Med Scand., vol. 195, no. 1–2, pp. 25–8, 1974.

[116] R. L. Veech, "Ketone ester effects on metabolism and transcription," J. Lipid Res., vol. 55, no. 10, pp. 2004–2006, Oct. 2014.

[117] A. Dąbek, M. Wojtala, L. Pirola, and A. Balcerczyk, "Modulation of cellular biochemistry, epigenetics and

metabolomics by ketone bodies. Implications of the ketogenic diet in the physiology of the organism and pathological states," Nutrients, vol. 12, no. 3. MDPI AG, 01-Mar-2020.

[118] P. Rojas-Morales, E. Tapia, and J. Pedraza-Chaverri, "Beta-Hydroxybutyrate: A signaling metabolite in starvation response?," Cell. Signal., vol. 28, no. 8, pp. 917–923, Aug. 2016.

[119] P. Rojas-Morales, J. Pedraza-Chaverri, and E. Tapia, "Ketone bodies, stress response, and redox homeostasis," Redox Biology, vol. 29. Elsevier B.V., p. 101395, 01-Jan-2020.

[120] J. C. Newman and E. Verdin, "β-hydroxybutyrate: Much more than a metabolite," Diabetes Res. Clin. Pract., vol. 106, no. 2, pp. 173–181, 2014.

[121] L. B. Achanta and C. D. Rae, "β-Hydroxybutyrate in the Brain: One Molecule, Multiple Mechanisms," Neurochem. Res., vol. 42, no. 1, pp. 35–49, Jan. 2017.

[122] A. L. Hartman and J. M. Rho, "The new ketone alphabet soup: BHB, HCA, and HDAC," Epilepsy Currents, vol. 14, no. 6. pp. 355–357, 2014.

[123] J. C. Newman and E. Verdin, "β-Hydroxybutyrate: A Signaling Metabolite," Annu. Rev. Nutr., vol. 37, no. 1, pp. 51–76, 2017.

[124] R. L. Veech, B. Chance, Y. Kashiwaya, H. a Lardy, and G. F. Cahill, "Ketone bodies, potential therapeutic uses.," IUBMB Life, vol. 51, pp. 241–247, 2001.

[125] M. Maalouf, J. M. Rho, and M. P. Mattson, "The neuroprotective properties of calorie restriction, the ketogenic diet, and ketone bodies," Brain Res. Rev., vol. 59, no. 2, pp. 293–315, Mar. 2009.

[126] A. K. P. Taggart et al., "(D)-β-hydroxybutyrate inhibits adipocyte lipolysis via the nicotinic acid receptor PUMA-G," J. Biol. Chem., vol. 280, no. 29, pp. 26649–26652, 2005.

[127] I. Kimura et al., "Short-chain fatty acids and ketones directly regulate sympathetic nervous system via G protein-coupled receptor 41 (GPR41)," Proc. Natl. Acad. Sci. U. S. A., vol. 108, no. 19, pp. 8030–8035, May 2011.

[128] S. P. Fu et al., "β-hydroxybutyric acid inhibits growth hormone-releasing hormone synthesis and secretion through the GPR109A/extracellular signal-regulated 1/2 signalling pathway in the hypothalamus," J. Neuroendocrinol., vol. 27, no. 3, pp. 212–222, Mar. 2015.

[129] D. Gambhir et al., "GPR109A as an anti-inflammatory receptor in retinal pigment epithelial cells and its relevance to diabetic retinopathy.," Invest. Ophthalmol. Vis. Sci., vol. 53, no. 4, pp. 2208–2217, 2012.

[130] M. Rahman et al., "The β-hydroxybutyrate receptor HCA2 activates a neuroprotective subset of macrophages.," Nat. Commun., vol. 5, no. May, p. 3944, May 2014.

[131] K. Zandi-Nejad et al., "The role of HCA2 (GPR109A) in regulating macrophage function," FASEB J., vol. 27, no. 11, pp. 4366–4374, Nov. 2013.

[132] S. P. Fu et al., "BHBA suppresses LPS-induced inflammation in BV-2 cells by inhibiting NF- B activation," Mediators Inflamm., vol. 2014, 2014.

[133] Y.-H. Youm et al., "The ketone metabolite β-hydroxybutyrate blocks NLRP3 inflammasome-mediated inflammatory disease.," Nat. Med., vol. 21, no. 3, pp. 263–9, 2015.

[134] H. R. Bae et al., "β-Hydroxybutyrate suppresses inflammasome formation by ameliorating endoplasmic reticulum stress via AMPK activation," Oncotarget, vol. 7, no. 41, pp. 66444–66454, 2016.

[135] E. L. Goldberg et al., "β-Hydroxybutyrate Deactivates Neutrophil NLRP3 Inflammasome to Relieve Gout Flares," Cell Rep., vol. 18, no. 9, pp. 2077–2087, Feb. 2017.

[136] K. Liu et al., "p53 β-hydroxybutyrylation attenuates p53 activity," Cell Death Dis., vol. 10, no. 3, p. 243, Mar. 2019.

[137] S. Chriett, A. Dąbek, M. Wojtala, H. Vidal, A. Balcerczyk, and L. Pirola, "Prominent action of butyrate over β-hydroxybutyrate as histone deacetylase inhibitor, transcriptional modulator and anti-inflammatory molecule," Sci. Rep., vol. 9, no. 1, pp. 1–14, Dec. 2019.

[138] X. Shi et al., "-Hydroxybutyrate Activates the NF-κB Signaling Pathway to Promote the Expression of Pro-Inflammatory Factors in Calf Hepatocytes," Cell. Physiol. Biochem., vol. 33, no. 4, pp. 920–932, 2014.

[139] C.-K. Huang et al., "Adipocytes promote malignant growth of breast tumours with monocarboxylate transporter 2 expression via β-hydroxybutyrate," Nat. Commun., vol. 8, p. 14706, 2017.

[140] T. Shimazu et al., "Suppression of Oxidative Stress by -Hydroxybutyrate, an Endogenous Histone Deacetylase Inhibitor," Science (80-.)., vol. 339, no. 6116, pp. 211–214, Jan. 2013.

[141] K. Tanegashima, Y. Sato-Miyata, M. Funakoshi, Y. Nishito, T. Aigaki, and T. Hara, "Epigenetic regulation of the glucose transporter gene Slc2a1 by β-hydroxybutyrate underlies preferential glucose supply to the brain of fasted mice," Genes to Cells, vol. 22, no. 1, pp. 71–83, Jan. 2017.

[142] G. Rando et al., "Glucocorticoid receptor-PPARα axis in fetal mouse liver prepares neonates for milk lipid catabolism," Elife, vol. 5, pp. 1–31, 2016.

[143] Z. Xie et al., "Metabolic Regulation of Gene Expression by Histone Lysine β-Hydroxybutyrylation," Mol. Cell, vol. 62, no. 2, pp. 194–206, Apr. 2016.

[144] L. Chen, Z. Miao, and X. Xu, "β-hydroxybutyrate alleviates depressive behaviors in mice possibly by increasing the histone3-lysine9-β-hydroxybutyrylation," Biochem. Biophys. Res. Commun., vol. 490, no. 2, pp. 117–122, Aug. 2017.

2

Chapter 2

Transcriptional profiling of PPARα-/- and CREB3L3-/- livers reveals disparate regulation of hepato-proliferative and metabolic functions of PPARα

Ruppert PMM, Park JG, Xu X, Hur KY, Lee AH, Kersten S.

BMC Genomics. 2019;20(1):1–19.

Abstract

Peroxisome Proliferator-Activated receptor α (PPARα) and cAMP-Responsive Element Binding Protein 3-Like 3 (CREB3L3) are transcription factors involved in the regulation of lipid metabolism in the liver. The aim of the present study was to characterize the interrelationship between PPARα and CREB3L3 in regulating hepatic gene expression. Male wild-type, PPARα-/-, CREB3L3-/- and combined PPARα/CREB3L3-/- mice were subjected to a 16-hour fast or 4 days of ketogenic diet. Whole genome expression analysis was performed on liver samples. Under conditions of overnight fasting, the effects of PPARα ablation and CREB3L3 ablation on plasma triglyceride, plasma β-hydroxybutyrate, and hepatic gene expression were largely disparate, and showed only limited interdependence. Gene and pathway analysis underscored the importance of CREB3L3 in regulating (apo)lipoprotein metabolism, and of PPARα as master regulator of intracellular lipid metabolism. A small number of genes, including Fgf21 and Mfsd2a, were under dual control of PPARα and CREB3L3. By contrast, a strong interaction between PPARα and CREB3L3 ablation was observed during ketogenic diet feeding. Specifically, the pronounced effects of CREB3L3 ablation on liver damage and hepatic gene expression during ketogenic diet were almost completely abolished by the simultaneous ablation of PPARα. Loss of CREB3L3 influenced PPARα signalling in two major ways. Firstly, it reduced expression of PPARα and its target genes involved in fatty acid oxidation and ketogenesis. In stark contrast, the hepatoproliferative function of PPARα was markedly activated by loss of CREB3L3. These data indicate that CREB3L3 ablation uncouples the hepatoproliferative and lipid metabolic effects of PPARα. Overall, except for the shared regulation of a very limited number of genes, the roles of PPARα and CREB3L3 in hepatic lipid metabolism are clearly distinct and are highly dependent on dietary status.

Keywords: Liver; CREB3L3; PPARα; Fasting; Ketogenic diet; Transcriptomics

Background

The liver plays a critical role in the metabolic response to changes in the diet. An important regulatory mechanism in the control of metabolism is via changes in the expression of relevant genes. Indeed, changes in nutrient composition and nutrient availability trigger profound changes in the hepatic expression of numerous genes involved in glucose and lipid metabolism. An important transcription factor that is involved in the adaptive response to changes in nutrient supply is PPARα [1, 2]. PPARα is a member of the family of nuclear receptors and part of the subfamily of Peroxisome Proliferators Activated Receptors, which also includes PPARβ/δ and PPARγ [3]. The PPARs share a common mode of action that involves heterodimerization with the nuclear receptor RXR (Retinoid X Receptor), followed by binding of the PPAR-RXR complex to specific DNA sequences in the regulatory regions of target genes [4-6]. Activation of transcription is triggered by binding of a ligand, which include fatty acids and fatty acid derivatives such as eicosanoids and oxidized fatty acids, as well as a variety of synthetic compounds collectively referred to as peroxisome proliferators [7].

Evidence abounds indicating that PPARα is crucial for the transcriptional regulation of hepatic lipid metabolism during fasting. Indeed, studies employing expression profiling of whole body or liver-specific PPARα-/- mice have demonstrated that PPARα induces the expression of hundreds of genes involved in nearly every branch of hepatic lipid metabolism [8-12]. Hence, PPARα can be aptly described as the master regulator of hepatic lipid metabolism, especially under conditions of elevated hepatic lipid load, as occurs during fasting, high fat feeding, and a ketogenic diet. In line with this notion, the absence of PPARα during fasting leads to a host of metabolic disturbances, including a fatty liver, elevated plasma non-esterified fatty acids, hypoglycemia and hypoketonemia [8-12].

Cyclic AMP-responsive element-binding protein 3 Like 3 (CREB3L3, encoded by Creb3l3) is a bZiP transcription factor that is highly expressed in the liver [13]. CREB3L3 is produced as an ER precursor form and is proteolytically activated in the Golgi to liberate the N-terminal portion that functions as a transcriptional activator [13]. Growing evidence implicates CREB3L3 in the regulation of glucose and lipid metabolism in the liver [14]. Specifically, CREB3L3 has been shown to stimulate gluconeogenesis [15] and glycogenolysis [16], plasma triglyceride clearance [17], and lipid droplet formation [18].

Both PPARα and CREB3L3 are activated in the liver by fasting and play important roles in the utilization of fatty acids for energy in the fasted state [8-10, 19]. Several lines of evidence point to an interaction between PPARα- and CREB3L3-mediated gene regulation. First, PPARα has been shown to regulate CREB3L3 expression in human and mouse hepatocytes [20], likely via a PPRE located upstream of exon 3 [21], indicating that CREB3L3

is a direct PPARα target gene. Second, there is strong evidence that PPARα and CREB3L3 cooperate in the regulation of certain genes such as *Fgf21*, encoding Fibroblast Growth Factor 21. Specifically, PPARα and CREB3L3 physically interact to form a complex that binds to an integrated CRE-PPAR-responsive element-binding motif in the *Fgf21* gene promoter [22]. The physical interaction between PPARα and CREB3L3 is enhanced by fasting and dependent on CREB3L3 acetylation at K294 [23]. More recently, it was shown that during fasting, PPARα and CREB3L3 also cooperate in the stimulation of hepatic gluconeogenesis by targeting genes such as *Pck1*, encoding Phosphoenolpyruvate Carboxykinase 1 [16]. Other genes that are under dual control of PPARα and CREB3L3 in liver include *Cidec*, encoding Cell Death Inducing DFFA Like Effector C [18, 24]. The data presented above suggest that part of the effects of PPARα may be mediated by CREB3L3 and point towards cooperativity in gene regulation by PPARα and CREB3L3. Based on the analysis of the phenotype of single and combined PPARα-/- and CREB3L3-/- mice, it was proposed that CREB3L3 co-operates with PPARα by directly and indirectly regulating the expression of genes involved in fatty acid oxidation and ketogenesis [25].

To further characterize the cooperativity between PPARα and CREB3L3 in hepatic gene regulation, we studied the effect of PPARα and CREB3L3 ablation, either individually or combined, on overall hepatic gene regulation using whole genome expression profiling, in mice after a 16-hour fast and after 4 days of ketogenic diet.

Results

Effect of PPARα and/or CREB3L3 ablation on fasting plasma metabolites

To study the potential interaction between PPARα and CREB3L3 in metabolic regulation in the fasted state, we first performed basic metabolic measurements in wild-type, PPARα-/-, CREB3L3-/-, and combined PPARα/CREB3L3-/- mice after 16 hours of fasting. Plasma triglyceride levels were markedly elevated in the CREB3L3-/-, but not in the PPARα-/- mice (Figure 1A). The hypertriglyceridemia in CREB3L3-/- mice was improved by the simultaneous ablation of PPARα, suggesting functional antagonism between PPARα and CREB3L3 in plasma triglyceride regulation (Figure 1A). As previously shown [9], PPARα ablation significantly increased plasma non-esterified fatty acid (NEFA) levels (Figure 1B), and decreased β-hydroxybutyrate levels (Figure 1C). In agreement with our previous report [19], NEFA and β-hydroxybutyrate levels were elevated in CREB3L3-/- mice, while levels in PPARα/CREB3L3-/- mice were similar to those in PPARα-/- mice (Figure 1B and 1C), suggesting a dominant effect of PPARα ablation. Interestingly, liver triglyceride levels were

elevated in both PPARα-/- and CREB3L3-/- mice compared with wild-type mice and were highest in the combined PPARα/CREB3L3-/- mice (Figure 1D). Plasma FGF21 levels were dramatically lower in PPARα-/-, CREB3L3-/-, and PPARα/CREB3L3-/- mice as compared with wild-type mice (Figure 1E). These data indicate the pronounced impact of PPARα and CREB3L3 deficiency on metabolic regulation during fasting.

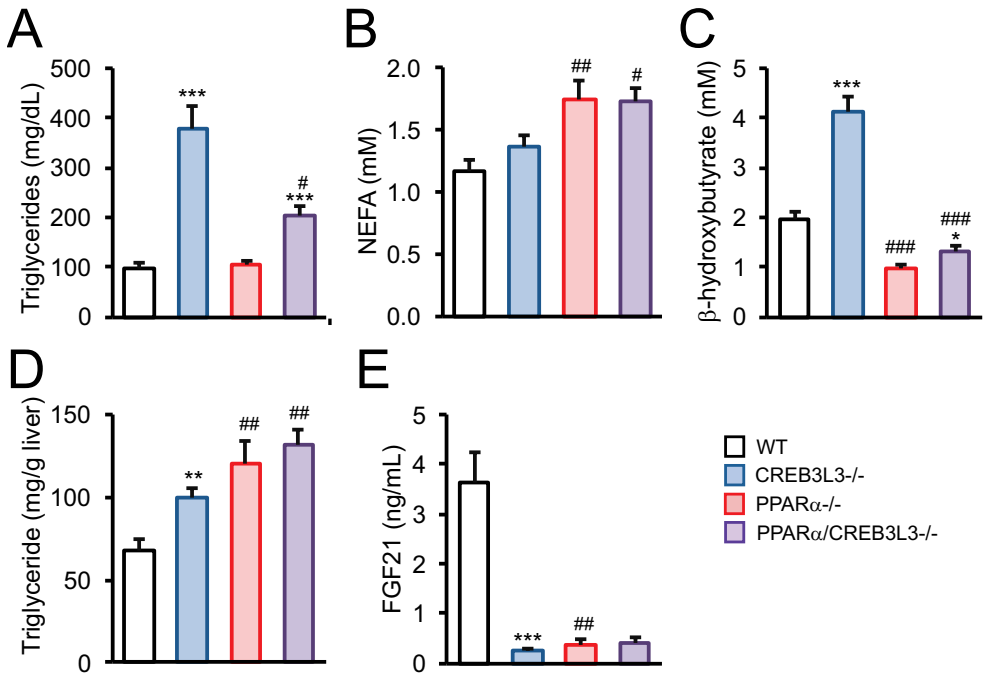

Figure 1. Effect of single and combined PPARα and CREB3L3 deficiency on metabolic parameters. PPARα-/-, CREB3L3-/- and combined PPARα/CREB3L3-/- mice were subjected to a 16-hour fast. A) Plasma triglycerides. WT, n=9; CREB3L3-/-, n=11; PPARα-/-, n=7; PPARα/CREB3L3-/-, n=6. B) Plasma non-esterified fatty acids (NEFA). WT, n=9; CREB3L3-/-, n=11; PPARα-/-, n=8; PPARα/CREB3L3-/-, n=6. C) Plasma β-hydroxybutyrate. WT, n=9; CREB3L3-/-, n=11; PPARα-/-, n=8; PPARα/CREB3L3-/-, n=6. D) Hepatic triglycerides. WT, n=7; CREB3L3-/-, n=9; PPARα-/-, n=6; PPARα/CREB3L3-/-, n=6. E) Plasma Fibroblast Growth Factor 21. WT, n=5; CREB3L3-/-, n=8; PPARα-/-, n=4; PPARα/CREB3L3-/-, n=4. Error bars represent SEM. Asterisk indicates significant effect of CREB3L3 deficiency in wild-type mice (blue vs. white bar) and in PPARα mice (purple vs red bar) according to Student's t-test (*P<0.05, **P<0.01, ***P<0.001). Pound sign indicates significant effect of PPARα deficiency in wild-type mice (red vs. white bar) and in CREB3L3 mice (purple vs. blue bar) according to Student's t-test (#P<0.05, ##P<0.01, ###P<0.001).

Effects of PPARα and CREB3L3 ablation on hepatic gene expression in the fasted state are largely independent

To study the potential interaction between PPARα and CREB3L3 in hepatic gene regulation in the fasted state, whole genome expression analysis was performed on liver samples of the four groups of mice after 16 hours of fasting. To study the magnitude of the effect of PPARα and CREB3L3 ablation on liver gene expression, we performed Volcano plot analysis. Interestingly, the effects of PPARα ablation were much more pronounced as compared to CREB3L3 ablation (Figure 2A). The combined ablation of PPARα and CREB3L3 had the most significant effect on gene regulation, pointing to a potential additive or synergistic effect of PPARα and CREB3L3 ablation on hepatic gene expression. Analysis of the number of significantly changed genes showed that in the fasted state, loss of PPARα altered the expression of 1097 genes, of which 553 genes were upregulated and 544 genes were downregulated (Figure 2B). Loss of CREB3L3 altered expression of 312 genes, of which 134 genes were upregulated and 178 genes were downregulated. Combined loss of PPARα and CREB3L3 altered the expression of 1917 genes, of which 1064 genes were upregulated and 853 genes were downregulated (Figure 2B). The fact that the number of significantly changed genes in the combined PPARα/CREB3L3-/- mice slightly exceeds the sum of significantly changed genes in the PPARα-/- and CREB3L3-/- mice suggests a modest synergistic effect of PPARα and CREB3L3 deficiency on hepatic gene regulation, dominated by PPARα.

To study the potential similarity between the effect of PPARα and CREB3L3 deficiency on liver gene expression, we performed principle component analysis (Figure 2C) and hierarchical clustering (Figure 2D). Both analyses indicated the separate clustering of the four experimental groups, with limited variation between the individual mice in each group, and the more pronounced effect of PPARα deficiency compared to CREB3L3 deficiency. In addition, both analyses showed that the whole genome effects of combined PPARα/CREB3L3 deficiency are largely taken up by PPARα deficiency (Figure 2C, D).

Hierarchical biclustering of samples and genes visualized in a heatmap further supported the conclusions reached above, showing the much more pronounced effect of PPARα deficiency on hepatic gene expression and the more significant contribution of PPARα towards the effect of combined PPARα/CREB3L3 deficiency (Figure 2E). The heat map also shows that for certain genes, the effects of PPARα and CREB3L3 deficiency are additive and seemingly independent, whereas for other genes the effect of PPARα and CREB3L3 deficiency appears to be synergistic and thus dependent.

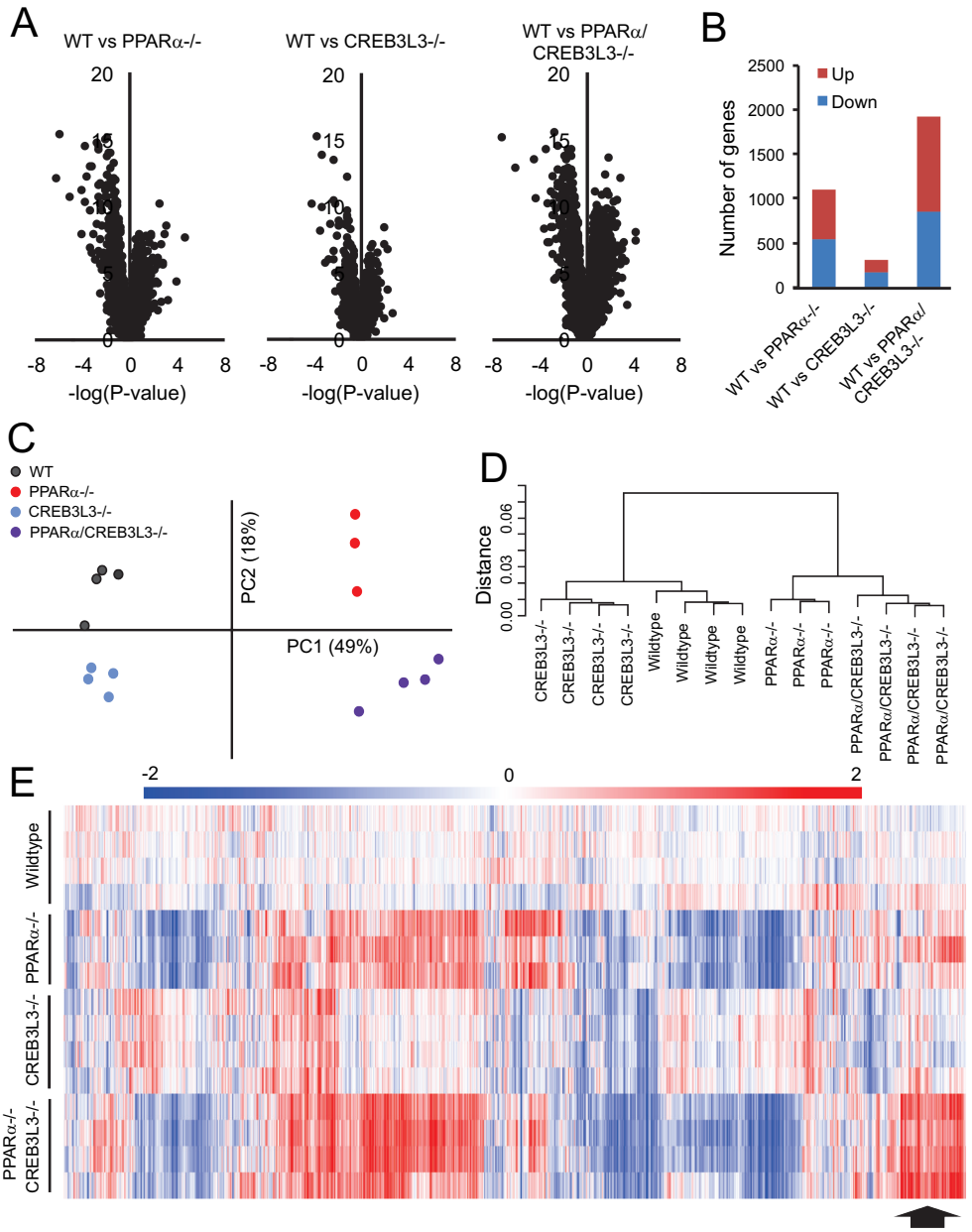

Figure 2. Largely independent effect of PPARα and CREB3L3 deficiency on hepatic gene expression in the fasted state. A) Volcano plot showing the relation between mean signal log ratio (2log[fold-change], x-axis) and the -10log of the IBMT P-value (y-axis) for the comparison between wild-type mice and PPARα-/- mice, CREB3L3-/- mice and combined PPARα/CREB3L3-/- mice after a 16-hour fast. B) Number of genes meeting significance criteria (fold change < -1.2 or > 1.2 and IBMT P<0.001) for the comparison between wild-type mice and PPARα-/- mice, CREB3L3-/- mice and combined PPARα/CREB3L3-/- mice after a 16-hour fast. Principle component analysis (C) and hierarchical clustering (D) of transcriptomics data from livers of wild-type, PPARα-/-, CREB3L3-/-, and combined

PPARα/CREB3L3-/- mice after a 16-hour fast. Distance criteria are based on Pearson correlation with average linkage. An IQR (Inter Quartile Range) filter of 0.5 was applied. E) Hierarchical biclustering of samples and genes visualized in a heatmap. Data were centered on wild-type mean. Clustering was done based on Pearson correlation with average linkage. Red indicates upregulated, blue indicates downregulated. The region in the heatmap that is suggestive of synergistic regulation by PPARα and CREB3L3 deficiency is indicated by a grey arrow.

A limited number of genes is commonly downregulated by PPARα and CREB3L3 deficiency in liver during fasting

The Venn diagram of significantly downregulated genes (Figure 3A) and scatter plot analysis (Figure 3B) confirmed that, in general, the effects of PPARα and CREB3L3 deficiency are disparate, with only a limited number of genes showing similar regulation in PPARα-/- and CREB3L3-/- mice. The list of 34 genes that were significantly downregulated in livers of PPARα-/-, CREB3L3-/-, and PPARα/CREB3L3-/- mice is presented in Supplemental Table 1. This list includes *Fgf21*, which is known to be under dual control of PPARα and CREB3L3, and *Mfsd2a*, a gene involved in lysophospholipid transport that is known to be under control of PPARα but not CREB3L3 [33, 34]. To examine whether any of these 34 genes may be directly regulated by PPARα, we determined the effect of the PPARα agonist Wy-14,643 on gene expression in the liver (Figure 3C). To examine whether any of these 34 genes may be directly regulated by CREB3L3, we determined the effect of adenoviral-mediated CREB3L3 overexpression on gene expression in the liver (Figure 3C). The results suggest that several of the 34 genes may be direct targets of both PPARα and CREB3L3, as they are markedly upregulated by PPARα and CREB3L3 activation. These genes include *Fgf21*, *Mfsd2a, Xrcc3*, *Suclg1*, *Tmem184a* and *Sel1l3*.

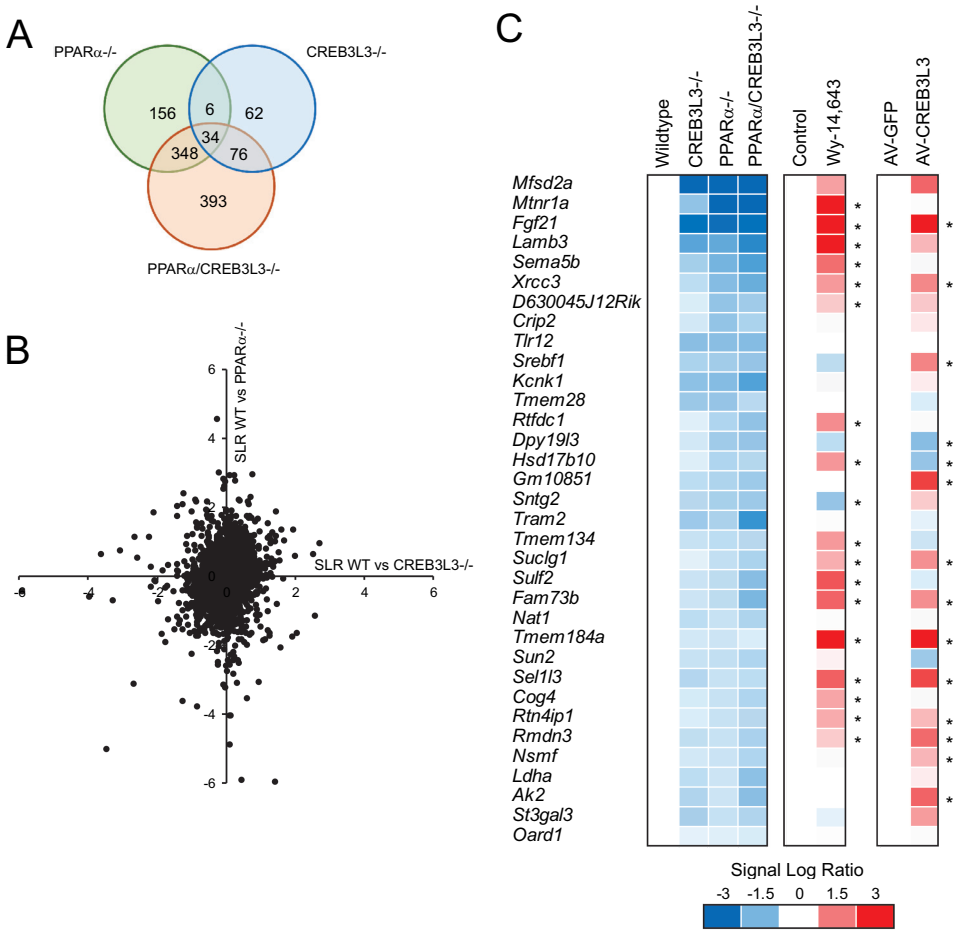

Figure 3. Limited overlap in effects of PPARα and CREB3L3 deficiency on hepatic gene expression in the fasted state. A) Venn diagram showing overlap in downregulated genes in PPARα-/-, CREB3L3-/-, and combined PPARα/CREB3L3-/- mice, in comparison with wild-type mice (IBMT P-value<0.001). B) Correlation plot showing gene expression changes in CREB3L3-/- mice in relation to wild-type mice (x-axis) and in PPARα-/- mice in relation to wild-type mice (y-axis) (expressed as signal log ratio, SLR). C) Comparative gene expression analysis in liver of wild-type, PPARα-/-, CREB3L3-/-, and combined PPARα/CREB3L3-/- mice after 16-hour fast. For comparison, gene expression changes in mouse liver after PPARα activation by 5-day treatment with the agonist Wy-14,643 are shown (GSE8316) [51], as well as gene expression changes in mouse liver after adenoviral-mediated over expression of CREB3L3. Asterisk indicates significantly different from control conditions according to IBMT P-value<0.001. The 34 genes shown are the commonly downregulated genes in livers of PPARα-/-, CREB3L3-/-, and PPARα/CREB3L3-/- mice in the fasted state (IBMT P-value<0.001).

To further explore the differential impact of PPARα and CREB3L3 deficiency on hepatic gene expression, the top 40 most significantly downregulated genes in each condition (PPARα-/-, CREB3L3-/-, and PPARα/CREB3L3-/-) were taken and visualized in a heatmap (Figure 4). The top 40 list of most significantly downregulated genes in the CREB3L3-/- mice contains the known CREB3L3 targets *Cidec*, *Apoa4*, and *Fgf21*. A relatively large portion of the genes downregulated in the CREB3L3-/- mice were also downregulated in the PPARα-/- mice and, especially, in the combined PPARα/CREB3L3-/- mice. For PPARα, only a very small portion of the genes downregulated in the PPARα-/- mice were also downregulated in the CREB3L3-/- mice, the exception being *Fgf21*, *Mfsd2a*, and *Mtnr1a*. Other typical PPARα target genes such as *Retsat*, *Cy4a14*, *Plin5*, *Fabp1*, *Acaa1b* and *Ehhadh* were exclusively downregulated in the PPARα-/- mice. For nearly all genes shown, the downregulation in the PPARα-/- mice was copied in the combined PPARα/CREB3L3-/- mice. The top 40 list of most significantly downregulated genes in the PPARα/CREB3L3-/- mice represents a combination of genes mainly controlled by PPARα (*Vnn1*, *Cyp4a14*, *Krt23*, *Slc27a1*), by CREB3L3 (*Cidec*, *Fabp2*), or both (*Fgf21*, *Mfsd2a*, *Mtnr1a*) (Figure 4).

A limited number of genes has been identified as direct or putative target of CREB3L3. The expression levels of these genes are illustrated in figure 5, showing that CREB3L3 deficiency leads to significant downregulation of genes involved in lipoprotein metabolism (*Apoc2, Apoa5, Apoa1, Scarb1*), lipid storage (*Cidec*), fatty acid binding (*Fabp2*), fatty acid desaturation and elongation (*Fads1, Fads2, Elovl2, Elovl5*), gluconeogenesis (*Pck1, G6pc*), and fatty acid oxidation (*Cpt1a*). Most of these genes were not or minimally affected by PPARα deficiency. Together, these data indicate that in the fasted state CREB3L3 and PPARα regulate different sets of genes, with some notable exceptions, suggesting that the transcription factors largely operate independently.

Figure 4. PPARα and CREB3L3 mostly regulate distinct genes in liver in the fasted state. Comparative gene expression analysis in liver of wild-type, PPARα-/-, CREB3L3-/-, and combined PPARα/CREB3L3-/- mice after a 16-hour fast, showing the top 50 most highly downregulated genes in CREB3L3-/- mice (left panel), PPARα-/- mice (middle panel), and combined PPARα/CREB3L3-/- (right panel) in the form a heatmap, using the mean expression of each group. Red indicates upregulated, blue indicates downregulated.

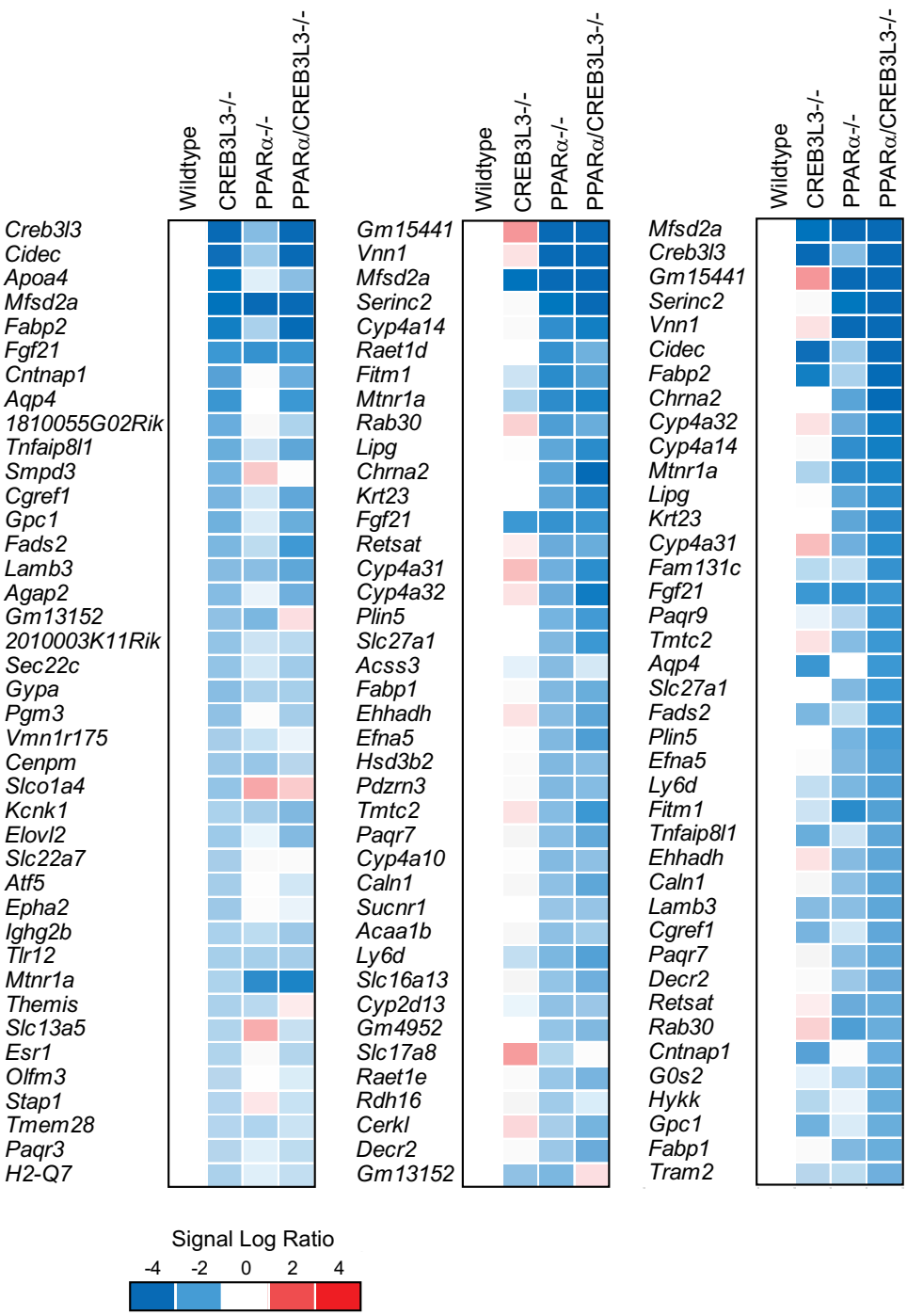
Wildtype
CREB3L3-/-
PPARα-/-
PPARα/CREB3L3-/-
Creb3l3
Cidec
Apoa4
Mfsd2a
Fabp2
Fgf21
Cntnap1
Aqp4
1810055G02Rik
Tnfaip8l1
Smpd3
Cgref1
Gpc1
Fads2
Lamb3
Agap2
Gm13152
2010003K11Rik
Sec22c
Gypa
Pgm3
Vmn1r175
Cenpm
Slco1a4
Kcnk1
Elovl2
Slc22a7
Atf5
Epha2
Ighg2b
Tlr12
Mtnr1a
Themis
Slc13a5
Esr1
Olfm3
Stap1
Tmem28
Paqr3
H2-Q7
Gm15441
Vnn1
Mfsd2a
Serinc2
Cyp4a14
Raet1d
Fitm1
Mtnr1a
Rab30
Lipg
Chrna2
Krt23
Fgf21
Retsat
Cyp4a31
Cyp4a32
Plin5
Slc27a1
Acss3
Fabp1
Ehhadh
Efna5
Hsd3b2
Pdzrn3
Tmtc2
Paqr7
Cyp4a10
Caln1
Sucnr1
Acaa1b
Ly6d
Slc16a13
Cyp2d13
Gm4952
Slc17a8
Raet1e
Rdh16
Cerkl
Decr2
Gm13152
Mfsd2a
Creb3l3
Gm15441
Serinc2
Vnn1
Cidec
Fabp2
Chrna2
Cyp4a32
Cyp4a14
Mtnr1a
Lipg
Krt23
Cyp4a31
Fam131c
Fgf21
Paqr9
Tmtc2
Aqp4
Slc27a1
Fads2
Plin5
Efna5
Ly6d
Fitm1
Tnfaip8l1
Ehhadh
Caln1
Lamb3
Cgref1
Paqr7
Decr2
Retsat
Rab30
Cntnap1
G0s2
Hykk
Gpc1
Fabp1
Tram2
Signal Log Ratio
-4
-2
0
2
4

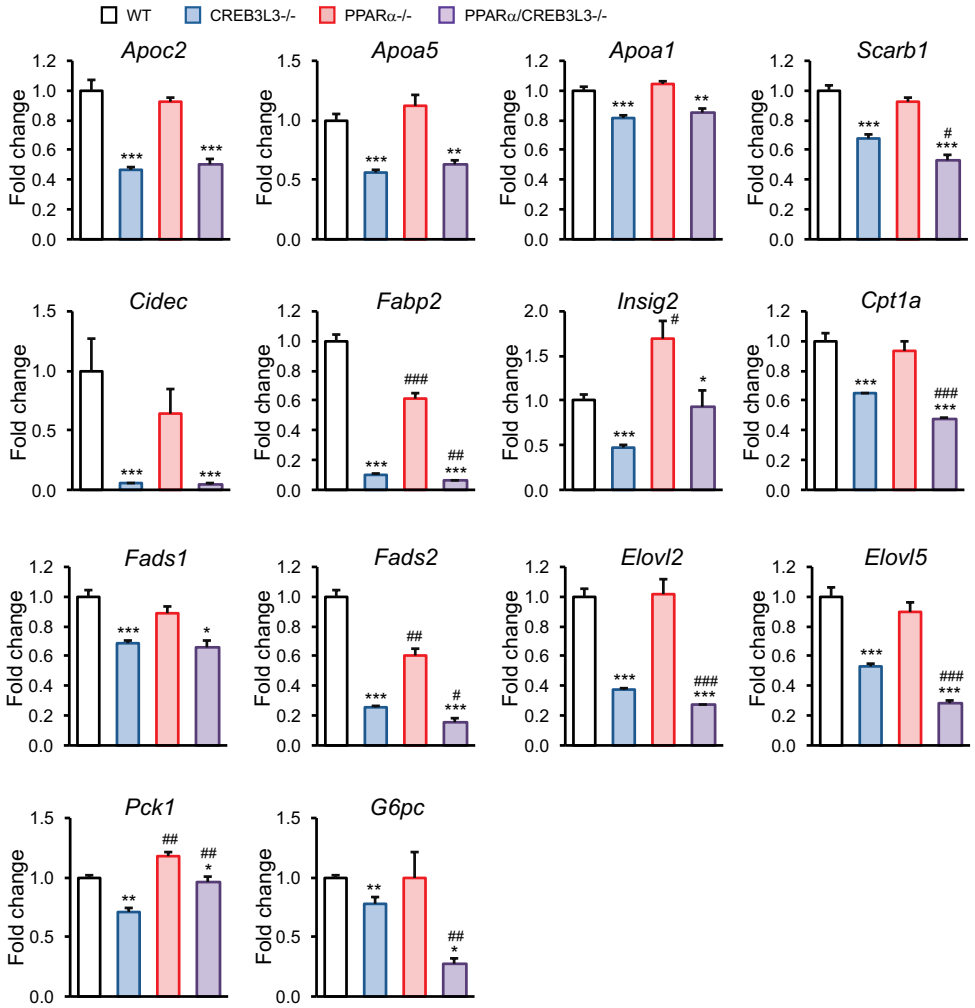

Figure 5. Microarray gene expression of selected genes previously shown to be under control of CREB3L3. All are significantly downregulated in liver of fasted CREB3L3-/- mice as compared to fasted wild-type mice (IBMT P-value<0.001). Asterisk indicates significant effect of CREB3L3 deficiency in wild-type mice (blue vs. white bar) and in PPARα mice (purple vs red bar) according to Student's t-test (*P<0.05, **P<0.01, ***P<0.001). Pound sign indicates significant effect of PPARα deficiency in wild-type mice (red vs. white bar) and in CREB3L3 mice (purple vs. blue bar) according to Student's t-test (#P<0.05, ##P<0.01, ###P<0.001).

CREB3L3 deficiency leads to downregulation of genesets related to lipoprotein and lipid transport

To gain more insight into the functional differences between PPARα and CREB3L3 deficiency, we compared the effects of PPARα and CREB3L3 deficiency at the level of pathways using geneset enrichment analysis (Figure 6A). Deficiency of PPARα led to the downregulation of numerous genesets that are known to be controlled by PPARα, mainly representing genesets related to peroxisomal and mitochondrial fatty acid catabolism and the electron transport chain. By contrast, deficiency of CREB3L3 led to the downregulation of genesets related to lipoprotein and lipid transport, as well as several genesets connected to immunity (Figure 6B). At the pathway level, minimal overlap was observed between the effect of PPARα and CREB3L3 deficiency (Figure 6C). In fact, out of 98 genesets that were significantly downregulated in PPARα-/- mice, only one geneset, named branched chain amino acid catabolism, was also downregulated in the CREB3L3-/- mice (Figure 6C). The commonly enriched genes within the geneset branched chain amino acid catabolism included *Auh*, *Hibch*, *Hibadh*, *Acad8*, *Ivd*, and *Hsd17B10*.

Consistent with the notion that the effects of combined PPARα/CREB3L3 deficiency are largely taken up by PPARα deficiency, the far majority of genesets downregulated in the combined PPARα/CREB3L3-/- mice were also downregulated in the PPARα-/- mice (Figure 6D). Indeed, the enrichment scores of the most highly downregulated genesets in the combined PPARα/CREB3L3-/- mice were very similar in the single PPARα-/- mice, suggesting that the functional impact of combined PPARα/CREB3L3-/- deficiency is mostly accounted for by deficiency of PPARα. The exception were two genesets related to lipoprotein and lipid transport, which had similar enrichment scores in the combined PPARα/CREB3L3-/- mice and single CREB3L3-/- mice (Figure 6D), suggesting that the regulation of these two genesets is driven by CREB3L3 deficiency.

Deficiency of PPARα led to the upregulation of genesets related to the unfolded protein response and inflammatory signalling (Supplemental Figure 1A). By contrast, deficiency of CREB3L3 led to upregulation of genesets related to cholesterol synthesis and protein translation (Supplemental Figure 1B). Consistent with this result, genes involved in cholesterol metabolism feature prominently among the top 40 most highly upregulated genes in CREB3L3-/- mice (Supplemental Figure 1C).

Overall, the above analyses indicate that the effects of PPARα and CREB3L3 deficiency on hepatic gene expression during fasting are very distinct. Only a limited number of genes is under regulation of both PPARα and CREB3L3. The PPARα/CREB3L3-/- mice reflect the combined effect of especially PPARα and to a lesser extent CREB3L3 deficiency, showing a minor degree of synergism.

Effect of PPARα and/or CREB3L3 deficiency on plasma metabolites during ketogenic diet

To further explore the cooperativity between PPARα and CREB3L3 in hepatic gene regulation, we compared the effect of PPARα and CREB3L3 deficiency under the condition of a ketogenic diet. Previously, this diet was shown to provoke a pronounced hepatic phenotype in CREB3L3-/- mice, characterized by hepatomegaly and signs of steatohepatitis [19, 25]. No difference in bodyweight between the four genotypes was observed before the start of the study (Figure 7A). Four days of ketogenic diet induced pronounced weight loss in all groups, which was most pronounced in the PPARα-/- mice and combined PPARα/CREB3L3-/- mice (Figure 7B). Interestingly, compared to the wild-type mice, the liver to body weight ratio was modestly increased in the PPARα-/- mice and combined PPARα/CREB3L3-/- mice, yet was highest in the CREB3L3-/- mice, suggesting hepatomegaly (Figure 7C) [19, 25]. Compared to the other three groups, CREB3L3-/- mice fed a ketogenic diet for 4 days also exhibited markedly elevated plasma alanine aminotransferase (ALT) activity (Figure 7D), suggesting liver damage. Plasma ALT levels were below 30 IU/L in all groups before starting the ketogenic diet (not shown). Elevated plasma ALT was accompanied by elevated liver and plasma triglycerides in CREB3L3-/- mice (Figure 7E,F). These parameters were also increased in the PPARα-/- mice. Plasma FGF21 levels followed a very different pattern and were about 50% decreased in the CREB3L3-/- mice, more than 90% decreased in the PPARα-/- mice, and nearly 99% decreased in the PPARα/CREB3L3-/- mice (Figure 7G). Overall, these data are in line with a previous report [25].

To study the magnitude of the effect of PPARα and CREB3L3 deficiency during ketogenic diet on liver gene expression, we performed Volcano plot analysis (Figure 8A). In contrast to what was observed in the fasted state, the effects of CREB3L3 deficiency during ketogenic diet were more pronounced as compared to PPARα deficiency. Strikingly, the effect of combined deficiency of PPARα and CREB3L3 on hepatic gene expression was less pronounced as compared to deficiency of only CREB3L3. Analysis of the number of significantly changed genes showed that loss of CREB3L3 altered the expression of 5878 genes, of which 3490 genes were upregulated and 2388 genes were downregulated (Figure 8B). Loss of PPARα altered expression of 2843 genes, of which 1616 genes were upregulated and 1227 genes were downregulated. Combined loss of PPARα and CREB3L3 altered the expression of 3707 genes, of which 1996 genes were upregulated and 1711 genes were downregulated. These observations indicate that deficiency of PPARα mitigates the effect of CREB3L3 deficiency on hepatic gene expression.

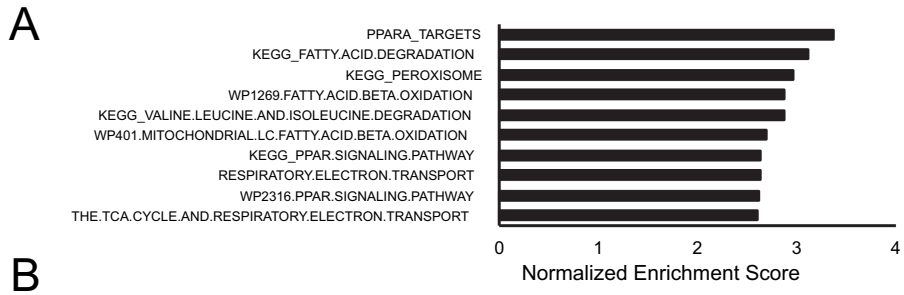
A
PPARA_TARGETS
KEGG_FATTY.ACID.DEGRADATION
KEGG_PEROXISOME
WP1269.FATTY.ACID.BETA.OXIDATION
KEGG_VALINE.LEUCINE.AND.ISOLEUCINE.DEGRADATION
WP401.MITOCHONDRIAL.LC.FATTY.ACID.BETA.OXIDATION
KEGG_PPAR.SIGNALING.PATHWAY
RESPIRATORY.ELECTRON.TRANSPORT
WP2316.PPAR.SIGNALING.PATHWAY
THE.TCA.CYCLE.AND.RESPIRATORY.ELECTRON.TRANSPORT
0 1 2 3 4
Normalized Enrichment Score

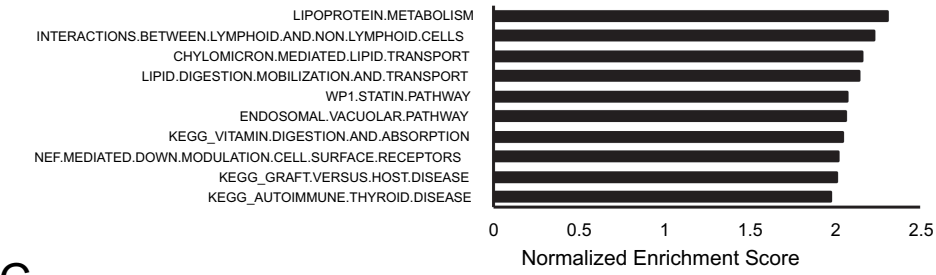
B
LIPOPROTEIN.METABOLISM
INTERACTIONS.BETWEEN.LYMPHOID.AND.NON.LYMPHOID.CELLS
CHYLOMICRON.MEDIATED.LIPID.TRANSPORT
LIPID.DIGESTION.MOBILIZATION.AND.TRANSPORT
WP1.STATIN.PATHWAY
ENDOSOMAL.VACUOLAR.PATHWAY
KEGG_VITAMIN.DIGESTION.AND.ABSORPTION
NEF.MEDIATED.DOWN.MODULATION.CELL.SURFACE.RECEPTORS
KEGG_GRAFT.VERSUS.HOST.DISEASE
KEGG_AUTOIMMUNE.THYROID.DISEASE
0 0.5 1 1.5 2 2.5
Normalized Enrichment Score

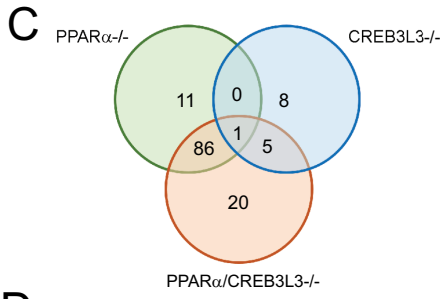
C
PPARα-/-
CREB3L3-/-
11
0
8
1
86
5
20
PPARα/CREB3L3-/-

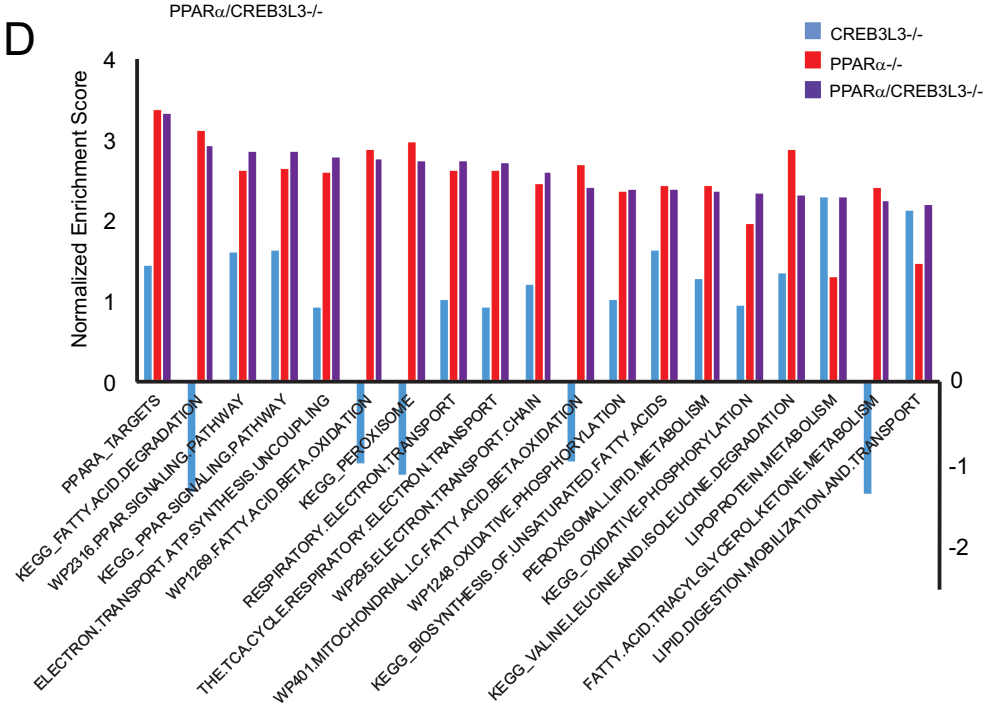
D
CREB3L3-/-
PPARα-/-
PPARα/CREB3L3-/-
Normalized Enrichment Score
4
3
2
1
0
0
-1
-2
PPARA_TARGETS
KEGG_FATTY.ACID.DEGRADATION
WP2316.PPAR.SIGNALING.PATHWAY
KEGG_PPAR.SIGNALING.PATHWAY
ELECTRON.TRANSPORT.ATP.SYNTHESIS.UNCOUPLING
WP1269.FATTY.ACID.BETA.OXIDATION
KEGG_PEROXISOME
RESPIRATORY.ELECTRON.TRANSPORT
THE.TCA.CYCLE.RESPIRATORY.ELECTRON.TRANSPORT.CHAIN
WP401.MITOCHONDRIAL.LC.FATTY.ACID.BETA.OXIDATION
KEGG_BIOSYNTHESIS.OF.UNSATURATED.FATTY.ACIDS
WP1248.OXIDATIVE.PHOSPHORYLATION
WP295.ELECTRON.TRANSPORT.CHAIN
PEROXISOMAL.LIPID.METABOLISM
KEGG_OXIDATIVE.PHOSPHORYLATION
KEGG_VALINE.LEUCINE.AND.ISOLEUCINE.DEGRADATION
LIPOPROTEIN.METABOLISM
FATTY.ACID.TRIACYLGLYCEROL.KETONE.METABOLISM
LIPID.DIGESTION.MOBILIZATION.AND.TRANSPORT

Figure 6. PPARα and CREB3L3 regulate distinct pathways in the liver in the fasted state. A) Top 10 downregulated genesets in liver of PPARα-/- compared with wild-type mice, determined by gene set enrichment analysis. B) Top 10 downregulated genesets in liver of CREB3L3-/- compared with wild-type mice, determined by gene set enrichment analysis. Genesets were ranked according to normalized enrichment score (NES). C) Venn diagram showing overlap in downregulated genesets (FDR q-value<0.1) in PPARα-/-, CREB3L3-/-, and combined PPARα/CREB3L3-/- mice, in comparison with wild-type mice. D) Top 20 downregulated gene sets in liver of combined PPARα/CREB3L3-/- mice compared with wild-type mice, determined by gene set enrichment analysis and ranked according to NES (purple). The NES of the same genesets for the comparison between wild-type and PPARα-/- (red) or CREB3L3-/- (blue) mice is shown as well.

Effects of CREB3L3 deficiency on hepatic gene expression during ketogenic diet are dependent on PPARα

To study the similarity between the three different genetic models in liver gene expression, we performed principle component analysis (Figure 8C) and hierarchical clustering (Figure 8D). Principle component analysis and hierarchical clustering of samples showed that the CREB3L3-/- mice formed a distinct cluster, underscoring the profound effect of CREB3L3 deficiency on hepatic gene expression during ketogenic diet. Surprisingly, the PPARα-/- mice and combined PPARα/CREB3L3-/- mice clustered together and were very distinct from the CREB3L3-/- mice. Hierarchical biclustering of samples and genes visualized in a heatmap further confirmed that at the level of hepatic gene expression, the PPARα-/- mice and combined PPARα/CREB3L3-/- mice were nearly indistinguishable, whereas the CREB3L3-/- mice showed a very different gene expression profile (Figure 8E). These data thus show that deficiency of CREB3L3 has no effect on hepatic gene expression in the absence of PPARα, indicating that the major liver phenotype triggered by CREB3L3 deficiency during ketogenic diet is dependent on PPARα.

Scatter plot analysis confirmed that the effects of PPARα and CREB3L3 deficiency on hepatic gene expression are very dissimilar, whereas the effect of PPARα deficiency and combined PPARα/CREB3L3 deficiency are similar (Supplemental Figure 2A). Venn diagram of significantly changed genes confirmed that deficiency of CREB3L3 leads to the up- and downregulation of a large set of genes that are not affected in the PPARα-/- or PPARα/CREB3L3-/- mice (Supplemental Figure 2B).

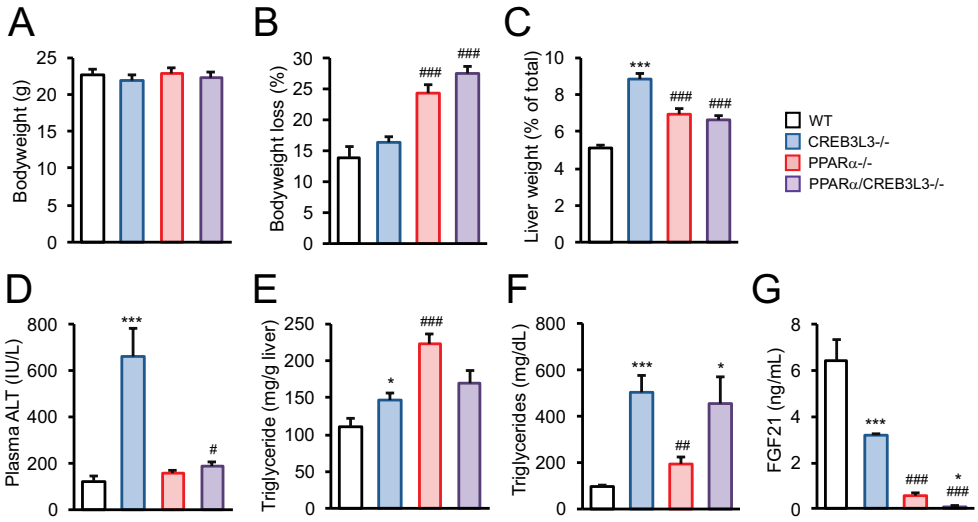

Figure 7. Effect of single and combined PPARα and CREB3L3 deficiency on metabolic parameters. PPARα-/-, CREB3L3-/- and combined PPARα/CREB3L3-/- mice were subjected to a 4 day ketogenic diet. A) Bodyweight before the ketogenic diet. WT, n=15; CREB3L3-/-, n=12; PPARα-/-, n=9; PPARα/CREB3L3-/-, n=10. B) Percentage bodyweight loss caused by the ketogenic diet. WT, n=15; CREB3L3-/-, n=12; PPARα-/-, n=10; PPARα/CREB3L3-/-, n=10. C) Liver weight as percentage of total bodyweight. WT, n=15; CREB3L3-/-, n=12; PPARα-/-, n=9; PPARα/CREB3L3-/-, n=10. D) Plasma alanine aminotransferase activity. WT, n=15; CREB3L3-/-, n=12; PPARα-/-, n=5; PPARα/CREB3L3-/-, n=6. E) Hepatic triglycerides. WT, n=10; CREB3L3-/-, n=7; PPARα-/-, n=5; PPARα/CREB3L3-/-, n=6. F) Plasma triglycerides. WT, n=10; CREB3L3-/-, n=7; PPARα-/-, n=5; PPARα/CREB3L3-/-, n=5. G) Plasma Fibroblast Growth Factor 21. WT, n=9; CREB3L3-/-, n=7; PPARα-/-, n=9; PPARα/CREB3L3-/-, n=5. Error bars represent SEM. Asterisk indicates significant effect of CREB3L3 deficiency in wild-type mice (blue vs. white bar) and in PPARα mice (purple vs red bar) according to Student's t-test (*P<0.05, **P<0.01, ***P<0.001). Pound sign indicates significant effect of PPARα deficiency in wild-type mice (red vs. white bar) and in CREB3L3 mice (purple vs. blue bar) according to Student's t-test (#P<0.05, ##P<0.01, ###P<0.001).

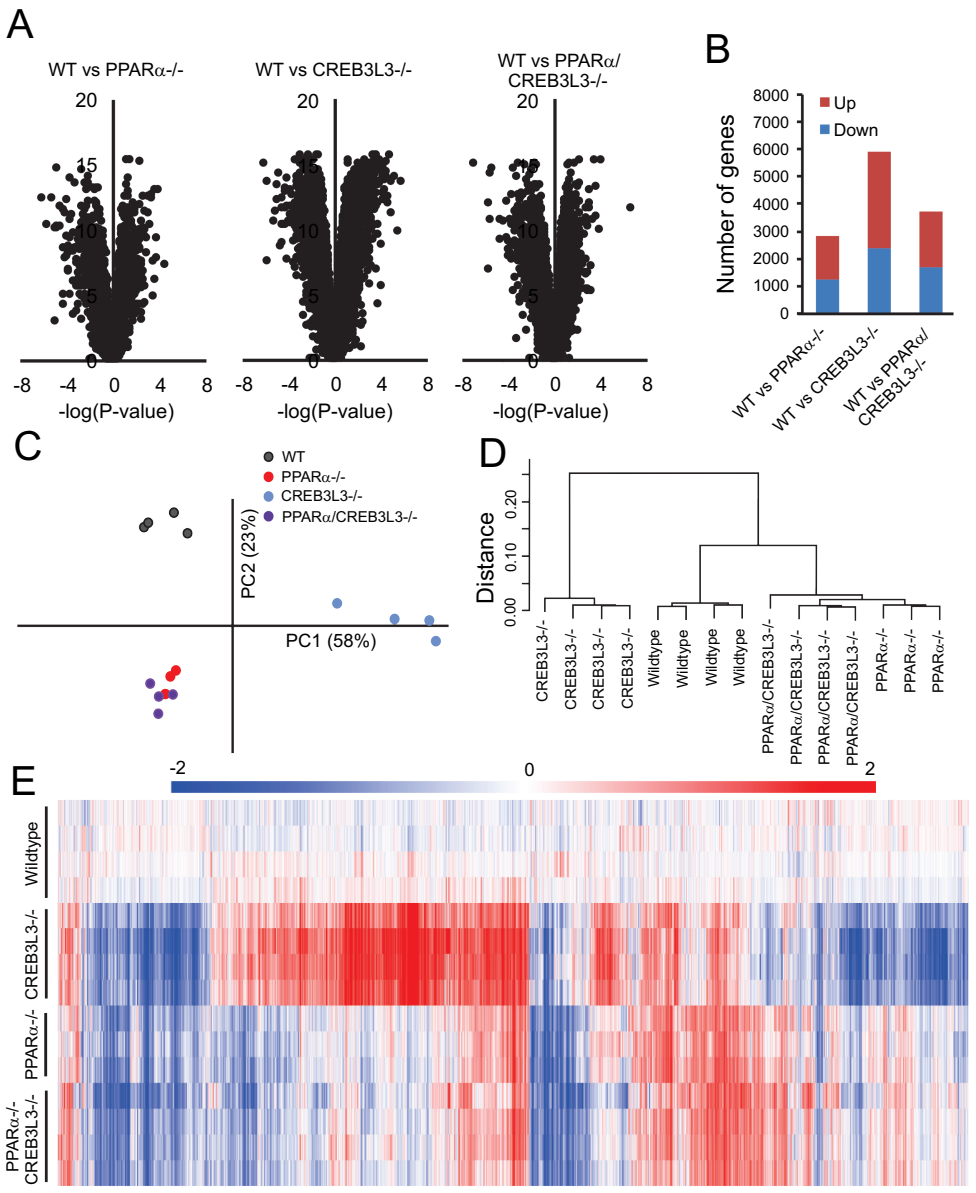

Figure 8. PPARα deficiency mitigates effect of CREB3L3 deficiency on hepatic gene expression during ketogenic diet. A) Volcano plot showing the relation between signal log ratio (^{2}log[fold-change], x-axis) and the -^{10}log of the IBMT P-value (y-axis) for the comparison between wild-type mice and PPARα-/- mice, CREB3L3-/- mice and combined PPARα/CREB3L3-/- mice after 4 days of ketogenic diet. B) Number of genes meeting significance criteria (fold change<-1.2 or >1.2 and IBMT P<0.001) for the comparison between wild-type mice and PPARα-/- mice, CREB3L3-/- mice and combined PPARα/CREB3L3-/- mice after 4 days of ketogenic diet. Principle component analysis (C) and hierarchical clustering (D) of transcriptomics data from liver of wild-type, PPARα-/-, CREB3L3-/-, and combined PPARα/CREB3L3-/- mice after a 4 day ketogenic diet. E) Hierarchical biclustering of samples and genes visualized in a heatmap. An IQR (Inter Quartile Range) filter of 0.5 was applied. Red indicates upregulated, blue indicates downregulated.

Induction of mitogenic genes in CREB3L3-/- mice during ketogenic diet is mediated by PPARα

To obtain more insight into the functional pathways affected by CREB3L3 deficiency on ketogenic diet, we performed gene set enrichment analysis. Surprisingly, many of the most highly downregulated genesets represented pathways of fatty acid and/or amino acid metabolism, including peroxisome, PPARα targets, and fatty acid degradation (Figure 9A). Enrichment scores for these latter genesets were similar in the PPARα-/- and PPARα/CREB3L3-/- mice (Figure 9A). A heatmap of the geneset PPARα targets shows the consistent downregulation of PPARα target genes across the 3 groups of mice (Figure 9B). These data suggest that CREB3L3 deficiency, as well as PPARα deficiency and combined PPARα/CREB3L3 deficiency, leads to reduced PPARα activity. In line with these data, the PPARα mRNA expression level was markedly reduced in the CREB3L3-/- mice (Figure 9C).

Gene set enrichment analysis also underscored the dramatic effect of CREB3L3 deficiency on hepatic gene expression. Indeed, 538 genesets met the statistical significance cut-off of FDR q-value<0.05, covering numerous biological processes, including immunity, cellular stress pathways, and DNA/RNA-related processes (not shown). Intriguingly, the 20 most upregulated genesets were all related to cell cycle/mitosis (Figure 10A). Enrichment scores for these genesets were much lower in the PPARα-/- and PPARα/CREB3L3-/- mice, indicating the selective induction of cell cycle/mitosis-related genes in the CREB3L3-/- mice (Figure 10A). A heatmap of the most enriched genes within the geneset Cell.Cycle.Mitotic demonstrates the pronounced upregulation of cell cycle genes in the CREB3L3-/- mice (Figure 10B). Strikingly, the upregulation is completely abolished upon additional deficiency of PPARα, suggesting that PPARα mediates the induction of cell cycle genes in CREB3L3-/- mice on ketogenic diet (Figure 10B). Consistent with the upregulation of cell cycle upon CREB3L3 deficiency, many of the most highly induced genes in the CREB3L3-/- mice on ketogenic diet were related to cell cycle (Figure 10C). Again, the upregulation of these genes was almost completely abolished in the PPARα-/- mice.

In line with the known mitogenic effect of PPARα activation on hepatocyte proliferation, pharmacological activation of PPARα *in vivo* has been shown to cause the induction of numerous genes and proteins involved in cell cycle control [35], which is specifically mediated by mouse PPARα and not human PPARα [36]. Previously, we found that treating mice with the specific PPARα agonist Wy-14,643 markedly induced numerous genesets related to cell cycle [2]. A heatmap of the most highly enriched genes in the geneset Mitotic.M.M.G1 phase underscores the marked induction of cell cycle-related genes by Wy-14,643, which is entirely PPARα dependent (Figure 10D). Strikingly, most of these genes are also highly upregulated in the CREB3L3-/- mice on ketogenic diet, which again is entirely PPARα dependent (Figure 10D), indicating that the pronounced upregulation of the cell

cycle in CREB3L3-/- mice is mediated by PPARα. Taken together, these data indicate that CREB3L3 deficiency uncouples the hepatoproliferative and lipid metabolic effects of PPARα.

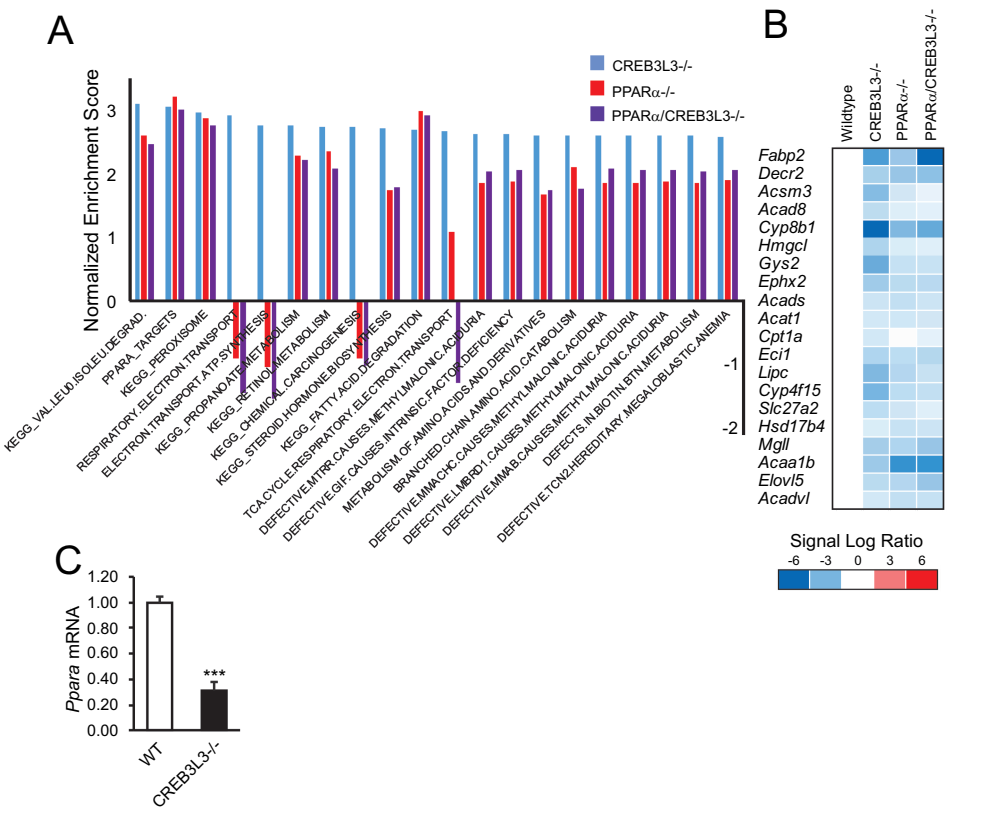

Figure 9. CREB3L3 deficiency during ketogenic diet leads to downregulation of PPARα targets. A) Top 20 downregulated genesets in liver of CREB3L3-/- mice compared with wild-type mice, determined by gene set enrichment analysis and ranked according to normalized enrichment score (NES)(blue). The NES of the same genesets for the comparison between wild-type and PPARα-/- (red) or combined PPARα/CREB3L3-/- (purple) mice is shown as well. B) Comparative gene expression analysis in liver of wild-type, PPARα-/-, CREB3L3-/-, and combined PPARα/CREB3L3-/- mice after a 4-day ketogenic diet. The genes shown are the 20 most highly enriched genes in CREB3L3-/- mice vs. wild-type mice that are part of the geneset PPARA targets. Red indicates upregulated, blue indicates downregulated. C) Mean PPARα mRNA expression level in liver of wild-type and CREB3L3-/- mice after a 4-day ketogenic diet. Asterisk indicates significantly different from wild-type mice according to Student's t-test (P<0.001).

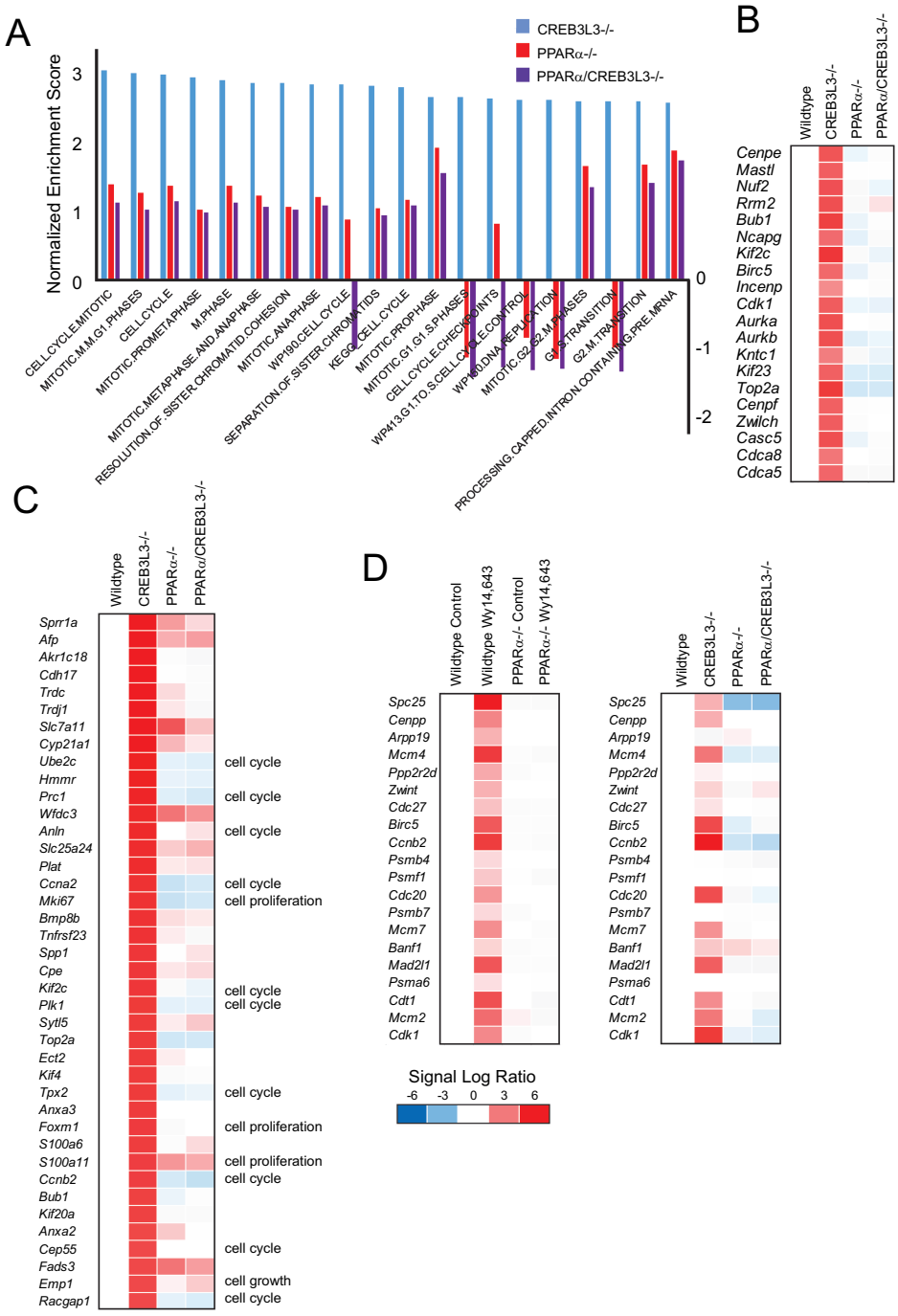
A
CREB3L3-/-
PPARα-/-
PPARα/CREB3L3-/-
Normalized Enrichment Score
3
2
1
0
0
-1
-2
CELLCYCLE,MITOTIC
MITOTIC,M.M.G1.PHASES
CELLCYCLE
MITOTIC,PROMETAPHASE
M.PHASE
MITOTIC,METAPHASE,AND,ANAPHASE
RESOLUTION.OF.SISTER.CHROMATID.COHESION
MITOTIC,ANAPHASE
WP190.CELL.CYCLE
SEPARATION.OF.SISTER.CHROMATIDS
KEGG_CELL_CYCLE
MITOTIC,PROPHASE
MITOTIC,G1.G1.S.PHASES
CELL.CYCLE,CHECKPOINTS
WP413.G1.TO.S.CELL.CYCLE.CONTROL
WP466.DNA.REPLICATION
MITOTIC,G2.G2.M.PHASES
G1.S.TRANSITION
G2.M.TRANSITION
PROCESSING.CAPPED.INTRON.CONTAINING.PRE.MRNA
B
Wildtype
CREB3L3-/-
PPARα-/-
PPARα/CREB3L3-/-
Cenpe
Mastl
Nuf2
Rrm2
Bub1
Ncapg
Kif2c
Birc5
Incenp
Cdk1
Aurka
Aurkb
Kntc1
Kif23
Top2a
Cenpf
Zwilch
Casc5
Cdca8
Cdca5
C
Wildtype
CREB3L3-/-
PPARα-/-
PPARα/CREB3L3-/-
Sprr1a
Afp
Akr1c18
Cdh17
Trdc
Trdj1
Slc7a11
Cyp21a1
Ube2c
Hmmr
Prc1
Wfdc3
Anln
Slc25a24
Plat
Ccna2
Mki67
Bmp8b
Tnfrsf23
Spp1
Cpe
Kif2c
Plk1
Sytl5
Top2a
Ect2
Kif4
Tpx2
Anxa3
Foxm1
S100a6
S100a11
Ccnb2
Bub1
Kif20a
Anxa2
Cep55
Fads3
Emp1
Racgap1
cell cycle
cell cycle
cell cycle
cell cycle
cell proliferation
cell cycle
cell cycle
cell cycle
cell proliferation
cell proliferation
cell cycle
cell cycle
cell growth
cell cycle
D
Wildtype Control
Wildtype Wy14,643
PPARα-/- Control
PPARα-/- Wy14,643
Spc25
Cenpp
Arpp19
Mcm4
Ppp2r2d
Zwint
Cdc27
Birc5
Ccnb2
Psmb4
Psmf1
Cdc20
Psmb7
Mcm7
Banf1
Mad2l1
Psma6
Cdt1
Mcm2
Cdk1
Signal Log Ratio
-6
-3
0
3
6
Wildtype
CREB3L3-/-
PPARα-/-
PPARα/CREB3L3-/-
Spc25
Cenpp
Arpp19
Mcm4
Ppp2r2d
Zwint
Cdc27
Birc5
Ccnb2
Psmb4
Psmf1
Cdc20
Psmb7
Mcm7
Banf1
Mad2l1
Psma6
Cdt1
Mcm2
Cdk1

Figure 10. CREB3L3 deficiency during ketogenic diet leads to upregulation of the cell cycle. A) Top 20 upregulated genesets in liver of CREB3L3-/- mice compared with wild-type mice, determined by gene set enrichment analysis and ranked according to normalized enrichment score (NES)(blue). The NES of the same genesets for the comparison between wild-type and PPARα-/- (red) or combined PPARα/CREB3L3-/- (purple) mice is shown as well. B) Comparative gene expression analysis in liver of wild-type, PPARα-/-, CREB3L3-/-, and combined PPARα/CREB3L3-/- mice after a 4-day ketogenic diet. The genes shown are the 20 most highly enriched genes in CREB3L3-/- mice vs. wild-type mice that are part of the geneset CELL.CYCLE.MITOTIC. C) Comparative gene expression analysis in liver of wild-type, PPARα-/-, CREB3L3-/-, and combined PPARα/CREB3L3-/- mice after a 4-day ketogenic diet, showing the top 40 most highly upregulated genes in CREB3L3-/- mice. D) Comparative gene expression analysis in liver of wild-type mice, wild-type mice treated with Wy-14,643 for 5 days, PPARα-/- mice, and PPARα-/- treated with Wy-14,643 for 5 days (left panel), and wild-type, PPARα-/-, CREB3L3-/-, and combined PPARα/CREB3L3-/- mice after a 4-day ketogenic diet (right panel). The genes shown are the 20 most highly enriched genes upon Wy-14.643 treatment that are part of the geneset MITOTIC.M.M.G1 PHASE. Red indicates upregulated, blue indicates downregulated.

Discussion

In this paper we studied the effect of individual and combined PPARα and CREB3L3 deficiency on hepatic gene expression after a 16-hour fast and a 4-day ketogenic diet. Under conditions of overnight fasting, the effect of PPARα deficiency and CREB3L3 deficiency on hepatic gene expression are largely independent, and only show a very limited degree of synergism. A small number of genes is under dual control of PPARα and CREB3L3, including *Fgf21* and *Mfsd2a*. Our data do not support a strong co-dependence of PPARα and CREB3L3 in hepatic gene regulation during fasting. By contrast, a strong interaction between PPARα and CREB3L3 exists during ketogenic diet feeding. Previously, it was shown that CREB3L3-/- mice on a ketogenic diet exhibit a strong phenotype characterized by hepatomegaly and steatohepatitis, and elevated expression of inflammatory marker genes [19, 25]. Here, using whole genome expression profiling, we corroborate these findings. In addition, we show that deficiency of CREB3L3 has virtually no effect on hepatic gene expression in the absence of PPARα, indicating that the major liver phenotype triggered by CREB3L3 deficiency during ketogenic diet is dependent on PPARα. Furthermore, we find that CREB3L3 has a dual impact on PPARα signalling during ketogenic diet. On the one hand, CREB3L3 deficiency leads to reduced expression of PPARα and PPARα target genes involved in fatty acid oxidation and ketogenesis. On the other hand, CREB3L3 deficiency leads to the marked activation of the hepatoproliferative effect of PPARα. Overall, our data suggest that CREB3L3 deficiency during ketogenic diet uncouples the mitogenic and lipid metabolic effects of PPARα in the liver.

It is unclear how CREB3L3 deficiency promotes liver damage and hepatoproliferation during ketogenic diet and how this effect is dependent on PPARα. It could be envisioned that

deficiency of CREB3L3 disrupts a certain metabolic pathway, such as fatty acid oxidation or fatty acid elongation and desaturation, leading to accumulation of intermediate lipid species that ligand-activate PPARα and specifically stimulate the mitogenic action of PPARα. In addition, these lipid species may promote liver damage. Additionally, it is possible that CREB3L3 deficiency alters a specific metabolic pathway, possibly involving accumulation of damaging intermediates, and that these effects are dependent on an enzyme/factor whose expression is maintained by PPARα. Insofar as CREB3L3 and PPARα regulate the expression of many genes, it is not possible to pinpoint the exact causal gene(s) downstream of CREB3L3 and PPARα.

Other examples exist of the uncoupling of the mitogenic and metabolic actions of PPARα. For example, human PPARα upregulates genes involved in fatty acid oxidation but not the cell cycle, as shown by studies in mice carrying human PPARα [36, 37]. Another example is the activation of mouse PPARα by dietary n-3 poly-unsaturated fatty acids, which leads to upregulation of PPARα targets involved in lipid metabolism but does not trigger hepatocyte proliferation [38]. These findings strongly indicate that the mechanisms by which PPARα affects lipid metabolism and hepatocyte proliferation are distinct [36, 37]. Mechanistically, how ligand-activated PPARα could selectively activate mitogenic and not metabolic pathways is unclear but could be related to the SPPARM concept [39-41]. According to this concept, different PPAR agonists have only partially overlapping effects on gene expression based on selective receptor-coregulator interactions. Borrowing from this notion, it can be hypothesized that the epigenetic mechanisms that drive the PPARα-dependent activation of genes involved in fatty acid oxidation and ketogenesis are different from the epigenetic mechanisms that support the induction of mitogenic pathways by PPARα, and additionally that these mechanisms are differentially affected by CREB3L3 deficiency.

Our data indicate that the roles of PPARα and CREB3L3 in the fasted state are very distinct, showing minimal overlap in target gene regulation (Figure 11A). As shown by previous whole genome expression analyses and supported by the present paper, PPARα governs the expression of a large number of genes involved in fatty acid oxidation and ketogenesis, as well as other pathways of intracellular and extracellular lipid metabolism [2]. Reduced fatty acid oxidation and ketogenesis causes the commonly observed fasting-induced hypoketonemia and elevated plasma free fatty acid levels in PPARα-/- mice [9-11, 42]. In the liver, the non-oxidized fatty acids are diverted towards re-esterification, explaining the fasting-induced steatosis in PPARα-/- mice [9-11, 42]. By contrast, CREB3L3 targets apolipoproteins, including *Apoa4*, *Apoc2*, *Apoa5*, and *Apoa1* [17, 43]. Reduced expression of the lipoprotein lipase activators *Apoc2* and *Apoa5*, and of *Fgf21*, which at pharmacological doses has been shown to stimulate plasma triglyceride clearance [44], likely explains the elevated plasma triglyceride levels in CREB3L3-/- mice via reduced plasma triglyceride clearance [17, 25, 43, 45]. This is in line with our previous observation that

CREB3L3 deficiency does not significantly influence triglyceride secretion [19]. Besides targeting lipoprotein metabolism, CREB3L3 regulates a relatively small number of genes involved in several distinct metabolic pathways, including *Fabp2* (fatty acid binding), *Cidec* (lipid storage), fatty acid desaturation (*Fads1*, *Fads2*), fatty acid elongation (*Elovl2*, *Elovl5*), and gluconeogenesis (*G6pc, Pck1*) (Figure 11A) [15-18]. Our data do not support the notion that CREB3L3 has an important role during fasting in regulating genes involved in fatty acid oxidation, with the exception of *Cpt1a* and *Hsd17b10*. This is supported by our previous data, showing a lack of effect of CREB3L3 deficiency on *ex vivo* fatty acid oxidation and fatty acid oxidation genes [19]. In contrast, Nakagawa and colleagues observed that CREB3L3 deficiency in the fasted state reduced expression of many genes involved in fatty acid oxidation, showing synergy with PPARα [25]. The reason for this discrepancy is not clear, but could be related to the different duration of fasting (16 hours vs. 24 hours). Interestingly, *Cpt1a* expression was not downregulated in the fasted state in PPARα-/- mice, which we had also observed in another set of samples [12], despite it being considered as the prototypical PPARα target gene. It can be hypothesized that the stimulatory effect of PPARα agonists on *Cpt1a* expression may be partly mediated by induction of CREB3L3.

An intriguing question is why CREB3L3 deficiency leads to a pronounced phenotype in mice fed a ketogenic but has much more limited effects in fasted mice. Direct comparison of hepatic gene expression in wild-type mice after fasting and ketogenic diet showed that expression of SREBP1 and its target genes involved in lipogenesis and cholesterogenesis was much higher after the ketogenic diet than after fasting (not shown). Previously, it was shown that CREB3L3 is a negative regulator of SREBP-1c production and hepatic lipogenesis [46], which is in line with our observation that genes involved in lipogenesis/cholesterogenesis are highly elevated in CREB3L3-/- mice under regular fasting conditions. Hence, placing CREB3L3-/- mice on a ketogenic diet is expected to lead to markedly increased lipogenesis/cholesterogenesis, which in turn may lead to the generation of a specific (set of) lipids that could trigger the mitogenic effect of PPARα (Figure 11B). The upregulation of cholesterogenesis upon CREB3L3 deficiency in the fasted state is seemingly at odds with a previous study that suggested that CREB3L3 stimulates lipogenesis and cholesterogenesis [47]. However, closer inspection at the individual gene levels shows substantial correspondence and indicates that CREB3L3 downregulates SREBP-dependent genes.

Despite lower expression of *Cidec*, which promotes lipid droplet formation [48, 49], PPARα-/-, CREB3L3-/-, and PPARα/CREB3L3-/- mice have elevated hepatic triglyceride levels. Similarly, expression of *Plin5*, which also promotes hepatic fat storage [50], is lower in PPARα-/- mice, despite these mice showing more pronounced steatosis. Accordingly, these data suggest that the elevated hepatic triglycerides in the PPARα-/-, CREB3L3-/-, and PPARα/CREB3L3-/- mice are not mediated by changes in *Cidec* and *Plin5* expression. It

should be noted that an increase in liver triglycerides does not necessarily have to be accompanied by elevated hepatic expression of *Cidec* and/or *Plin5*.

One limitation of our study is that we used whole body PPARα-/- and CREB3L3-/- mice. Ideally, it would have been better to use liver-specific PPARα and CREB3L3 deficient mice. Nevertheless, due to the high expression of PPARα and CREB3L3 in liver, we believe the results presented here reflect the hepatic function of the two transcription factors [2, 13]. An additional limitation is that we did not unveil the molecular details of the interaction between PPARα and CREB3L3 during ketogenic diet. These aspects should be further addressed in future studies.

Conclusion

We find that PPARα and CREB3L3 regulate distinct genes in the liver during fasting, with the exception of a limited number of common targets such as *Fgf21*. Strikingly, deficiency of CREB3L3 in mice during ketogenic diet uncouples the hepatoproliferative and metabolic effects of PPARα. Our data underscore the distinct functions of PPARα and CREB3L3 in the regulation of hepatic gene expression.

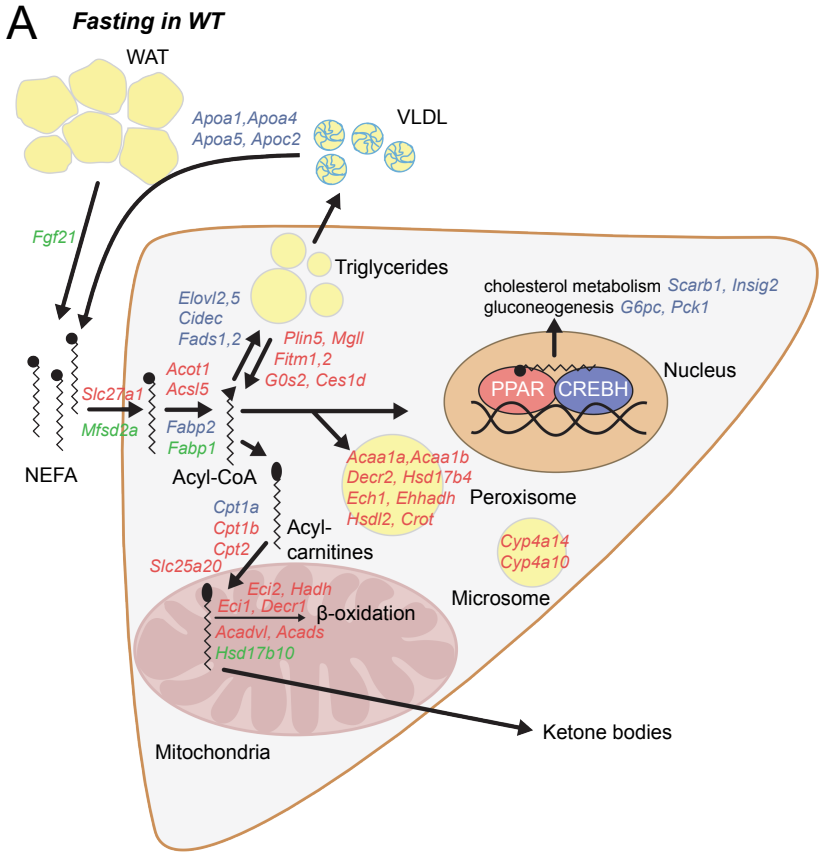

Figure 11. PPARα and CREB3L3 cooperate to regulate hepatic lipid metabolism. A) The cartoon illustrates the distinct roles of CREB3L3 and PPARα in the regulation of hepatic lipid metabolism during fasting. CREB3L3 stimulates genes involved in lipoprotein metabolism (*Apoc2, Apoa5, Apoa1*), lipid storage (*Cidec*), fatty acid binding (Fabp2), fatty acid desaturation and elongation (*Fads1, Fads2, Elovl2, Elovl5*), gluconeogenesis (*Pck1,G6pc*), and fatty acid oxidation (*Cpt1a, Hsd17b10*). PPARα stimulates genes involved in peroxisomal fatty acid oxidation (*Acaa1, Decre2, Ehhadh, Ech1*), mitochondrial fatty acid oxidation (*Slc25a20, Cpt2, Acadvl, Hadh*), microsomal fatty acid oxidation (*Cyp4a10, Cyp4a14*), fatty acid binding and (de)activation (*Fabp1, Acsl5, Acot1*), triglyceride hydrolysis (*Plin5, Fitm1, G0s2, Mgll*). Genes significantly decreased in CREB3L3-/- mice in the fasted state are in blue (IBMT P-value<0.001). Genes significantly decreased in PPARα-/- mice in the fasted state are in red. Genes significantly decreased in both genotypes are shown in green.

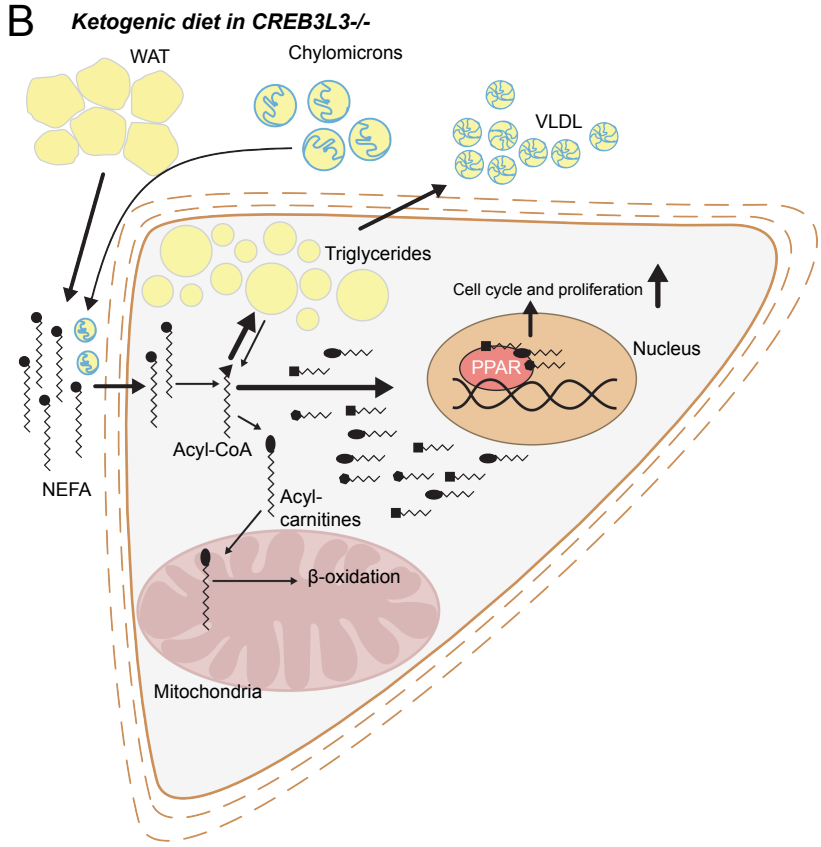

B) Overview of the effect of CREB3L3 deficiency after 4 days of ketogenic diet feeding. It is hypothesized that CREB3L3 deficiency during ketogenic diet leads to accumulation of certain lipid species that (ligand) activate PPARα. In turn, PPARα activation leads to hepatocyte proliferation and hepatomegaly. Additional effects of CREB3L3 deficiency include steatosis and enhanced liver damage.

Methods

Animal experiments

CREB3L3-/- mice were backcrossed onto a C57BL/6 background at least 10 times [17]. PPARα-/- mice that had been backcrossed on a pure C57Bl/6J background for more than 10 generations were acquired from Jackson Laboratories (no. 008154, B6;129S4-Pparatm1Gonz/J) [26]. The two lines were interbred to generate combined PPARα/CREB3L3-/- mice. Mice were housed in a specific pathogen free facility at the Weill Cornell Medical College on a 12h light/dark cycles and fed ad libitum standard chow diet (PicoLab Rodent diet 20, #5058, Lab diet). The four different mouse lines (wild-type, PPARα-/-, CREB3L3-/-, and PPARα/CREB3L3-/-) were either fasted for 16 hours or fed a ketogenic diet for 4 days (# F3666, Bio-Serv). The mice used for experiments were all male and approximately 8 weeks old. The euthanasia was carried out at around 10 a.m., with the ketogenic diet group being non-fasted (ad libitum fed). Blood was collected via orbital puncture under isoflurane anaesthesia. Immediately thereafter, the mice were euthanized by cervical dislocation. Tissues were excised and immediately frozen in liquid nitrogen followed by storage at −80°C.

For the adenoviral-mediated CREB3L3 overexpression, two-month-old male mice were injected intravenously via the tail vein at a dose of 3 × 10^9 particles of the adenoviruses per g body weight in 0.15 ml of saline. Mice injected with GFP-expressing adenovirus were used as control. Mice were euthanized four days after adenovirus injection and livers of three mice per group were used for whole genome expression profiling as detailed below. All animal experiments were approved by the Institutional Animal Care and Use Committee at Weill Cornell Medical College (Protocol #2012–0048) and performed in accordance with the approved guidelines.

Biochemical assays

Plasma triglycerides, non-esterified fatty acids, ketone bodies, alanine aminotransferase, and FGF21 concentrations were determined using assay kits (Serum Triglyceride Determination Kit, Sigma; NEFA-HR (2), Wako Chemicals; Autokit Total Ketone Bodies, Wako Chemicals; ALT Kit, Bio-Quant; Mouse/Rat FGF-21 Quantikine ELISA Kit, R&D Systems; Human FGF-21 Quantikine ELISA Kit, R&D Systems). Lipids were extracted from liver tissues with chloroform/methanol mixture (2:1 v/v), as described previously [27].

Transcriptomics

Microarray analysis was performed on liver samples using 3-4 biological replicates per group. Total RNA was extracted from cells using TRIzol reagent (Life Technologies, Bleiswijk, The Netherlands) and subsequently purified using the RNeasy Micro kit (Qiagen, Venlo, The Netherlands). RNA integrity was verified with RNA 6000 Nano chips on an Agilent 2100 bioanalyzer (Agilent Technologies, Amsterdam, The Netherlands). Purified RNA (100 ng) was labelled with the Ambion WT expression kit (Carlsbad, CA) and hybridized to an Affymetrix Mouse Gene 1.1 ST array plate (Affymetrix, Santa Clara, CA). Hybridization, washing, and scanning were carried out on an Affymetrix GeneTitan platform according to the manufacturer's instructions. Normalized expression estimates were obtained from the raw intensity values applying the robust multi-array analysis preprocessing algorithm available in the Bioconductor library AffyPLM with default settings [28, 29]. Probe sets were defined according to Dai et al. [30]. In this method probes are assigned to Entrez IDs as a unique gene identifier. In this study, probes were reorganized based on the Entrez Gene database, build 37, version 1 (remapped CDF v22). The P values were calculated using an Intensity-Based Moderated T-statistic (IBMT) [31]. Genes were defined as significantly changed when $P < 0.001$.

Gene set enrichment analysis (GSEA) was used to identify gene sets that were enriched among the upregulated or downregulated genes [32]. Genes were ranked based on the IBMT-statistic and subsequently analyzed for over- or underrepresentation in predefined gene sets derived from Gene Ontology, KEGG, National Cancer Institute, PFAM, Biocarta, Reactome and WikiPathways pathway databases. Only gene sets consisting of more than 15 and fewer than 500 genes were taken into account. Statistical significance of GSEA results was determined using 1,000 permutations.

Statistical Analysis

Statistical analysis of the transcriptomics data was performed as described in the previous paragraph. Statistical analysis of the other parameters was performed by two-way ANOVA and Student's t-test. Data are presented as mean ± SEM. $P<0.05$ was considered statistically significant.

Additional files

Supplementary Material: Supplemental Table 1. List of 34 genes that were commonly downregulated in livers of PPARα-/-, CREB3L3-/-, and PPARα/CREB3L3-/- mice in the fasted state. Supplemental Table 2. Specific functions of the genes connected to cell cycle illustrated in figures 10B and C. Supplemental figure 1. PPARα and CREB3L3 regulate distinct pathways in liver during fasting. Supplemental figure 2. Similar effects of PPARα and combined PPARα/CREB3L3 ablation on hepatic gene expression.

Abbreviations

PPAR, Peroxisome Proliferator-Activated Receptor

CREB3L3, cAMP-Responsive Element Binding Protein 3-Like 3

GSEA, Gene Set Enrichment Analysis

NEFA, non-esterified fatty acids

SPPARM, Selective PPAR Modulator

Declarations

Ethics approval for animal study

All animal experiments were approved by the Institutional Animal Care and Use Committee at Weill Cornell Medical College (Protocol #2012–0048) and performed in accordance with the approved guidelines.

Consent for publication

Not applicable.

Availability of data and material

The datasets generated and/or analyzed during the current study are available in the Gene Expression Omnibus repository: GSE121096.

Competing interests

The authors declare that they have no competing interests.

Funding

This research was supported by CVON ENERGISE grant CVON2014-02.

Authors' contributions

SK and AHL conceived and designed the study. JGP, XX and KYH acquired the data. PMMR and SK analysed and interpreted the data. SK drafted the manuscript. PMMR substantively revised it. All authors read and approved the final manuscript.

Acknowledgements

Not applicable.

References

[1] I. Issemann, S. Green, Activation of a member of the steroid hormone receptor superfamily by peroxisome proliferators, Nature, 347 (1990) 645-650.

[2] S. Kersten, Integrated physiology and systems biology of PPARalpha, Molecular metabolism, 3 (2014) 354-371.

[3] B. Gross, M. Pawlak, P. Lefebvre, B. Staels, PPARs in obesity-induced T2DM, dyslipidaemia and NAFLD, Nat Rev Endocrinol, (2016).

[4] K.L. Gearing, M. Gottlicher, M. Teboul, E. Widmark, J.A. Gustafsson, Interaction of the peroxisome-proliferator-activated receptor and retinoid X receptor, Proc Natl Acad Sci U S A, 90 (1993) 1440-1444.

[5] I. Issemann, R.A. Prince, J.D. Tugwood, S. Green, The retinoid X receptor enhances the function of the peroxisome proliferator activated receptor, Biochimie, 75 (1993) 251-256.

[6] H. Keller, C. Dreyer, J. Medin, A. Mahfoudi, K. Ozato, W. Wahli, Fatty acids and retinoids control lipid metabolism through activation of peroxisome proliferator-activated receptor-retinoid X receptor heterodimers, Proc Natl Acad Sci U S A, 90 (1993) 2160-2164.

[7] S. Kersten, R. Stienstra, The role and regulation of the peroxisome proliferator activated receptor alpha in human liver, Biochimie, 136 (2017) 75-84.

[8] T. Hashimoto, W.S. Cook, C. Qi, A.V. Yeldandi, J.K. Reddy, M.S. Rao, Defect in peroxisome proliferator-activated receptor alpha-inducible fatty acid oxidation determines the severity of hepatic steatosis in response to fasting, J Biol Chem, 275 (2000) 28918-28928.

[9] S. Kersten, J. Seydoux, J.M. Peters, F.J. Gonzalez, B. Desvergne, W. Wahli, Peroxisome proliferator-activated receptor alpha mediates the adaptive response to fasting, J Clin Invest, 103 (1999) 1489-1498.

[10] T.C. Leone, C.J. Weinheimer, D.P. Kelly, A critical role for the peroxisome proliferator-activated receptor alpha (PPARalpha) in the cellular fasting response: the PPARalpha-null mouse as a model of fatty acid oxidation disorders, Proc Natl Acad Sci U S A, 96 (1999) 7473-7478.

[11] M. Regnier, A. Polizzi, Y. Lippi, E. Fouche, G. Michel, C. Lukowicz, S. Smati, A. Marrot, F. Lasserre, C. Naylies, A. Batut, F. Viars, J. Bertrand-Michel, C. Postic, N. Loiseau, W. Wahli, H. Guillou, A. Montagner, Insights into the role of hepatocyte PPARalpha activity in response to fasting, Mol Cell Endocrinol, (2017).

[12] L.M. Sanderson, M.V. Boekschoten, B. Desvergne, M. Muller, S. Kersten, Transcriptional profiling reveals divergent roles of PPARalpha and PPARbeta/delta in regulation of gene expression in mouse liver, Physiol Genomics, 41 (2010) 42-52.

[13] K. Zhang, X. Shen, J. Wu, K. Sakaki, T. Saunders, D.T. Rutkowski, S.H. Back, R.J. Kaufman, Endoplasmic reticulum stress activates cleavage of CREBH to induce a systemic inflammatory response, Cell, 124 (2006) 587-599.

[14] A.H. Lee, The role of CREB-H transcription factor in triglyceride metabolism, Curr Opin Lipidol, 23 (2012) 141-146.

[15] M.W. Lee, D. Chanda, J. Yang, H. Oh, S.S. Kim, Y.S. Yoon, S. Hong, K.G. Park, I.K. Lee, C.S. Choi, R.W. Hanson, H.S. Choi, S.H. Koo, Regulation of hepatic gluconeogenesis by an ER-bound transcription factor, CREBH, Cell Metab, 11 (2010) 331-339.

[16] H. Kim, Z. Zheng, P.D. Walker, G. Kapatos, K. Zhang, CREBH Maintains Circadian Glucose Homeostasis by Regulating Hepatic Glycogenolysis and Gluconeogenesis, Mol Cell Biol, 37 (2017).

[17] J.H. Lee, P. Giannikopoulos, S.A. Duncan, J. Wang, C.T. Johansen, J.D. Brown, J. Plutzky, R.A. Hegele, L.H. Glimcher, A.H. Lee, The transcription factor cyclic AMP-responsive element-binding protein H regulates triglyceride metabolism, Nat Med, 17 (2011) 812-815.

[18] X. Xu, J.G. Park, J.S. So, A.H. Lee, Transcriptional activation of Fsp27 by the liver-enriched transcription factor CREBH promotes lipid droplet growth and hepatic steatosis, Hepatology, 61 (2015) 857-869.

[19] J.G. Park, X. Xu, S. Cho, K.Y. Hur, M.S. Lee, S. Kersten, A.H. Lee, CREBH-FGF21 axis improves hepatic steatosis by suppressing adipose tissue lipolysis, Scientific reports, 6 (2016) 27938.

[20] M. Rakhshandehroo, G. Hooiveld, M. Muller, S. Kersten, Comparative analysis of gene regulation by the transcription factor PPARalpha between mouse and human, PLoS One, 4 (2009) e6796.

[21] H. Danno, K.A. Ishii, Y. Nakagawa, M. Mikami, T. Yamamoto, S. Yabe, M. Furusawa, S. Kumadaki, K. Watanabe, H. Shimizu, T. Matsuzaka, K. Kobayashi, A. Takahashi, S. Yatoh, H. Suzuki, N. Yamada, H. Shimano, The liver-enriched transcription factor CREBH is nutritionally regulated and activated by fatty acids and PPARalpha, Biochem Biophys Res Commun, 391 (2010) 1222-1227.

[22] H.B. Kim, R. Mendez, Z. Zheng, L. Chang, J. Cai, R. Zhang, K. Zhang, Liver-Enriched Transcription Factor CREBH Interacts with Peroxisome Proliferator-Activated Receptor alpha to Regulate Metabolic Hormone FGF21, Endocrinology, (2014) en20131490.

[23] H. Kim, R. Mendez, X. Chen, D. Fang, K. Zhang, Lysine Acetylation of CREBH Regulates Fasting-Induced Hepatic Lipid Metabolism, Mol Cell Biol, 35 (2015) 4121-4134.

[24] M.A. de la Rosa Rodriguez, S. Kersten, Regulation of lipid droplet-associated proteins by peroxisome proliferator-activated receptors, Biochim Biophys Acta, 1862 (2017) 1212-1220.

[25] Y. Nakagawa, A. Satoh, H. Tezuka, S.I. Han, K. Takei, H. Iwasaki, S. Yatoh, N. Yahagi, H. Suzuki, Y. Iwasaki, H. Sone, T. Matsuzaka, N. Yamada, H. Shimano, CREB3L3 controls fatty acid oxidation and ketogenesis in synergy with PPARalpha, Scientific reports, 6 (2016) 39182.

[26] S.S. Lee, T. Pineau, J. Drago, E.J. Lee, J.W. Owens, D.L. Kroetz, P.M. Fernandez-Salguero, H. Westphal, F.J. Gonzalez, Targeted disruption of the alpha isoform of the peroxisome proliferator-activated receptor gene in mice results in abolishment of the pleiotropic effects of peroxisome proliferators, Mol Cell Biol, 15 (1995) 3012-3022.

[27] J.H. Lee, T. Wada, M. Febbraio, J. He, T. Matsubara, M.J. Lee, F.J. Gonzalez, W. Xie, A novel role for the dioxin receptor in fatty acid metabolism and hepatic steatosis, Gastroenterology, 139 (2010) 653-663.

[28] B.M. Bolstad, R.A. Irizarry, M. Astrand, T.P. Speed, A comparison of normalization methods for high density oligonucleotide array data based on variance and bias, Bioinformatics, 19 (2003) 185-193.

[29] R.A. Irizarry, B.M. Bolstad, F. Collin, L.M. Cope, B. Hobbs, T.P. Speed, Summaries of Affymetrix GeneChip probe level data, Nucleic Acids Res, 31 (2003) e15.

[30] M. Dai, P. Wang, A.D. Boyd, G. Kostov, B. Athey, E.G. Jones, W.E. Bunney, R.M. Myers, T.P. Speed, H. Akil, S.J. Watson, F. Meng, Evolving gene/transcript definitions significantly alter the interpretation of GeneChip data, Nucleic Acids Res, 33 (2005) e175.

[31] M.A. Sartor, C.R. Tomlinson, S.C. Wesselkamper, S. Sivaganesan, G.D. Leikauf, M. Medvedovic, Intensity-based hierarchical Bayes method improves testing for differentially expressed genes in microarray experiments, BMC Bioinformatics, 7 (2006) 538.

[32] A. Subramanian, P. Tamayo, V.K. Mootha, S. Mukherjee, B.L. Ebert, M.A. Gillette, A. Paulovich, S.L. Pomeroy, T.R. Golub, E.S. Lander, J.P. Mesirov, Gene set enrichment analysis: a knowledge-based approach for interpreting genome-wide expression profiles, Proc Natl Acad Sci U S A, 102 (2005) 15545-15550.

[33] J.H. Berger, M.J. Charron, D.L. Silver, Major facilitator superfamily domain-containing protein 2a (MFSD2A) has roles in body growth, motor function, and lipid metabolism, PLoS One, 7 (2012) e50629.

[34] L.N. Nguyen, D. Ma, G. Shui, P. Wong, A. Cazenave-Gassiot, X. Zhang, M.R. Wenk, E.L. Goh, D.L. Silver, Mfsd2a is a transporter for the essential omega-3 fatty acid docosahexaenoic acid, Nature, 509 (2014) 503-506.

[35] J.M. Peters, T. Aoyama, R.C. Cattley, U. Nobumitsu, T. Hashimoto, F.J. Gonzalez, Role of peroxisome proliferator-activated receptor alpha in altered cell cycle regulation in mouse liver, Carcinogenesis JID - 8008055, 19 (1998) 1989-1994.

[36] C. Cheung, T.E. Akiyama, J.M. Ward, C.J. Nicol, L. Feigenbaum, C. Vinson, F.J. Gonzalez, Diminished hepatocellular proliferation in mice humanized for the nuclear receptor peroxisome proliferator-activated receptor alpha, Cancer Res, 64 (2004) 3849-3854.

[37] Q. Yang, T. Nagano, Y. Shah, C. Cheung, S. Ito, F.J. Gonzalez, The PPAR alpha-humanized mouse: a model to investigate species differences in liver toxicity mediated by PPAR alpha, Toxicol Sci, 101 (2008) 132-139.

[38] L.M. Sanderson, P.J. de Groot, G.J. Hooiveld, A. Koppen, E. Kalkhoven, M. Muller, S. Kersten, Effect of synthetic dietary triglycerides: a novel research paradigm for nutrigenomics, PLoS ONE, 3 (2008) e1681.

[39] B.L. Balint, L. Nagy, Selective modulators of PPAR activity as new therapeutic tools in metabolic diseases, Endocrine, metabolic & immune disorders drug targets, 6 (2006) 33-43.

[40] H.S. Camp, O. Li, S.C. Wise, Y.H. Hong, C.L. Frankowski, X. Shen, R. Vanbogelen, T. Leff, Differential activation of peroxisome proliferator-activated receptor-gamma by troglitazone and rosiglitazone, Diabetes, 49 (2000) 539-547.

[41] H. Duez, B. Lefebvre, P. Poulain, I.P. Torra, F. Percevault, G. Luc, J.M. Peters, F.J. Gonzalez, R. Gineste, S. Helleboid, V. Dzavik, J.C. Fruchart, C. Fievet, P. Lefebvre, B. Staels, Regulation of human apoA-I by gemfibrozil and fenofibrate through selective peroxisome proliferator-activated receptor alpha modulation, Arterioscler Thromb Vasc Biol, 25 (2005) 585-591.

[42] C.N. Brocker, D.P. Patel, T.J. Velenosi, D. Kim, T. Yan, J. Yue, G. Li, K.W. Krausz, F.J. Gonzalez, Extrahepatic PPARalpha modulates fatty acid oxidation and attenuates fasting-induced hepatosteatosis in mice, J Lipid Res, (2018).

[43] X. Xu, J.G. Park, J.S. So, K.Y. Hur, A.H. Lee, Transcriptional regulation of apolipoprotein A-IV by the transcription factor CREBH, J Lipid Res, 55 (2014) 850-859.

[44] C. Schlein, S. Talukdar, M. Heine, A.W. Fischer, L.M. Krott, S.K. Nilsson, M.B. Brenner, J. Heeren, L. Scheja, FGF21 Lowers Plasma Triglycerides by Accelerating Lipoprotein Catabolism in White and Brown Adipose Tissues, Cell Metab, 23 (2016) 441-453.

[45] Y. Nakagawa, F. Oikawa, S. Mizuno, H. Ohno, Y. Yagishita, A. Satoh, Y. Osaki, K. Takei, T. Kikuchi, S.I. Han, T. Matsuzaka, H. Iwasaki, K. Kobayashi, S. Yatoh, N. Yahagi, M. Isaka, H. Suzuki, H. Sone, S. Takahashi, N. Yamada, H. Shimano, Hyperlipidemia and hepatitis in liver-specific CREB3L3 knockout mice generated using a one-step CRISPR/Cas9 system, Scientific reports, 6 (2016) 27857.

[46] A.K. Min, J.Y. Jeong, Y. Go, Y.K. Choi, Y.D. Kim, I.K. Lee, K.G. Park, cAMP response element binding protein H mediates fenofibrate-induced suppression of hepatic lipogenesis, Diabetologia, 56 (2013) 412-422.

[47] C. Zhang, G. Wang, Z. Zheng, K.R. Maddipati, X. Zhang, G. Dyson, P. Williams, S.A. Duncan, R.J. Kaufman, K. Zhang, Endoplasmic reticulum-tethered transcription factor cAMP responsive element-binding protein, hepatocyte specific, regulates hepatic lipogenesis, fatty acid oxidation, and lipolysis upon metabolic stress in mice, Hepatology, 55 (2012) 1070-1082.

[48] K. Matsusue, A physiological role for fat specific protein 27/cell death-inducing DFF45-like effector C in adipose and liver, Biol Pharm Bull, 33 (2010) 346-350.

[49] M.J. Xu, Y. Cai, H. Wang, J. Altamirano, B. Chang, A. Bertola, G. Odena, J. Lu, N. Tanaka, K. Matsusue, T. Matsubara, P. Mukhopadhyay, S. Kimura, P. Pacher, F.J. Gonzalez, R. Bataller, B. Gao, Fat-Specific Protein 27/CIDEC Promotes Development of Alcoholic Steatohepatitis in Mice and Humans, Gastroenterology, 149 (2015) 1030-1041 e1036.

[50] C. Wang, Y. Zhao, X. Gao, L. Li, Y. Yuan, F. Liu, L. Zhang, J. Wu, P. Hu, X. Zhang, Y. Gu, Y. Xu, Z. Wang, Z. Li, H. Zhang, J. Ye, Perilipin 5 improves hepatic lipotoxicity by inhibiting lipolysis, Hepatology, 61 (2015) 870-882.

[51] M. Rakhshandehroo, L.M. Sanderson, M. Matilainen, R. Stienstra, C. Carlberg, P.J. de Groot, M. Muller, S. Kersten, Comprehensive analysis of PPARalpha-dependent regulation of hepatic lipid metabolism by expression profiling, PPAR Res, 2007 (2007) 26839.

Supplemental Material

Supplemental Table 1. List of 34 genes that were significantly downregulated in livers of PPARα-/-, CREB3L3-/-, and PPARα/CREB3L3-/- mice in the fasted state (IBMT P- value<0.001).

Mfsd2a	Major Facilitator Superfamily Domain Containing 2A
Mtnr1a	Melatonin Receptor 1A
Fgf21	Fibroblast Growth Factor 21
Lamb3	Laminin Subunit Beta 3
Sema5b	Semaphorin 5B
Xrcc3	X-Ray Repair Cross Complementing 3
D630045J12Rik	RIKEN cDNA D630045J12 gene
Crip2	Cysteine Rich Protein 2
Tlr12	Toll-like Receptor 12
Srebf1	Sterol Regulatory Element Binding Transcription Factor 1
Kcnk1	Potassium Two Pore Domain Channel Subfamily K Member 1
Tmem28	Transmembrane Protein 28
Rtfdc1	Replication Termination Factor 2
Dpy19l3	Dpy-19 Like C-Mannosyltransferase 3
Hsd17b10	Hydroxysteroid 17-Beta Dehydrogenase 10
Gm10851	Predicted gene 10851
Sntg2	Syntrophin Gamma 2
Tram2	Translocation Associated Membrane Protein 2
Tmem134	Transmembrane Protein 134
Suclg1	Succinate-CoA Ligase Alpha Subunit
Sulf2	Sulfatase 2
Fam73b	Mitoguardin 2
Nat1	N-acetyl transferase 1
Tmem184a	Transmembrane protein 184a
Sun2	Sad1 and UNC84 domain containing 2
Sel1l3	Sel-1 suppressor of lin-12-like 3 (C. elegans)
Cog4	Component Of Oligomeric Golgi Complex 4
Rtn4ip1	Reticulon 4 Interacting Protein 1
Rmdn3	Regulator Of Microtubule Dynamics 3
Nsmf	NMDA Receptor Synaptonuclear Signaling And Neuronal Migration Factor
Ldha	Lactate dehydrogenase A
Ak2	Adenylate kinase 2
St3gal3	*S*T3 beta-galactoside alpha-2,3-sialyltransferase 3
Oard1	O-acyl-ADP-ribose deacylase 1

Supplemental Table 2. Specific functions of the genes connected to cell cycle illustrated in figures 10B and C.

Cenpe, Centrosome-associated protein E	required for stable spindle microtubule capture at kinetochores	Promoting cell cycle progression
Mastl, microtubule-associated serine/threonine kinase		Possibly Pro
Nuf2, NDC80 kinetochore complex component NUF2	Yeast Nuf2 disappears from the centromere during meiotic prophase when centromeres lose their connection to the spindle pole body, and plays a regulatory role in chromosome segregation	Likely pro
Rrm2	catalyzes the formation of deoxyribonucleotides from ribonucleotides	Pro
Bub1, BUB1 mitotic checkpoint serine/threonine kinase	The encoded protein functions in part by phosphorylating members of the mitotic checkpoint complex and activating the spindle checkpoint	Pro
Ncapg, non-SMC condensin I complex subunit G	subunit of condensin complex, which is involved in condensation and stabilization of chromosomes during mitosis	Likely pro
Kif2c**,** Kinesin family member 2c	depolymerize microtubules at the plus end, thereby promoting mitotic chromosome segregation	Pro
Birc5, baculoviral IAP repeat containing 5	inhibitor of apoptosis (IAP) gene family, which encode negative regulatory proteins that prevent apoptotic cell death	Possibly Pro
Incep, inner centromere protein		Pro
Cdk1		Pro
Aurka, aurora kinase A	involved in microtubule formation and/or stabilization at the spindle pole during chromosome segregation	Pro
Aurkb, same as Aurka		Pro
Kntc1, kinetochore associated 1	involved in mechanisms to ensure proper chromosome segregation	Pro
Kif23, kinesin family member 23	This protein has been shown to cross-bridge antiparallel microtubules and drive microtubule movement in vitro	Pro
Top2a, DNA topoisomerase II alpha		Pro
Cenpf, centromere protein F		Pro
Zwilch, zwilch kinetochore protein		Likely Pro
Casc5, kinetochore scaffold	interacts with at least 5 different kinetochore proteins and two checkpoint kinases	Likely Pro
Cdca8, cell division cycle associated 8	Spindle formation	Pro
Cdca5 – same as Cdca8		Pro
Ube2c, ubiquitin conjugating enzyme E2 C	The encoded protein is required for the destruction of mitotic cyclins and for cell cycle progression	Pro
Prc1, protein regulator of cytokinesis 1	present at high levels during the S and G2/M phases of mitosis but its levels drop dramatically when the cell exits mitosis and enters the G1 phase. It is located in the nucleus during interphase, becomes associated with mitotic spindles in a highly dynamic manner during mitosis, and localizes to the cell mid-body during cytokinesis. This protein has been shown to be a substrate of several cyclin-dependent kinases (CDKs). It is necessary for polarizing parallel microtubules and concentrating the factors responsible for contractile ring assembly	Pro
Anln, anillin actin binding protein	This gene encodes an actin-binding protein that plays a role in cell growth and migration, and in cytokinesis	Likely Pro

Ccna2, cyclin A2	his protein binds and activates cyclin-dependent kinase 2 and thus promotes transition through G1/S and G2/M	Pro
Mki67, marker of proliferation Ki-67	"necessary for cellular proliferation"	Possibly Pro
Plk1, polo like kinase 1	Depletion of this protein in cancer cells dramatically inhibited cell proliferation and induced apoptosis	Pro
Tpx2, microtubule nucleation factor	controls spindle integrity, genome stability	Likely Pro
Foxm1, forkhead box M1	The encoded protein is phosphorylated in M phase and regulates the expression of several cell cycle genes, such as cyclin B1 and cyclin D1	Pro
S100a11, S100 calcium binding protein A11	involved in the regulation of a number of cellular processes such as cell cycle progression and differentiation	Possibly Pro
Ccnb2, cyclin B2	essential components of the cell cycle regulatory machinery	Likely pro
Cep55, centrosomal protein 55		Possibly Pro
Emp1, epithelial membrane protein 1		?
Racgap1, Rac GTPase activating protein	This protein plays a regulatory role in cytokinesis, cell growth, and differentiation	Possibly Pro

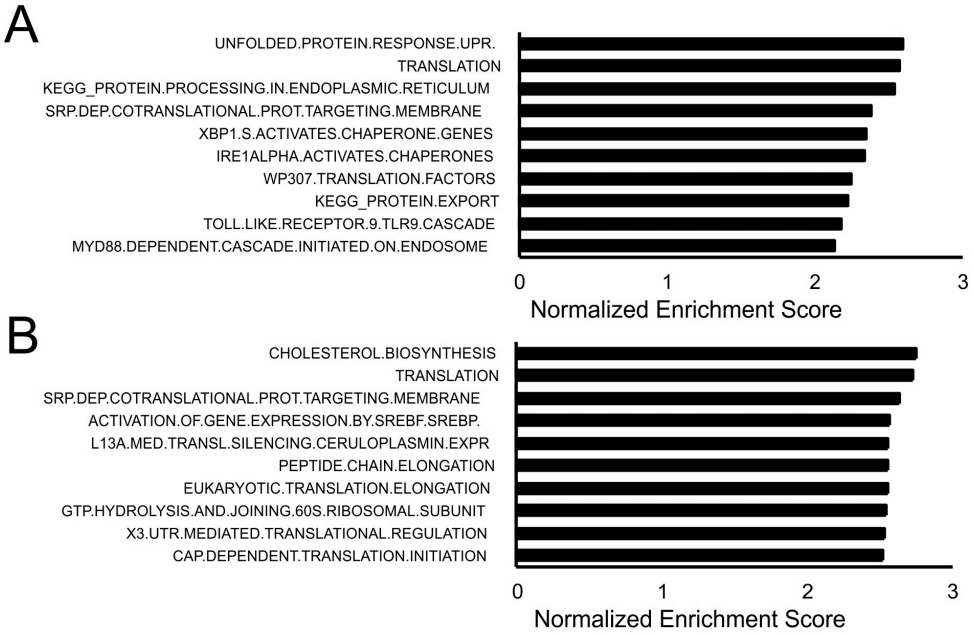

Supplemental figure 1. PPARα and CREB3L3 regulate distinct pathways in liver during fasting. Top 10 upregulated gene sets in liver of (A) PPARα-/- mice and (B) CREB3L3-/- mice compared to wildtype mice, as determined by gene set enrichment analysis. Gene sets were ranked according to normalized enrichment score. C) Comparative gene expression analysis in liver of wildtype, PPARα-/-, CREB3L3- /-, and PPARα/CREB3L3-/- mice after a 16h fast, showing the top 40 most highly upregulated genes in PPARα-/- mice (left panel) and CREB3L3-/- mice (right panel).

C

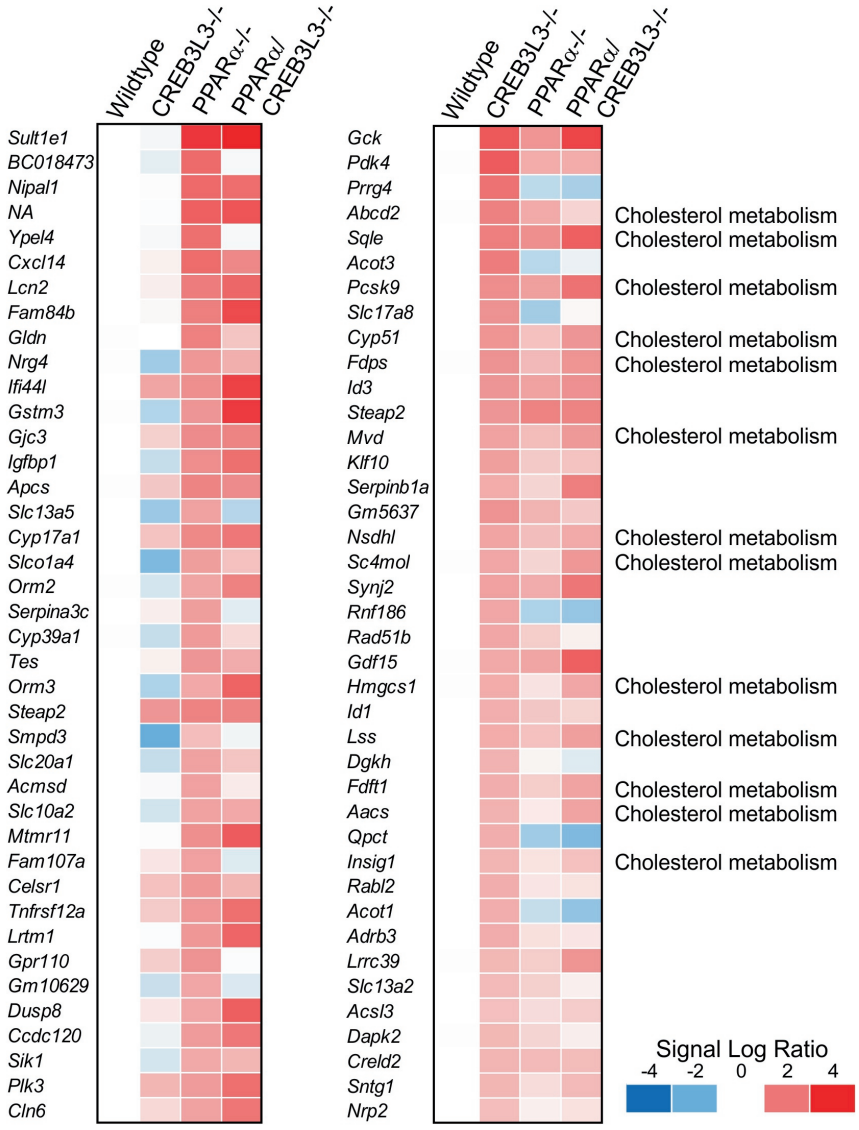
Wildtype
CREB3L3-/-
PPARα-/-
PPARα/ CREB3L3-/-
Sult1e1
BC018473
Nipal1
NA
Ypel4
Cxcl14
Lcn2
Fam84b
Gldn
Nrg4
Ifi44l
Gstm3
Gjc3
Igfbp1
Apcs
Slc13a5
Cyp17a1
Slco1a4
Orm2
Serpina3c
Cyp39a1
Tes
Orm3
Steap2
Smpd3
Slc20a1
Acmsd
Slc10a2
Mtmr11
Fam107a
Celsr1
Tnfrsf12a
Lrtm1
Gpr110
Gm10629
Dusp8
Ccdc120
Sik1
Plk3
Cln6
Gck
Pdk4
Prrg4
Abcd2
Sqle
Acot3
Pcsk9
Slc17a8
Cyp51
Fdps
Id3
Steap2
Mvd
Klf10
Serpinb1a
Gm5637
Nsdhl
Sc4mol
Synj2
Rnf186
Rad51b
Gdf15
Hmgcs1
Id1
Lss
Dgkh
Fdft1
Aacs
Qpct
Insig1
Rabl2
Acot1
Adrb3
Lrrc39
Slc13a2
Acsl3
Dapk2
Creld2
Sntg1
Nrp2
Cholesterol metabolism
Cholesterol metabolism
Cholesterol metabolism
Cholesterol metabolism
Cholesterol metabolism
Cholesterol metabolism
Cholesterol metabolism
Cholesterol metabolism
Cholesterol metabolism
Cholesterol metabolism
Cholesterol metabolism
Cholesterol metabolism
Signal Log Ratio
-4 -2 0 2 4

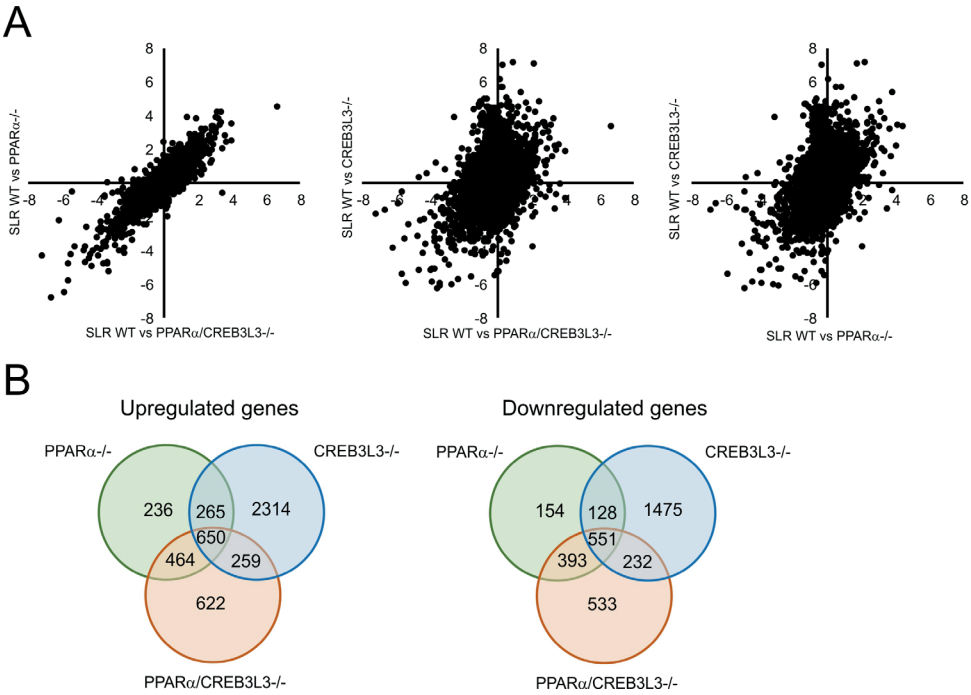

Supplemental figure 2. Similar effects of PPARα and combined PPARα/CREB3L3 ablation on hepatic gene expression. A) Correlation plot showing comparative hepatic gene expression changes in PPARα- /-, CREB3L3-/-, and combined PPARα/CREB3L3-/- mice in relation to wildtype mice after a 4 day ketogenic diet (expressed as signal log ratio, SLR). B) Venn diagram showing overlap in upregulated genes (left panel) and downregulated genes (right panel) in PPARα-/-, CREB3L3- /-, and combined PPARα/CREB3L3-/- mice, in comparison with wildtype mice (IBMT P value<0.001).

3

Chapter 3

Fasting induces ANGPTL4 and reduces LPL activity in human adipose tissue

Ruppert PMM†, Michielsen CCJR†, Hazebroek EJ, Pirayesh A, Olivecrona G, Afman LA, Kersten S.

† equal contribution

Mol Metab. 2020 Jun 3;101033.

Abstract

Objective: Studies in mice have shown that the decrease in lipoprotein lipase (LPL) activity in adipose tissue upon fasting is mediated by induction of the inhibitor ANGPTL4. Here, we aimed to validate this concept in humans by determining the effect of a prolonged fast on ANGPTL4 and LPL gene and protein expression in human subcutaneous adipose tissue.

Methods: To that end, twenty-three volunteers ate a standardized meal at 18.00h and fasted until 20.00h the next day. Blood was drawn and periumbilical adipose tissue biopsies were collected 2h and 26h after the meal.

Results: Consistent with previous mouse data, LPL activity in human adipose tissue was significantly decreased by fasting (-60%), concurrent with increased ANGPTL4 mRNA (+90%) and decreased ANGPTL8 mRNA (-94%). ANGPTL4 protein levels in adipose tissue were also significantly increased by fasting (+46%), whereas LPL mRNA and protein levels remained unchanged. In agreement with the adipose tissue data, plasma ANGPTL4 levels increased upon fasting (+100%), whereas plasma ANGPTL8 decreased (-79%). Insulin, levels of which significantly decreased upon fasting, downregulated ANGPTL4 mRNA and protein in primary human adipocytes. By contrast, cortisol, levels of which significantly increased upon fasting, upregulated ANGPTL4 mRNA and protein in primary human adipocytes, as did fatty acids.

Conclusion: ANGPTL4 levels in human adipose tissue are increased by fasting, likely via increased plasma cortisol and free fatty acids and decreased plasma insulin, resulting in decreased LPL activity.

This clinical trial was registered with identifier NCT03757767.

Keywords: adipose tissue, lipoprotein lipase, triglycerides, insulin, fatty acids

Introduction

Elevated plasma triglyceride levels are associated with elevated risk of atherosclerotic cardiovascular disease [1]–[4]. Triglycerides are mainly transported in the blood as part of intestine-derived chylomicrons and liver-derived very-low density lipoproteins (VLDLs). The triglycerides in these lipoprotein particles are cleared from the bloodstream through the action of lipoprotein lipase (LPL) [5], [6]. Adipocytes and myocytes produce and secrete large amounts of LPL, which is subsequently transported to the luminal side of the capillary endothelium by glycosylphosphatidylinositol-anchored high-density lipoprotein binding protein 1 (GPIHBP1) [7]–[9]. As a result, mutations in GPIHBP1 or LPL can lead to severe hypertriglyceridemia. In line with the physiological fluctuations in lipid requirement in various tissues, the activity of LPL is highly variable. For example, LPL activity in adipose tissue is decreased by fasting to reduce lipid storage [10]–[15]. Besides regulation via changes in LPL gene transcription, LPL activity is primarily controlled at the post-translational level [12], [13], [16], [17]. Key factors involved in post-translational regulation of LPL include fatty acids, which inhibit LPL via product inhibition [18], and the apolipoproteins C1, C2, C3 and A5. In addition, LPL is regulated by three members of the Angiopoietin-like protein family (ANGPTL): ANGPTL3, ANGPTL4 and ANGPTL8 [19].

The current literature places ANGPTL3, ANGPTL4 and ANGPTL8 at the center of the physiological partitioning of circulating triglycerides among various metabolic tissues [19], [20]. ANGPTL3 is secreted by the liver as a complex with ANGPTL8 and regulates postprandial LPL activity in adipose tissue and muscle in an endocrine fashion [21], [22]. Whereas the production of ANGPTL3 is relatively insensitive to feeding and fasting, the synthesis of ANGPTL8 is highly induced by feeding, which is mediated by insulin [23]. After feeding, the combined action of ANGPTL3/ANGPTL8 reduces the clearance of plasma triglycerides in brown adipose tissue, heart, and muscle, thereby rerouting plasma triglycerides to white adipose tissue and ensuring the replenishment of triglyceride stores [21], [22], [24], [25]. By contrast, ANGPTL4 has emerged as the dominant regulator of LPL activity in the fasted state. Befitting its original name fasting-induced adipose factor (FIAF), *Angptl4* was cloned as a fasting-induced gene in murine adipose tissue and liver [26]. Subsequent studies demonstrated that ANGPTL4 inhibits LPL activity and raises plasma triglyceride levels in mice [27]–[29]. Olivecrona found that *Angptl4* mRNA in rat adipose tissue turns over rapidly and that changes in *Angptl4* mRNA expression are inversely correlated to LPL activity, both during the fed-to-fasted and fasted-to-fed transitions [30]. Consistent with a predominant role of ANGPTL4 during fasting, transgenic ANGPTL4 overexpression markedly reduces plasma triglyceride clearance in mice in the fasted but not in the fed state, leading to a reduced uptake of TG-derived fatty acids by numerous tissues such as adipose tissue [31]. Conversely, ANGPTL4 deficiency in mice is associated

with enhanced clearance of plasma triglycerides and uptake of TG-derived fatty acids into adipose tissue in the fasted state [32]. Furthermore, the fasting-induced decrease in adipose tissue LPL activity was abolished in *Angptl4*-/- mice, indicating that ANGPTL4 mediates the repression of LPL activity during fasting [14]. ANGPTL4 inhibits LPL activity by promoting LPL unfolding via direct protein-protein interactions [33]. In mouse adipose tissue, this action of ANGPTL4 triggers LPL cleavage and subsequent degradation [34], [35]. The existence of a mechanism regulating LPL degradation/turnover during fasting and requiring the induction of a gene separate from *Lpl* was already suggested prior to the cloning of ANGPTL4 [13], [16].

The predominant role of ANGPTL4 in LPL regulation during fasting is likely at least partly related to the upregulation of ANGPTL4 mRNA and protein levels in mouse adipose tissue by fasting [14], [26], [32], [34], [35]. In addition, recent evidence suggests that the inhibitory effect of ANGPTL4 on LPL is counteracted by ANGPTL8, levels of which decrease in adipose tissue during fasting [36]. At the whole body level, the upregulation of ANGPTL4 during fasting ensures that triglycerides are directed to non-adipose tissues to be used as fuel rather than being stored. The importance of ANGPTL4 in the regulation of human plasma triglyceride metabolism is supported by human genetic studies, which have shown that carriers of the E40K mutation and other inactivating variants have reduced plasma triglyceride concentrations and reduced risk of coronary artery disease [37], [38]. The crucial role of ANGPTL4 in governing plasma lipid levels in mice and humans has made ANGPTL4 an attractive therapeutic target for correcting dyslipidemia and associated cardiovascular disorders.

While there is overwhelming support for the role of ANGPTL4 as a fasting-induced inhibitor of LPL activity in rodent adipose tissue, evidence on ANGPTL4 in human adipose tissue is lacking. We have previously shown that human plasma ANGPTL4 levels increase with caloric restriction and during extended fasting [39] and that tissue ANGPTL4 and LPL protein levels negatively correlate in a cross-sectional analysis of human adipose tissue samples [40]. However, whether fasting influences ANGPTL4 protein levels and LPL activity in human adipose tissue remains unclear. Accordingly, the primary objective of this study is to determine the effect of a prolonged fast on ANGPTL4 gene and protein expression in human subcutaneous adipose tissue. An additional aim is to study the effect of a prolonged fast on LPL gene expression, LPL protein expression, and on LPL activity in subcutaneous adipose tissue. To characterize the mechanisms for the regulation of ANGPTL4 by fasting in human adipose tissue, we performed in vitro studies using primary human adipocytes.

Materials and methods

FASTING study

The FASTING study was approved by the Medical Ethics Committee of Wageningen University and registered at ClinicalTrials.gov, identifier: NCT03757767. In short, 24 healthy volunteers aged 40-70 years (median age 55 years) with a BMI of 22-30 kg/m^2 (median BMI 25 kg/m^2) were asked to consume a standardized meal until full (ad libitum), consisting of 22 energy% protein, 24 energy% fat, 51 energy% carbohydrate and 476 kJ per 100 gram. Two hours after consumption of the standardized meal, blood samples and a subcutaneous adipose tissue biopsy were taken. Twenty-four hours later, a second subcutaneous adipose tissue biopsy was taken and again blood samples were drawn. After consumption of the standardized meal until after the second measurements, subjects were only allowed to drink water. The subcutaneous adipose tissue samples were obtained by needle biopsy from the periumbilical area under local anesthesia. The samples were rinsed to eliminate blood and were immediately frozen in liquid nitrogen. All samples were stored in aliquots at -80°C.

Isolation and differentiation of human stromal vascular fraction

Anonymous samples of subcutaneous and visceral adipose tissue were collected from the abdominal region of patients undergoing elective cosmetic surgery at the Amsterdam Plastic Surgery, Amsterdam, The Netherlands (subcutaneous) or bariatric surgery for weight management at the Department of Bariatric Surgery, Rijnstate Hospital/Vitalys Clinic, Arnhem, The Netherlands (visceral). All study subjects gave written informed consent for the use of the tissue.

Material was collected in DMEM supplemented with 1% PS and 1% bovine serum albumin (BSA; Sigma-Aldrich). Upon arrival in the lab, the material was minced with scissors immediately and digested in collagenase-containing medium (DMEM with 3.2 mM CaCl2, 1.5 mg/ml collagenase type II (C6885, Sigma-Aldrich), 10% FBS, 0.5% BSA, and 15 mM HEPES) for 45-60 min at 37°C, with occasional vortexing. Cells were filtered through a 100-µm cell strainer (Falcon) to remove remaining cell clumps and lymph nodes. The cell suspension subsequently was centrifuged at 1600 rpm for 10 min and the pellet was resuspended in erythrocyte lysis buffer (155 mM NH_4Cl, 12 mM $NaHCO_3$, 0.1 mM EDTA). Upon incubation for 2 min at room temperature, cells were centrifuged at 1200 rpm for 5 min and the pelleted cells were resuspended in Growth medium (DMEM + 10% FBS + 1% P/S) and plated.

Upon confluence, the stromal vascular fraction (SVF) from subcutaneous origin were differentiated according to the standard protocol for 3T3-L1 cells with addition of 1 µM rosiglitazone [41]. Briefly, confluent SVFs were plated in 1:1 surface ratio, and differentiation was induced 2 days afterwards by switching to a differentiation induction cocktail (DMEM containing 10% FBS, 1% P/S, 0.5 mM isobutylmethylxanthine, 1 µM dexamethasone, 7 µg/ml insulin and 1 µM rosiglitazone) for 3 days. Subsequently, cells were maintained in Growth medium with addition of 7 µg/mL insulin for 3-6 days and switched to Growth medium only for 3 days, after which experiments have been performed. Average rate of differentiation was at least 80% as determined by eye.

SVFs from visceral origin were differentiated according to the 3D protocol described by Emont et al. [42] due to the very low differentiation rate of visceral preadipocytes when differentiated in a 2D well format. Briefly, pre-adipocytes were seeded at a concentration of 300,000 cells/500 µL collagen gel in a 24-well plate format. Pre-adipocytes were resuspended in Growth medium to a concentration of $6x10^6$ cells/mL, of which, per well, 50 µL were mixed with 100 µL 5x DMEM (Biozol, #1-25K34-I), 50 µL FBS and 50 µL 0.1N NaOH and 250 µL collagen solution (Corning, #354249), in this order, to create the 3D gel. After each step the solution was carefully mixed by pipetting up and down. Collagen solution was previously diluted to 8 mg/mL with 0.02N Acetic acid. The 3D gel was allowed to polymerize for 10-20 min in the incubator after which 0.5 mL of Growth medium were added per well. Differentiation was induced the next day according to the protocol described for the differentiation of subcutaneous pre-adipocytes. All cells were maintained in a humidified incubator at 37 ºC with 5% CO_2.

Cell culture treatments

Treatments of primary cells were done within 2 days after reaching differentiation. Cells were maintained in DMEM containing 10% FBS and 1% P/S until treatment with insulin (500 nM), cortisol (1 µM), dexamethasone (1 µM), or a mixture of oleate and palmitate (2:1, 300 µM total) for 24h. In a separate experiment, primary cells were incubated with 40 µg/mL cycloheximide for indicated durations. All compounds were from Sigma-Aldrich.

RNA isolation & Quantitative real-time PCR

Total RNA from subcutaneous adipose tissue from the FASTING study was isolated using TRIzol reagent (Thermo Fisher Scientific, the Netherlands) and purified using the Qiagen RNeasy Mini kit (Qiagen, the Netherlands). Total RNA from in vitro studies was isolated homogenizing in TRIzol (Thermo Fisher Scientific) either with a Qiagen Tissue Lyser II

(Qiagen, Venlo, The Netherlands) (visceral) or by pipetting up and down (subcutaneous). Reverse transcription was performed using the iScript™ cDNA Synthesis Kit (Biorad, the Netherlands) according to the manufacturer's protocol using 400-750 ng RNA for in vitro studies and 350 ng from human adipose tissue. Quantitative PCR amplifications were done on a CFX 384 Bio-Rad thermal cycler (Bio-Rad, the Netherlands) using SensiMix PCR reagents (Bioline, GC Biotech, the Netherlands). Gene expression values were normalized to one of housekeeping genes. Primer sequences of genes are provided in Supplemental Table 1.

Western blots

Protein lysates were made of subcutaneous adipose tissue from participants included in the FASTING study. The material was lysed in RIPA lysis buffer (25 mM Tris-HCl pH 7.6, 150 mM NaCl, 1% NP-40, 1% sodium; deoxycholate, 0.1% SDS; Thermo Fisher Scientific, the Netherlands) supplemented with protease and phosphatase inhibitors (Roche, The Netherlands) to make 20% protein lysates. After a 30-minute incubation on ice, the lysates were spun down at 13.000 rpm at 4 °C for 15 min in order to get rid of non-dissolved material and fat. Following the transfer of the infranatant to a clean tube, this procedure was repeated twice to get rid of excess fat. Protein concentrations of lysates were determined with BCA reagent (Thermo Fisher Scientific, the Netherlands). Next, lysates were mixed with 4x LSB loading buffer and denatured at 95 °C for 5 minutes. For each participant, 10 µg of protein was loaded per lane on 26- wells Criterion 8-16% TGX gels (Bio-Rad, the Netherlands) and separated by SDS gel electrophoresis. Separated proteins were transferred to a PVDF membrane by means of a Transblot Turbo System (Bio-Rad, the Netherlands). Primary antibodies (goat anti-human LPL antibody (Santa Cruz Biotechnology, #Y-20) and rabbit anti-human ANGPTL4 antibody (1187) [43] were used at a ratio of 1:1000 (#Y-20) or 1:5000 (1187). Rabbit anti-human GAPDH was used at 1:2000 (Cell signaling, #2118). All primary antibodies were incubated overnight at 4 °C. Corresponding secondary antibodies (HRP-conjugated) (Sigma-Aldrich, the Netherlands) were used at a 1:5000 dilution. All incubations were done in Tris-buffered saline, pH 7.5, with 0.1% Tween-20 (TBS-T) and 5% dry milk, whereas all washing steps were done in TBS-T without dry milk. Blots were visualized using the ChemiDoc MP system and Clarity ECL substrate (Bio-Rad, the Netherlands). Quantification of bands was performed using ImageLab software (Bio-Rad, the Netherlands).

Quantification of plasma parameters

Blood samples were collected in EDTA-coated tubes and centrifuged at 4°C for 15 min at 10000 g. Plasma was collected and stored at -80°C. Measurements of plasma levels of non-esterified fatty acids (NEFA) and beta-hydroxybutyrate were performed using kits from WAKO Diagnostics (Cat: 3055 and 417-73501/413-73601, WAKO Diagnostics, Germany) according to the manufacturer's protocol. Glucose, insulin, and triglycerides as well as total-, HDL-, and LDL-cholesterol were determined in lithium heparin plasma samples by hospital Gelderse Vallei, Ede, The Netherlands.

Plasma ANGPTL4 concentrations were determined using the ELISA kit from R&D systems (Cat: DY3485, R&D systems, the Netherlands) according to the manufacturer's protocol. Plasma Cortisol concentrations were determined using the ELISA kit from R&D systems (Cat: KGE008B R&D systems, the Netherlands) according to the manufacturer's protocol.

Plasma ANGPTL8 concentrations were determined by a sandwich ELISA assay using two monoclonal antibodies: a capture antibody to the N-terminal domain and detection antibody to the C-terminal domain (Hobbs, manuscript in preparation).

LPL activity measurements

Frozen subcutaneous adipose tissues biopsies were homogenized in 9 volumes of buffer at pH 8.2 containing 0.025 M ammonia, 1% Triton X-100, 0.1% SDS and protease inhibitor cocktail tablets (Complete Mini, Roche Diagnosis, Germany) using a Polytron PT 3000 Homogenizer (Kinematica). The homogenates were centrifuged for 15 min at 10,000 rpm, 4°C. Aliquots of the supernatants were used for determination of LPL activity as previously described using a phospholipid-stabilized emulsion of soy bean triacylglycerols and 3H-oleic acid-labeled triolein with the same composition as Intralipid 10% (Fresenius Kabi, Uppsala, Sweden) [13]. The incubation was at 25°C for 100 or 120 min. One milliunit of enzyme activity corresponds to 1 nmol of fatty acids released per min. Enzyme activity is expressed per g wet tissue weight. Protein contents in homogenates of adipose tissue were measured using Markwell's modified Lowry method [44].

Statistical analyses

Differences in plasma parameters, LPL activity, and subcutaneous adipose tissue gene expression between the fed and fasted state were evaluated using a paired Student's t-test. Individuals are always represented by the same color in the various fed-fasted line graphs. Differences in gene expression in the primary adipocytes were evaluated by unpaired Student's t-test. P-values < 0.05 were considered statistically significant.

Results

Between October and December 2018, 38 individuals were assessed for eligibility of which 14 were excluded from participation (Figure 1). The remaining 24 participants were invited to the research facilities for the FASTING study. One participant dropped out of the study, due to personal reasons that were not related to the study. The remaining 23 participants completed the study.

The main objective of this study was to determine the effect of a prolonged fast on ANGPTL4 gene and protein expression in human subcutaneous adipose tissue, and to link these effects with changes in LPL expression and activity. To that end, 23 healthy middle-aged men and women underwent a 24h fast. Participants received a standardized meal at 18.00h, followed by blood sampling and collection of an adipose tissue biopsy at 20.00h, representing the fed state. At 20.00h the next day, a second blood sample and adipose tissue biopsy were collected. Accordingly, the two blood samples and adipose tissue biopsies were taken at the same time, thereby avoiding the potential influence of circadian rhythmicity. The participant characteristics are listed in Table 1.

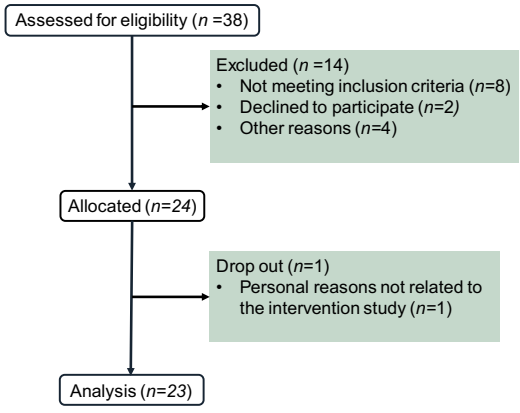

Figure 1: Flow chart of the FASTING study.

Table 1: Participants characteristics

Participants, n	24
Gender, n males (%)	8 (33%)
Age, years	43–71
Weight, kg	76.5 ± 10.5
BMI, kg/m^2	25.3 ± 2.4
Plasma cholesterol, mM	5.76 ± 0.96
HDL cholesterol, mM	1.68 ± 0.32
LDL cholesterol, mM	3.02 ± 0.84

Fasting significantly increased plasma levels of non-esterified fatty acids and β-hydroxybutyrate, and significantly decreased plasma triglycerides (Figure 2). The direction of the change is consistent with the known stimulatory effect of fasting on adipose tissue lipolysis and hepatic ketogenesis, and the inhibitory effect on plasma triglyceride secretion. Plasma glucose levels showed a more mixed response with most individuals showing a decrease, while 6 individuals showed an increase (Figure 2). Overall, these parameters confirm compliance to the fasting protocol.

In agreement with data from rats and mice [14], fasting led to a marked decrease in adipose tissue LPL activity (-60%, $p<0.001$) (Figure 3A), which was consistently observed in all participants. To determine the potential cause of the decrease in LPL activity, we measured the mRNA levels of LPL, ANGPTL4 and ANGPTL8 by qPCR in a subsection of the participants. LPL mRNA was slightly lower after the 24h fast but the difference did not reach statistical significance (Figure 3B). In most but not all individuals, adipose ANGPTL4 mRNA levels went up by fasting, with a mean increase of nearly two-fold (+90%, $p<0.001$). By contrast, ANGPTL8 mRNA levels went down drastically by fasting (-94%, $p<0.001$) (Figure 3B).

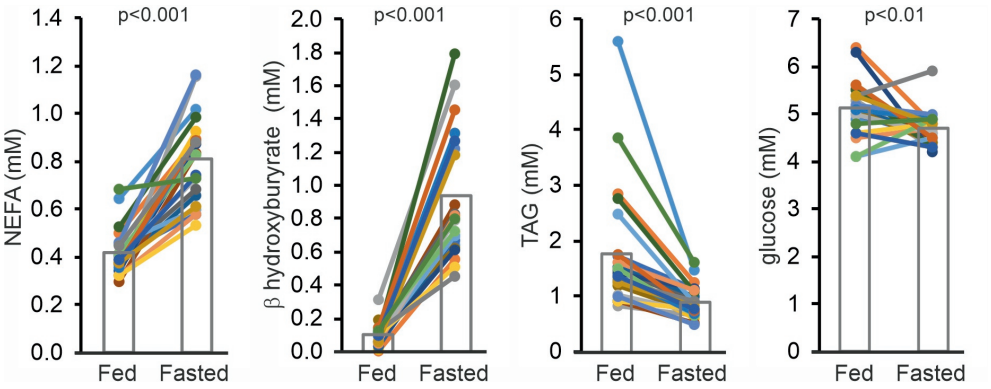

Figure 2: Influence of fasting on plasma metabolites. Plasma concentrations of non-esterified fatty acids (NEFA), β-hydroxybutyrate, triacylglycerol (TAG) and glucose after 2h (Fed) and 26h (Fasted) of fasting. Each line represents one individual. Individuals are depicted in the same color in all figures. Bars represent group means (N = 23).

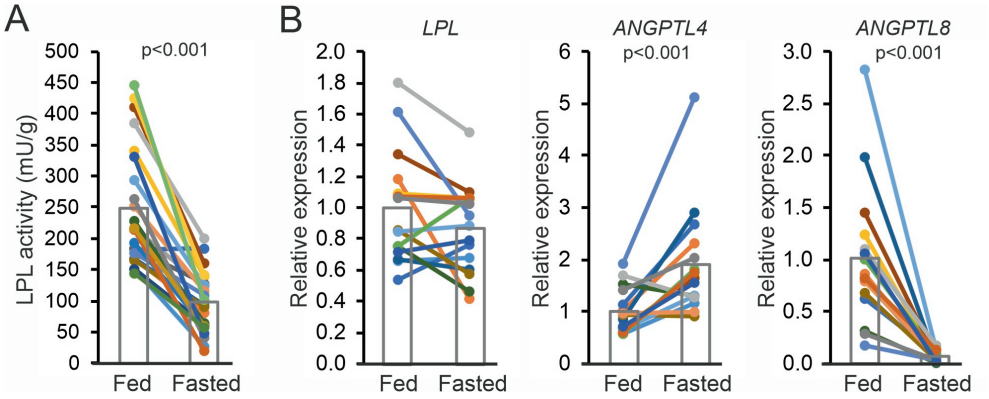

Figure 3: Fasting reduces LPL activity and increases *ANGPTL4* mRNA expression in human adipose tissue biopsies. A) LPL activity measured in subcutaneous adipose tissue samples collected after 2h (Fed) and 26h (Fasted) of fasting. Every line represents one individual and bars represent group means (N = 23). B) Relative mRNA levels for *LPL*, *ANGPTL4* and *ANGPTL8* in subcutaneous adipose tissue biopsies collected after 2h (Fed) and 26h (Fasted) of fasting, as determined by qPCR. Each line represents one individual and bars represent group means (N = 16). Individuals are depicted in the same color in all figures. The lower number of samples is due to limited availability of biopsy material. Statistical differences were assessed using the paired Student's t-test.

To determine if the increase in ANGPTL4 mRNA by fasting was accompanied by an increase in ANGPTL4 protein, we assessed ANGPTL4 protein levels in the subcutaneous adipose tissue biopsies using Western blot. As shown previously [43], only full length ANGPTL4 was detectable in human adipose tissue, which is in contrast to human liver where we observed substantial N-terminal ANGPTL4 cleavage product (Supplemental figure 1A). In most but not all individuals, the level of full length ANGPTL4 protein increased upon fasting (+46%, $p<0.05$). Conversely, the mean LPL protein level was lower after fasting, although this decrease did not reach statistical significance (Figure 4A,B). To determine if changes in ANGPTL4 mRNA and protein levels were associated with changes in plasma ANGPTL4 levels, we measured the plasma ANGPTL4 concentration before and after fasting using ELISA. In agreement with previous data [39], plasma ANGPTL4 concentrations went up in all participants (+100%, $p<0.001$) (Figure 4C). As the ANGPTL4 ELISA only measures full length and C-terminal ANGPTL4 [45], we also determined plasma levels of N-terminal ANGPTL4 by Western blot. Fasting modestly yet significantly induced plasma N-terminal ANGPTL4 levels (+15%, $p<0.05$) (Figure 4D). By contrast, plasma ANGPTL8 concentrations were decreased by fasting in all participants (-79%, $p<0.001$) (Figure 4E).

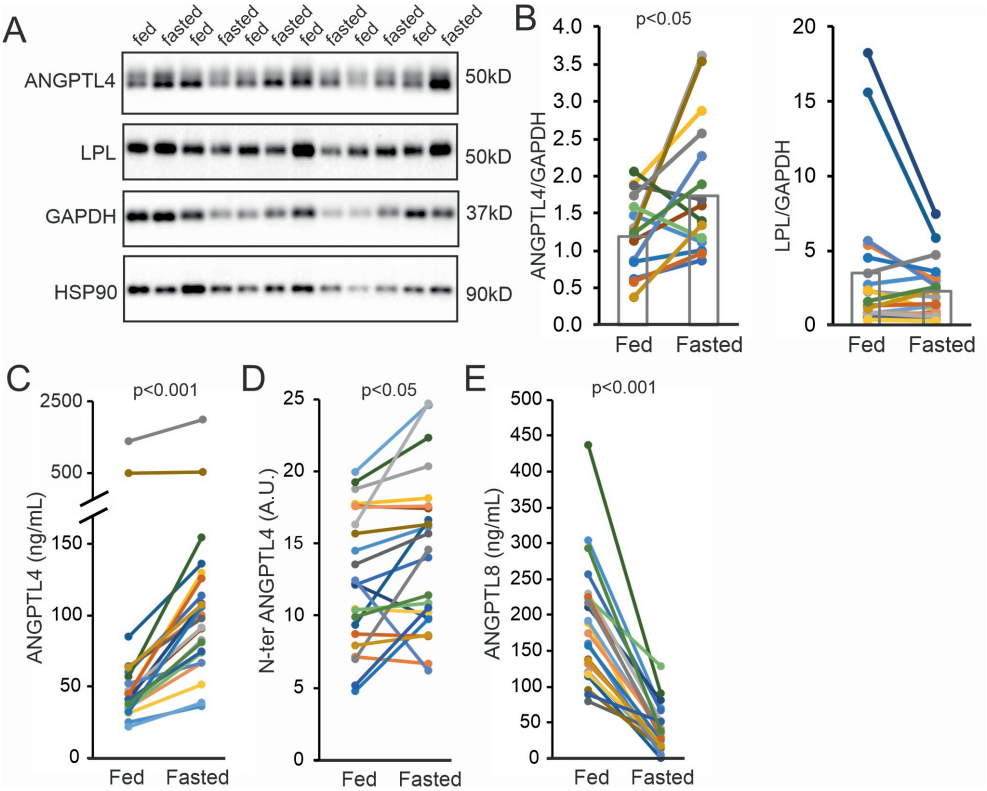

Figure 4: Fasting increases ANGPTL4 protein in human adipose tissue and plasma. A) Representative Western blots for ANGPTL4, LPL, GAPDH and HSP90 in subcutaneous adipose tissue samples of 6 individuals collected after 2h (Fed) and 26h (Fasted) of fasting. B) Quantitative analysis of ANGPTL4 and LPL protein levels in subcutaneous adipose tissue normalized to GAPDH. Each line represents one individual and bars representing group means (N = 19 resp. 20. C) Plasma levels of ANGPTL4 after 2h (Fed) and 26h (Fasted) of fasting as determined by ELISA (N = 23). D) Plasma levels of N-terminal ANGPTL4 after 2h (Fed) and 26h (Fasted) of fasting as determined by Western blot (N = 23). E) Plasma levels of ANGPTL8 after 2h (Fed) and 26h (Fasted) of fasting as determined by ELISA (N = 23). Individuals are depicted in the same color in all figures.

The expression of ANGPTL4 in adipose tissue of mice is known to be under control of various stimuli and transcriptional regulators. For instance, ANGPTL4 expression was previously found to be repressed by insulin [46]. In our study, fasting drastically reduced plasma levels of insulin (-95%, p<0.001) (Figure 5A), suggesting the increase in adipose ANGPTL4 levels during fasting might be related to the decline in plasma insulin. To investigate whether insulin lowers ANGPTL4 expression in vivo, we extracted data from a transcriptomics dataset of adipose tissue biopsies from human subjects before and after 3 hours intravenously maintained euglycemic hyperinsulinemia [47]. Strikingly, ANGPTL4 mRNA

levels were markedly reduced by insulin in vivo in both insulin-sensitive and resistant individuals (Figure 5B). By contrast, ANGPTL8 mRNA levels went up, especially in the insulin-sensitive individuals (Figure 5B). These data support a possible role of insulin in the regulation of ANGPTL4 expression in human adipose tissue during fasting, but do not indicate whether insulin has a direct role in regulating ANGPTL4 in human adipose tissue. To address this question, we cultured primary human adipocytes. In these cells, full length ANGPTL4 protein was easily detectable by immunoblot, whereas N-terminal ANGPTL4 was absent (Supplemental figure 1B). The lack of ANGPTL4 cleavage in cultured human adipocytes is supported by experiments in human Lisa-2 adipocytes (Supplemental figure 1C) and SGBS adipocytes [43], [48]. Levels of ANGPTL4 protein declined rapidly after treatment with cycloheximide, indicating that ANGPTL4 has a fast turnover in human adipocytes (Figure 5C, D).

In primary adipocytes from visceral and subcutaneous adipose tissue, insulin significantly reduced *ANGPTL4* mRNA after 24h treatment (Figure 5E). In visceral adipocytes, insulin also markedly decreased ANGPTL4 protein levels (Figure 5F). In line with data from mouse adipocytes [35], [46], these data indicate the insulin directly suppresses ANGPTL4 gene and protein expression in human adipocytes. Besides insulin, another factor that may be involved in regulating ANGPTL4 levels during fasting is cortisol. Fasting significantly increased plasma cortisol concentrations in the human volunteers (Figure 6A). In the primary human adipocytes, cortisol as well as dexamethasone significantly increased ANGPTL4 mRNA and protein levels (Figure 6B). Interestingly, free fatty acids, plasma levels of which were elevated during fasting (Figure 2), also increased ANGPTL4 mRNA and protein levels (Figure 6B). These data suggest that the increase in ANGPTL4 production in adipose tissue upon fasting is likely mediated by increased plasma cortisol and free fatty acids, and decreased plasma insulin.

Consistent with the increase in *ANGPTL8* mRNA levels in adipose tissue after insulin infusion, insulin markedly increased *ANGPTL8* mRNA levels in primary human adipocytes (Figure 6C). Cortisol and dexamethasone also induced *ANGPTL8* mRNA but to a smaller extent. Intriguingly, *LPL* mRNA levels in the primary human adipocytes were significantly increased by insulin, cortisol, and dexamethasone (Figure 6C).

As ANGPTL4 and ANGPTL8 are regulated by insulin, we hypothesized that *ANGPTL4* and *ANGPTL8* mRNA levels in human adipose tissue may respond to weight loss, which is known to increase insulin sensitivity. To that end, we analyzed adipose gene expression data from subjects before and after 5 weeks on a very-low-calorie diet (500 Kcal/day), followed by a 4-week weight maintenance diet based on their individual energy requirements [49]. Intriguingly, after 5 weeks of very-low-calorie diet, when subjects were in a hypocaloric state and actively losing weight, *ANGPTL4* and *ANGPTL8* mRNA levels were significantly

increased and decreased, respectively. By contrast, after weight loss and in a eucaloric state of weight stability, *ANGPTL4* and *ANGPTL8* mRNA had returned to pre-weight loss values. *LPL* mRNA largely followed *ANGPTL8* mRNA. These data indicate that *ANGPTL4*, *ANGPTL8*, and *LPL* mRNA in human adipose tissue are not affected by weight loss as such but respond to a negative energy balance.

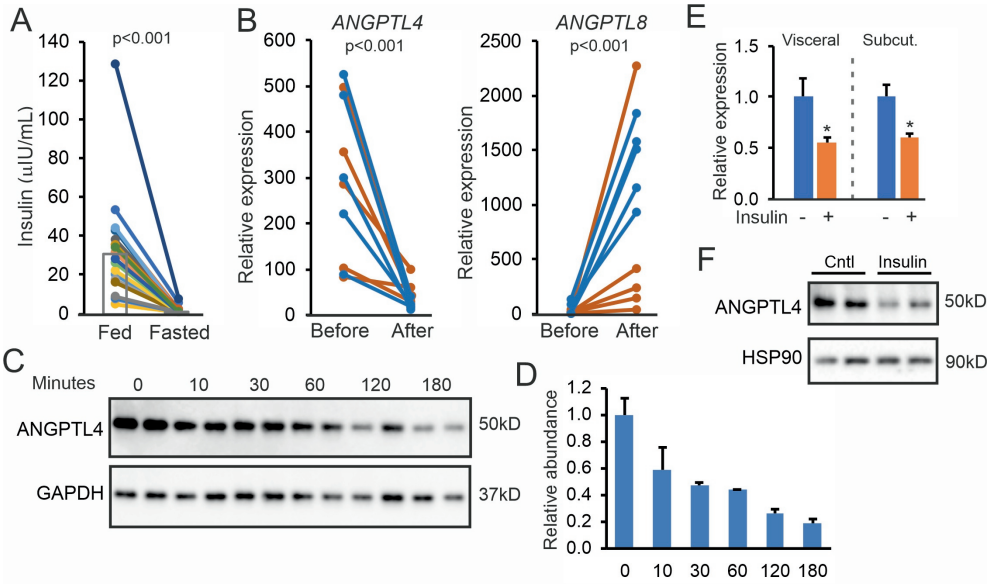

Figure 5: Insulin downregulates ANGPTL4 *in vivo* and *in vitro*. A) Plasma insulin concentration after 2h (Fed) and 26h (Fasted) of fasting. Each line represents one individual. Individuals are depicted in the same color in all figures. Bars represent group means (N = 23). B) Adipose tissue mRNA levels of *ANGPTL4* and *ANGPTL8* in insulin-sensitive (blue lines) and insulin-resistant (orange lines) subjects before and after a hyperinsulinemic clamp. Data were extracted from GSE26637. C) Western blot for ANGPTL4 and GAPDH in primary human subcutaneous adipocytes treated with cycloheximide for different durations. D) Quantification of the ANGPTL4 levels relative to GAPDH. E) ANGPTL4 mRNA in primary human visceral and subcutaneous adipocytes treated with 500 nM insulin for 24h. F) Western blot for ANGPTL4 and HSP90 in primary human visceral adipocytes treated with insulin. HSP90 was blotted as a loading control. Statistical differences for in vitro experiments were assessed using the unpaired Student's t-test. *p<0.05, relative to control treatment.

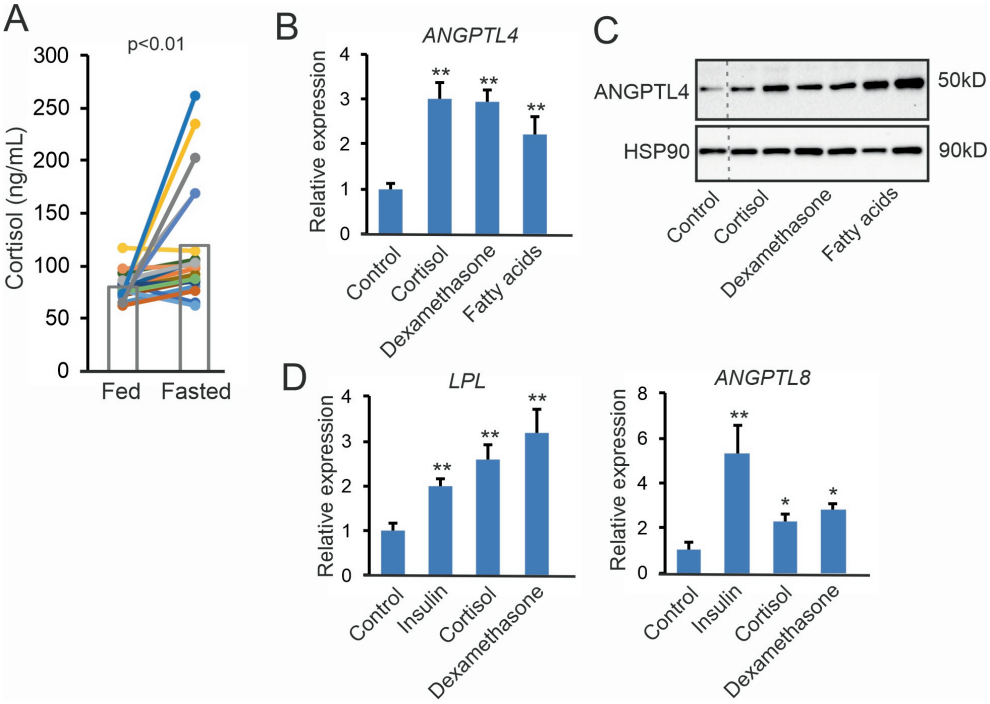

Figure 6: Corticosteroids and fatty acids upregulate ANGPTL4 primary human adipocytes. A) Plasma cortisol concentration after 2h (Fed) and 26h (Fasted) of fasting. Each line represents one individual. Individuals are depicted in the same color in all figures. Bars represent group means (N = 23). *ANGPTL4* mRNA (B) and ANGPTL4 protein levels (C) in primary human visceral adipocytes treated with cortisol (1 µM), dexamethasone (1 µM), or a mixture of oleate and palmitate (2:1, 300 µM total) for 24h. HSP90 was blotted as a loading control. D) *LPL* and *ANGPTL8* mRNA in primary human subcutaneous adipocytes treated with insulin (500 nM), cortisol (1 µM), or dexamethasone (1 µM) for 24h. Statistical differences for in vitro experiments were assessed using the unpaired Student's t-test. *p<0.05, **p<0.01, ***p<0.001, relative to control treatment.

Discussion

In this paper we show that a 24h fast in human volunteers markedly reduces LPL activity in subcutaneous adipose tissue, concomitant with significant increases in adipose tissue *ANGPTL4* mRNA, adipose tissue ANGPTL4 protein, and plasma ANGPTL4 levels. By contrast, fasting decreases adipose tissue *ANGPTL8* mRNA and plasma ANGPTL8 levels. In cultured human adipocytes, insulin significantly decreased ANGPTL4 mRNA and protein, whereas cortisol and fatty acids had the opposite effect. Inasmuch as plasma insulin levels decrease upon fasting, and plasma cortisol and free fatty acid levels increase upon fasting, the increase in ANGPTL4 production in adipose tissue upon fasting is likely mediated by changes in these factors. Overall, our results strongly support the notion derived from studies in rodents that local upregulation of ANGPTL4 mediates the decrease in LPL activity and associated lipid storage in adipose tissue during fasting in humans. Consistent with its role as rapidly inducible regulator of LPL activity during fasting, we found that ANGPTL4 protein in human adipocytes turns over rapidly, at a rate that is faster than the turnover rate of LPL protein and activity determined in rat adipose tissue [13], [14].

LPL activity controls plasma triglyceride clearance [6]. The activity of LPL is differentially regulated in various tissues in accordance with the local physiological needs for fatty acids. In agreement with observations made in rodents [10]–[14], studies in human volunteers have shown that LPL activity in adipose tissue is reduced by fasting [50]–[54], thereby diverting circulating triglycerides to other tissues. An important and previously unaddressed question was whether the fasting-induced decrease in adipose LPL activity in humans is driven by corresponding changes in LPL expression or whether it is mainly due to a post-translational mechanism via ANGPTL4. Biochemical studies combined with studies in mice have shown that ANGPTL4 is upregulated by fasting in mouse adipose tissue [14], [26], [32], [35] and promotes the unfolding of LPL [33], thereby activating the intracellular cleavage and subsequent degradation of LPL [34], [35]. The present data indicate that ANGPTL4 is upregulated by fasting in human adipose tissue, concurrent with a marked decrease in LPL activity and a lack of change in *LPL* mRNA. Although the human data are inevitably correlative, they are highly consistent with conservation of the post-translational control of adipose tissue LPL activity during fasting between rodents and humans via ANGPTL4.

Previously, we showed that ANGPTL4 promotes the degradation of LPL in adipose tissue of mice, thereby reducing the amount of LPL available on the capillary surface [34]. We also found that ANGPTL4 and LPL protein levels negatively correlate in a cross-sectional analysis of human adipose tissue samples from obese individuals [40]. In this study, we observed that the increase in ANGPTL4 protein levels in human adipose tissue upon fasting was not paralleled by a significant decrease in LPL protein. A number of possibilities may explain

these findings. First, the method of detecting LPL via immunoblot may not be sufficiently precise to pick up small changes in LPL levels. Here, it should be noted that the mean LPL protein level was lower after fasting but this change did not reach statistical significance. Second, the immunoblot may measure the wrong LPL pool. Here, it would have been useful to be able to distinguish between EndoH-sensitive and EndoH-resistant LPL, which in mouse adipose tissue can be used to differentiate between inactive ER-resident LPL and active LPL in the Golgi and on the cell surface, respectively. However, we were unable to visualize EndoH-sensitive and EndoH-resistant LPL in human adipose tissue. Hence, it is possible that in human adipose tissue, most of the immunoreactive LPL is inactive and in the ER. Third, the timing of sampling of the adipose tissue biopsies in relation to the meal may not have been optimal. Indeed, in mice, the level of LPL protein in adipose tissue is higher in the refed state than in the ad libitum fed state [34]. Fourth, it cannot be excluded that in human adipocytes, ANGPTL4 only unfolds LPL and inhibits LPL activity, but does not regulate LPL degradation and LPL protein levels.

A number of factors may contribute to the upregulation of ANGPTL4 mRNA and protein levels in human adipose tissue during fasting. Expression of *ANGPTL4* in mouse or human adipocytes is known to be regulated via several different signals, including hypoxia (stimulatory), insulin (inhibitory) [35], [46], glucocorticoids (stimulatory) [55], tumor necrosis factor α (stimulatory) [56], and PPARγ agonists (stimulatory) [43]. We show that ANGPTL4 levels in human adipocytes are also increased by fatty acids, confirming regulation in other cell types [39], [57]. In addition, we find that ANGPTL4 levels in human adipocytes are decreased and increased by insulin and glucocorticoids, respectively. Induction by glucocorticoids is mediated by binding of the glucocorticoid receptor to the 3'-untranslated region of exon 7 [55]. Inhibition of *Angptl4* expression by insulin in mouse adipocytes is likely mediated by the PI3K/Foxo1 pathway [46]. Overall, the data suggest that the increased ANGPTL4 production in adipose tissue upon fasting is likely mediated by changes in plasma levels of insulin, cortisol, and fatty acids.

Intriguingly, ANGPTL4 was less sensitive to the suppressive effect of insulin in subcutaneous adipocytes than visceral adipocytes. This is in line with our previous finding that ANGPTL4 mRNA levels are higher in subcutaneous adipose tissue than in visceral adipose tissue [40], which in turn is in agreement with the finding that the LPL activity/mass ratio is lower in subcutaneous than visceral adipose tissue [58]. Why insulin less effectively lowers ANGPTL4 in subcutaneous adipocytes is not clear.

Clearance of plasma triglycerides is promoted by insulin. Accordingly, the impaired action of insulin in type 2 diabetes leads to reduced plasma triglyceride clearance, which in turn contributes to elevated post-prandial lipid excursions and fasting dyslipidemia [59]. Taking into consideration the repression of adipocyte ANGPTL4 mRNA by insulin [35], [46],

upregulation of ANGPTL4 in insulin resistance may contribute to the postprandial dyslipidemia in insulin-resistant individuals via inhibition of LPL. In support, type 2 diabetics present with elevated circulating ANGPTL4 levels [60]. Contradicting this scenario, however, the reduction in adipose ANGPTL4 mRNA during a hyperinsulinemic clamp was similar in insulin-sensitive and resistant individuals. In addition, weight loss, despite an improvement in insulin sensitivity, did not influence ANGPTL4 mRNA levels in human adipose tissue. Existing data on the relation between insulin resistance and adipose tissue LPL activity are mixed as well. In a group of 26 subjects varying in insulin sensitivity, insulin resistance was negatively correlated with adipose tissue LPL activity [61]. Consistent with these data, in type 2 diabetic men, adipose tissue LPL activity was significantly reduced compared to matched non-diabetic subjects, while the differences were more modest in women [62]. By contrast, Olivecrona found that the induction of adipose tissue LPL activity with feeding was similar in type 2 diabetes patients and matched healthy controls, suggesting that dysregulation of adipose LPL is not involved in the postprandial hypertriglyceridaemia in type 2 diabetes [63]. Overall, these data make it difficult to assign a role for aberrant ANGPTL4 regulation in post-prandial hypertriglyceridemia in type 2 diabetes.

We found that human adipose tissue and adipocytes only produce full length ANGPTL4. Based on the inability to detect full length ANGPTL4 in human plasma, it could be reasoned that ANGPTL4 produced in adipose tissue does not end up in the circulation, suggesting it has a local role. Alternatively, adipose tissue-derived full length ANGPTL4 may undergo cleavage in the circulation. As the plasma concentration of full length ANGPTL4 is probably very low, the ANGPTL4 ELISA, which is able to detect full length and C-terminal ANGPTL4 but not N-terminal ANGPTL4 [45], in essence measures plasma levels of C-terminal ANGPTL4.

In this paper we find that adipose tissue ANGPTL8 expression is markedly reduced by fasting. Most of the published data relate to the role of ANGPTL8 in the liver, where in the fed state ANGPTL8 forms a complex with ANGPTL3 and supports the inhibition of plasma triglyceride clearance by ANGPTL3 in brown adipose tissue, heart, and muscle, thereby rerouting plasma triglycerides to white adipose tissue for storage [22], [24]. Recently, evidence was presented that ANGPTL8, via direct protein interaction, may interfere with the ability of ANGPTL4 to inhibit LPL [36]. Presumably, in the fed state, when ANGPTL8 expression is high, ANGPTL8 suppresses ANGPTL4 function, thereby promoting adipose tissue LPL activity. The extent to which adipose tissue contributes to the changes in plasma ANGPTL8 during fasting is unclear. Interestingly, in human adipocytes, ANGPTL8 mRNA was upregulated by cortisol and dexamethasone, although to a lesser extent than by insulin. The impact of the induction of ANGPTL8 by glucocorticoids on LPL activity needs further investigation.

This paper has limitations. First, our study cannot demonstrate a direct causal link between the upregulation of ANGPTL4 in human adipose tissue during fasting and the decrease in LPL activity. Nevertheless, the plethora of pre-clinical data combined with our data strongly suggest that upregulation of ANGPTL4, and possibly the downregulation of ANGPTL8, causes the decrease in adipose tissue LPL activity in humans during fasting. Second, we were unable to visualize LPL protein in the human primary adipocytes. For reasons that are unclear, LPL is very hard to detect in primary adipocytes compared to adipose tissue, and its migration is dubious.

In conclusion, our data support the notion that upregulation of ANGPTL4 mediates the decrease in LPL activity and associated lipid storage in adipose tissue during fasting in humans. The increase in ANGPTL4 production in human adipose tissue by fasting is likely mediated by increased plasma cortisol and free fatty acids, and decreased plasma insulin.

Acknowledgements/Grant support

We thank Madelene Ericsson and Rakel Nyrén (Department of Medical Biosciences/Physiological Chemistry, Umeå University, Sweden) for their technical assistance with the LPL activity measurements, and Lisa Pool, Morena Bertuzzi and Noa Kapteyn (Wageningen University) for helping out with the experiments in human adipocytes.

This work was supported by the Netherlands Heart Foundation (CVON ENERGISE grant CVON2014–02).

Declaration of interest

None

Author contributions

Philip M. M. Ruppert Conceptualization, Methodology, Validation, Formal analysis, Investigation, Writing – Original draft, Writing – Review & Editing, Visualization, Supervision

Charlotte C.J.R. Michielsen Conceptualization, Methodology, Formal analysis, Investigation, Resources, Data curation, Writing – Review & Editing, Visualization

Eric J. Hazebroek Resources, Writing – Review & Editing

Ali Pirayesh Resources, Writing – Review & Editing

Gunilla Olivecrona Resources, Writing – Review & Editing

Lydia A. Afman Conceptualization, Writing – Review & Editing, Supervision, Project administration, Funding acquisition

Sander Kersten Conceptualization, Formal analysis, Writing – Original draft, Writing – Review & Editing, Visualization, Supervision, Project administration, Funding acquisition

References

[1] P. B. Sandesara, S. S. Virani, S. Fazio, and M. D. Shapiro, "The Forgotten Lipids: Triglycerides, Remnant Cholesterol, and Atherosclerotic Cardiovascular Disease Risk," *Endocr. Rev.*, vol. 40, no. 2, pp. 537–557, Apr. 2019.

[2] A. Onat, I. Sari, M. Yazici, G. Can, G. Hergenç, and G. Ş. Avci, "Plasma triglycerides, an independent predictor of cardiovascular disease in men: A prospective study based on a population with prevalent metabolic syndrome," *Int. J. Cardiol.*, vol. 108, no. 1, pp. 89–95, Mar. 2006.

[3] J. E. Hokanson and M. A. Austin, "Plasma triglyceride level is a risk factor for cardiovascular disease independent of high-density lipoprotein cholesterol level: A metaanalysis of population-based prospective studies," *Eur. J. Cardiovasc. Prev. Rehabil.*, vol. 3, no. 2, pp. 213–219, 1996.

[4] K. Musunuru and S. Kathiresan, "Surprises From Genetic Analyses of Lipid Risk Factors for Atherosclerosis.," *Circ. Res.*, vol. 118, no. 4, pp. 579–85, Feb. 2016.

[5] I. J. Goldberg, R. H. Eckel, and N. A. Abumrad, "Regulation of fatty acid uptake into tissues: Lipoprotein lipase- And CD36-mediated pathways," *J. Lipid Res.*, vol. 50 Suppl, no. SUPPL., pp. S86-90, Apr. 2009.

[6] S. Kersten, "Physiological regulation of lipoprotein lipase," *Biochim. Biophys. Acta - Mol. Cell Biol. Lipids*, vol. 1841, no. 7, pp. 919–933, 2014.

[7] C. N. Goulbourne *et al.*, "The GPIHBP1-LPL complex is responsible for the margination of triglyceride-rich lipoproteins in capillaries," *Cell Metab.*, vol. 19, no. 5, pp. 849–860, May 2014.

[8] A. P. Beigneux *et al.*, "Autoantibodies against GPIHBP1 as a Cause of Hypertriglyceridemia," *N. Engl. J. Med.*, vol. 376, no. 17, pp. 1647–1658, Apr. 2017.

[9] B. S. J. Davies *et al.*, "GPIHBP1 is responsible for the entry of lipoprotein lipase into capillaries," *Cell Metab.*, vol. 12, no. 1, pp. 42–52, Jul. 2010.

[10] C. H. Hollenberg, "Effect of nutrition on activity and release of lipase from rat adipose tissue," *Am. J. Physiol. Content*, vol. 197, no. 3, pp. 667–670, Sep. 1959.

[11] A. Cherkes and R. S. Gordon, "The liberation of lipoprotein lipase by heparin from adipose tissue incubated in vitro," *J. Lipid Res.*, vol. 1, no. 1, pp. 97–101, Oct. 1959.

[12] M. Bergö, G. Olivecrona, and T. Olivecrona, "Forms of lipoprotein lipase in rat tissues: In adipose tissue the proportion of inactive lipase increases on fasting," *Biochem. J.*, vol. 313, no. 3, pp. 893–898, Feb. 1996.

[13] M. Bergö, G. Wu, T. Ruge, and T. Olivecrona, "Down-regulation of adipose tissue lipoprotein lipase during fasting requires that a gene, separate from the lipase gene, is switched on," *J. Biol. Chem.*, vol. 277, no. 14, pp. 11927–11932, Apr. 2002.

[14] O. Kroupa *et al.*, "Linking nutritional regulation of Angptl4, Gpihbp1, and Lmf1 to lipoprotein lipase activity in rodent adipose tissue.," *BMC Physiol.*, vol. 12, p. 13, 2012.

[15] T. Ruge, G. Wu, T. Olivecrona, and G. Olivecrona, "Nutritional regulation of lipoprotein lipase in mice," *Int. J. Biochem. Cell Biol.*, vol. 36, no. 2, pp. 320–329, 2004.

[16] M. H. Doolittle, O. Ben-Zeev, J. Elovson, D. Martin, and T. G. Kirchgessner, "The Response of Lipoprotein Lipase to Feeding and Fasting. Evidence for Posttranslational Regulation," *Journal of Biological Chemistry*, 15-Mar-1990. [Online]. Available: http://www.jbc.org/content/265/8/4570.abstract. [Accessed: 03-Apr-2020].

[17] C. F. Semenkovich, M. Wims, L. Noe, J. Etienne, and L. Chan, "Insulin regulation of lipoprotein lipase activity in 3T3-L1 adipocytes is mediated at posttranscriptional and posttranslational levels.," *J. Biol. Chem.* , vol. 264, no. 15, pp. 9030–9038, May 1989.

[18] G. BENGTSSON and T. OLIVECRONA, "Lipoprotein Lipase: Mechanism of Product Inhibition," *Eur. J. Biochem.*, vol. 106, no. 2, pp. 557–562, 1980.

[19] W. Dijk and S. Kersten, "Regulation of lipid metabolism by angiopoietin-like proteins," *Curr. Opin. Lipidol.*, vol. 27, no. 3, pp. 249–256, Jun. 2016.

[20] R. Zhang, "The ANGPTL3-4-8 model, a molecular mechanism for triglyceride trafficking," *Open Biol.*, vol. 6, no. 4, p. 150272, 2016.

[21] X. Chi *et al.*, "ANGPTL8 promotes the ability of ANGPTL3 to bind and inhibit lipoprotein lipase," *Mol. Metab.*, vol. 6, no. 10, pp. 1137–1149, Oct. 2017.

[22] J. F. Haller *et al.*, "ANGPTL8 requires ANGPTL3 to inhibit lipoprotein lipase and plasma triglyceride clearance," *J. Lipid Res.*, vol. 58, no. 6, pp. 1166–1173, Jun. 2017.

[23] R. Zhang, "Lipasin, a novel nutritionally-regulated liver-enriched factor that regulates serum triglyceride levels," *Biochem. Biophys. Res. Commun.*, vol. 424, no. 4, pp. 786–792, Aug. 2012.

[24] Y. Wang *et al.*, "Mice lacking ANGPTL8 (Betatrophin) manifest disrupted triglyceride metabolism without impaired glucose homeostasis," *Proc. Natl. Acad. Sci.*, vol. 110, no. 40, pp. 16109–16114, Oct. 2013.

[25] Y. Wang *et al.*, "Hepatic ANGPTL3 regulates adipose tissue energy homeostasis," *Proc. Natl. Acad. Sci. U. S. A.*, vol. 112, no. 37, pp. 11630–11635, Sep. 2015.

[26] S. Kersten *et al.*, "Characterization of the fasting-induced adipose factor FIAF, a novel peroxisome proliferator-activated receptor target gene.," *J. Biol. Chem.*, vol. 275, no. 37, pp. 28488–93, Sep. 2000.

[27] K. Yoshida, T. Shimizugawa, M. Ono, and H. Furukawa, "Angiopoietin-like protein 4 is a potent hyperlipidemia-inducing factor in mice and inhibitor of lipoprotein lipase," *J. Lipid Res.*, vol. 43, no. 11, pp. 1770–1772, Nov. 2002.

[28] A. Köster *et al.*, "Transgenic angiopoietin-like (Angptl)4 overexpression and targeted disruption of Angptl4 and Angptl3: Regulation of triglyceride metabolism," *Endocrinology*, vol. 146, no. 11, pp. 4943–4950, 2005.

[29] S. Mandard *et al.*, "The fasting-induced adipose factor/angiopoietin-like protein 4 is physically associated with lipoproteins and governs plasma lipid levels and adiposity," *J. Biol. Chem.*, vol. 281, no. 2, pp. 934–944, Jan. 2006.

[30] V. Sukonina, A. Lookene, T. Olivecrona, and G. Olivecrona, "Angiopoietin-like protein 4 converts lipoprotein lipase to inactive monomers and modulates lipase activity in adipose tissue.," *Proc. Natl. Acad. Sci. U. S. A.*, vol. 103, no. 46, pp. 17450–5, Nov. 2006.

[31] L. Lichtenstein *et al.*, "Angptl4 Upregulates Cholesterol Synthesis in Liver via Inhibition of LPL- and HL-Dependent Hepatic Cholesterol Uptake," *Arterioscler. Thromb. Vasc. Biol.*, vol. 27, no. 11, pp. 2420–2427, Nov. 2007.

[32] E. M. Cushing, X. Chi, K. L. Sylvers, S. K. Shetty, M. J. Potthoff, and B. S. J. Davies, "Angiopoietin-like 4 directs uptake of dietary fat away from adipose during fasting.," *Mol. Metab.*, vol. 6, no. 8, pp. 809–818, 2017.

[33] S. Mysling *et al.*, "The angiopoietin-like protein ANGPTL4 catalyzes unfolding of the hydrolase domain in lipoprotein lipase and the endothelial membrane protein GPIHBP1 counteracts this unfolding," *Elife*, vol. 5, no. 45, pp. 1–23, Dec. 2016.

[34] W. Dijk, A. P. Beigneux, M. Larsson, A. Bensadoun, S. G. Young, and S. Kersten, "Angiopoietin-like 4 (ANGPTL4) promotes intracellular degradation of lipoprotein lipase in adipocytes.," *J. Lipid Res.*, vol. 7, no. 11, pp. 956–963, 2016.

[35] W. Dijk, P. M. M. Ruppert, L. J. Oost, and S. Kersten, "Angiopoietin-like 4 promotes the intracellular cleavage of lipoprotein lipase by PCSK3/furin in adipocytes," *J. Biol. Chem.*, vol. 1, no. 3, p. jbc.RA118.002426, 2018.

[36] O. Kovrov, K. K. Kristensen, E. Larsson, M. Ploug, and G. Olivecrona, "On the mechanism of angiopoietin-like protein 8 for control of lipoprotein lipase activity," *J. Lipid Res.*, p. jlr.M088807, Jan. 2019.

[37] F. E. Dewey *et al.*, "Inactivating Variants in ANGPTL4 and Risk of Coronary Artery Disease.," *N. Engl. J. Med.*, vol. 374, no. 12, pp. 1123–33, Mar. 2016.

[38] K. Abid *et al.*, "ANGPTL4 variants E40K and T266M are associated with lower fasting triglyceride levels and predicts cardiovascular disease risk in type 2 diabetic Tunisian population," *Lipids Health Dis.*, vol. 15, no. 1, 2016.

[39] S. Kersten *et al.*, "Caloric restriction and exercise increase plasma ANGPTL4 levels in humans via elevated free fatty acids.," *Arterioscler. Thromb. Vasc. Biol.*, vol. 29, no. 6, pp. 969–74, Jun. 2009.

[40] W. Dijk, S. Schutte, E. O. Aarts, I. M. C. Janssen, L. Afman, and S. Kersten, "Regulation of angiopoietin-like 4 and lipoprotein lipase in human adipose tissue," *J. Clin. Lipidol.*, vol. 12, no. 3, pp. 773–783, 2018.

[41] S. Alex *et al.*, "Short-Chain Fatty Acids Stimulate Angiopoietin-Like 4 Synthesis in Human Colon Adenocarcinoma Cells by Activating Peroxisome Proliferator-Activated Receptor," *Mol. Cell. Biol.*, vol. 33, no. 7, pp. 1303–1316, 2013.

[42] M. P. Emont *et al.*, "Using a 3D Culture System to Differentiate Visceral Adipocytes In Vitro," *Endocrinology*, vol. 156, no. 12, pp. 4761–4768, Dec. 2015.

[43] S. Mandard *et al.*, "The direct peroxisome proliferator-activated receptor target fasting-induced adipose factor (FIAF/PGAR/ANGPTL4) is present in blood plasma as a truncated protein that is increased by fenofibrate treatment," *J. Biol. Chem.*, vol. 279, no. 33, pp. 34411–34420, Aug. 2004.

[44] M. A. K. Markwell, S. M. Haas, L. L. Bieber, and N. E. Tolbert, "A modification of the Lowry procedure to simplify protein determination in membrane and lipoprotein samples," *Anal. Biochem.*, vol. 87, no. 1, pp. 206–210, Jun. 1978.

[45] J. T. Jonker *et al.*, "Dietary modulation of plasma angiopoietin-like protein 4 concentrations in healthy volunteers and in patients with type 2 diabetes," *Am. J. Clin. Nutr.*, vol. 97, no. 2, pp. 255–260, Feb. 2013.

[46] T. Yamada, N. Ozaki, Y. Kato, Y. Miura, and Y. Oiso, "Insulin downregulates angiopoietin-like protein 4 mRNA in 3T3-L1 adipocytes," *Biochem. Biophys. Res. Commun.*, vol. 347, no. 4, pp. 1138–1144, Sep. 2006.

[47] J. Soronen *et al.*, "Adipose tissue gene expression analysis reveals changes in inflammatory, mitochondrial respiratory and lipid metabolic pathways in obese insulin-resistant subjects," *BMC Med. Genomics*, vol. 5, 2012.

[48] M. Wabitsch, S. Brüderlein, I. Melzner, M. Braun, G. Mechtersheimer, and P. Möller, "LiSa-2, a novel human liposarcoma cell line with a high capacity for terminal adipose differentiation.," *Int. J. cancer*, vol. 88, no. 6, pp. 889–94, Dec. 2000.

[49] N. J. T. Roumans, R. G. Vink, F. G. Bouwman, P. Fazelzadeh, M. A. Van Baak, and E. C. M. Mariman, "Weight loss-induced cellular stress in subcutaneous adipose tissue and the risk for weight regain in overweight and obese adults," *Int. J. Obes.*, vol. 41, no. 6, pp. 894–901, Jun. 2017.

[50] R. V. Farese, T. J. Yost, and R. H. Eckel, "Tissue-specific regulation of lipoprotein lipase activity by insulin/glucose in normal-weight humans," *Metabolism*, vol. 40, no. 2, pp. 214–216, Feb. 1991.

[51] P. MÅRIN, M. REBUFFÉ-SCRIVE, and P. BJÖRNTORP, "Uptake of triglyceride fatty acids in adipose tissue in vivo in man," *Eur. J. Clin. Invest.*, vol. 20, no. 2Part1, pp. 158–165, Apr. 1990.

[52] T. J. Yost, D. R. Jensen, B. R. Haugen, and R. H. Eckel, "Effect of dietary macronutrient composition on tissue-specific lipoprotein lipase activity and insulin action in normal-weight subjects," *Am. J. Clin. Nutr.*, vol. 68, no. 2, pp. 296–302, Aug. 1998.

[53] M. R. Taskinen and E. A. Nikkilä, "Basal and postprandial lipoprotein lipase activity in adipose tissue during caloric restriction and refeeding," *Metabolism*, vol. 36, no. 7, pp. 625–630, Jul. 1987.

[54] T. Ruge, M. Svensson, J. W. Eriksson, and G. Olivecrona, "Tissue-specific regulation of lipoprotein lipase in humans: effects of fasting," *Eur. J. Clin. Invest.*, vol. 35, no. 3, pp. 194–200, Mar. 2005.

[55] S. K. Koliwad *et al.*, "Angiopoietin-like 4 (ANGPTL4, fasting-induced adipose factor) is a direct glucocorticoid receptor target and participates in glucocorticoid-regulated triglyceride metabolism," *J. Biol. Chem.*, vol. 284, no. 38, pp. 25593–25601, Sep. 2009.

[56] E. Makoveichuk, E. Vorrsjö, T. Olivecrona, and G. Olivecrona, "TNF-α decreases lipoprotein lipase activity in 3T3-L1 adipocytes by up-regulation of angiopoietin-like protein 4," *Biochim. Biophys. Acta - Mol. Cell Biol. Lipids*, vol. 1862, no. 5, pp. 533–540, May 2017.

[57] H. Staiger *et al.*, "Muscle-derived angiopoietin-like protein 4 is induced by fatty acids via peroxisome proliferator-activated receptor (PPAR)-δ and is of metabolic relevance in humans," *Diabetes*, vol. 58, no. 3, pp. 579–589, Mar. 2009.

[58] T. Ruge, V. Sukonina, T. Myrnäs, M. Lundgren, J. W. Eriksson, and G. Olivecrona, "Lipoprotein lipase activity/mass ratio is higher in omental than in subcutaneous adipose tissue," *Eur. J. Clin. Invest.*, vol. 36, no. 1, pp. 16–21, Jan. 2006.

[59] M.-R. Taskinen and J. Borén, "New insights into the pathophysiology of dyslipidemia in type 2 diabetes," *Atherosclerosis*, vol. 239, no. 2, pp. 483–495, Apr. 2015.

[60] L. J. McCulloch, L. R. Bramwell, B. Knight, and K. Kos, "Circulating and tissue specific transcription of angiopoietin-like protein 4 in human Type 2 diabetes," *Metabolism.*, vol. 106, p. 154192, 2020.

[61] D. Panarotto, P. Rémillard, L. Bouffard, and P. Maheux, "Insulin resistance affects the regulation of lipoprotein lipase in the postprandial period and in an adipose tissue-specific manner," in *European Journal of Clinical Investigation*, 2002, vol. 32, no. 2, pp. 84–92.

[62] M. R. Taskinen, E. A. Nikkilä, T. Kuusi, and K. Harno, "Lipoprotein lipase activity and serum lipoproteins in untreated Type 2 (insulin-independent) diabetes associated with obesity," *Diabetologia*, vol. 22, no. 1, pp. 46–50, Jan. 1982.

[63] J. W. Eriksson, J. Burén, M. Svensson, T. Olivecrona, and G. Olivecrona, "Postprandial regulation of blood lipids and adipose tissue lipoprotein lipase in type 2 diabetes patients and healthy control subjects," *Atherosclerosis*, vol. 166, no. 2, pp. 359–367, Feb. 2003.

Supplemental Material

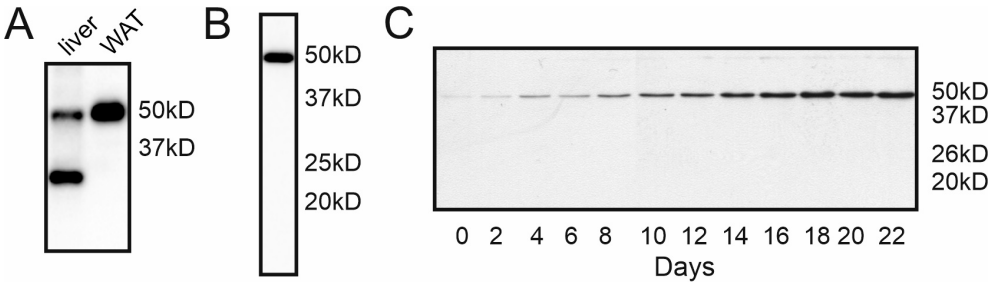

Supplementary figure 1. ANGPTL4 is produced in human adipose tissue as full length protein. A) Immunoblot for ANGPTL4 of human liver and human subcutaneous adipose tissue. B) Immunoblot for ANGPTL4 of human primary adipocytes. C) Immunoblot for ANGPTL4 during adipogenic differentiation of human Lisa-2 adipocytes [1].

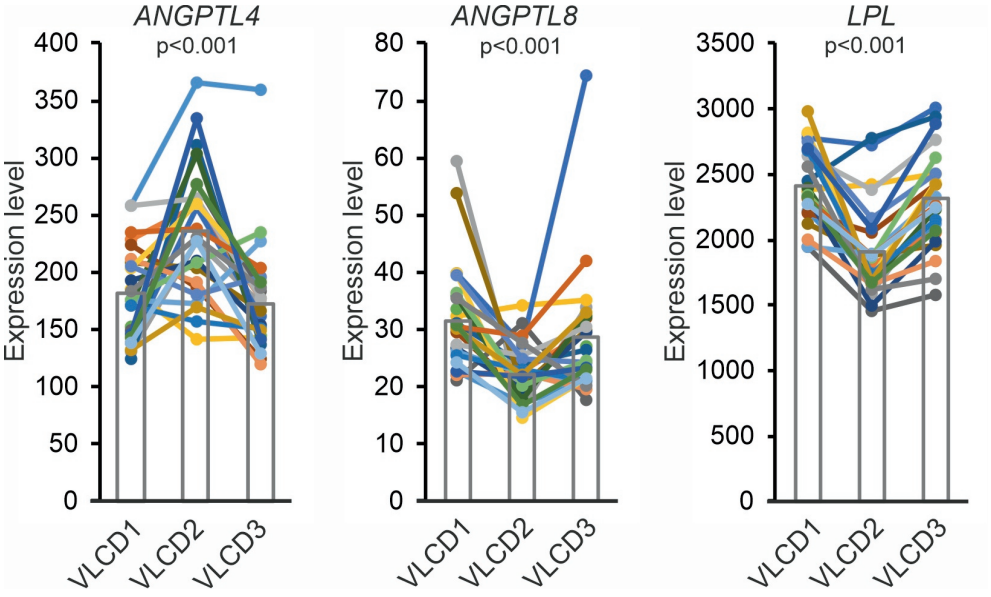

Supplementary figure 2. Adipose tissue mRNA levels of *ANGPTL4*, *ANGPTL8* and *LPL* are altered during severe hypocaloric diet but are unaffected by weight loss per se. Microarray-based gene expression of *ANGPTL4*, *ANGPTL8* and *LPL* in adipose tissue of subjects before weight loss (VLCD1), after 5 weeks of very low calorie diet (500 Kcal/day, VLCD2), and after 4 weeks of weight maintenance (VLCD3) (GSE77962) [2].

Supplementary table 1. Primer sequences used for qPCR in this study

Gene	Forward primer	Reverse Primer
ANGPTL4	CACAGCCTGCAGACACAACTC	GGAGGCCAAACTGGCTTTGC
ANGPTL8	CAGAAGGTGCTACGGGACAG	AAATTCTCGGTAGGCAGGGC
LPL	CATTCCCGGAGTAGCAGAGT	GGCCACAAGTTTTGGCACC
BACTIN	AGAAAATCTGGCACCACACC	AGAGGCGTACAGGGATAGCA

Supplemental References

[1] M. Wabitsch, S. Brüderlein, I. Melzner, M. Braun, G. Mechtersheimer, and P. Möller, "LiSa-2, a novel human liposarcoma cell line with a high capacity for terminal adipose differentiation.," *Int. J. cancer*, vol. 88, no. 6, pp. 889–94, Dec. 2000.

[2] R. G. Vink *et al.*, "Adipose tissue gene expression is differentially regulated with different rates of weight loss in overweight and obese humans," *Int. J. Obes.*, vol. 41, no. 2, pp. 309–316, Feb. 2017.

Chapter 4

Angiopoietin-like 4 promotes the intracellular cleavage of lipoprotein lipase by furin in adipocytes

Dijk W†, Ruppert PMM†, Oost LJ, Kersten S.

† equal contribution

J Biol Chem. 2018;11(3):jbc.RA118.002426.

Abstract

Lipoprotein lipase (LPL) catalyzes the breakdown of circulating triglycerides in muscle and fat. LPL is inhibited by several proteins, including Angiopoietin-like 4 (ANGPTL4), and may be cleaved by members of the PCSK family. Here, we aimed to investigate the cleavage of LPL in adipocytes by PCSKs and study the potential involvement of ANGPTL4. A substantial portion of LPL in mouse and human adipose tissue was cleaved into N- and C-terminal fragments. Treatment of different adipocytes with the PCSK- inhibitor Dec-RVKR-CMK markedly decreased LPL cleavage, indicating LPL is cleaved by PCSKs. Silencing of Pcsk3/furin significantly decreased LPL cleavage in cell culture medium and lysates of 3T3-L1 adipocytes. Remarkably, PCSK-mediated cleavage of LPL in adipocytes was diminished by Angptl4 silencing and was decreased in adipocytes and adipose tissue of Angptl4-/- mice. Differences in LPL cleavage between Angptl4-/- and wild-type mice were abrogated by treatment with Dec-RVKR-CMK. Induction of ANGPTL4 in adipose tissue during fasting enhanced PCSK-mediated LPL cleavage, concurrent with decreased LPL activity, in wild-type but not Angptl4-/- mice. In adipocytes, after removal of cell surface LPL by heparin, levels of N-terminal LPL were still markedly higher in wild-type compared to Angptl4-/- adipocytes, suggesting that stimulation of PCSK-mediated LPL cleavage by ANGPTL4 occurs intracellularly. Finally, treating adipocytes with insulin increased full-length LPL and decreased N-terminal LPL in an ANGPTL4-dependent manner. In conclusion, ANGPTL4 promotes PCSK-mediated intracellular cleavage of LPL in adipocytes, likely contributing to regulation of LPL in adipose tissue. Our data provide further support for an intracellular action of ANGPTL4 in adipocytes.

Keywords: Angiopoietin-like 4, lipoprotein lipase, lipoprotein metabolism, adipocyte, furin, triglycerides

Introduction

Elevated levels of plasma triglycerides are increasingly recognized as an important causal risk factor for coronary artery disease (1). Plasma triglyceride levels are determined by the balance between the secretion of triglycerides by the liver and small intestine and the clearance of triglycerides in muscle and fat tissue. The rate of triglyceride clearance is determined by the enzyme lipoprotein lipase (LPL), which catalyzes the hydrolysis of triglycerides at the capillary endothelium (2). LPL is produced by myocytes and adipocytes and is transported toward the endothelial cell surface by the protein GPIHBP1 (glycosylphosphatidylinositol-anchored high density lipoprotein binding protein 1) (3). In order to match the tissue uptake of fatty acids in accordance with the local needs, the activity of LPL is tightly regulated, primarily at the post-translational level (4).

Angiopoietin-like 3 (ANGPTL3), Angiopoietin-like 4 (ANGPTL4) and Angiopoietin-like 8 (ANGPTL8) are three members of the angiopoietin-like protein family that are involved in the post-translational regulation of LPL (5). ANGPTL3 and ANGPTL8 are secreted by the liver as hepatokines and cooperate to inhibit the activity of LPL in oxidative tissues such as heart and brown fat, with a primary action in the fed state (6–9). By contrast, ANGPTL4 is produced by several tissues and appears to mainly function locally in a tissue-specific manner (5). Studies have shown that ANGPTL4 plays a major role in the regulation of LPL activity during various physiological conditions such as exercise, fasting and cold exposure (10–12). ANGPTL4 inactivates LPL by promoting the unfolding of the protein, leading to the conversion of the catalytically active LPL dimer into inactive monomers (13, 14). Although ANGPTL4 is able to inhibit LPL activity in the subendothelial spaces and on the endothelial surface (15, 16), recently we provided evidence that ANGPTL4 and LPL also interact intracellularly, causing the degradation of LPL (17). However, the specific steps involved in the intracellular degradation of LPL by ANGPTL4 remain unclear.

Members of the proprotein convertase subtilisin/kexin (PCSK) protein family (PCSK1-7, SKI-1/S1P and PCSK9) are calcium-dependent serine endopeptidases that convert proproteins into their active forms by cleavage (18, 19). PCSK1-7 recognize and cleave substrates at specific lysine- and/or arginine-containing basic amino acid sequences (18). Despite overlap in substrate recognition, their functions are tissue-specific and dependent on their cellular localization. For example, PCSK3 (Furin) is primarily found in the *trans*-Golgi network, in the endosomes, and on the cell surface, while PCSK5 (PC5/6) and PCSK6 (PACE4) are primarily present on the cell surface (19). PCSKs have been repeatedly implicated in the regulation of lipoprotein metabolism. The best-known example is PCSK9, which raises plasma low-density lipoprotein cholesterol (LDL-C) levels. Specifically, PCSK9 promotes the degradation of the LDL receptor in endosomes/lysosomes, resulting in a reduced clearance of LDL-C (20). Other examples include the cleavage of ANGPTL3 and ANGPTL4 by PCSKs *in vitro* and *in vivo*

(21–24). Interestingly, it has been demonstrated that LPL is also subject to cleavage by PCSKs, at least *in vitro* (25, 26). Specifically, a cleavage site was identified at residues 321-324, which is in the middle of a stretch of 60 amino acids that is 100% conserved between mouse and human LPL (26), yielding an N- and C-terminal LPL cleavage fragment. However, to what extent LPL is cleaved *in vivo* in adipocytes has remained unclear. In addition, the potential role of ANGPTL4 has not been investigated. Accordingly, the aim of the present study was to investigate the mechanism underlying the cleavage of LPL in adipocytes and to explore the potential role of ANGPTL4.

Results

LPL is cleaved in human and mouse adipose tissue

To examine whether LPL is cleaved *in vivo* in white adipose tissue, we performed Western blot for LPL in human adipose tissue using antibodies directed against the N- or C-terminal portion of human LPL (27). Both antibodies gave rise to two bands, corresponding to full length LPL (slightly above 50 kDa), and the N-terminal or C-terminal LPL cleavage fragment at around 30 kDa or 20- 25 kDa, respectively (Figure 1A). These data indicate that LPL is cleaved in human adipose tissue. Using two different antibodies directed against the C-terminal part of human LPL, it was observed that treatment with Endoglycosidase H (EndoH), an enzyme that cleaves asparagine- linked mannose-rich oligosaccharides, did not alter the migration of full length and C-terminal LPL (Figure 1B). By contrast, treatment with PNGase—which removes most N-linked oligosaccharides—altered the migration of full length LPL but not C-terminal LPL (Figure 1B). Adipose tissue of different human subjects always showed a substantial proportion of LPL in the truncated form (Figure 1C). Similarly, using an antibody directed against the N-terminal portion of mouse LPL, immunoblotting of mouse adipose tissue yielded two bands, corresponding to full length LPL and the N-terminal LPL cleavage fragment) (Figure 1D) (28). Whereas part of mouse full length LPL changed migration after treatment with EndoH, the N-terminal LPL cleavage product did not change migration. Treatment with PNGase altered the migration of both full length and N-terminal LPL (Figure 1D). LPL was also found to be cleaved in mouse heart but not in mouse bone marrow-derived macrophages (Figure 1E). Overall, these data indicate that: 1) LPL is cleaved into N- and C- terminal cleavage fragments in human and mouse adipose tissue. 2) Human and mouse LPL is glycosylated in the N-terminal region (29, 30, 26, 31).

LPL is cleaved in adipose tissue by PCSKs

Previously, members of the proprotein convertase subtilisin/kexin (PCSK) family were suggested to cleave LPL at residues 321-324 to yield nearly complete N-terminal and C-terminal domains (26). To examine whether the observed N- terminal LPL was the result of PCSK-mediated cleavage, mature 3T3-L1 and 3T3-F442a adipocytes, as well as primary adipocytes and white adipose tissue explants from mice were treated with the inhibitor Dec-RVKR-CMK (dec- CMK) to block PCSK activity (32). In all adipocyte models, incubation with dec-CMK resulted in the almost complete disappearance of N-terminal LPL in cell culture medium and cell lysates, indicating that LPL is cleaved by PCSKs in adipocytes (Figure 2).

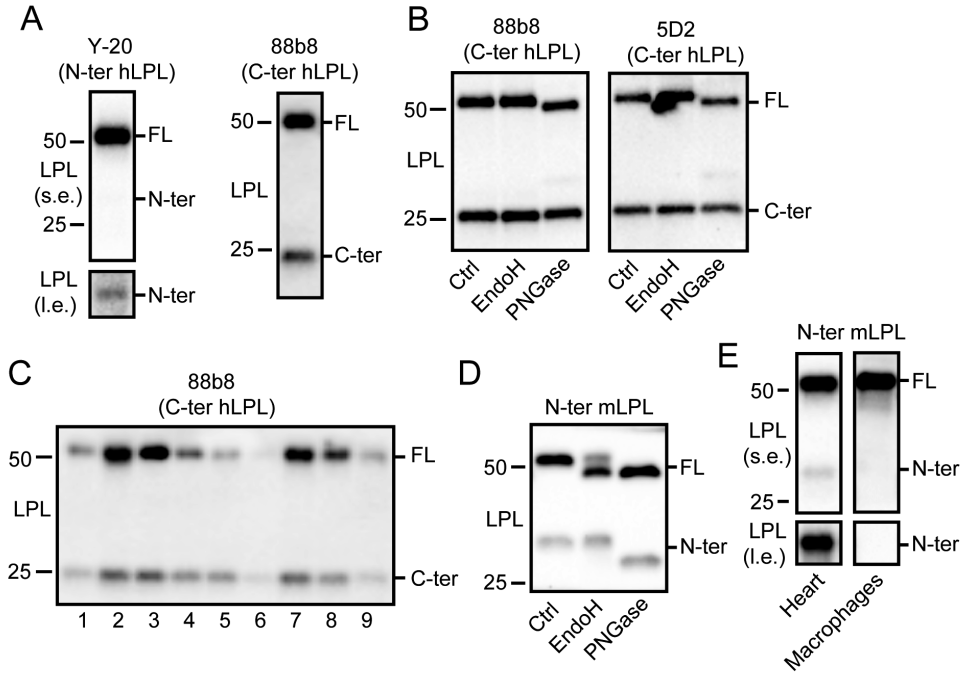

Figure 1. Cleavage of LPL in human and mouse adipose tissue. (A) Western blot of lysates of human adipose tissue using antibodies against the N-terminal (Y-20) and C-terminal (88b8) portion of hLPL. (B) Western blot of lysates of human adipose tissue treated with endoglycosidase H (EndoH) or PNGase, using two different antibodies against hLPL, 88b8 and 5D2 (27). (C) Western blot of lysates of human adipose tissue of different subjects enrolled in the MONDIAL study, using an antibody against hLPL (88b8). (D) Western blot of lysates of mouse adipose tissue treated with endoglycosidase H (EndoH) or PNGase, using an antibody against mLPL (28). (E) Western blot of lysates of mouse heart and bone marrow-derived macrophages. Molecular weight markers are indicated. l.e., long exposure; s.e., short exposure.

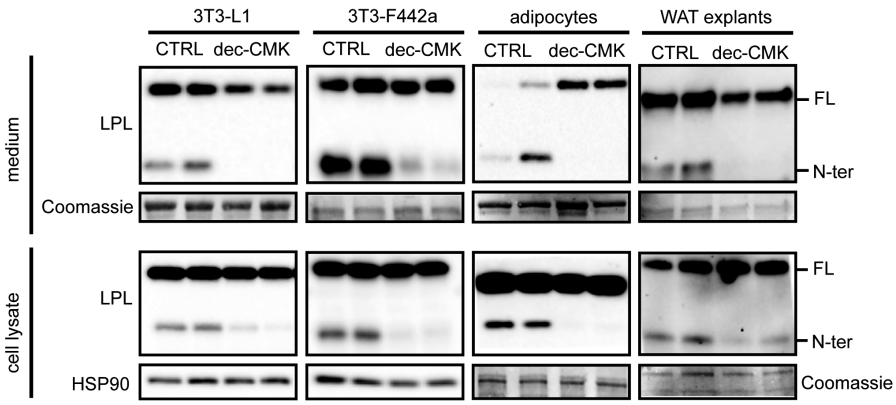

Figure 2. LPL is cleaved by PCSKs in adipocytes. (A) Western blots of cell culture medium (*upper panels*) and cell lysates (*lower panels*) of mature 3T3-L1 adipocytes, mature 3T3-F442a adipocytes, primary adipocytes differentiated from the stromal vascular fraction of adipose tissue from mice, and adipose tissue explants from mice, that were treated with 50 µM Dec-RVKR-CMK (dec-CMK) for 9h. Western blots were probed with antibodies against mLPL and HSP90 (as a loading control). Coomassie blue staining was performed as loading control for cell culture medium, primary adipocytes and WAT explants. WAT, white adipose tissue.

PCSK3 is expressed in adipose tissue and cleaves adipocyte LPL

To assess whether adipocyte LPL is cleaved by PCSKs intracellularly and/or upon secretion, we treated 3T3-L1 adipocytes with heparin to release LPL bound to heparin sulphate proteoglycans (HSPG) from the cell surface. As expected, heparin treatment resulted in a pronounced increase of LPL in the cell culture medium, along with a reduction of LPL in the cell lysates (Figure 3). In line with the notion that binding of LPL to HSPG is mainly mediated by C-terminal and not N-terminal LPL (29, 33), heparin did not influence the amount of N-terminal LPL in the cell culture medium and cell lysates (Figure 3). These data indicate that little or no N-terminal LPL is bound to HSPGs on the cell surface and that N-terminal LPL in cell lysates must originate from intracellular LPL cleavage, from where it is secreted.

Given that LPL is cleaved intracellularly by PCSKs, a promising candidate that may catalyze LPL cleavage in adipocytes is PCSK3, as PCSK3 is activated and active intracellularly in the *trans*-Golgi (19). Expression profiling showed that PCSK3 is most highly expressed in liver and kidney, with comparatively low but clearly detectable PCSK3 expression in adipose tissue (Figure 4A). To assess whether PCSK3 might be involved in LPL cleavage in adipocytes, we silenced *Pcsk3* in mature 3T3-L1 adipocytes by means of siRNA. SiRNA-mediated silencing resulted in a 90% reduction in *Pcsk3* expression levels (Figure 4B). In line with a role for PCSK3 in LPL cleavage, silencing of *Pcsk3* significantly reduced the amount of LPL

cleavage in cell culture medium and cell lysates (Figure 4C). These data are in line with a previous finding that PCSK3 is able to cleave LPL in a stable HEK293 cell line expressing LPLmyc (26).

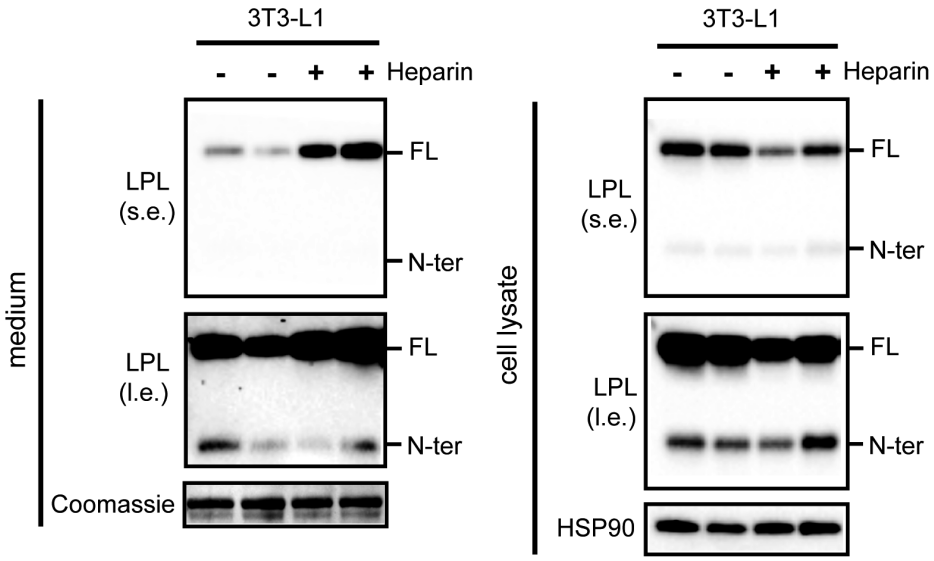

Figure 3. Amino-terminal LPL cannot be released from the cell surface by heparin. (A) Western blots of cell culture medium (*left*) or cell lysates (*right*) of mature 3T3-L1 adipocytes that were treated with 10 IU/ mL heparin for 20 minutes. Western blots were probed with antibodies against mLPL and HSP90 (as loading control). Coomassie blue staining was performed as loading control for cell culture medium. l.e., long exposure; s.e., short exposure.

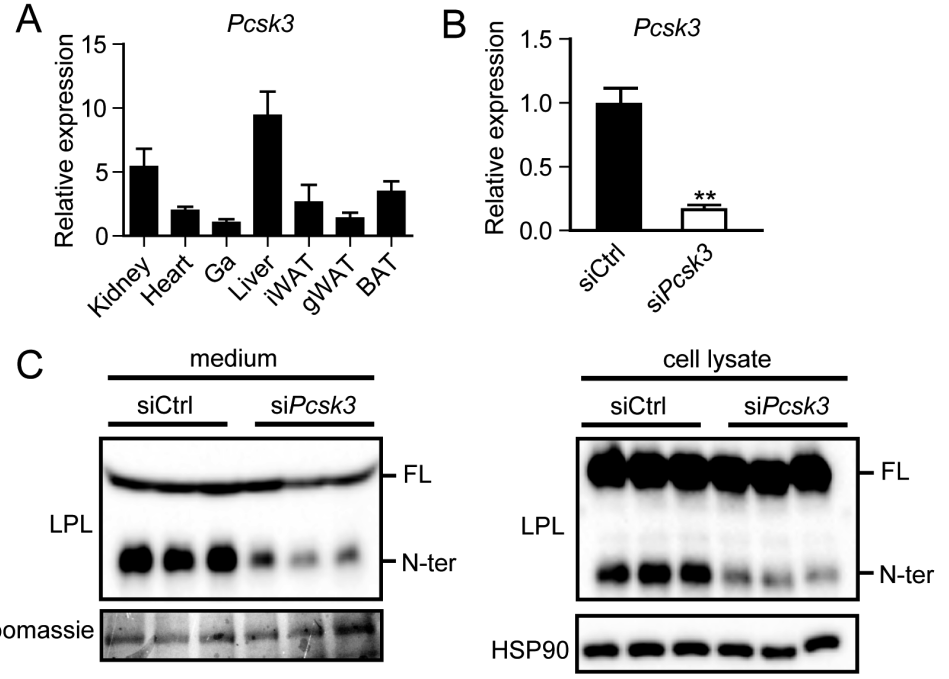

Figure 4. PCSK3 is well expressed in adipose tissue and cleaves adipocyte LPL. (A) *Pcsk3* mRNA levels in different tissues from C57BL/6 mice (n=4). (B) *Pcsk3* mRNA levels in fully differentiated 3T3-L1 adipocytes that were trypsinized, replated at 70% confluency, and treated with si*Pcsk3* or siCtrl for 48h. Asterisk indicates significantly different from siCtrl according to Student's t-test; $p<0.01$. (C) Western blots of cell culture medium (*left panel*) and cell lysates (*right panel*) of fully differentiated 3T3-L1 adipocytes that were trypsinized, replated at 70% confluency, and treated with si*Pcsk3* or siCtrl for 48h. Western blots were probed with antibodies against mLPL and HSP90 (as a loading control). Coomassie blue staining was performed as loading control for cell culture medium.

Amino-terminal LPL is cleared by the lysosomes

Previously, PCSK-mediated cleavage was shown to promote the inactivation of endothelial lipase, a family member of LPL (26). Similarly, cleavage of LPL by PCSKs might also serve to inactivate LPL (26). To assess the fate of cleaved LPL and to study whether it may be further subject to lysosomal degradation in adipocytes, we incubated mature 3T3-L1 adipocytes and primary adipocytes with Bafilomycin A1 (BafA1) to inhibit lysosomal degradation. In agreement with previous studies, treatment of adipocytes with BafA1 significantly increased proteins levels of full-length LPL in cell lysates and to a lesser extent in the cell culture medium (Figure 5A & Figure 5B) (34). Interestingly, in both 3T3-L1 and primary adipocytes, BafA1 also increased the amount of N-terminal LPL in cell lysates and medium, suggesting that at least part of the N- terminal LPL is cleared by lysosomes (Figure 5A & Figure 5B). The increase in LPL protein abundance in primary and 3T3-L1 adipocytes upon BafA1 treatment cannot be attributed to an increase in *Lpl* mRNA (Figure 5C & Figure 5D).

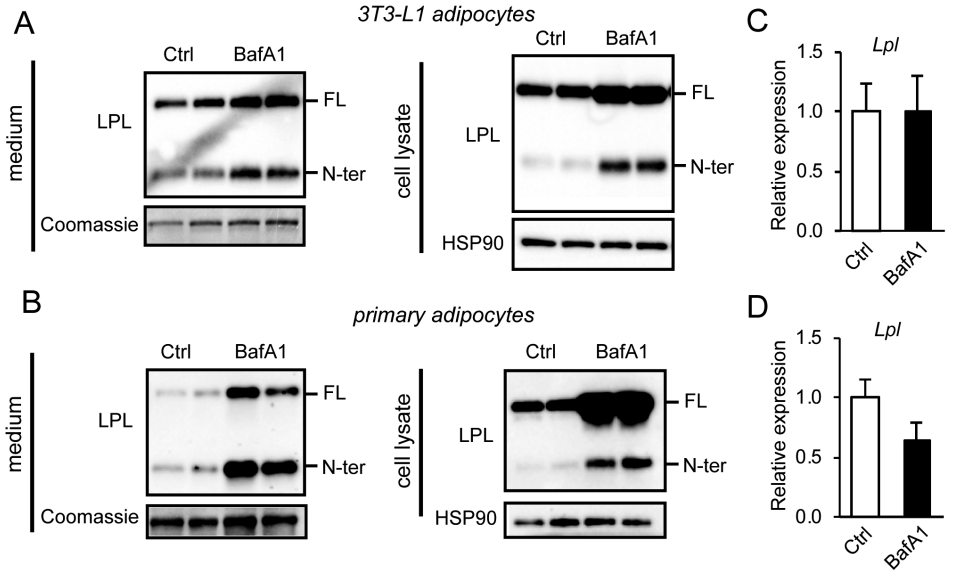

Figure 5. Amino-terminal LPL is cleared by the lysosomes. (A) Western blots of cell culture medium (*left panel*) and cell lysates (*right panel*) of mature 3T3-L1 adipocytes that were treated with 100 nM Bafilomycin A1 (BafA1) for 10h. (B) Western blots of cell culture medium (*left panel*) and cell lysates (*right panel*) of primary adipocytes differentiated from the stromal vascular fraction of adipose tissue that were treated with 100 nM Bafilomycin A1 (BafA1) for 10h. Western blots were probed with antibodies against LPL and HSP90. Coomassie blue staining was performed as loading control for cell culture medium. (C) *Lpl* mRNA in mature 3T3-L1 adipocytes treated with 100 nM Bafilomycin A1 (BafA1) for 10h. (D) *Lpl* mRNA in primary mouse adipocytes treated with 100 nM Bafilomycin A1 (BafA1) for 10h.

ANGPTL4 promotes PCSK-mediated cleavage of adipocyte LPL

An important regulator of LPL in adipose tissue is ANGPTL4. Indeed, ANGPTL4 is highly abundant in mouse adipose tissues, where it exists as a glycosylated protein (Figure 6A). Treatment with PNGase, which removes most N-linked glycans, and a Protein Deglycosylation Mix, which removes N-linked glycans as well as simple and some complex O-linked glycans, altered the mobility of ANGPTL4, indicating removal of carbohydrate side-chains (Figure 6A). However, EndoH, which removes N-linked mannose-rich glycans, had no effect, suggesting that most of carbohydrate side-chains on ANGPTL4 contain complex sugars. (22). Recently, we found that ANGPTL4 promotes the intracellular degradation of LPL in adipocytes (17). To explore the connection between PCSK- mediated cleavage of LPL and ANGPTL4- induced LPL degradation, we investigated whether ANGPTL4 is able to enhance PCSK- mediated LPL cleavage. To that end, we assessed the effect of siRNA-mediated *Angptl4* silencing on LPL cleavage in 3T3-L1 adipocytes. The approximately 80% reduction in *Angptl4* mRNA (Figure 6B) was accompanied by a marked decrease in N-terminal LPL in 3T3-L1 cell lysate, and a modest increase in full length LPL in cell lysates and medium (Figure 6C). These results suggest that ANGPTL4 may promote LPL cleavage in adipocytes. To further investigate this notion, we determined the accumulation of N-terminal LPL in adipose tissue of *Angptl4*-/- and wild-type mice. Corroborating our previous findings, levels of full-length LPL were notably higher in adipose tissue of *Angptl4*-/- mice compared to wild-type mice (Figure 7A) (17). Consistent with a stimulatory effect of ANGPTL4 on cleavage of LPL, levels of N-terminal LPL were significantly lower in adipose tissue of *Angptl4*-/- mice (Figure 7A). Of note, LPL activity was significantly higher in adipose tissue of *Angptl4*-/- mice compared to wild-type mice, confirming the increase in full length LPL protein (Figure 7B).

To examine whether levels of N-terminal LPL respond to changes in endogenous ANGPTL4 production, we measured ANGPTL4 and LPL under conditions of fasting/refeeding. Samples were treated with EndoH to distinguish between EndoH-resistant LPL (LPL in the Golgi and the cell surface) and EndoH-sensitive LPL (LPL in the ER). As previously observed (17, 35), ANGPTL4 levels in white adipose tissue were elevated in the fasted state compared to the refed state (Figure 7C), which was accompanied by a decrease in full length (EndoH-resistant) LPL and an increase in N-terminal LPL (Figure 7D). Strikingly, levels of N-terminal LPL were lower in *Angptl4-/-* mice. Moreover, the difference in levels of N-terminal LPL between the fasted and refed state was abolished in *Angptl4-/-* mice (Figure 7D).

To further understand the mechanism underlying the differential abundance of N- terminal LPL in adipose tissue of wild-type and Angptl4-/- mice, we shifted our experiments to primary adipocytes. Similar to whole adipose tissue, primary adipocytes of Angptl4-/- mice also showed higher levels of full length LPL and lower levels of N-terminal LPL as compared

to wild- type adipocytes (Figure 8A). Treatment with the PCSK inhibitor dec-CMK fully abrogated these differences, indicating that PCSK-mediated LPL cleavage mediates the differences in N-terminal LPL between Angptl4-/- and wild-type mice (Figure 8B). To investigate whether stimulation of PCSK-mediated LPL cleavage by ANGPTL4 may initiate the complete degradation of LPL, we treated primary adipocytes with cycloheximide to arrest protein synthesis and measured the decline in full length and N-terminal LPL by Western blot. The rate of decline of N-terminal LPL and to a lesser extent full length LPL was notably lower in Angptl4-/- adipocytes than in wildtype adipocytes, indicating that ANGPTL4 accelerates the degradation of LPL (Figure 8C). These data suggest that induction of PCSK-mediated LPL cleavage by ANGPTL4 is part of the degradation pathway of LPL.

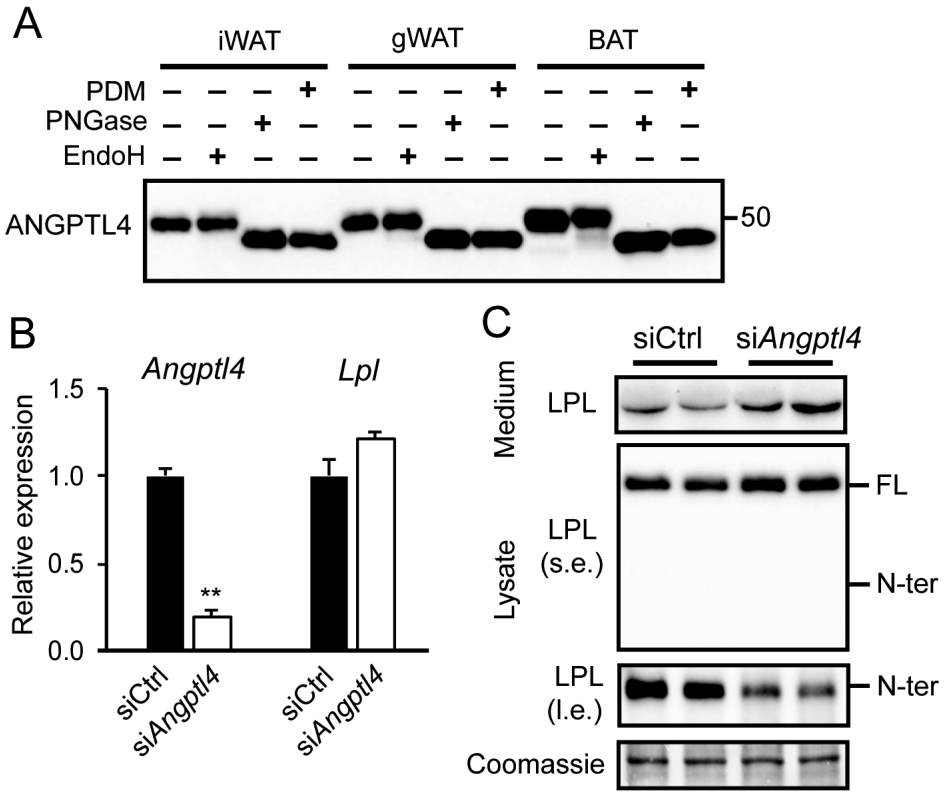

Figure 6. ANGPTL4 silencing reduces LPL cleavage. (A) Western blot of lysate of inguinal white (iWAT), gonadal white (gWAT), and interscapular brown (BAT) adipose tissue treated with protein deglycosylation mix (PDM), endoglycosidase H (EndoH), or PNGase, using an antibody against mANGPTL4. (B) *Lpl* and *Angptl4* mRNA levels in fully differentiated 3T3-L1 adipocytes that were treated with si*Angptl4* or siCtrl for 48h. Asterisk indicates significantly different from siCtrl according to Student's t-test; p<0.01. (C) Western blots of cell culture medium and cell lysates of mature 3T3-L1 adipocytes that were treated with si*Angptl4* or siCtrl for 48h, using an antibody against mLPL. Coomassie blue staining served as loading control. l.e., long exposure; s.e., short exposure.

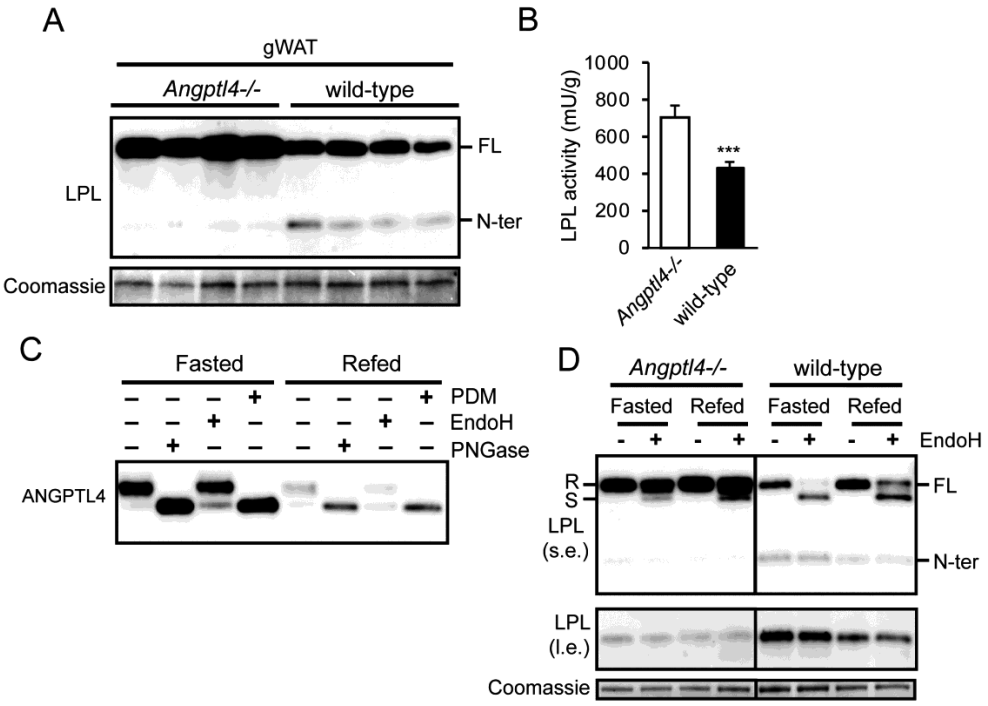

Figure 7. ANGPTL4 regulates LPL cleavage in adipose tissue during fasting. (A) Western blot of cell lysates of gonadal adipose tissue (gWAT) from *Angptl4*-/- and wild-type mice, using an antibody against mLPL. Coomassie blue staining was performed as loading control. (B) LPL activity in gonadal adipose tissue of *Angptl4*-/- mice (n=7) and wild-type mice (n=14). Values are mean ± SEM. Asterisks indicates significantly different from *Angptl4*-/- mice according to Student's t-test (P<0.001). Samples were from *ad libitum* fed mice. (C) Western blot of cell lysates of gonadal adipose tissue of fasted and refed wild-type mice treated with protein deglycosylation mix (PDM), endoglycosidase H (EndoH), or PNGase, using an antibody against mANGPTL4. (D) Western blot of cell lysates of gonadal adipose tissue of fasted and refed *Angptl4*-/- and wild-type mice treated with endoglycosidase H (EndoH), using an antibody against mLPL. Separate boxes for *Angptl4*-/- and wild-type mice indicates that all samples were run on the same gel with the same exposure time but that intermediate lanes were removed. Part of this Western blot at different exposure has been previously published (17). EndoH-resistant LPL (complex oligosaccharides: Golgi and cell surface LPL) is indicated with R. EndoH-sensitive LPL (high-mannose oligosaccharides, ER LPL) is indicated with S. l.e., long exposure; s.e., short exposure.

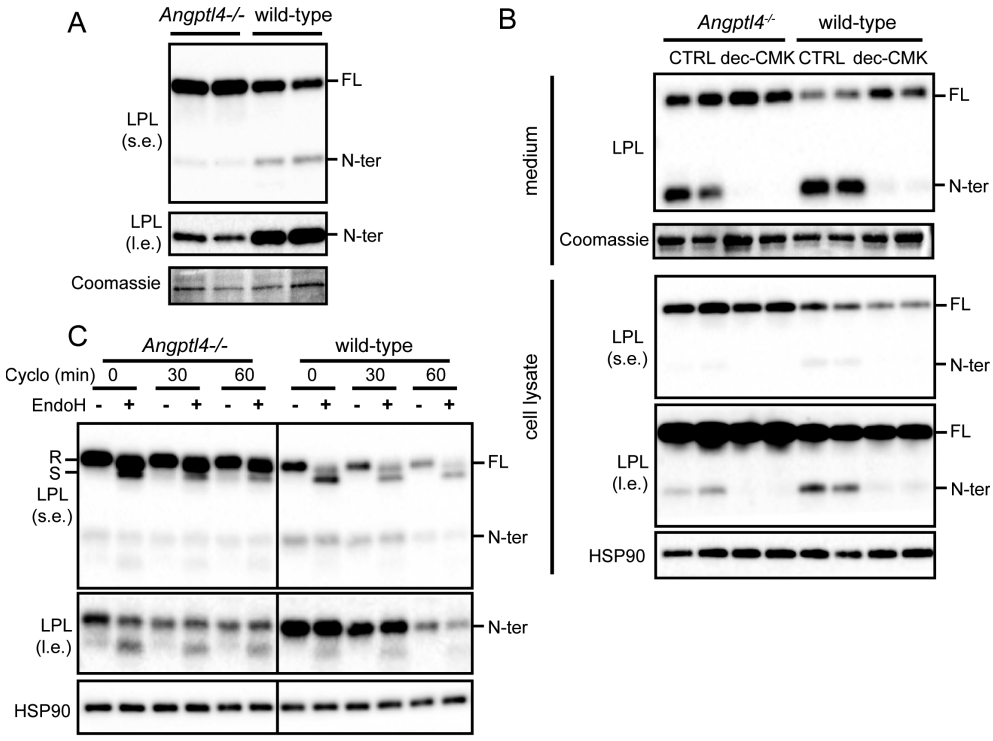

Figure 8. ANGPTL4 promotes PCSK-mediated cleavage of adipocyte LPL. (A) Western blot of cell lysates of primary adipocytes differentiated from the stromal vascular fraction of adipose tissue from *Angptl4*-/- and wild-type mice, using an antibody against mLPL. Coomassie blue staining was performed as loading control. (B) Western blots of cell culture medium (*upper panels*) and cell lysates (*lower panels*) of primary adipocytes differentiated from the stromal vascular fraction of adipose tissue from *Angptl4*-/- and wild-type mice that were treated with 50 µM dec-CMK for 9h. Western blots were probed with antibodies against mLPL and HSP90. Coomassie blue staining was performed as a loading control for cell culture medium. (C) Western blot of cell lysates of primary adipocytes differentiated from the stromal vascular fraction of adipose tissue from *Angptl4*-/- and wild-type mice. Adipocytes were treated with cycloheximide (Cyclo) for 0, 30 or 60 min. Adipocyte lysates were treated with Endoglycosidase H (EndoH). Western blots were probed with antibodies against mLPL and HSP90. EndoH-resistant LPL (complex oligosaccharides: Golgi and cell surface LPL) is indicated with R. EndoH-sensitive LPL (high-mannose oligosaccharides, ER LPL) is indicated with S. l.e., long exposure; s.e., short exposure.

Induction of PCSK-mediated LPL cleavage by ANGPTL4 occurs intracellularly

Finally, to unequivocally establish that stimulation of PCSK-mediated LPL cleavage by ANGPTL4 occurs intracellularly, we determined the levels of full length and N-terminal LPL in medium and lysate of wild-type and *Angptl4-/-* adipocytes treated with heparin for 20 minutes. As previously shown (17), the heparin-induced release of full length LPL into the medium was higher in *Angptl4-/-* than in wild-type adipocytes (Figure 9A). In concordance with these data, the reduction in cellular LPL content by heparin was more pronounced in *Angptl4-/-* than in wild-type adipocytes. Consistent with the inability of N- terminal LPL to bind to HSPG, heparin treatment did not cause any release of N-terminal LPL into the medium. Importantly, even after removal of the heparin-releasable pool of LPL, the levels of N-terminal LPL were still markedly higher in wild-type than in *Angptl4-/-* adipocytes (Figure 9B). These data indicate that the stimulation of PCSK-mediated LPL cleavage by ANGPTL4 happens inside the cell and not on the cell surface.

As a final experiment, we studied the effect of insulin. Injection of insulin was previously shown to decrease *Angptl4* mRNA and increase LPL activity in adipose tissue of rats (12). To study whether downregulation of *Angptl4* by insulin leads to corresponding changes in the different LPL forms, we treated primary adipocytes with insulin and determined the levels of full length and N-terminal LPL in the lysates. Insulin reduced *Angptl4* mRNA in primary adipocytes by about 50%, and did not have a noticeable effect on *Lpl* and *Pcsk3* mRNA (Figure 10A). Interestingly, whereas insulin treatment increased levels of full length LPL, it modestly decreased levels of N-terminal LPL (Figure 10B). These effects were observed specifically in wild-type adipocytes, but not *Angptl4-/-* adipocytes. The increase in full length LPL in response to insulin and in *Angptl4-/-* adipocytes was accounted for by an increase in EndoH-resistant LPL (Figure 10C). These data indicate that the downregulation of *Angptl4* by insulin in adipocytes leads to reduced LPL cleavage.

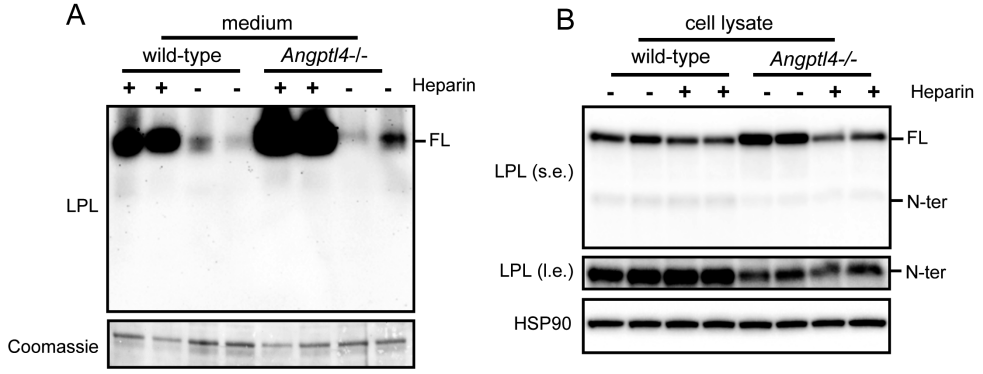

Figure 9. ANGPTL4 promotes LPL cleavage inside adipocytes. Western blots of cell culture medium (A) and cell lysates (B) of primary adipocytes differentiated from the stromal vascular fraction of adipose tissue from *Angptl4*-/- and wild-type mice treated with 10 IU/mL heparin for 20 min. Western blots were probed with antibodies against mLPL and HSP90. Coomassie blue staining was performed as loading control for cell culture medium. l.e., long exposure; s.e., short exposure.

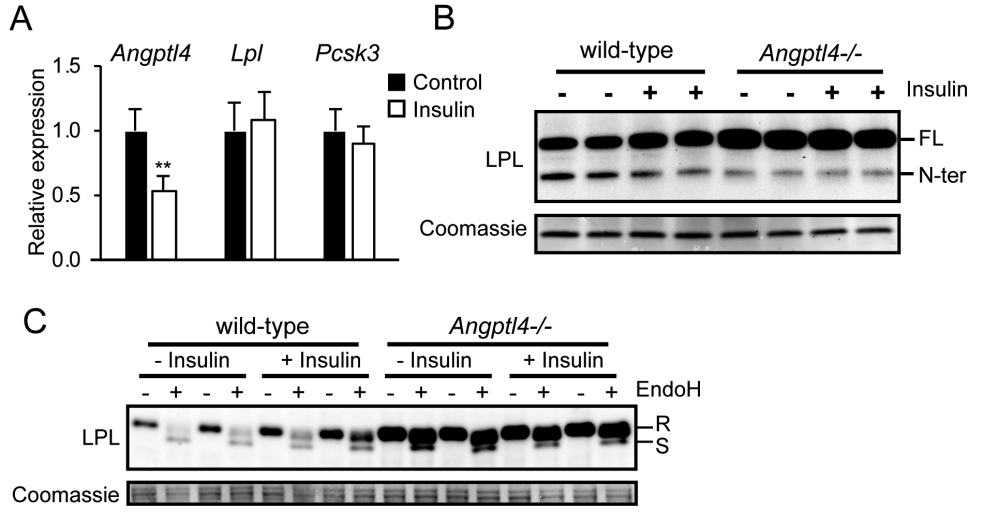

Figure 10. Downregulation of *Angptl4* by insulin reduces LPL cleavage. (A) Expression of *Angptl4* and *Lpl* in primary mouse adipocytes treated with insulin (500 nM) for 12 hours. Asterisk indicates significantly different from control according to Student's t-test; $p<0.01$. (B) Western blot of cell lysates of primary adipocytes differentiated from the stromal vascular fraction of adipose tissue from wild-type and *Angptl4*-/- mice treated with 500 nM insulin for 12 hours. (C) Western blot of cell lysates of primary adipocytes differentiated from the stromal vascular fraction of adipose tissue from wild-type and *Angptl4*-/- mice treated with 500 nM insulin for 12 hours. Adipocyte lysates were treated with Endoglycosidase H (EndoH). Western blots were probed with antibodies against mLPL. Coomassie blue staining was performed as loading control. EndoH-resistant LPL (complex oligosaccharides: Golgi and cell surface LPL) is indicated with R. EndoH- sensitive LPL (high-mannose oligosaccharides, ER LPL) is indicated with S.

Discussion

Little is known about the cleavage of LPL in adipocytes. Here, we provide *in vitro* and *in vivo* evidence that LPL undergoes substantial cleavage in mouse and human adipocytes to yield N- and C-terminal fragments. The cleavage of LPL in adipocytes is at least partly mediated by PCSK3 (Furin) and likely represents an initial step in the intracellular degradation of LPL. Importantly, we find that ANGPTL4 stimulates the intracellular cleavage of LPL by PCSKs. Induction of ANGPTL4 levels in adipose tissue during fasting enhanced PCSK-mediated LPL cleavage, concurrent with decreased LPL levels and activity, suggesting that stimulation of LPL cleavage by ANGPTL4 contributes to suppression of LPL levels in adipocytes during fasting. Conversely, suppression of ANGPTL4 by insulin in adipocytes reduced PCSK-mediated LPL cleavage, concurrent with increased LPL levels. Induction of PCSK-mediated LPL cleavage by ANGPTL4 occurs inside the cell, thereby providing further support for an intracellular mode of action of ANGPTL4 in adipocytes.

ANGPTL4 is a well-established inhibitor of LPL that mediates the reduction in LPL activity in adipose tissue during fasting (12, 36). Through this action, ANGPTL4 reduces uptake of plasma triglyceride-derived fatty acids into adipose tissue during fasting, thereby raising plasma triglyceride levels (12, 36). Genetic studies strongly support a role of ANGPTL4 in regulating LPL activity in humans (37, 38). Specifically, carriers of an inactivating variant of the *ANGPTL4* gene have lower plasma triglyceride levels than non- carriers, and a lower risk of coronary artery disease (37, 38). At the biochemical level, ANGPTL4 promotes the unfolding of LPL (14), leading to the dissociation of the catalytically active, dimeric form of LPL to catalytically inactive monomers (13). Previously, we showed that ANGPTL4 and LPL interact already before being secreted by the cell, at least in adipocytes, causing the intracellular degradation of LPL (17). Specifically, we observed that *Angptl4*-/- adipocytes secrete markedly more LPL compared with wild-type adipocytes. Our studies also indicated that the increase in ANGPTL4 protein during fasting diverts LPL away from secretion towards degradation, strongly suggesting that ANGPTL4 is the long sought after factor responsible for the redistribution of LPL mass in adipocytes during fasting (39). The data in the present paper suggest that induction of LPL cleavage in adipocytes by ANGPTL4 represents an intermediate stage in the degradation pathway of LPL triggered by ANGPTL4 and activated during fasting (Figure 11). As a consequence, less LPL is available for transport to the endothelium to carry out the hydrolysis of circulating triglycerides. At the molecular level, it can be hypothesized that the ANGTL4-induced unfolding of LPL and dissociation of LPL dimers unmasks the PCSK cleavage site at residues 321- 324, thereby rendering LPL more susceptible to cleavage and subsequent degradation (13, 14, 26).

Besides being subject to further intracellular degradation, the N- and C-terminal LPL cleavage fragments can also be secreted (17). It is possible that C-terminal LPL is retained

on the cell surface via HSPG. This is not the case for N-terminal LPL, which lacks the ability to bind HSPG. Cleavage of LPL may also occur extracellularly (25, 26) (Figure 11).

As indicated above, the induction of PCSK-mediated LPL cleavage by ANGPTL4 occurs intracellularly, strengthening the notion that ANGPTL4 is able to act inside the cell. Preliminary evidence from our group indicates that ANGPTL4 may also influence the secretion of other proteins. There is evidence that the intracellular mode of action of ANGPTL4 extends to ANGPTL3 as well (40), and as such may provide a new mechanistic framework underlying certain functional properties of this class of proteins.

Interestingly, a previous report indicated that liver-derived ANGPTL3 also enhances the cleavage of LPL, possibly by serving as a cofactor for PCSKs (25). This action was suggested to lead to inactivation of LPL and the release of LPL from the endothelial cell surface. Since ANGPTL3 and LPL are not produced in the same cell, the effect of ANGPTL3 on PCSK-mediated LPL cleavage is likely extracellular. A previous study in the Huh7 human liver cell line hinted at a similar stimulatory effect on LPL cleavage by ANGPTL4 (21). These data suggest that the induction of PCSK-mediated LPL cleavage may be a common property of ANGPTL3 and ANGPTL4. An interesting twist to the story is that PCSKs not only cleave LPL but also ANGPTL4 and ANGPTL3, releasing their N-terminal domain (21, 22, 24, 41). Since the N-terminal domains of ANGPTL4 and ANGPTL3 mediate the inhibition of LPL, the cleavage of ANGPTL4 and ANGPTL3 may potentiate LPL inhibition. All together, these data raise the possibility that PCSKs might reduce LPL activity by two complementary cleavage mechanisms (21, 24).

We found that PCSK3 is for a large part responsible for the intracellular cleavage of LPL in mouse adipocytes. Previously, PCSK3 was already found to be the primary convertase responsible for cleavage of endothelial lipase in hepatocytes (24). In contrast to PCSK3, which localizes to the *trans*-Golgi and the endosomes, other PCSKs such as PCSK5 (PC5/6) and PCSK6 (PACE4) are mainly activated and present on the cell surface, anchored to HSPGs (19). Similar to PCSK3, PCSK5 and PCSK6 are widely expressed, recognize similar target sequences and share multiple target proteins (19). Hence, it is possible that the observed extracellular cleavage of LPL, leading to the release of cleavage products in the cell culture medium, reflects the action of PCSK5 and PCSK6. Indeed, *in vitro* transfection studies have shown that LPL can also be cleaved by PCSK5 and PCSK6 (26, 25). Interestingly, in our experiments, PCSK inhibition did not lead to an increase in full length LPL. The reason remains unclear.

An interesting question concerns the rationale behind PCSK3-mediated cleavage of LPL. PCSK3 catalyzes the maturation of a variety of proproteins, including growth factors and pathogen recognizing proteins (42), and is essential for proper embryonal development (43). Whereas the action of PCSK3 towards certain proproteins results in their activation,

the PCSK- mediated cleavage of endothelial lipase results in the inactivation of the protein (24, 26). Similarly, it is likely that the PCSK3-mediated cleavage of LPL serves to inactivate LPL rather than to activate LPL. Consistent with this notion, cleaved LPL products that were found in human pre- heparin plasma had little LPL activity (44). Furthermore, mutations G409R or E410V in the human *LPL* gene that are characterized by enhanced cleavage of LPL *in vitro* cause a severe chylomicronaemia (45). Our data support the idea that PCSK-mediated cleavages of LPL serves to inactivate LPL and indicate that N-terminal LPL is efficiently cleared by the lysosomes.

Besides being part of the degradation of LPL, it can be hypothesized that PCSK-mediated cleavage of LPL may serve to separate the N- and C-terminal fragments of LPL, which each might have specific physiological functions that complement or extend beyond LPL's capacity to hydrolyze triglycerides. For example, the C- terminal domain of LPL was previously found to mediate the margination of triglyceride-rich lipoproteins to the endothelium (46). However, it is questionable whether the C-terminal domain alone is capable of translocating to the endothelium *via* GPIHBP1 (47). Likewise, the separate fragments are unlikely to bind to HSPGs on the cell surface, as both monomeric LPL and C-terminal LPL have a much lower affinity for HSPGs compared to full-length dimeric LPL (48, 49). Overall, there is insufficient evidence that the N- and C-terminal fragments of LPL carry specific biological functions and thus that the cleavage of LPL serves any other purpose than LPL degradation.

In conclusion, we demonstrate that LPL is cleaved in adipocytes by PCSK3 and that this cleavage is stimulated by the LPL inhibitor ANGPTL4. We propose that the stimulation of LPL cleavage by ANGPTL4 is part of the degradation pathway of LPL in adipocytes during fasting.

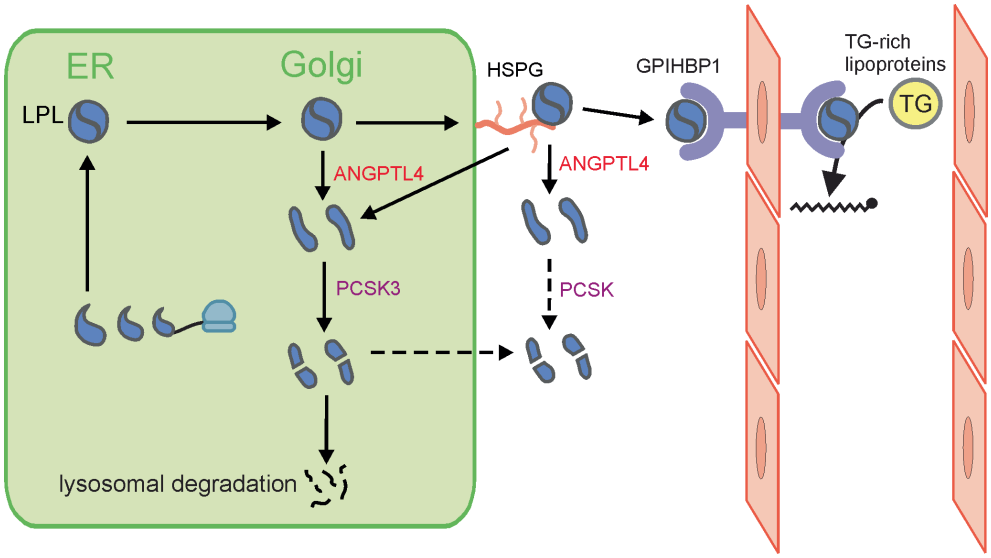

Figure 11. Schematic model of the role of ANGPTL4 in intracellular LPL processing. ANGPTL4 causes the intracellular unfolding of LPL and dissociation of LPL dimers into monomers, rendering LPL more prone to cleavage by PCSK3. Cleaved LPL is further subject to degradation in lysosomes. This action of ANGPTL4 leads to reduced secretion of LPL and reduced delivery of LPL to the endothelial surface by GPIHBP1. Besides being subject to further intracellular degradation, the N- and C-terminal LPL cleavage fragments can also be secreted. Cleavage of LPL may also occur extracellularly (25, 26). PCSK3 = Proprotein convertase subtilisin/kexin type 3, GPIHBP1= glycosylphosphatidylinositol anchored high density lipoprotein binding protein 1, HSPG = heparan sulphate proteoglycans, ER = endoplasmic reticulum.

Experimental procedures

All animal experiments were performed in accordance with Directive 2010/63/EU from the European Union. All animal studies were reviewed and approved by the Animal Ethics Committee of Wageningen University.

Chemicals

AICAR, dexamethasone, IBMX, insulin, rosiglitazone, and intralipid were from Sigma. Dec-RVKR-CMK was from Cayman Chemicals (*via* Sanbio, Uden, The Netherlands). A769662 was from Tocris (Tocris Bioscience, Bristol, United Kingdom).

Human adipose tissue

Human adipose tissue was obtained from the cross-sectional MONDIAL cohort (51). Briefly, the MONDIAL study (as an acronym for Markers of Organ health in Non-diabetic and Diabetics; Intestine, Adipose tissue & Liver) was a cross-sectional study in patients undergoing bariatric surgery at Rijnstate hospital/Vitalys clinics in Arnhem, the Netherlands. In this study, tissue samples were obtained from residual biological material from patients undergoing either a primary laparoscopic Roux-en-Y gastric bypass or a primary laparoscopic gastric sleeve procedure. The study was approved by the local ethics committee of Rijnstate hospital.

Mouse studies

Wild-type and *Angptl4*-/- mice on a C57Bl/6 background were used that were bred and maintained in the same facility for more than 20 generations(52). *Angptl4*-/- mice were generated via homologous recombination of embryonic stem cells, and lack part of the *Angptl4* gene, resulting in a non-functional ANGPTL4 protein. The *Angptl4*-/- mice were imported to our animal facility in 2006 as strain B6.129P2-Lp139tm1 N10 from Taconic (Germantown, NY, USA) (kind gift of Dr. Anja Köster, Eli Lilly, Indianapolis, IN, USA). Mice were individually housed in temperature- and humidity-controlled specific pathogen-free conditions. Mice had ad libitum access to food and water. For the fasting experiment, male wild-type and *Angptl4*-/- mice between the age of 4-6 months were used. Fasted mice were fasted from 15:00 h and sacrificed the next day between 9:00 h and 10:00 h. Refed mice were fasted from 15:00 h, refed with chow the next day at 6:00 h and sacrificed between 9:00 h and 10:00 h. Mice were anaesthetized with a mixture of isoflurane (1.5%), nitrous oxide (70%) and oxygen (30%). Blood was collected by orbital puncture into EDTA tubes.

Mice were killed by cervical dislocation, after which tissues were excised and directly frozen in liquid nitrogen. For the tissue panel, wild-type mice (n=4) were euthanized and multiple tissues were harvested, snap-frozen in liquid nitrogen and stored at -80˚ C until further analyses.

Cell culture

3T3-L1 fibroblasts (P7-P16) were maintained in DMEM (Lonza, Verviers, Belgium) supplemented with 10% newborn calf serum (NCS) (Lonza) and 1% penicillin/streptomycin (P/S) (Lonza). Two days post-confluency, cells were switched to DMEM, supplemented with 10% fetal bovine serum (FBS), 1% P/S, 0.5 mM IBMX, 10 µM dexamethasone, 5 µg/mL insulin for 2 days. Subsequently, cells were maintained in DMEM supplemented with 10% FBS, 1% P/S, and 5 µg/mL insulin for 6 days and switched to DMEM with 10% FBS and 1% P/S for 3 days, after which experiments were performed as indicated in figure legends (53). To examine the accumulation of amino-terminal LPL on the cell surface, mature 3T3-L1 adipocytes were incubated with 10 IU/mL heparin for 20 minutes.

3T3-F442a cells (P8-P14, Sigma) were maintained in DMEM (Lonza), supplemented with 10% NCS and 1% P/S. At confluency, cells were switched to DMEM (Lonza) supplemented with 10% FBS, 1% P/S and 5 µg/mL insulin (Sigma) to stimulate differentiation. During differentiation, medium was changed every 2/3 days. After 10 days, cells were switched back to regular medium and used for experiments 2/3 days later.

For isolation and differentiation of primary adipocytes, inguinal WAT was removed from *Angptl4*-/- and wild-type mice and placed in DMEM supplemented with 1% P/S and 1% bovine serum albumin (BSA) (Sigma-Aldrich) (17). Material from 2–3 mice was pooled, minced with scissors, and digested in collagenase-containing medium [DMEM with 3.2 mM $CaCl_2$, 1.5 mg/mL collagenase type II (C6885, Sigma-Aldrich), 10% FBS, 0.5% BSA, and 15 mM HEPES] for 1 h at 37°C. Following digestion, the cells were filtered through a 100 µm cell strainer (Falcon) to remove remaining cell clumps. The cell suspension was centrifuged at 1600 rpm for 10 min, after which the supernatant was removed and the pellet was resuspended in erythrocyte lysis buffer (155 mM NH_4Cl, 12 mM $NaHCO_3$, 0.1 mM EDTA). Upon incubation for 2–3 minutes at room temperature, cells were centrifuged at 1200 rpm for 5 min and the pelleted cells were resuspended in DMEM + 10% FCS + 1% P/S and plated. Upon confluency, the cells were differentiated according to the protocol as described above for 3T3-L1 cells, with the addition of 1 µM rosiglitazone during the initial differentiation step.

For WAT explants, gonadal WAT was taken from wild-type mice and *Angptl4*-/- mice and placed in DMEM supplemented with 1% P/S and 1% BSA. Fat pads were minced into small

pieces and divided into small mounds of WAT (~50–100 mg of tissue). WAT explants were placed into wells containing medium (DMEM with 1% P/S and 10% FCS) and incubated as indicated in the figure legends. Next, the medium was harvested and explant weights were determined. Explants were immediately lysed to prepare protein extracts.

siRNA-mediated knockdown

Dharmacon ON-TARGETplus SMARTpool siRNAs against mouse *Pcsk3* and *Angptl4* were purchased from Thermo Fisher-Scientific. siRNAs were diluted in Dharmacon 1x siRNA buffer (final concentration 20 mM KCl, 6 mM HEPES pH 7.5, 0.2 mM $MgCL_2$). Transfections for *Pcsk3* were performed with Lipofectamine RNAiMAX transfection reagent (Life Technologies, Bleiswijk, The Netherlands) at a concentration of 10 nM siRNA and 1.5 µL transfection reagent for a 24-wells plate. Transfections for Angptl4 were performed at a concentration of 25 nM siRNA and 2 µL Lipofectamine in a 24-wells plate. To examine the impact of either knockdown on LPL cleavage, mature 3T3-L1 adipocytes were washed with PBS, trypsinized and collected in DMEM. Following centrifugation at 1250 rpm for 5 minutes, pelleted cells were re-suspended and filtered through a 70 µM cell strainer. Adipocytes were plated at 70% confluency and two hours later siRNAs complexed to Lipofectamine were added. Cleavage of LPL was examined after 48 hours of incubation.

Western blots

Mouse or human fat pads, WAT explants, differentiated primary adipocytes, and differentiated 3T3-L1 and 3T3-F442a adipocytes were lysed in RIPA buffer (25 mM Tris-HCl pH 7.6, 150 mM NaCl, 1% NP-40, and 0.1% SDS; Thermo Fisher-Scientific, Landsmeer, The Netherlands) supplemented with protease and phosphatase inhibitors (Roche Diagnostics, Almere, The Netherlands). Following homogenization, lysates were placed on ice for 30 minutes and centrifuged 2–3 times at 13,000 rpm for 10 min at 4˚C to remove fat and cell debris. Concentration of protein lysates was determined by using a bicinchoninic acid (BCA) assay (Thermo Fisher-Scientific). Protein lysates (10–30 µg protein per lane) or medium aliquots (10–15 µL) were loaded onto 8-16% or 10% Criterion gels (Bio-Rad, Veenendaal, The Netherlands). Next, proteins were transferred onto a PVDF membrane using the Transblot Turbo System (Bio-Rad). Membranes were probed with a goat anti-mouse LPL antibody (28); mouse anti-human LPL antibodies 88b8 and 5D2 (27), a rabbit anti-mouse HSP90 antibody (Cell Signaling Technology, #4874); a rat anti-mouse ANGPTL4 antibody (Kairos 142-2, Adipogen); a mouse anti-mouse β-TUBULIN (sc-5274, Santa Cruz); or a rabbit anti-mouse PCSK3 (Abcam, ab183495) at 1:5000 (mLPL), 1:2000 (HSP90) or 1:1000 (PCSK3, ANGPTL4, hLPL and β-TUBULIN) dilutions. Blocking and the incubation of primary and

secondary antibodies were all done in Tris-buffered saline, pH 7.5, 0.1% Tween-20 (TBS-T), and 5% w/v skimmed milk. In between, membranes were washed in TBS-T. Quantification was performed with the ChemiDoc MP system (Bio-Rad) and Clarity ECL substrate (Bio-Rad). Equal loading of medium samples was verified by Coomassie blue staining.

Glycosylation of ANGPTL4 & LPL

Glycosylation of ANGPTL4 and LPL was analyzed by western blotting, as described above, after digestion of 10-20 µg with EndoH, PNGase or Protein Deglycosylation Mix (New England Biolabs), according to the manufacturer's instructions.

RNA isolation and qPCR

To isolate RNA, tissues or cells were homogenized using TRIzol (Thermo Fisher-Scientific) in a Qiagen Tissue lyser II (Qiagen, Venlo, The Netherlands) or by pipetting up and down. RNA was reverse transcribed using the First Strand cDNA synthesis kit (Thermo Fisher-Scientific). qPCR analyses were done on a CFX384 Real-Time PCR platform (Bio-Rad) with the SensiMix PCR mix from Bioline (GC biotech, Alphen aan de Rijn, The Netherlands).

Acknowledgements

This study was supported by grant 12CVD04 from the Fondation Leducq.

We kindly thank Anne Beigneux and Katsuyuki Nakajima for providing the antibodies 88b8 and 5D2 against human LPL, André Bensadoun for providing the antibody against mouse LPL, and Merel Defour for cDNA of the mouse tissue panel. The authors thank Sophie Schutte and Lydia Afman for the permission to use human adipose tissue material from the MONDIAL cohort.

Conflict of Interest

The authors declare that they have no conflicts of interest with the contents of this article.

References

1. Musunuru, K., and Kathiresan, S. (2016) Surprises From Genetic Analyses of Lipid Risk Factors for Atherosclerosis. Circ. Res. 118, 579–85

2. Bensadoun, A. (1991) Lipoprotein lipase. Annu. Rev. Nutr. 11, 217–37

3. Davies, B. S. J., Beigneux, A. P., Barnes, R. H., Tu, Y., Gin, P., Weinstein, M. M., Nobumori, C., Nyrén, R., Goldberg, I., Olivecrona, G., Bensadoun, A., Young, S. G., and Fong, L. G. (2010) GPIHBP1 Is Responsible for the Entry of Lipoprotein Lipase into Capillaries. Cell Metab. 12, 42–52

4. Kersten, S. (2014) Physiological regulation of lipoprotein lipase. Biochim. Biophys. Acta. 1841, 919–933

5. Dijk, W., and Kersten, S. (2016) Regulation of lipid metabolism by angiopoietin-like proteins. Curr. Opin. Lipidol. 27, 249–56

6. Wang, Y., Quagliarini, F., Gusarova, V., Gromada, J., Valenzuela, D. M., Cohen, J. C., and Hobbs, H. H. (2013) Mice lacking ANGPTL8 (Betatrophin) manifest disrupted triglyceride metabolism without impaired glucose homeostasis. Proc. Natl. Acad. Sci. U. S. A. 110, 16109–14

7. Wang, Y., McNutt, M. C., Banfi, S., Levin, M. G., Holland, W. L., Gusarova, V., Gromada, J., Cohen, J. C., and Hobbs, H. H. (2015) Hepatic ANGPTL3 regulates adipose tissue energy homeostasis. Proc. Natl. Acad. Sci. U. S. A. 112, 11630–5

8. Haller, J. F., Mintah, I. J., Shihanian, L. M., Stevis, P., Buckler, D., Alexa-Braun, C. A., Kleiner, S., Banfi, S., Cohen, J. C., Hobbs, H. H., Yancopoulos, G. D., Murphy, A. J., Gusarova, V., and Gromada, J. (2017) ANGPTL8 requires ANGPTL3 to inhibit lipoprotein lipase and plasma triglyceride clearance. J. Lipid Res. 58, 1166–73

9. Chi, X., Britt, E. C., Shows, H. W., Hjelmaas, A. J., Shetty, S. K., Cushing, E. M., Li, W., Dou, A., Zhang, R., and Davies, B. S. J. (2017) ANGPTL8 promotes the ability of ANGPTL3 to bind and inhibit lipoprotein lipase. Mol. Metab. 6, 1137–49

10. Catoire, M., Alex, S., Paraskevopulos, N., Mattijssen, F., Evers-van Gogh, I., Schaart, G., Jeppesen, J., Kneppers, A., Mensink, M., Voshol, P. J., Olivecrona, G., Tan, N. S., Hesselink, M. K. C., Berbée, J. F., Rensen, P. C. N., Kalkhoven, E., Schrauwen, P., and Kersten, S. (2014) Fatty acid-inducible ANGPTL4 governs lipid metabolic response to exercise. Proc. Natl. Acad. Sci. U. S. A. 111, E1043-52

11. Dijk, W., Heine, M., Vergnes, L., Boon, M. R., Schaart, G., Hesselink, M. K. C., Reue, K., van Marken Lichtenbelt, W. D., Olivecrona, G., Rensen, P. C. N., Heeren, J., and Kersten, S. (2015) ANGPTL4 mediates shuttling of lipid fuel to brown adipose tissue during sustained cold exposure. Elife. 4, e08428

12. Kroupa, O., Vorrsjö, E., Stienstra, R., Mattijssen, F., Nilsson, S. K., Sukonina, V., Kersten, S., Olivecrona, G., and Olivecrona, T. (2012) Linking nutritional regulation of Angptl4, Gpihbp1, and Lmf1 to lipoprotein lipase activity in rodent adipose tissue. BMC Physiol. 12, 13

13. Sukonina, V., Lookene, A., Olivecrona, T., and Olivecrona, G. (2006) Angiopoietin-like protein 4 converts lipoprotein lipase to inactive monomers and modulates lipase activity in adipose tissue. Proc. Natl. Acad. Sci. U. S. A. 103, 17450–5

14. Mysling, S., Kristensen, K. K., Larsson, M., Kovrov, O., Bensadouen, A., Jørgensen, T. J., Olivecrona, G., Young, S. G., and Ploug, M. (2016) The angiopoietin-like protein ANGPTL4 catalyzes unfolding of the hydrolase domain in lipoprotein lipase and the endothelial membrane protein GPIHBP1 counteracts this unfolding. Elife. 5, e20958

15. Makoveichuk, E., Vorrsjö, E., Olivecrona, T., and Olivecrona, G. (2013) Inactivation of lipoprotein lipase in 3T3-L1 adipocytes by angiopoietin-like protein 4 requires that both proteins have reached the cell surface. Biochem. Biophys. Res. Commun. 441, 941–6

16. Desai, U., Lee, E.-C., Chung, K., Gao, C., Gay, J., Key, B., Hansen, G., Machajewski, D., Platt, K. a, Sands, A. T., Schneider, M., Van Sligtenhorst, I., Suwanichkul, A., Vogel, P., Wilganowski, N., Wingert, J., Zambrowicz, B. P., Landes, G., and Powell, D. R. (2007) Lipid-lowering effects of anti-angiopoietin-like 4 antibody

recapitulate the lipid phenotype found in angiopoietin-like 4 knockout mice. Proc. Natl. Acad. Sci. U. S. A. 104, 11766–71

17. Dijk, W., Beigneux, A. P., Larsson, M., Bensadoun, A., Young, S. G., and Kersten, S. (2016) Angiopoietin-like 4 (ANGPTL4) promotes intracellular degradation of lipoprotein lipase in adipocytes. J. Lipid Res. 58, 7250–7

18. Turpeinen, H., Ortutay, Z., and Pesu, M. (2013) Genetics of the first seven proprotein convertase enzymes in health and disease. Curr. Genomics. 14, 453–67

19. Seidah, N. G., Sadr, M. S., Chrétien, M., and Mbikay, M. (2013) The multifaceted proprotein convertases: their unique, redundant, complementary, and opposite functions. J. Biol. Chem. 288, 21473–81

20. Lagace, T. A. (2014) PCSK9 and LDLR degradation. Curr. Opin. Lipidol. 25, 387–93

21. Lei, X., Shi, F., Basu, D., Huq, A., Routhier, S., Day, R., and Jin, W. (2011) Proteolytic processing of angiopoietin-like protein 4 by proprotein convertases modulates its inhibitory effects on lipoprotein lipase activity. J. Biol. Chem. 286, 15747–56

22. Mandard, S., Zandbergen, F., Tan, N. S., Escher, P., Patsouris, D., Koenig, W., Kleemann, R., Bakker, A., Veenman, F., Wahli, W., Müller, M., and Kersten, S. (2004) The direct peroxisome proliferator-activated receptor target fasting-induced adipose factor (FIAF/PGAR/ANGPTL4) is present in blood plasma as a truncated protein that is increased by fenofibrate treatment. J. Biol. Chem. 279, 34411–20

23. Chomel, C., Cazes, A., Faye, C., Bignon, M., Gomez, E., Ardidie-Robouant, C., Barret, A., Ricard-Blum, S., Muller, L., Germain, S., and Monnot, C. (2009) Interaction of the coiled-coil domain with glycosaminoglycans protects angiopoietin-like 4 from proteolysis and regulates its antiangiogenic activity. FASEB J. 23, 940–9

24. Essalmani, R., Susan-Resiga, D., Chamberland, A., Asselin, M.-C., Canuel, M., Constam, D., Creemers, J. W., Day, R., Gauthier, D., Prat, A., and Seidah, N. G. (2013) Furin is the primary in vivo convertase of angiopoietin-like 3 and endothelial lipase in hepatocytes. J. Biol. Chem. 288, 26410–8

25. Liu, J., Afroza, H., Rader, D. J., and Jin, W. (2010) Angiopoietin-like protein 3 inhibits lipoprotein lipase activity through enhancing its cleavage by proprotein convertases. J. Biol. Chem. 285, 27561–70

26. Jin, W., Fuki, I. V., Seidah, N. G., Benjannet, S., Glick, J. M., and Rader, D. J. (2005) Proprotein convertases [corrected] are responsible for proteolysis and inactivation of endothelial lipase. J. Biol. Chem. 280, 36551–9

27. Allan, C. M., Larsson, M., Hu, X., He, C., Jung, R. S., Mapar, A., Voss, C., Miyashita, K., Machida, T., Murakami, M., Nakajima, K., Bensadoun, A., Ploug, M., Fong, L. G., Young, S. G., and Beigneux, A. P. (2016) An LPL-specific monoclonal antibody, 88B8, that abolishes the binding of LPL to GPIHBP1. J. Lipid Res. 57, 1889–1898

28. Weinstein, M. M., Yin, L., Beigneux, A. P., Davies, B. S. J., Gin, P., Estrada, K., Melford, K., Bishop, J. R., Esko, J. D., Dallinga-Thie, G. M., Fong, L. G., Bensadoun, A., and Young, S. G. (2008) Abnormal patterns of lipoprotein lipase release into the plasma in GPIHBP1-deficient mice. J. Biol. Chem. 283, 34511–8

29. Davis, R. C., Wong, H., Nikazy, J., Wang, K., Han, Q., and Schotz, M. C. (1992) Chimeras of hepatic lipase and lipoprotein lipase. Domain localization of enzyme-specific properties. J. Biol. Chem. 267, 21499–504

30. Ben-Zeev, O., Stahnke, G., Liu, G., Davis, R. C., and Doolittle, M. H. (1994) Lipoprotein lipase and hepatic lipase: the role of asparagine-linked glycosylation in the expression of a functional enzyme. J. Lipid Res. 35, 1511–23

31. Chajek-Shaul, T., Friedman, G., Knobler, H., Stein, O., Etienne, J., and Stein, Y. (1985) Importance of the different steps of glycosylation for the activity and secretion of lipoprotein lipase in rat preadipocytes studied with monensin and tunicamycin. Biochim. Biophys. Acta (BBA)/Lipids Lipid Metab. 837, 123–34

32. Garten, W., Hallenberger, S., Ortmann, D., Schäfer, W., Vey, M., Angliker, H., Shaw, E., and Klenk, H. D. (1994) Processing of viral glycoproteins by the subtilisin-like endoprotease furin and its inhibition by specific peptidylchloroalkylketones. Biochimie. 76, 217–25

33. Lutz, E. P., Merkel, M., Kako, Y., Melford, K., Radner, H., Breslow, J. L., Bensadoun, A., and Goldberg, I. J. (2001) Heparin-binding defective lipoprotein lipase is unstable and causes abnormalities in lipid delivery to tissues. J. Clin. Invest. 107, 1183–92

34. Cisar, L. A., Hoogewerf, A. J., Cupp, M., Rapport, C. A., and Bensadoun, A. (1989) Secretion and degradation of lipoprotein lipase in cultured adipocytes. Binding of lipoprotein lipase to membrane heparan sulfate proteoglycans is necessary for degradation. J. Biol. Chem. 264, 1767–74

35. Kersten, S., Mandard, S., Tan, N. S., Escher, P., Metzger, D., Chambon, P., Gonzalez, F. J., Desvergne, B., and Wahli, W. (2000) Characterization of the fasting-induced adipose factor FIAF, a novel peroxisome proliferator-activated receptor target gene. J. Biol. Chem. 275, 28488–93

36. Cushing, E. M., Chi, X., Sylvers, K. L., Shetty, S. K., Potthoff, M. J., and Davies, B. S. J. (2017) Angiopoietin-like 4 directs uptake of dietary fat away from adipose during fasting. Mol. Metab. 6, 809–18

37. Dewey, F. E., Gusarova, V., O'Dushlaine, C., Gottesman, O., Trejos, J., Hunt, C., Van Hout, C. V., Habegger, L., Buckler, D., Lai, K.-M. V., Leader, J. B., Murray, M. F., Ritchie, M. D., Kirchner, H. L., Ledbetter, D. H., Penn, J., Lopez, A., Borecki, I. B., Overton, J. D., Reid, J. G., Carey, D. J., Murphy, A. J., Yancopoulos, G. D., Baras, A., Gromada, J., and Shuldiner, A. R. (2016) Inactivating Variants in ANGPTL4 and Risk of Coronary Artery Disease. N. Engl. J. Med. 374, 1123–33

38. Myocardial Infarction Genetics and CARDIoGRAM Exome Consortia Investigators, Stitziel, N. O., Stirrups, K. E., Masca, N. G. D., Erdmann, J., Ferrario, P. G., König, I. R., Weeke, P. E., Webb, T. R., Auer, P. L., Schick, U. M., Lu, Y., Zhang, H., Dube, M.-P., Goel, A., Farrall, M., Peloso, G. M., Won, H.-H., Do, R., van Iperen, E., Kanoni, S., Kruppa, J., Mahajan, A., Scott, R. A., Willenberg, C., Braund, P. S., van Capelleveen, J. C., Doney, A. S. F., Donnelly, L. A., Asselta, R., Merlini, P. A., Duga, S., Marziliano, N., Denny, J. C., Shaffer, C. M., El-Mokhtari, N. E., Franke, A., Gottesman, O., Heilmann, S., Hengstenberg, C., Hoffman, P., Holmen, O. L., Hveem, K., Jansson, J.-H., Jöckel, K.-H., Kessler, T., Kriebel, J., Laugwitz, K. L., Marouli, E., Martinelli, N., McCarthy, M. I., Van Zuydam, N. R., Meisinger, C., Esko, T., Mihailov, E., Escher, S. A., Alvar, M., Moebus, S., Morris, A. D., Müller-Nurasyid, M., Nikpay, M., Olivieri, O., Lemieux Perreault, L.-P., AlQarawi, A., Robertson, N. R., Akinsanya, K. O., Reilly, D. F., Vogt, T. F., Yin, W., Asselbergs, F. W., Kooperberg, C., Jackson, R. D., Stahl, E., Strauch, K., Varga, T. V, Waldenberger, M., Zeng, L., Kraja, A. T., Liu, C., Ehret, G. B., Newton-Cheh, C., Chasman, D. I., Chowdhury, R., Ferrario, M., Ford, I., Jukema, J. W., Kee, F., Kuulasmaa, K., Nordestgaard, B. G., Perola, M., Saleheen, D., Sattar, N., Surendran, P., Tregouet, D., Young, R., Howson, J. M. M., Butterworth, A. S., Danesh, J., Ardissino, D., Bottinger, E. P., Erbel, R., Franks, P. W., Girelli, D., Hall, A. S., Hovingh, G. K., Kastrati, A., Lieb, W., Meitinger, T., Kraus, W. E., Shah, S. H., McPherson, R., Orho-Melander, M., Melander, O., Metspalu, A., Palmer, C. N. A., Peters, A., Rader, D., Reilly, M. P., Loos, R. J. F., Reiner, A. P., Roden, D. M., Tardif, J.-C., Thompson, J. R., Wareham, N. J., Watkins, H., Willer, C. J., Kathiresan, S., Deloukas, P., Samani, N. J., and Schunkert, H. (2016) Coding Variation in ANGPTL4, LPL, and SVEP1 and the Risk of Coronary Disease. N. Engl. J. Med. 374, 1134–44

39. Doolittle, M. H., Ben-Zeev, O., Elovson, J., Martin, D., and Kirchgessner, T. G. (1990) The response of lipoprotein lipase to feeding and fasting. Evidence for posttranslational regulation. J. Biol. Chem. 265, 4570–7

40. Xu, Y.-X., Redon, V., Yu, H., Querbes, W., Pirruccello, J., Liebow, A., Deik, A., Trindade, K., Wang, X., Musunuru, K., Clish, C. B., Cowan, C., Fizgerald, K., Rader, D., and Kathiresan, S. (2018) Role of angiopoietin-like 3 (ANGPTL3) in regulating plasma level of low-density lipoprotein cholesterol. Atherosclerosis. 268, 196–206

41. Ono, M., Shimizugawa, T., Shimamura, M., Yoshida, K., Noji-Sakikawa, C., Ando, Y., Koishi, R., and Furukawa, H. (2003) Protein Region Important for Regulation of Lipid Metabolism in Angiopoietin-like 3 (ANGPTL3): ANGPTL3 is cleaved and activated in vivo. J. Biol. Chem. 278, 41804–41809

42. Molloy, S. S., Anderson, E. D., Jean, F., and Thomas, G. (1999) Bi-cycling the furin pathway: from TGN localization to pathogen activation and embryogenesis. Trends Cell Biol. 9, 28–35

43. Roebroek, A. J., Umans, L., Pauli, I. G., Robertson, E. J., van Leuven, F., Van de Ven, W. J., and Constam, D. B. (1998) Failure of ventral closure and axial rotation in embryos lacking the proprotein convertase Furin. Development. 125, 4863–76

44. Kern, P. A., Martin, R. A., Carty, J., Goldberg, I. J., and Ong, J. M. (1990) Identification of lipoprotein lipase immunoreactive protein in pre- and postheparin plasma from normal subjects and patients with type I hyperlipoproteinemia. J. Lipid Res. 31, 17–26

45. Gin, P., Goulbourne, C. N., Adeyo, O., Beigneux, A. P., Davies, B. S. J., Tat, S., Voss, C. V., Bensadoun, A., Fong, L. G., and Young, S. G. (2012) Chylomicronemia mutations yield new insights into interactions between lipoprotein lipase and GPIHBP1. Hum. Mol. Genet. 21, 2961–72

46. Goulbourne, C. N., Gin, P., Tatar, A., Nobumori, C., Hoenger, A., Jiang, H., Grovenor, C. R. M., Adeyo, O., Esko, J. D., Goldberg, I. J., Reue, K., Tontonoz, P., Bensadoun, A., Beigneux, A. P., Young, S. G., and Fong, L. G. (2014) The GPIHBP1-LPL complex is responsible for the margination of triglyceride-rich lipoproteins in capillaries. Cell Metab. 19, 849–60

47. Mysling, S., Kristensen, K. K., Larsson, M., Beigneux, A. P., Gårdsvoll, H., Fong, L. G., Bensadouen, A., Jørgensen, T. J., Young, S. G., and Ploug, M. (2016) The acidic domain of the endothelial membrane protein GPIHBP1 stabilizes lipoprotein lipase activity by preventing unfolding of its catalytic domain. Elife. 5, e12095

48. Lookene, A., Nielsen, M. S., Gliemann, J., and Olivecrona, G. (2000) Contribution of the carboxy-terminal domain of lipoprotein lipase to interaction with heparin and lipoproteins. Biochem. Biophys. Res. Commun. 271, 15–21

49. Lookene, A., Chevreuil, O., Ostergaard, P., and Olivecrona, G. (1996) Interaction of lipoprotein lipase with heparin fragments and with heparan sulfate: stoichiometry, stabilization, and kinetics. Biochemistry. 35, 12155–63

50. Ge, H., Yang, G., Huang, L., Motola, D. L., Pourbahrami, T., and Li, C. (2004) Oligomerization and regulated proteolytic processing of angiopoietin-like protein 4. J. Biol. Chem. 279, 2038–45

51. Dijk, W., Schutte, S., Aarts, E. O., Janssen, I. M. C., Afman, L., and Kersten, S. (2018) Regulation of angiopoietin-like 4 and lipoprotein lipase in human adipose tissue. J. Clin. Lipidol. 12, 773-83

52. Köster, A., Chao, Y. B., Mosior, M., Ford, A., Gonzalez-DeWhitt, P. A., Hale, J. E., Li, D., Qiu, Y., Fraser, C. C., Yang, D. D., Heuer, J. G., Jaskunas, S. R., and Eacho, P. (2005) Transgenic angiopoietin-like (angptl)4 overexpression and targeted disruption of angptl4 and angptl3: regulation of triglyceride metabolism. Endocrinology. 146, 4943–50

53. Alex, S., Lange, K., Amolo, T., Grinstead, J. S., Haakonsson, A. K., Szalowska, E., Koppen, A., Mudde, K., Haenen, D., Al-Lahham, S., Roelofsen, H., Houtman, R., van der Burg, B., Mandrup, S., Bonvin, A. M. J. J., Kalkhoven, E., Müller, M., Hooiveld, G. J., and Kersten, S. (2013) Short-chain fatty acids stimulate angiopoietin-like 4 synthesis in human colon adenocarcinoma cells by activating peroxisome proliferator-activated receptor γ. Mol. Cell. Biol. 33, 1303–16

5

Chapter 5

Characterization of ANGPTL4 function in macrophages and adipocytes using Angptl4-knockout and Angptl4-hypomorphic mice

Oteng A-B†, Ruppert PMM†, Boutens L, Dijk W, van Dierendonck XAMH, Olivecrona G, Stienstra R, Kersten S

† equal contribution

J Lipid Res. 2019 Oct;6600(10):1741–54.

Abstract

ANGPTL4 regulates plasma lipids, making it an attractive target for correcting dyslipidemia. However, ANGPTL4 inactivation in mice fed a high fat diet causes chylous ascites, an acute-phase response, and mesenteric lymphadenopathy. Here, we studied the role of ANGPTL4 in lipid uptake in macrophages and in the above-mentioned pathologies using Angptl4-hypomorphic and Angptl4–/– mice. Angptl4 expression in peritoneal and bone marrow-derived macrophages was highly induced by lipids. Recombinant ANGPTL4 decreased lipid uptake in macrophages, whereas deficiency of ANGPTL4 increased lipid uptake, upregulated lipid-induced genes, and increased respiration. ANGPTL4 deficiency did not alter LPL protein levels in macrophages. Angptl4-hypomorphic mice with partial expression of a truncated N-terminal ANGPTL4 exhibited reduced fasting plasma triglyceride, cholesterol, and non-esterified fatty acid levels, strongly resembling Angptl4–/– mice. However, during high fat feeding, Angptl4-hypomorphic mice showed markedly delayed and attenuated elevation in plasma serum amyloid A and much milder chylous ascites than Angptl4–/– mice, despite similar abundance of lipid-laden giant cells in mesenteric lymph nodes. In conclusion, ANGPTL4 deficiency increases lipid uptake and respiration in macrophages without affecting LPL protein levels. Compared with the absence of ANGPTL4, low levels of N-terminal ANGPTL4 mitigate the development of chylous ascites and an acute-phase response in mice.

Keywords: Angiopoietin-like 4; lipoprotein lipase; dyslipidaemia; macrophage foam cells; inflammation; glucose homeostasis.

Introduction

Elevated plasma triglyceride levels are increasingly considered as an independent risk factor for cardiovascular diseases (1–3). Triglycerides circulate in the blood in two major forms: as chylomicrons carrying the dietary triglycerides, and as very-low density lipoproteins carrying endogenously produced triglycerides (4). The clearance of plasma triglycerides is primarily mediated by the action of lipoprotein lipase (LPL). This secretory enzyme is produced by parenchymal cells of fat tissue, skeletal muscle, and heart, as well as by macrophages. With the help of the endothelial protein glycosylphosphatidylinositol-anchored high-density lipoprotein binding protein 1 (GPIHBP1), LPL is transferred from the surface of the sub-endothelial myocytes and adipocytes to the luminal side of the capillary endothelium. There, LPL hydrolyses the triglycerides contained in the triglyceride-rich lipoproteins to release fatty acids for uptake by the underlying tissues (5–8). The activity of LPL is regulated post-translationally by numerous factors, many of which are produced in the liver, including several apolipoproteins. In addition, LPL activity is governed by several members of the family of Angiopoietin-like proteins: ANGPTL3 (9) ANGPTL4 (10–12), and ANGPTL8 (13–15).

ANGPTL3 is produced in the liver and cooperates with ANGPTL8 to inhibit LPL activity in peripheral tissues (15–17). The role of ANGPTL3/ANGPTL8 in LPL regulation is particularly important in the fed state (18). By contrast, ANGPTL4 mainly plays a role in LPL regulation in the fasted state (19). Individuals who carry an inactive variant of ANGPTL4 exhibit lower levels of circulating triglycerides and have decreased odds of developing coronary heart disease (20, 21). In mice, overexpression of ANGPTL4 potently represses LPL activity and leads to hypertriglyceridemia, whereas deletion of ANGPTL4 stimulates LPL activity and drastically reduces plasma triglyceride levels (18, 22). In contrast to ANGPTL3, which functions as an endocrine factor, ANGPTL4 likely serves as a local regulator of LPL in tissues where LPL and ANGPTL4 are co-produced (23). Inhibition of LPL is mediated by the N-terminal coiled-coiled domain of ANGPTL4, causing the unfolding and inactivation of LPL, which may be accompanied by a change in the aggregation state of LPL (19, 24, 25). In adipocytes, ANGPTL4 promotes the cleavage and subsequent degradation of LPL, thereby preventing the delivery of LPL to the endothelial surface (26, 27). The important role of ANGPTL4 in governing plasma lipid levels in humans has made ANGPTL4 an attractive therapeutic target for correcting dyslipidemia and associated cardiovascular disorders.

However, we and others have shown that disabling ANGPTL4, either via monoclonal antibody-mediated or genetic inactivation, leads to a highly pro-inflammatory and ultimately lethal phenotype in mice fed a high saturated fat diet (28, 29). This marked phenotype includes mesenteric lymphadenopathy—characterized by the presence of lipid-laden Touton giant cells in mesenteric lymph nodes—as well as fibrinopurulent peritonitis,

chylous ascites, and marked elevation of acute-phase proteins in plasma, such as serum amyloid A and haptoglobin (29, 30). Accumulation of lipids in mesenteric lymph nodes was also observed in several female monkeys treated with an anti-ANGPTL4 antibody (21). Although there is so far no evidence pointing to the occurrence of abdominal lymphadenopathy in humans homozygous for an inactive ANGPTL4 variant (21), currently the therapeutic prospects of whole body ANGPLT4 inactivation are not very favourable.

The deleterious effects of ANGPTL4 inactivation in mesenteric lymph nodes were previously attributed to the role of ANGPTL4 as LPL inhibitor in macrophages. Specifically, ANGPTL4 inactivation would increase LPL activity, leading to excessive lipid uptake in macrophages and a concomitant pro-inflammatory response (29). We have shown that recombinant ANGPTL4 represses lipid uptake into peritoneal macrophages incubated with chyle (29). However, whether endogenous ANGPTL4 suppresses lipid uptake into macrophages was not addressed. Accordingly, the first aim of our paper was to examine the influence of endogenous ANGPTL4 on lipid uptake and utilization in macrophages and explore the underlying mechanisms.

The mouse model that revealed the effect of ANGPTL4 inactivation on mesenteric lymphadenopathy and other pathologies is a whole body ANGPTL4 knock-out model characterized by the deletion of exons 2 and 3 and part of intron 1, leading to the absence of ANGPTL4 protein (31). Whether other and milder forms of genetic ANGPTL4 inactivation in mice provoke a similar phenotype upon feeding a high saturated fat diet is unclear. Accordingly, the second aim of our paper was to further investigate the role of ANGPTL4 in the aforementioned pathologies using *Angptl4*-hypomorphic mice.

Materials and Methods

Animal studies

Animal studies were performed in male purebred wild-type (WT), *Angptl4*^{hyp} and *Angptl4*$^{-/-}$ mice. All mice were on the same C57Bl/6 background strain. The *Angptl4*^{hyp} mice were a kind donation from Dr. Nguan Soon Tan (Nanyang Technological University, Singapore). The *Angptl4*^{hyp} mice can also be classified as *Angptl4* knockout-first mice (32), which upon stepwise crossing with mice expressing flippase recombinase and Cre recombinase can be used to generate a tissue-specific *Angptl4* knockout mouse model (33, 34). The sequence of the *Angptl4* construct is available at: https://www.i-dcc.org/imits/targ_rep/alleles/5215/escell-clone-genbank-file

High fat diet intervention: Eleven to 16-week-old mice (10 wild-type, 11 *Angptl4*^{hyp} and 8 *Angptl4*$^{-/-}$) were fed a high fat diet containing 45 energy percent as triglycerides (D12451, Research Diets Inc., New Brunswick, NJ). The high fat feeding of the 3 groups of mice was not done in parallel. After week 2 and 4 of the intervention, blood samples were collected to measure plasma serum amyloid A (SAA). After 20 weeks, blood was collected via orbital puncture under isoflurane anaesthesia. Immediately thereafter, the mice were euthanized by cervical dislocation. Tissues were excised and immediately frozen in liquid nitrogen followed by storage at −80°C. The animal studies were approved by the Local Animal Ethics Committee of Wageningen University (AVD104002015236: 2016.W-0093.005, 2016.W-0093.007).

Fasting intervention: Mice were fed a standard chow diet since weaning. Mice were either kept on chow or fasted for 24 hours and euthanized between 9.00 and 11.00 hours. Blood was collected via orbital puncture under isoflurane anaesthesia. Immediately thereafter, the mice were euthanized by cervical dislocation. Tissues were excised and immediately frozen in liquid nitrogen followed by storage at −80°C.

Intraperitoneal glucose tolerance test: After 18 weeks of high fat diet, the mice were fasted for 5 hours prior to the glucose tolerance test. The mice were injected intraperitoneally with glucose (1g/kg body weight) (Baxter, Deerfield, IL, USA). Blood samples from tail vein bleeding were tested for glucose levels at different time points following glucose injection using a GLUCOFIX Tech glucometer and glucose sensor test strips (GLUCOFIX Tech, Menarini Diagnostics, Valkenswaard, The Netherlands).

Histology

Haematoxylin and eosin staining was performed on the mesenteric lymph nodes. During the mice sections, lymph nodes were isolated into plastic cassettes and immediately fixated in 4% paraformaldehyde. The tissues were processed and embedded into paraffin blocks. Thin sections of the blocks were made at 5 µm using a microtome and placed onto Superfrost glass slides followed by overnight incubation at 37°C. The tissues were stained in Mayer hematoxylin solution for 10 minutes and in eosin for 10 seconds at room temperature with intermediate washings in ethanol. The tissues were allowed to dry at room temperature followed by imaging using light microscope.

Quantification of plasma parameters

Blood samples were collected into EDTA-coated tubes and centrifuged at 4°C for 15 min at 10,000 *g*. Plasma was collected and stored at -80°C. ELISA kits were used to measure plasma serum amyloid (SAA) (Tridelta Development Ltd, Ireland) and haptoglobin (Abcam, Cambridge, UK) according to manufacturer's protocol. Measurement of plasma levels of triglycerides, non-esterified fatty acids (NEFA) and glycerol were performed using kits from HUMAN Diagnostics (Wiesbaden, Germany) according to manufacturer's protocol. Plasma levels of cholesterol and glucose were also measured using kits from Diasys Diagnostics Systems (Holzheim, Germany) according to manufacturer's protocol.

LPL activity measurements

LPL activity levels in epididymal white adipose tissues were measured in triplicate with a [^{3}H] triolein-labeled lipid emulsion as previously described (35). Protein contents in homogenates of adipose tissue were measured using Markwell's modified Lowry method (36).

Cell Culture

Bone marrow cells were isolated from femurs of wild-type or *Angptl4*$^{-/-}$ mice following standard protocol and differentiated into macrophages (bone marrow-derived macrophages) in 6-8 days in Dulbecco's modified eagle's medium (DMEM; Lonza, Verviers, Belgium) containing 10% fetal bovine serum (FBS) and 1% Penicillin/Streptomycin (PS) supplemented with 20% L929-conditioned medium (L929). After 6-8 days, non-adherent cells were removed and adherent cells were washed and plated in 6-, 12-, or 48 well plates in DMEM/FBS/PS + 5% L929. After 24 hours, the cells were washed with PBS and treated. Peritoneal macrophages were obtained by infusion, and subsequent collection of ice-cold PBS from the abdominal cavity, and frozen directly or brought into culture in DMEM containing 10% FBS and 1% PS. RAW264.7 macrophages were cultured in DMEM containing 10% FBS and 1% P/S. All cells were maintained in a humidified incubator at 37°C with 5% CO_2.

Inguinal white adipose tissue from 3-4 WT, *Angptl4*^{hyp} and *Angptl4*$^{-/-}$ mice was collected and placed in DMEM supplemented with 1% PS and 1% bovine serum albumin (BSA; Sigma-Aldrich). Material was minced with scissors and digested in collagenase-containing medium (DMEM with 3.2 mM $CaCl_2$, 1.5 mg/ml collagenase type II (C6885, Sigma-Aldrich), 10% FBS, 0.5% BSA, and 15 mM HEPES) for 1 h at 37°C, with occasional vortexing. Cells were filtered through a 100-µm cell strainer (Falcon) to remove remaining cell clumps and lymph nodes.

The cell suspension subsequently was centrifuged at 1600 rpm for 10 min and the pellet was resuspended in erythrocyte lysis buffer (155 mM NH_4Cl, 12 mM $NaHCO_3$, 0.1 mM EDTA). Upon incubation for 2 min at room temperature, cells were centrifuged at 1200 rpm for 5 min and the pelleted cells were resuspended in DMEM + 10% FBS + 1% P/S and plated. Upon confluence, the cells were differentiated according to the protocol as described previously (14, 15). Briefly, confluent SVFs were plated in 1:1 surface ratio, and differentiation was induced 2 days afterwards by switching to a differentiation induction cocktail (DMEM containing 10% FBS, 1% P/S, 0.5 mM isobutylmethylxanthine, 1 µM dexamethasone, 7 µg/ml insulin and 1 µM rosiglitazone) for 3 days. Subsequently, cells were maintained in DMEM supplemented with 10% FBS, 1% P/S, and 7 µg/ml insulin for 3-6 days and switched to DMEM with 10% FBS and 1% P/S for 3 days. Average rate of differentiation was at least 80% as determined by eye.

Cell culture experiments and chemical treatments

Bone marrow-derived macrophages (BMDM) and peritoneal macrophages were exposed to 0.5 mM intralipid or 0.5 mM oleic acid (Sigma-Aldrich) for 6 hours in DMEM/PS media. The oleic acid was conjugated to BSA at a ratio of 2:1 (BSA:oleic acid). BMDM were also treated with synthetic PPAR agonists; 1 µM Wy14643, 1 µM rosiglitazone, 1 µM L165041, 1 µM GW501516 or vehicle control for 6 hours. All PPAR agonists were obtained from Sigma-Aldrich. Peritoneal macrophages and RAW264.7 cells were incubated for 6 hours with lymph (final triglyceride concentration of 2 mM, which was collected from rats provided with palm-oil based high fat diet overnight). BMDM were co-incubated for 6 hours with 10 µM orlistat (Sigma-Aldrich) and 0.5 mM intralipid. RAW264.7 macrophages treated with 0.5 mM intralipid or lymph was incubated with or without 0.5 µg/mL recombinant ANGPTL4 (R&D Systems, Abingdon, UK). In a separate experiment, BMDM of wild-type and *Angptl4*$^{-/-}$ mice were exposed to ER to Golgi transport inhibitors Monensin (10 µM, 3 hours, Cayman Chemicals) and Brefeldin A (5 µg/mL, 4 hours, Sigma-Aldrich), proteasomal degradation inhibitor MG132 (40 µM, 4 hours, Sigma-Aldrich) and lysosomal degradation inhibitors e64d (20 µM, 24 hours, Sigma-Aldrich) and Leupeptin (5 µM, 16 hours, Cayman Chemicals).

Oil red-O staining

Oil red-O staining was performed in RAW264.7 cells incubated with intralipid or lymph in the presence or absence of recombinant ANGPTL4. A stock of oil red O (Sigma) was prepared by dissolving 0.5 g in 500 ml of isopropanol. Working concentrations were made by dissolving stock concentrations with water (3 stock : 2 water) and filtered. Treated cells were washed twice with PBS, followed by fixation with 4% formalin for 30 min. The cells

were then washed twice with PBS and incubated with oil red-O dye for 20 min. The stained cells were washed 3 times with ddH_2O after which cells were visualised under a light microscope and pictures taken.

Bodipy staining

For visualization of lipid droplets, BMDM of wild-type and *Angptl4*$^{-/-}$ mice were washed with PBS, fixated in 4% formalin and subsequently stained with 1 ng/mL Bodipy 493/503 (ThermoFisher Scientific, Landsmeer, The Netherlands).

RNA isolation and quantitative real-time PCR

Total RNA was isolated from tissues and cells by homogenizing in TRIzol (Thermo Fisher Scientific) either with a QIagen Tissue Lyser II (Qiagen, Venlo, The Netherlands) or by pipetting up and down. Reverse transcription was performed using the iScript™ cDNA Synthesis Kit (Biorad) according to the manufacturer's protocol. Quantitative PCR amplifications were done on a CFX384 real-time PCR platform (Bio-Rad) with the SensiMix PCR mix from Bioline (GC Biotech, Alphen aan de Rijn, The Netherlands). Primer sequences of genes are provided in Supplemental Table 1. Gene expression values were normalized to the housekeeping gene *36b4* (*Rplp0*, ribosomal protein lateral stalk subunit P0).

Microarray analysis

RNeasy mini columns (Qiagen, Venlo, the Netherlands) were used to isolate RNA from mouse peritoneal macrophages that were incubated for 6 hours with 0.5 mM intralipid in the presence or absence of 2.5 μg/mL recombinant ANGPTL4. RNA quality was verified on an Agilent 2100 Bioanalyzer (Agilent Technologies, Amsterdam, The Netherlands) using 6000 Nano Chips according to manufacturer's instructions. RNA was considered suitable for array hybridization only if RNA integrity number exceeded 8.0. RNA from 3 samples per group was pooled for microarray analysis. One hundred nanogram of RNA was used for Whole Transcript cDNA synthesis (Affymetrix, Santa Clara, CA). Hybridization, washing, and scanning of Affymetrix GeneChip Mouse Gene 1.0 ST Arrays were carried out according to standard Affymetrix protocols. Scans of the Affymetrix arrays were processed using packages from the Bioconductor project. Arrays were normalized using the Robust Multi-array Average method (37, 38). Probe sets were defined by assigning probes to unique gene identifiers, e.g. Entrez ID (39). Changes in gene expression were calculated as signal log ratio's between treatment and control. These ratios were used to create heatmaps within Excel.

Affymetrix GeneChip analysis was carried out on WT mouse BMDM incubated with oleate (250 µM) for 5 hours (40). CEL files were downloaded from the internet via Gene Expression Omnibus (GSE77104) and processed as described above.

Extracellular flux analysis

Real-time oxygen consumption rates (OCR) of BMDM from wild-type and *Angptl4*$^{-/-}$ mice were assessed using XF-96 Extracellular Flux Analyzer (Seahorse, Bioscience, Santa Clara, CA, USA). Basal metabolic rates of BMDM seeded in quintuplicate were determined during three consecutive measurements in unbuffered Seahorse medium (8.3 g DMEM powder, 0.016 g phenol red and 1.85 g NaCl in 1 L milli-Q, pH 7.4 at 37°C, sterile-filtered) containing 25 mM glucose and 2 mM L-glutamine. Measurements were performed after 6 hour treatment with intralipid (0.5 mM) in the presence or absence of recombinant ANGPTL4 (0.5ug/mL). After basal measurements, three consecutive measurements were made following addition of 1.5 µM oligomycin, 1.5 µM carbonyl cyanide-4-(trifluoromethoxy)phenylhydrazone (FCCP) and combination of 2 µM antimycin A and 1 µM rotenone. Pyruvate (1 mM) was added together with FCCP to fuel maximal respiration. All compounds used during the Seahorse runs were acquired from Merck. Signals were normalized to relative DNA content in the wells using the Quanti-iT^{TM} dsDNA Assay kit (ThermoFisher).

Western immunoblotting

To isolate protein, mouse fat pads, differentiated primary adipocytes, primary macrophages and whole adipose tissues were lysed in RIPA Lysis and Extraction Buffer (25 mM Tris-HCl, pH 7.6, 150 mM NaCl, 1% Nonidet P-40, and 0.1% SDS; Thermo Fisher Scientific) supplemented with protease and phosphatase inhibitors (Roche Diagnostics, Almere, The Netherlands). Following homogenization, lysates were placed on ice for 30 min and centrifuged 2–3 times at 13,000 rpm for 10 min at 4°C to remove fat and cell debris. Concentration of protein lysates was determined using a bicinchoninic acid assay (Thermo Fisher Scientific). For assessment of LPL release, BMDM were treated for 20 mins with 10 IU/mL heparin (# 012866-08, LEO Pharma). For assessment of glycosylation of LPL, 2—30 µg of proteins was digested with endoglycosidase H (EndoH), (New England BioLabs) according to manufacturer's protocol. Protein lysates (10–30 µg of protein/lane) were loaded onto 8–16% or 10% Criterion gels (Bio-Rad, Veenendaal, The Netherlands). Next, proteins were transferred onto a polyvinylidene difluoride membrane using the Transblot Turbo System (Bio-Rad). Membranes were probed with a goat anti-mouse LPL antibody (41), a rabbit anti-mouse HSP90 antibody (#4874S, Cell Signaling), a rat anti-mouse

ANGPTL4 antibody (Kairos 142-2, Adipogen) and a rabbit anti-mouse ANGPTL4 antibody (742) (42) at 1:5000 (mLPL), 1:2000 (HSP90), or 1:1000 (ANGPTL4) dilutions. Blocking and the incubation of primary and secondary antibodies were all done in TBS, pH 7.5, 0.1% Tween 20 (TBS-T), and 5% (w/v) skimmed milk at 1:5000. In between, membranes were washed in TBS-T. Quantification was performed with the ChemiDoc MP system (Bio-Rad) and Clarity ECL substrate (Bio-Rad). Equal loading of medium samples was verified with HSP90.

Statistical Analysis

Statistical analyses were performed using one-way ANOVA followed by Tukey HSD test or by Student's t test. Data are presented as mean ± SEM (animal experiments) or mean ± SD (cell culture studies). $P < 0.05$ was considered statistically significant.

Results

Angptl4 expression is sensitive to lipids and regulates lipid uptake in macrophages

We previously suggested that enhanced LPL-mediated lipid uptake in macrophages may be at the basis of the mesenteric lymphadenopathy in *Angptl4*$^{-/-}$ mice fed a high fat diet (29). To better understand the role of endogenous ANGPTL4 in lipid uptake in macrophages, we first studied the regulation of *Angptl4* expression by lipids in macrophages. Treatment of peritoneal macrophages with oleic acid markedly increased *Angptl4* mRNA (Fig. 1A). Similarly, treatment of peritoneal and bone marrow-derived macrophages with intralipid markedly induced *Angptl4* mRNA (Fig. 1B). Interestingly, analysis of a publicly available transcriptomics dataset indicated that *Angptl4* is the most highly induced gene in BMDM upon treatment with oleic acid (Fig. 1C) (43). Treatment of BMDM with the synthetic PPARγ agonist rosiglitazone and the synthetic PPARδ agonists L165041 and GW501516 markedly increased *Angptl4* mRNA (Fig. 1D). By contrast, the PPARα agonist Wy14643 had no effect on *Angptl4* expression. These data suggest that the effect of lipid treatment on *Angptl4* expression in BMDM might be mediated by PPARδ and/or PPARγ.

To study the effect of exogenous ANGPTL4 on lipid uptake in macrophages, RAW264.7 macrophages were treated with intralipid in the presence or absence of recombinant ANGPTL4. ANGPTL4 clearly reduced lipid accumulation, as shown by decreased Oil Red O staining (Fig. 2A). Similar results were obtained in peritoneal macrophages incubated with lymph, an endogenous lipid source (Fig. 2B). Transcriptomics analysis of peritoneal macrophages treated with intralipid showed that the induction of lipid-sensitive genes by intralipid was almost completely abolished in the presence of recombinant ANGPTL4 (Fig. 2C).

To study the effect of endogenous ANGPTL4 on lipid uptake in macrophages, wild-type and *Angptl4*$^{-/-}$ BMDM were treated with intralipid. Lipid accumulation was distinctly higher in *Angptl4*$^{-/-}$ macrophages than in wild-type macrophages, as shown by Bodipy staining (Fig. 2D). This effect could be abolished by treatment with orlistat, a serine hydrolase inhibitor of LPL (Fig. 2D). Consistent with enhanced lipid uptake in *Angptl4*$^{-/-}$ macrophages, the effect of intralipid on the expression of lipid-sensitive genes was much more pronounced in *Angptl4*$^{-/-}$ BMDM than in wild-type BMDM (Fig. 2E). Similar results were obtained in peritoneal wild-type

and *Angptl4*$^{-/-}$ macrophages upon loading with lymph (Fig. 2F). Together, these data strongly suggest that ANGPTL4 controls lipid uptake in macrophages via regulation of LPL.

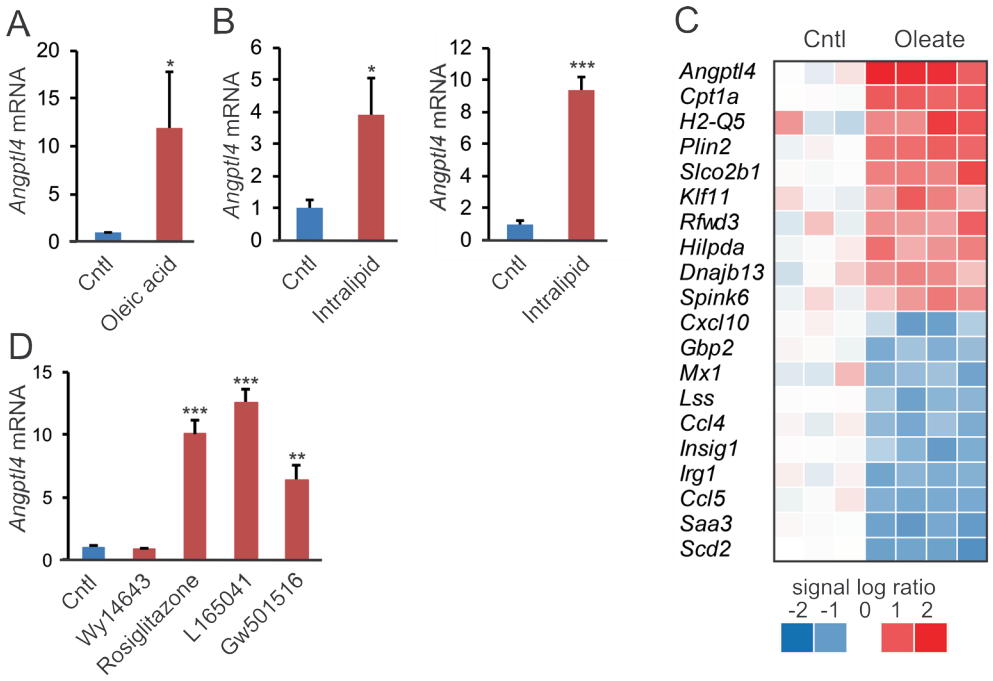

Figure 1. Angptl4 expression is induced in primary macrophages by lipid stimulation or PPAR agonists. (A) Angptl4 expression in peritoneal macrophages treated with 0.5 mM oleic acid for 6 hours. (B) Angptl4 expression in peritoneal macrophages (left) and BMDM (right) treated for 6 hours with 0.5 mM intralipid. (C) Heatmap of top 10 most upregulated and top 10 most downregulated genes in BMDM treated for 5 hours with 250 uM oleic acid or BSA (vehicle control) (GSE77104) (43). (D) Angptl4 expression in BMDM treated for 6 hours with 1 μM of PPAR agonists Wy14643 (PPARα), GW501516 (PPARδ), L165041 (PPARδ) and rosiglitazone (PPARγ) or vehicle (DMSO). mRNA expression was normalized to 36b4. Data are mean ± SD from 3 biological replicates; *p < 0.05, **p < 0.01 and ***p < 0.001 relative to vehicle control.

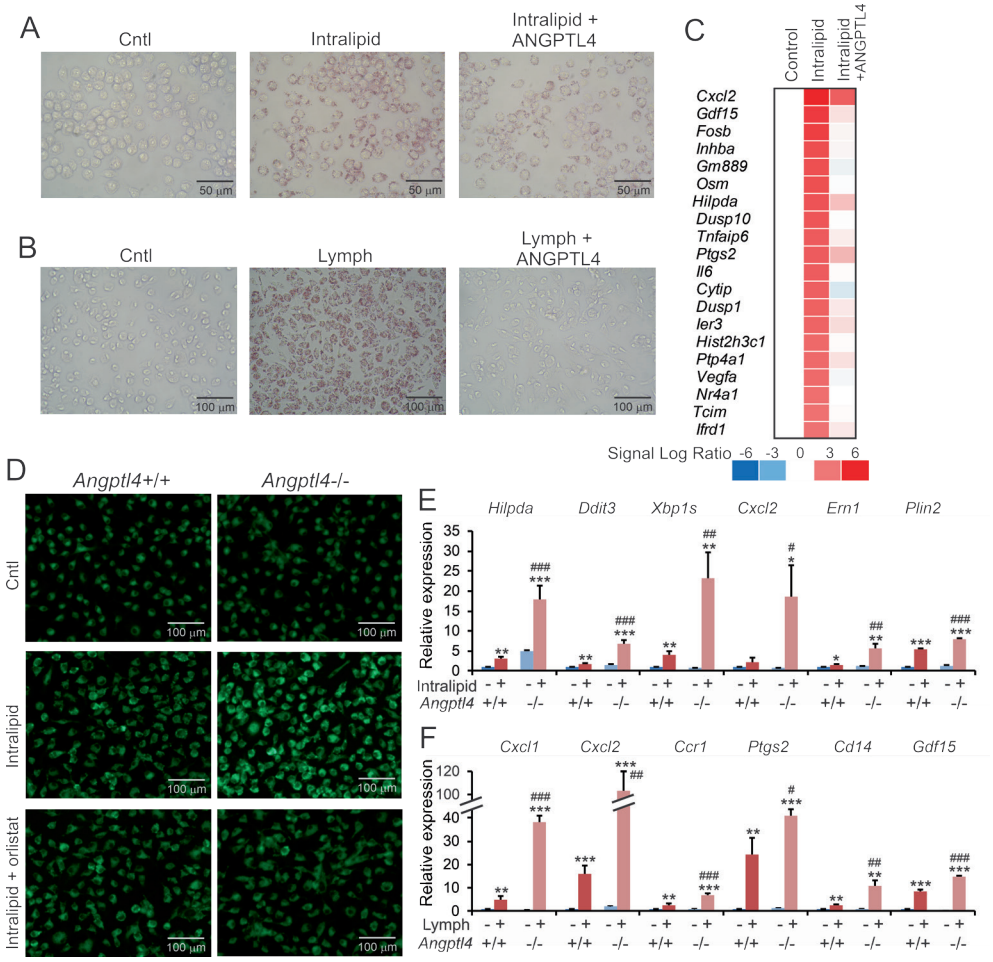

Figure 2. ANGPTL4 deficiency promotes macrophage lipid uptake and magnifies the induction of lipid-sensitive genes. (A) Oil red O staining of lipid droplets in RAW264.7 macrophages treated with 0.5 mM intralipid for 6 hours in the presence or absence of 0.5 µg/mL recombinant ANGPTL4. (B) Oil red O staining of lipid droplets in peritoneal macrophages treated for 6 hours with lymph (final triglyceride concentration of 2 mM) in the presence or absence of 0.5 µg/mL recombinant ANGPTL4. (C) Microarray heatmap showing expression profile of lipid-sensitive genes in peritoneal macrophages treated for 6 hours with 0.5 mM intralipid in the presence or absence of recombinant ANGPTL4. (D) Bodipy staining of *Angptl4*$^{+/+}$ and *Angptl4*$^{-/-}$ BMDM cultured with regular culture medium (Cntl), or for 6 hours with 0.5 mM intralipid with or without orlistat. (E-F) mRNA expression of lipid sensitive genes in *Angptl4*$^{+/+}$ and *Angptl4*$^{-/-}$ BMDM treated for 6 hours with 0.5 mM intralipid (E) or peritoneal macrophages treated for 6 hours with lymph (final triglyceride concentration of 2 mM) (F). mRNA expression was normalized to *36b4*. Data are mean ± SD from 3 biological replicates; *p < 0.05, **p < 0.01 and ***p < 0.001 relative to untreated wild-type; and #p < 0.05, ##p < 0.01 and ###p < 0.001 relative to wild-type + intralipid/lymph.

ANGPTL4 deficiency increases respiration in BMDM but does not influence LPL levels

To test if differences in lipid uptake between the genotypes are reflected in fuel utilization, we measured real time metabolic fluxes in BMDM using the Seahorse machine (Fig. 3A). Interestingly, after intralipid treatment, basal and maximal respiration was significantly higher in *Angptl4*$^{-/-}$ than wild-type macrophages (Fig. 3B). Treatment with exogenous ANGPTL4 resulted in slightly lower basal and maximal respiration in *Angptl4*$^{-/-}$ BMDM, but this effect was not statistically significant. These data suggest that the inhibitory effect of endogenous ANGPTL4 on LPL-mediated lipid uptake in macrophages is accompanied by a decrease in fuel utilization.

We previously showed in primary adipocytes that ANGPTL4 deficiency is paralleled by elevated LPL protein levels (26). To study the influence of ANGPTL4 deficiency on LPL protein in macrophages, we performed Western blot for LPL in BMDM from wild-type and *Angptl4*$^{-/-}$ mice, with and without intralipid treatment. In contrast to what was observed in adipocytes, ANGPTL4 deficiency did not have any effect on LPL protein in macrophages and did not alter the ratio between the active, endonuclease H-resistant form and the inactive, endonuclease-sensitive form of LPL (Fig. 3C). In addition, the amount of LPL that could be released into the medium by treatment of the macrophages with heparin did not differ between the two genotypes (Fig. 3D).

Additional experiments showed that inhibition of ER to Golgi transport by Monensin and Brefeldin A increased intracellular LPL levels, as did inhibition of proteasomal degradation by MG132, albeit to a lesser extent (Fig. 3E). By contrast, inhibition of lysosomal proteases using Leupeptin and e64d did not alter intracellular LPL accumulation in BMDM (Fig. 3E). These data suggest that unlike LPL in adipocytes, LPL in macrophages is not subject to lysosomal degradation but instead is broken down—at least partly—via proteasomal degradation. Interestingly, none of these effects were influenced by ANGPTL4 deficiency (Fig. 3E). These data indicate that in macrophages, inhibition of LPL activity by ANGPTL4 is not accompanied by a decrease in LPL protein levels.

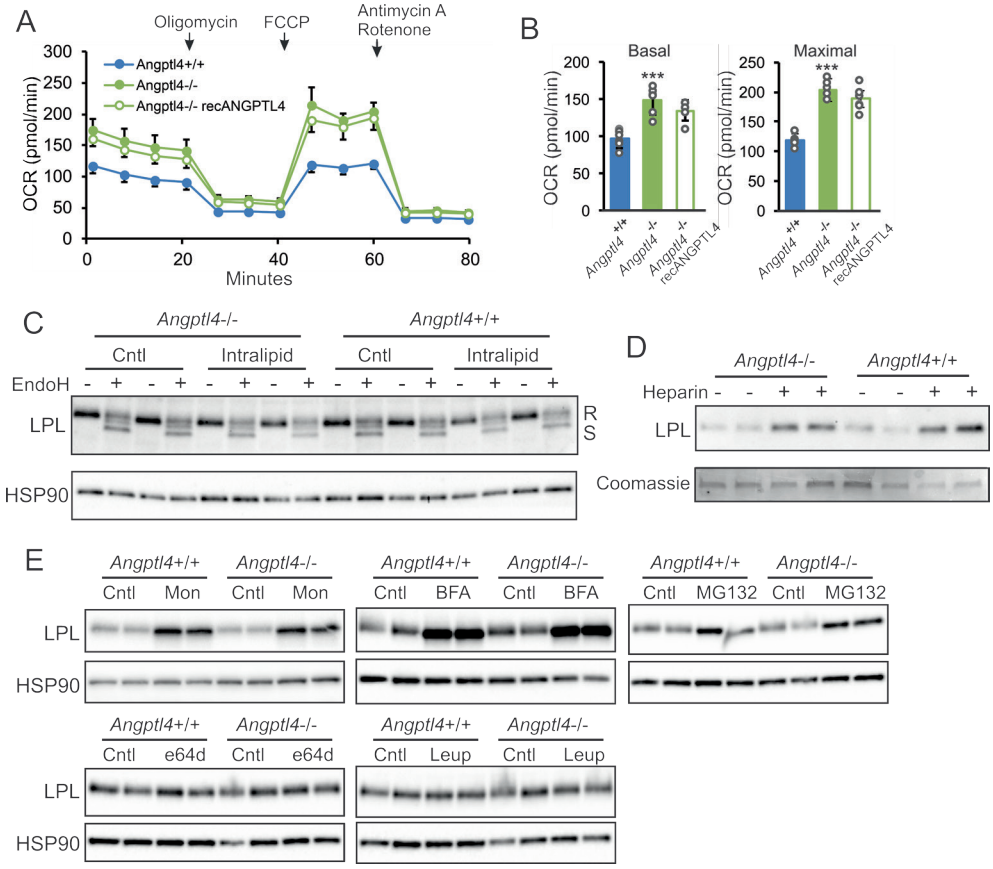

Figure 3. ANGPTL4 deficiency increases respiration in BMDM but does not influence LPL abundance. (A) Real time changes in oxygen consumption rate (OCR) in BMDM from *Angptl4*$^{+/+}$ and *Angptl4*$^{-/-}$ mice in presence or absence of recombinant ANGPTL4, treated with 0.5 mM intralipid for 6 hours, and assessed in unbuffered medium during sequential injections with Oligomycin, FCCP, and antimycin A + rotenone. (B) Basal (left) and maximal (right) oxygen consumption rate (OCR) in BMDM from *Angptl4*$^{+/+}$ and *Angptl4*$^{-/-}$ mice in presence or absence of recombinant ANGPTL4 (0.5 µg/mL), incubated with 0.5 mM intralipid for 6 hours. Measurements were done in quintuplicates in unbuffered medium. Data are mean ± SD; ***p < 0.001. (C) Immunoblot of LPL in *Angptl4*$^{+/+}$ and *Angptl4*$^{-/-}$ BMDM treated for 6 hours with or without 0.5 mM intralipid in the presence or absence of endonuclease-H. (D) Immunoblot of LPL from culture medium of *Angptl4*$^{+/+}$ and *Angptl4*$^{-/-}$ BMDM treated with or without heparin. (E) Immunoblot of LPL in *Angptl4*$^{+/+}$ and *Angptl4*$^{-/-}$ BMDM treated with or without ER to Golgi transport inhibitors Monensin (Mon; 10 µM for 3 hours) and Brefeldin A (BFA; 5 µg/mL for 4 hours), proteasomal degradation inhibitor MG132 (40 µM for 4 hours) and lysosomal degradation inhibitors e64d (20 µM for 24 hours) and Leupeptin (Leup; 5 µM for 16 hours). HSP90 or Coomassie staining serve as loading control.

Angptl4-hypomorphic mice show partial expression of N-terminal exons and truncated ANGPTL4 protein in adipose tissue and primary adipocytes

The second objective of this paper was to investigate whether in addition to the *Angptl4*$^{-/-}$ model, an alternative model of genetic *Angptl4* inactivation also leads to a deleterious phenotype in mice fed a high saturated fat diet. To that end, we used *Angptl4* knockout first mice. The *Angptl4* knockout first allele contains in intron 3 a reading frame–independent LacZ gene trap cassette followed by a promoter-driven selection cassette (Fig. 4A). The *Angptl4* knockout first allele was designed to create tissue-specific *Angptl4*$^{-/-}$ mice by subsequent crossing with mice expressing the FLP and Cre recombinase enzymes. Interestingly, based on sequence analysis, it can be predicted that when omitting the FLP and Cre recombinase reaction steps, the *Angptl4* knockout first allele might lead to the production of a whole body mutant 32 kDa ANGPTL4 protein covering amino acid residues 1-186, followed by 102 amino acids originating from the EN2a splice acceptor site and the internal ribosome entry site (Fig. 4B). Accordingly, we hypothesized that the *Angptl4* knockout first allele may give rise to a truncated ANGPTL4 protein that contains the N-terminal domain responsible for LPL inhibition. In the remainder of the paper, we will refer to the ANGPTL4 knockout first mice as *Angptl4*^{hyp} mice, as explained below.

To carefully characterize the *Angptl4*^{hyp} mice, we performed qPCR for *Angptl4* using cDNA obtained from adipose tissue and primary adipocytes of wild-type, *Angptl4*^{hyp} and *Angptl4*$^{-/-}$ mice. Primers were designed to amplify parts of the cDNA encoded by specific exons. Remarkably, whereas no *Angptl4* expression using any of the primers could be detected in adipose tissue and adipocytes of *Angptl4*$^{-/-}$ mice, substantial *Angptl4* expression (approx. 30-50% of wild-type level) for exon 1-3 was found in the *Angptl4*^{hyp} mice (Fig. 4C, D). By contrast, no amplification was observed in the *Angptl4*^{hyp} mice using primers directed against the cDNA encoded by exons 4-7 (Fig. 4C, D). A similar expression profile of the *Angptl4* exons was observed in the liver of *Angptl4*^{hyp} mice (Supplemental Fig. 1A). Further PCR analysis of the cDNA suggested the presence of an mRNA comprising *Angptl4* exons 1 to 3, the EN2a splice acceptor site, and more than 50% of the IRES site, but without the LacZ gene (Supplemental table 2). These data indicate that the *Angptl4*^{hyp} mice produce a mutated cDNA that may lead to the production of a truncated ANGPTL4 protein.

To verify this notion, we performed Western blot on adipose tissue of the three types of mice using a monoclonal antibody directed against mouse ANGPTL4. A strong ANGPTL4 band at 50 kDa was observed in the wild-type mice (Fig. 4E). At this position, a weak band was observed in the *Angptl4*^{hyp} and *Angptl4*$^{-/-}$ mice, which is likely non-specific. Interestingly, a band of around 32 kDa corresponding to the predicted size for the truncated ANGPTL4 protein was observed in the *Angptl4*^{hyp} mice but not in the *Angptl4*$^{-/-}$ mice (Fig. 4E). To verify that the designated bands indeed represent ANGPTL4, we used the same

samples to perform Western blot using a polyclonal antibody directed against an epitope close to the N-terminus of ANGPTL4. Similar results were obtained (Fig. 4E). These analyses confirm that the *Angptl4*^{hyp} mice produce a truncated ANGPTL4 protein containing the LPL inhibitory domain, at levels that are far below the levels in wild-type mice. Accordingly, the *Angptl4*^{hyp} mice represent a hypomorph. In line with previous studies, LPL protein levels were increased in adipose tissue of *Angptl4*$^{-/-}$ mice (Fig. 4E) (26, 27). LPL protein levels were also increased in *Angptl4*^{hyp} mice compared to wild-type mice (Fig. 4E, Supplemental Fig. 1B). Similarly, primary adipocytes of *Angptl4*^{hyp} mice expressed low levels of a truncated N-terminal ANGPTL4 protein (Fig. 4F, Supplemental Fig. 1C). Consistent with an effect of truncated ANGPTL4 on LPL abundance, LPL protein levels in *Angptl4*^{hyp} adipocytes were markedly lower than in *Angptl4*$^{-/-}$ adipocytes, yet higher than in wild-type adipocytes (Fig. 4F).

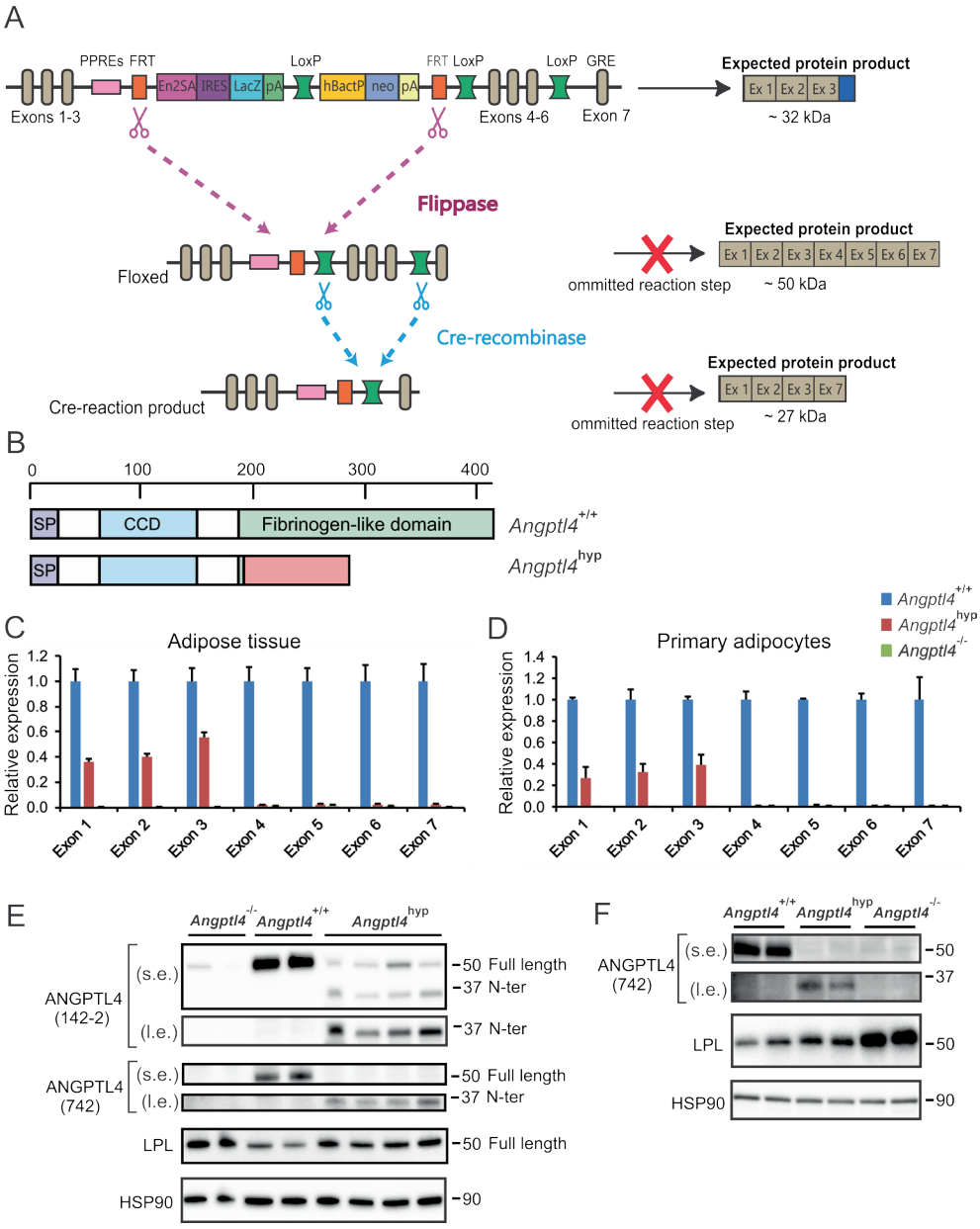

Figure. 4. Hypomorphic ANGPTL4 mice show reduced ANGPTL4 expression and reduced regulation on LPL. (A) Schematic map of the *Angptl4* locus by knockout first-allele strategy. (B) Full ANGPTL4 protein (upper scheme) and predicted sequence of truncated ANGPTL4 (lower scheme) based on sequence analysis of the knockout first-allele mice. mRNA expression of all 7 exons of *Angptl4* in epididymal adipose tissue (C) and primary adipocytes (D) of *Angptl4*$^{-/-}$ and *Angptl4*^{hyp} mice relative to wild-type mice. Western blot showing full-length and N-terminal ANGPTL4, and LPL in adipose tissue (E) and primary adipocytes (F) of the *Angptl4*$^{-/-}$, *Angptl4*^{hyp} and wild-type mice. mRNA expression was normalized to *36b4*. Data are mean ± SEM. N = 7 to 11 mice/group. s.e. and l.e. indicate short exposure and long exposure, respectively.

Angptl4^{hyp} and Angptl4$^{-/-}$ mice have similar plasma triglycerides and adipose LPL protein levels after a 24-hour fast

In line with the alternative name fasting-induced adipose factor, the effects of *Angptl4* inactivation or overexpression on lipid metabolism are most prominent in the fasted state. Accordingly, we measured basic plasma parameters in the three types of mice in the fasted and fed state. Fasting plasma levels of triglycerides, cholesterol, and non-esterified fatty acids were very similar between the *Angptl4*^{hyp} and *Angptl4*$^{-/-}$ mice, and were significantly lower compared to the wild-type mice (Fig. 5A). These data suggest that *Angptl4*^{hyp} and *Angptl4*$^{-/-}$ mice are highly similar and that the low levels of N-terminal ANGPTL4 protein in the *Angptl4*^{hyp} mice have no discernible impact on plasma lipid parameters in the fasted state.

Consistent with previous studies (35, 44), *Angptl4* mRNA in adipose tissue was significantly increased by fasting (Fig. 5B). Interestingly, fasting did not influence *Angptl4* mRNA in the *Angptl4*^{hyp} mice. In line with these data and fitting with previous studies (27, 45), ANGPTL4 protein levels in wild-type adipose tissue were increased by fasting, concomitant with a decrease in LPL protein levels (Fig. 5C, Supplemental Fig. 1D). By contrast, levels of truncated ANGPTL4 protein remained unchanged or tended to decrease during fasting in the *Angptl4*^{hyp} mice, while LPL protein levels went up (Fig. 5C, Supplemental Fig. 1D,E).

As previously shown (27), LPL protein was higher in *Angptl4*$^{-/-}$ mice compared with wild-type mice (Fig. 5C). Importantly, the decrease in LPL protein upon fasting was abrogated in *Angptl4*$^{-/-}$ mice, indicating that the increase in ANGPTL4 mediates the reduction in LPL protein upon fasting. Interestingly, in the fed state, LPL protein levels were lower in *Angptl4*^{hyp} than *Angptl4*$^{-/-}$ mice, whereas in the fasted, LPL protein levels were similar in *Angptl4*^{hyp} and *Angptl4*$^{-/-}$ mice (Fig. 5C, Supplemental Fig. 1D). These data suggest that small amounts of N-terminal ANGPTL4 in adipose tissue can decrease LPL protein levels, presumably by promoting LPL degradation, specifically in the fed and not the fasted state.

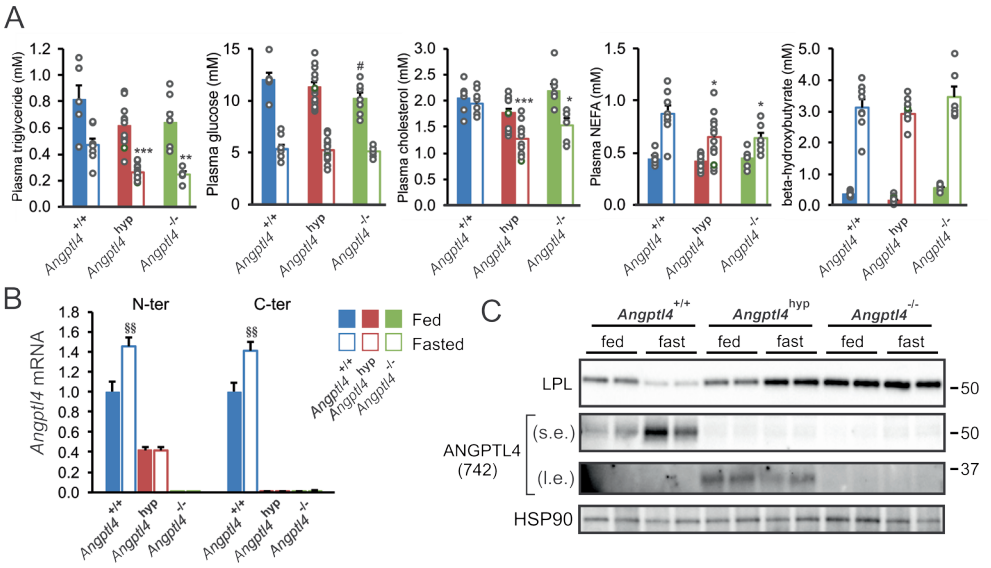

Figure 5. Similar regulation on plasma metabolites and LPL between *Angptl4*^{hyp} and *Angptl4*$^{-/-}$ mice after 24-hour fast. (A) Plasma levels of triglycerides, glucose, cholesterol, non-esterified fatty acids (NEFA) and β-hydroxybutyrate in fed (closed bars) and fasted (opened bars) mice. (B) mRNA expression from N-terminal (left column) and C-terminal (right column) regions of *Angptl4* in epididymal adipose tissues of fed (closed bars) and fasted (opened) mice. (C) Western blot of LPL and ANGPTL4 in epididymal adipose tissues from the 3 groups of mice in fed and fasted state. mRNA expression was normalized to *36b4.* Data are mean ± SEM. N = 7 to 11 mice/group. *p < 0.05, **p < 0.01 and ***p < 0.001 represent significance in fasted group relative to wild-type fasted mice; #p < 0.05 represent significance in fed group relative to wild-type fed mice; and §§p < 0.01 relative to wild-type fed mice. s.e. and l.e. indicate short exposure and long exposure, respectively.

Angptl4^{hyp} mice show attenuated chylous ascites and acute inflammation but similar levels of lymphadenopathy as Angptl4$^{-/-}$ mice

We have previously shown that *Angptl4*$^{-/-}$ mice respond poorly to high saturated fat diet characterized by the formation of lipid-laden Touton giant cells in mesenteric lymph nodes, accumulation of chylous ascites in peritoneum and acute inflammation (30). To determine the influence of low levels of N-terminal ANGPTL4 on the development of mesenteric lymphadenopathy, chylous ascites and other pathologies, the three groups of mice were fed a standard high fat diet rich in saturated fat for 20 weeks. Whereas the *Angptl4*$^{-/-}$ mice showed a rapid and marked increase in serum amyloid A levels upon high fat feeding, serum amyloid A levels in the *Angptl4*^{hyp} mice only went up after 20 weeks of high fat feeding (Fig. 6A). At this time point, hepatic expression of several acute-phase proteins in *Angptl4*^{hyp} mice was significantly lower than or approximating the levels in *Angptl4*$^{-/-}$ mice (Fig. 6B). Besides a delayed increase in serum amyloid A, the development of chylous ascites was much reduced in the *Angptl4*^{hyp} mice compared to the *Angptl4*$^{-/-}$ mice. Whereas 7 out of 8 *Angptl4*$^{-/-}$ mice showed very pronounced ascites several weeks after starting the high fed diet, leading to premature death in 6 *Angptl4*$^{-/-}$ mice (30), at the end of the 20 weeks of high fat feeding, all *Angptl4*^{hyp} mice survived, with only 2 out of 11 *Angptl4*^{hyp} mice showing ascites, which was also very mild (Fig. 6C) (29, 30). The mesenteric adipose tissue of the *Angptl4*^{hyp} mice with ascites showed the characteristic mesenteric panniculitis, but this was less severe than in the *Angptl4*$^{-/-}$ mice (Fig. 6D). Of note, the frequency rate, severity of ascites and full survival in the *Angptl4*^{hyp} mice remained unchanged when extending the high fat feeding to 36 weeks in 7 *Angptl4*^{hyp} mice (data not shown). Despite the much milder ascites and slower progression of the inflammatory phenotype, after 20 weeks of high fat feeding nearly all mesenteric lymph nodes in the *Angptl4*^{hyp} mice contained multiple lipid-laden Touton giant cells (Fig. 6E). Specifically, Touton giant cells were present in mesenteric lymph nodes of 10 out of 11 *Angptl4*^{hyp} mice, 7 out of 8 *Angptl4*$^{-/-}$ mice but in none of the wild-type mice. A summary of the clinical outcomes in the 3 groups of mice is presented in Supplemental Table 3.

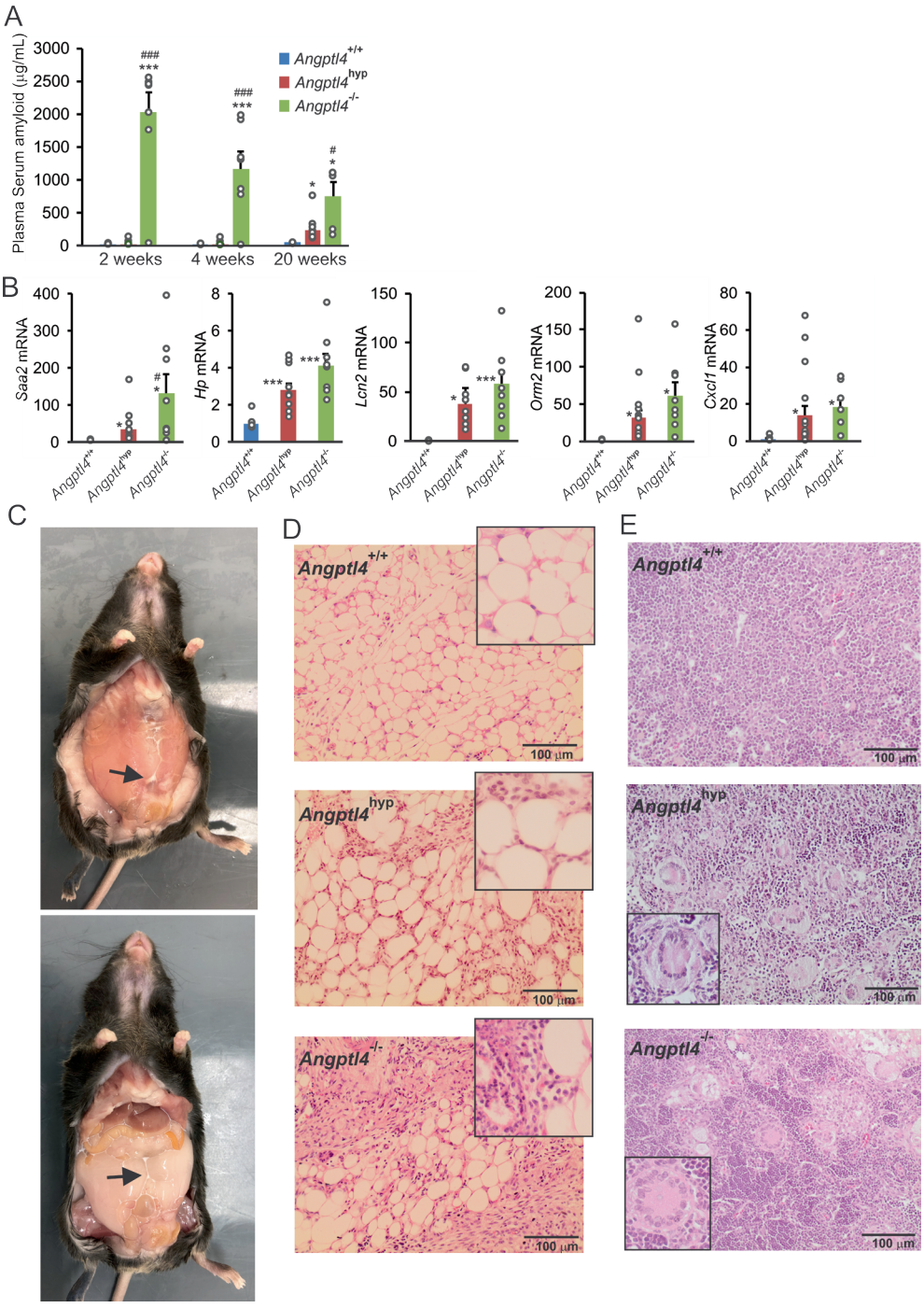
A
Plasma Serum amyloid (µg/mL)
3000
2500
2000
1500
1000
500
0
2 weeks
4 weeks
20 weeks
Angptl4+/+
Angptl4hyp
Angptl4-/-
B
Saa2 mRNA
Hp mRNA
Lcn2 mRNA
Orm2 mRNA
Cxcl1 mRNA
C
D
E
Angptl4+/+
Angptl4hyp
Angptl4-/-
100 µm

Figure 6. *Angptl4*^{hyp} mice have less severe pathological phenotypes in response to 20-weeks of high fat diet compared to *Angptl4*$^{-/-}$ mice. (A) Plasma levels of serum amyloid A after 2, 4 and 20 weeks of high fat diet. (B) Relative hepatic expression of pro-inflammatory markers in three groups of mice. (C) Pictures showing levels of ascites formation in the peritoneum of *Angptl4*^{hyp} mice. Arrows pointing towards ascites. (D) H&E staining depicting mesenteric panniculitis in *Angptl4*^{hyp} mice. (E) Images showing Touton giant cells in the mesenteric lymph nodes of *Angptl4*^{hyp} and *Angptl4*$^{-/-}$ mice but not wildtype mice. Images are 200x magnification; insert is 400x magnification. mRNA expression was normalized to *36b4.* Data are mean ± SEM. N = 7 to 11 mice/group. *p < 0.05, **p < 0.01 and ***p < 0.001 relative to wild-type.

Angptl4^{hyp} mice show increased LPL activity and improved glucose tolerance compared to wild-type mice

Consistent with the role of ANGPTL4 as LPL inhibitor, after 20 weeks of high fat feeding, adipose tissue LPL activity was significantly higher in *Angptl4*^{hyp} mice than in wild-type mice (Fig. 7A). By contrast, adipose tissue LPL activity was not increased in *Angptl4*$^{-/-}$ mice, which is likely related to the steatitis in these animals (29). Interestingly, whereas plasma levels of triglycerides and cholesterol were significantly lower in both *Angptl4*^{hyp} and *Angptl4*$^{-/-}$ mice than in wild-type mice, plasma glycerol and non-esterified fatty acid levels were only lower in the *Angptl4*^{hyp} mice, which again may be related to the steatitic phenotype of the *Angptl4*$^{-/-}$ adipose tissue (Fig. 7B). To study the impact of ANGPTL4 deficiency on glucose homeostasis, we measured plasma glucose and performed a glucose tolerance test. Plasma glucose levels were significantly lower in *Angptl4*$^{-/-}$ mice than in wild-type and *Angptl4*^{hyp} mice (Fig. 7C), while glucose tolerance was dramatically or modestly improved in *Angptl4*$^{-/-}$ and *Angptl4*^{hyp} mice, respectively, compared with wild-type mice (Fig. 7D). Overall, the LPL activity and plasma metabolites levels in *Angptl4*^{hyp} mice are consistent with the known role of ANGPTL4 in intra- and extracellular lipolysis (46). By contrast, LPL activity and plasma metabolite levels in *Angptl4*$^{-/-}$ mice fed a high fat diet likely partly reflect the severe inflammatory phenotype in these animals (29, 30).

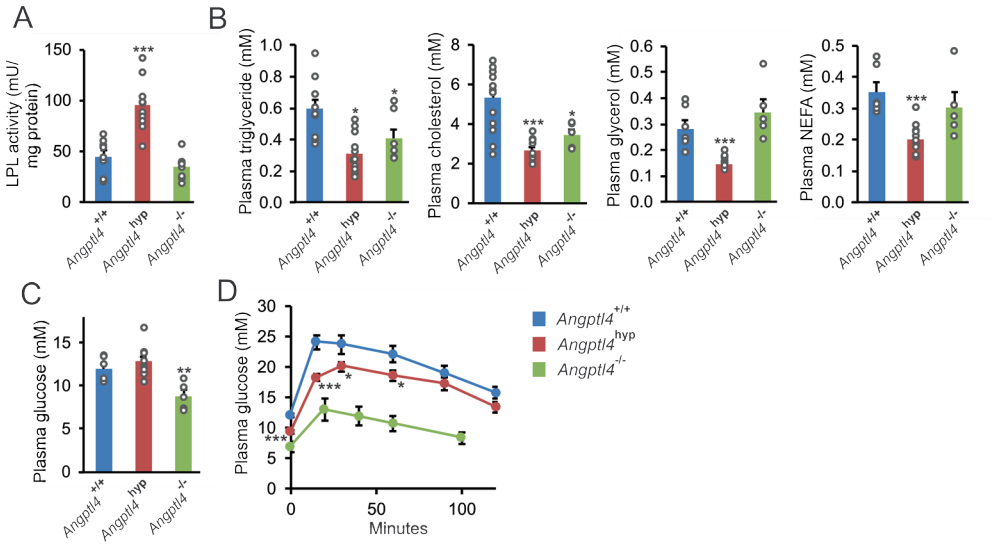

Figure 7. Increased LPL activity and improved glucose tolerance in *Angptl4*^{hyp} mice after 20 week of high fat diet. (A) LPL activity in epididymal adipose tissue of *Angptl4*^{hyp}, *Angptl4*$^{-/-}$ and wild-type mice (B) Plasma concentrations of triglycerides, cholesterol, glycerol and non-esterified fatty acids (NEFA) in the 3 groups of mice. Plasma glucose levels (C) and glucose tolerance test (D) in the 3 groups of mice. Data are mean ± SEM. N = 7 to 11 mice/group. *p < 0.05, **p < 0.01 and ***p < 0.001 relative to wild-type. No statistical analysis could be done on glucose tolerance in *Angptl4*$^{-/-}$ mice due to the use of different time points.

Discussion

In this paper we addressed two independent questions relevant to the mesenteric lymphadenopathy phenotype in *Angptl4*$^{-/-}$ mice fed a high fat diet: 1) what is the influence of endogenous ANGPTL4 on lipid uptake and utilization in macrophages, and 2) what is the role of N-terminal ANGPTL4 in the development of mesenteric lymphadenopathy, inflammation, and ascites.

Our study confirms previous data indicating that *Angptl4* expression in macrophages is highly induced by lipids (29, 47, 48). This induction is likely mediated by PPARδ and/or PPARγ, as shown by the marked upregulation of *Angptl4* mRNA by PPARδ and PPARγ agonists in BMDM. Importantly, the present study shows that not only external ANGPTL4 but also endogenously produced ANGPTL4 inhibits lipid uptake in macrophages. The elevated lipid uptake in *Angptl4*$^{-/-}$ macrophages increases the expression of various lipid-sensitive genes involved in inflammation and ER stress, such as *Hilpda*, *Ddit3, Ptgs2* and *Cxcl2*. Interestingly, the elevated lipid uptake in *Angptl4*$^{-/-}$ macrophages was accompanied by increased mitochondrial respiration, suggesting that enhanced lipid uptake may stimulate cellular respiration. As the effect on cellular respiration was observed for endogenous and not exogenous ANGPTL4, it might reflect an intracellular mechanism of action of ANGPTL4. Together, our findings demonstrate an important role of ANGPTL4 in regulating lipid uptake and utilization in macrophages.

It is well established that ANGPTL4 inactivates LPL by promoting LPL unfolding (24, 49). Recently, we found that ANGPTL4 has a local role in adipocytes by promoting the intracellular cleavage and subsequent degradation of LPL (26, 27). In stark contrast to adipocytes, ANGPTL4 deficiency in macrophages did not lead to the accumulation of full length, rapidly-releasable LPL, while the cleaved, N-terminal LPL portion was not detectable in our hands. The lack of effect of ANGPTL4 on LPL protein levels in macrophages may be because macrophage LPL is not degraded via the lysosomal pathway but via the proteasomal pathway. The difference in LPL degradation pathway and in the effect of ANGPTL4 on LPL levels between adipocytes and macrophages could be connected to how LPL is presented on the cell surface. Specifically, it is conceivable that LPL on the surface of macrophages is not internalized for degradation, unlike LPL in adipocytes, and that ANGPTL4 only causes the unfolding and inactivation of LPL after both proteins have been secreted (50, 51). Overall, these findings suggest that the location and cellular mechanism of LPL inactivation by ANGPTL4 may be different in different cells.

Previously, we showed that *Angptl4*$^{-/-}$ mice fed a diet rich in saturated fat develop an inflammatory and ultimately lethal phenotype characterized by the formation of Touton giant cells in mesenteric lymph nodes, chylous ascites, and fibrinopurulent peritonitis (29,

30). By comparing *Angplt4*$^{-/-}$ mice with an *Angptl4*-hypomorphic model, here we show that a low-level expression of a truncated N-terminal ANGPTL4 does not prevent Touton giant cell formation, yet drastically mitigates the acute-phase response and the development of chylous ascites upon high fat feeding. Importantly, the development of fibrinopurulent peritonitis and the death of the animals is completely prevented by the expression of the truncated N-terminal ANGPTL4. Although the severity of the clinical phenotype was attenuated, activation of the acute-phase response and chylous ascites were still observed in a substantial number of *Angptl4*^{hyp} mice.

Strictly, we cannot fully exclude that N-terminal ANGPTL4 influences ascites independently of LPL inhibition. However, two lines of reasoning support an action of N-terminal ANGPTL4 on ascites via LPL. First, LPL protein levels in *Angptl4*^{hyp} adipocytes were lower than in *Angplt4*$^{-/-}$ adipocytes, paralleled by a marked reduction in ascites severity. These data suggest that a low level of N-terminal ANGPTL4 decreases LPL abundance. Second, chronic injection of a monoclonal antibody that is directed against N-terminal ANGPTL4 and abolishes its ability to inhibit LPL causes ascites in mice fed a HFD (28). Collectively, we favor the notion that the attenuation of the ascites phenotype in *Angptl4*^{hyp} mice compared to *Angplt4*$^{-/-}$ mice is related to reduced LPL activity via N-terminal ANGPTL4, and accordingly that the ascites in *Angplt4*$^{-/-}$ mice fed a high fat diet is directly connected to enhanced LPL activity.

Our observation that partial deficiency of ANGPTL4 leads to undesirable clinical consequences in mice suggests that therapeutic approaches that only partially inactivate ANGPTL4 and/or are aimed at whole body inactivation of ANGPTL4 may still carry the risk of major side effects in humans. By contrast, tissue-specific inactivation, in particular adipose tissue-specific and possibly liver-specific inactivation of ANGPTL4, hold considerably more promise for improving dyslipidemia and reducing coronary artery disease risk without leading to deleterious side-effects [33].

In line with a predominant role of ANGPTL4 in lipid metabolism during fasting, plasma levels of triglycerides, cholesterol and non-esterified fatty acids were lower in *Angptl4*$^{-/-}$ mice compared with wild-type mice specifically in the fasted but not the fed state. Interestingly, in the fasted state, plasma triglyceride, cholesterol, and non-esterified fatty acid levels were similar in *Angptl4*^{hyp} and *Angptl4*$^{-/-}$ mice, which was accompanied by similar levels of LPL protein in the adipose tissue. Accordingly, the expression of low levels of N-terminal ANGPTL4 does not influence LPL protein levels in the fasted state. By contrast, in the fed state, LPL protein levels in adipose tissue were lower in *Angptl4*^{hyp} mice than in *Angptl4*$^{-/-}$ mice, suggesting that a low level of N-terminal ANGPTL4 decreases LPL protein, likely by promoting LPL degradation. The reason why N-terminal ANGPTL4 in *Angptl4*^{hyp} mice has a more pronounced effect on LPL in the fed state than in the fasted state is unclear. Why

fasting fails to alter *Angptl4* mRNA in *Angptl4*^{hyp} mice is also unclear. It can be hypothesized that is due to a disrupted transcriptional regulation by the glucocorticoid receptor via exon 7, as this mechanism is responsible for the induction of *Angptl4* expression by fasting in wild-type adipose tissue (52, 53). Despite the minimal effect of fasting on levels of N-terminal ANGPTL4 in *Angptl4*^{hyp} mice, LPL protein levels increased, suggesting an additional regulatory mechanism of LPL protein.

In addition to regulating plasma lipid levels, recent reports also suggest a role of ANGPTL4 in glucose homeostasis (54–56). Using different models, ANGPTL4 deficiency in mice was found to lead to improved glucose tolerance. Consistent with the study by Gusarova et al (57), we found that *Angptl4*$^{-/-}$ mice chronically fed a high fat diet have drastically lower basal plasma glucose levels and improved glucose tolerance. However, these mice have numerous clinical abnormalities, which prohibits any conclusion on the direct effect of ANGPTL4 deficiency on glucose homeostasis. *Angptl4*^{hyp} mice fed a high fat diet showed a much milder clinical phenotype, concomitant with a more modest yet statistically significant improvement in glucose tolerance, yet acute-phase protein levels were still elevated compared with wild-type mice. This observation again makes it difficult to derive a solid conclusion on the direct effect of ANGPTL4 deficiency on glucose homeostasis. We previously found that *Angptl4*$^{-/-}$ mice fed a diet high in unsaturated fat, which does not exhibit any clinical complications, were more glucose tolerant than wild-type mice fed the same diet (55). In addition, it was shown that adipocyte-specific ANGPTL4-deficient mice have markedly improved glucose and insulin tolerance after one month and to a lesser extent five months of high fat feeding, which was suggested to be due to LPL-mediated redistribution of ectopic fat stores to adipose tissue (54). While growing evidence thus connects ANGPTL4 with glucose homeostasis, further studies are necessary to delineate potential mechanisms.

Another interesting question concerns the significance of the lipid-laden Touton giant cells for the onset of the debilitating side-effects after high fat feeding. A causal role had been previously questioned by the observation that *Angptl4*$^{-/-}$ mice fed a diet high in trans fatty acids develop Touton cells but do not show elevated systemic inflammation or ascites and survive the intervention (30). Here we find that *Angptl4*^{hyp} mice fed a regular high fat diet, despite showing a much milder inflammation and ascites than *Angptl4*$^{-/-}$ mice, carry similar numbers of Touton giant cells in their mesenteric lymph nodes. These data reinforce the notion that the formation of lipid-laden Touton giant cells is uncoupled from activation of an acute-phase response and chylous ascites (30).

Two previous publications have used the *Angptl4*^{hyp} mice to generate floxed *Angptl4* mice, which in turn were used to generated adipocyte- or brown fat-specific ANGPTL4-deficient mice (33, 34). Deficiency of ANGPTL4 was shown by dramatically reduced qPCR-based

amplification of introns 4-5, which covers the region removed by Cre-mediated excision. No information was presented on ANGPTL4 protein levels. Based on our results and calculations, it is possible that in both mouse models there still is significant expression of a truncated N-terminal ANGPTL4 protein derived from exons 1-3 containing the LPL-inhibitory domain. It can be argued that this truncated ANGPTL4 might have influenced the metabolic phenotype.

In conclusion, we find that ANGPTL4 deficiency increases lipid uptake and respiration in macrophages without affecting LPL protein levels. Furthermore, in comparison to *Angptl4*$^{-/-}$ mice, mice expressing low levels of N-terminal ANGPTL4 show a reduced acute-phase response and markedly attenuated chylous ascites following high fat feeding. These findings have significant clinical implications since any therapeutic strategy would likely reduce but not completely inactivate ANGPTL4.

Acknowledgements/Grant support

We thank Madelene Ericsson and Rakel Nyrén (Department of Medical Biosciences/Physiological Chemistry, Umeå University, Sweden) for their technical assistance with the LPL activity measurements, and Imke Vohs (Wageningen University) for her assistance with the H&E staining.

This work was supported by the Graduate School Voeding, Levensmiddelentechnologie, Agro-Biotechnologie en Gezondheid (VLAG) (Wageningen University) and CVON ENERGISE grant CVON2014–02.

The authors declare that there are no conflicts of interest associated with this manuscript.

References

1. Hokanson, J. E., and M. A. Austin. 1996. Plasma triglyceride level is a risk factor for cardiovascular disease independent of high-density lipoprotein cholesterol level: A metaanalysis of population-based prospective studies. Eur. J. Cardiovasc. Prev. Rehabil. 3: 213–219.

2. Onat, A., I. Sari, M. Yazici, G. Can, G. Hergenç, and G. Ş. Avci. 2006. Plasma triglycerides, an independent predictor of cardiovascular disease in men: A prospective study based on a population with prevalent metabolic syndrome. Int. J. Cardiol. 108: 89–95.

3. Sandesara, P. B., S. S. Virani, S. Fazio, and M. D. Shapiro. 2018. The Forgotten Lipids: Triglycerides, Remnant Cholesterol, and Atherosclerotic Cardiovascular Disease Risk. Endocr. Rev. [online] https://academic.oup.com/edrv/advance-article/doi/10.1210/er.2018-00184/5126386.

4. Goldberg, I. J., R. H. Eckel, and R. McPherson. 2011. Triglycerides and heart disease: Still a hypothesis? Arterioscler. Thromb. Vasc. Biol. 31: 1716–1725.

5. Kersten, S. 2014. Physiological regulation of lipoprotein lipase. Biochim. Biophys. Acta. 1841: 919–33. [online] http://www.ncbi.nlm.nih.gov/pubmed/24721265.

6. Davies, B. S. J., A. P. Beigneux, R. H. Barnes, Y. Tu, P. Gin, M. M. Weinstein, C. Nobumori, R. Nyrén, I. Goldberg, G. Olivecrona, A. Bensadoun, S. G. Young, and L. G. Fong. 2010. GPIHBP1 is responsible for the entry of lipoprotein lipase into capillaries. Cell Metab. 12: 42–52.

7. Beigneux, A. P., K. Miyashita, M. Ploug, D. J. Blom, M. Ai, M. F. Linton, W. Khovidhunkit, R. Dufour, A. Garg, M. A. McMahon, C. R. Pullinger, N. P. Sandoval, X. Hu, C. M. Allan, M. Larsson, T. Machida, M. Murakami, K. Reue, P. Tontonoz, I. J. Goldberg, P. Moulin, S. Charrière, L. G. Fong, K. Nakajima, and S. G. Young. 2017. Autoantibodies against GPIHBP1 as a Cause of Hypertriglyceridemia. N. Engl. J. Med. NEJMoa1611930. [online] http://www.nejm.org/doi/10.1056/NEJMoa1611930.

8. Goulbourne, C. N., P. Gin, A. Tatar, C. Nobumori, A. Hoenger, H. Jiang, C. R. M. Grovenor, O. Adeyo, J. D. Esko, I. J. Goldberg, K. Reue, P. Tontonoz, A. Bensadoun, A. P. Beigneux, S. G. Young, and L. G. Fong. 2014. The GPIHBP1-LPL complex is responsible for the margination of triglyceride-rich lipoproteins in capillaries. Cell Metab. 19: 849–860.

9. Conklin, D., D. Gilbertson, D. W. Taft, M. F. Maurer, T. E. Whitmore, D. L. Smith, K. M. Walker, L. H. Chen, S. Wattler, M. Nehls, and K. B. Lewis. 1999. Identification of a mammalian angiopoietin-related protein expressed specifically in liver. Genomics. 62: 477–482.

10. KIM, I., H.-G. KIM, H. KIM, H.-H. KIM, S. K. PARK, C.-S. UHM, Z. H. LEE, and G. Y. KOH. 2000. Hepatic expression, synthesis and secretion of a novel fibrinogen/angiopoietin-related protein that prevents endothelial-cell apoptosis. Biochem. J. 346: 603–610.

11. Kersten, S., S. Mandard, N. S. Tan, P. Escher, D. Metzger, P. Chambon, F. J. Gonzalez, B. Desvergne, and W. Wahli. 2000. Characterization of the fasting-induced adipose factor FIAF, a novel peroxisome proliferator-activated receptor target gene. J. Biol. Chem. 275: 28488–28493.

12. Yoon, J. C., T. W. Chickering, E. D. Rosen, B. Dussault, Y. Qin, A. Soukas, J. M. Friedman, W. E. Holmes, and B. M. Spiegelman. 2000. Peroxisome proliferator-activated receptor gamma target gene encoding a novel angiopoietin-related protein associated with adipose differentiation. Mol. Cell. Biol. 20: 5343–9. [online] http://www.pubmedcentral.nih.gov/articlerender.fcgi?artid=85983&tool=pmcentrez&rendertype=abstract.

13. Zhang, R. 2012. Lipasin, a novel nutritionally-regulated liver-enriched factor that regulates serum triglyceride levels. Biochem. Biophys. Res. Commun. 424: 786–792. [online] http://dx.doi.org/10.1016/j.bbrc.2012.07.038.

14. Quagliarini, F., Y. Wang, J. Kozlitina, N. V. Grishin, R. Hyde, E. Boerwinkle, D. M. Valenzuela, A. J. Murphy, J. C. Cohen, and H. H. Hobbs. 2012. Atypical angiopoietin-like protein that regulates ANGPTL3. Proc. Natl. Acad. Sci. 109: 19751–19756.

15. Ren, G., J. Y. Kim, and C. M. Smas. 2012. Identification of RIFL, a novel adipocyte-enriched insulin target gene with a role in lipid metabolism. Am. J. Physiol. Metab. 303: E334–E351.

16. Chi, X., E. C. Britt, H. W. Shows, A. J. Hjelmaas, S. K. Shetty, E. M. Cushing, W. Li, A. Dou, R. Zhang, and B. S. J. Davies. 2017. ANGPTL8 promotes the ability of ANGPTL3 to bind and inhibit lipoprotein lipase. Elsevier GmbH. [online] http://www.sciencedirect.com/science/article/pii/S2212877817303307.

17. Haller, J. F., I. J. Mintah, L. M. Shihanian, P. Stevis, D. Buckler, C. A. Alexa-Braun, S. Kleiner, S. Banfi, J. C. Cohen, H. H. Hobbs, G. D. Yancopoulos, A. J. Murphy, V. Gusarova, and J. Gromada. 2017. ANGPTL8 requires ANGPTL3 to inhibit lipoprotein lipase and plasma triglyceride clearance. J. Lipid Res. 58: jlr.M075689. [online] http://www.ncbi.nlm.nih.gov/pubmed/28413163.

18. Köster, A., Y. B. Chao, M. Mosior, A. Ford, P. A. Gonzalez-DeWhitt, J. E. Hale, D. Li, Y. Qiu, C. C. Fraser, D. D. Yang, J. G. Heuer, S. R. Jaskunas, and P. Eacho. 2005. Transgenic angiopoietin-like (Angptl)4 overexpression and targeted disruption of Angptl4 and Angptl3: Regulation of triglyceride metabolism. Endocrinology. 146: 4943–4950.

19. Lichtenstein, L., J. F. P. Berbée, S. J. Van Dijk, K. W. Van Dijk, A. Bensadoun, I. P. Kema, P. J. Voshol, M. Müller, P. C. N. Rensen, and S. Kersten. 2007. Angptl4 upregulates cholesterol synthesis in liver via inhibition of LPL- and HL-dependent hepatic cholesterol uptake. Arterioscler. Thromb. Vasc. Biol. 27: 2420–2427.

20. Abid, K., T. Trimeche, D. Mili, M. A. Msolli, I. Trabelsi, S. Nouira, and A. Kenani. 2016. ANGPTL4 variants E40K and T266M are associated with lower fasting triglyceride levels and predicts cardiovascular disease risk in Type 2 diabetic Tunisian population. Lipids Health Dis. 15: 63. [online] http://lipidworld.biomedcentral.com/articles/10.1186/s12944-016-0231-6.

21. Dewey, F. E., V. Gusarova, C. O'Dushlaine, O. Gottesman, J. Trejos, C. Hunt, C. V. Van Hout, L. Habegger, D. Buckler, K.-M. V. Lai, J. B. Leader, M. F. Murray, M. D. Ritchie, H. L. Kirchner, D. H. Ledbetter, J. Penn, A. Lopez, I. B. Borecki, J. D. Overton, J. G. Reid, D. J. Carey, A. J. Murphy, G. D. Yancopoulos, A. Baras, J. Gromada, and A. R. Shuldiner. 2016. Inactivating Variants in ANGPTL4 and Risk of Coronary Artery Disease. N. Engl. J. Med. 374: 1123–1133. [online] http://www.nejm.org/doi/10.1056/NEJMoa1510926.

22. Mandard, S., F. Zandbergen, E. Van Straten, W. Wahli, F. Kuipers, M. Müller, and S. Kersten. 2006. The fasting-induced adipose factor/angiopoietin-like protein 4 is physically associated with lipoproteins and governs plasma lipid levels and adiposity. J. Biol. Chem. 281: 934–944.

23. Dijk, W., and S. Kersten. 2016. Regulation of lipid metabolism by angiopoietin-like proteins. Curr. Opin. Lipidol. 27: 249–256.

24. Mysling, S., K. K. Kristensen, M. Larsson, O. Kovrov, A. Bensadouen, T. J. D. Jørgensen, G. Olivecrona, S. G. Young, and M. Ploug. 2016. The angiopoietin-like protein angptl4 catalyzes unfolding of the hydrolase domain in lipoprotein lipase and the endothelial membrane protein gpihbp1 counteracts this unfolding. Elife. 5: 18.

25. Sukonina, V., A. Lookene, T. Olivecrona, and G. Olivecrona. 2006. Angiopoietin-like protein 4 converts lipoprotein lipase to inactive monomers and modulates lipase activity in adipose tissue. Proc. Natl. Acad. Sci.

26. Dijk, W., P. M. M. Ruppert, L. J. Oost, and S. Kersten. 2018. Angiopoietin-like 4 promotes the intracellular cleavage of lipoprotein lipase by PCSK3/furin in adipocytes. J. Biol. Chem. 293: 14134–14145.

27. Dijk, W., A. P. Beigneux, M. Larsson, A. Bensadoun, S. G. Young, and S. Kersten. 2016. Angiopoietin-like 4 (ANGPTL4) promotes intracellular degradation of lipoprotein lipase in adipocytes. J. Lipid Res. 7: 956–963. [online] http://ebooks.cambridge.org/ref/id/CBO9781107415324A009%5Cnhttp://www.ncbi.nlm.nih.gov/pubmed/27034464.

28. Desai, U., E. C. Lee, K. Chung, C. Gao, J. Gay, B. Key, G. Hansen, D. Machajewski, K. A. Platt, A. T. Sands, M. Schneider, I. Van Sligtenhorst, A. Suwanichkul, P. Vogel, N. Wilganowski, J. Wingert, B. P. Zambrowicz, G. Landes, and D. R. Powell. 2007. Lipid-lowering effects of anti-angiopoietin-like 4 antibody recapitulate the lipid phenotype found in angiopoietin-like 4 knockout mice. Proc Natl Acad Sci U S A. 104: 11766–11771. [online] http://www.ncbi.nlm.nih.gov/pubmed/17609370.

29. Lichtenstein, L., F. Mattijssen, N. J. de Wit, A. Georgiadi, G. J. Hooiveld, R. van der Meer, Y. He, L. Qi, A. Köster, J. T. Tamsma, N. S. Tan, M. Müller, and S. Kersten. 2010. Angptl4 Protects against Severe Proinflammatory Effects of Saturated Fat by Inhibiting Fatty Acid Uptake into Mesenteric Lymph Node Macrophages. Cell Metab. 12: 580–592. [online] http://linkinghub.elsevier.com/retrieve/pii/S1550413110003943.

30. Oteng, A.-B., A. Bhattacharya, S. Brodesser, L. Qi, N. S. Tan, and S. Kersten. 2017. Feeding Angptl4- / - mice trans fat promotes foam cell formation in mesenteric lymph nodes without leading to ascites. J. Lipid Res. 58: 1–36.

31. Dijk, W., M. Heine, L. Vergnes, M. R. Boon, G. Schaart, M. K. C. Hesselink, K. Reue, W. D. van Marken Lichtenbelt, G. Olivecrona, P. C. N. Rensen, J. Heeren, and S. Kersten. 2015. ANGPTL4 mediates shuttling of lipid fuel to brown adipose tissue during sustained cold exposure. Elife. 4: 1–23.

32. Skarnes, W. C., B. Rosen, A. P. West, M. Koutsourakis, W. Bushell, V. Iyer, A. O. Mujica, M. Thomas, J. Harrow, T. Cox, D. Jackson, J. Severin, P. Biggs, J. Fu, M. Nefedov, P. J. De Jong, A. F. Stewart, and A. Bradley. 2011. A conditional knockout resource for the genome-wide study of mouse gene function. Nature. 474.

33. Singh, A. K., B. Aryal, B. Chaube, N. Rotllan, L. Varela, T. L. Horvath, Y. Suárez, and C. Fernández-Hernando. 2018. Brown adipose tissue derived ANGPTL4 controls glucose and lipid metabolism and regulates thermogenesis. Mol. Metab. 11: 59–69. [online] https://doi.org/10.1016/j.molmet.2018.03.011.

34. Aryal, B., A. K. Singh, X. Zhang, L. Varela, N. Rotllan, L. Goedeke, B. Chaube, J.-P. Camporez, D. F. Vatner, T. L. Horvath, G. I. Shulman, Y. Suárez, and C. Fernández-Hernando. 2018. Absence of ANGPTL4 in adipose tissue improves glucose tolerance and attenuates atherogenesis. JCI Insight. 3.

35. Kroupa, O., E. Vorrsjö, R. Stienstra, F. Mattijssen, S. K. Nilsson, S. Kersten, G. Olivecrona, and T. Olivecrona. 2012. Linking nutritional regulation of Angptl4 , Gpihbp1 , and Lmf1 to lipoprotein lipase activity in rodent adipose tissue. 1–15.

36. Markwell, M. A. K., S. M. Haas, L. L. Bieber, and N. E. Tolbert. 1978. A modification of the Lowry procedure to simplify protein determination in membrane and lipoprotein samples. Anal. Biochem. 87: 206–210.

37. Bolstad, B. M., R. A. Irizarry, M. Astrand, and T. P. Speed. 2003. A comparison of normalization methods for high density oligonucleotide array data based on variance and bias. Bioinformatics. 19: 185–193.

38. Irizarry, R. A., B. Hobbs, F. Collin, Y. D. Beazer-Barclay, K. J. Antonellis, U. Scherf, and T. P. Speed. 2003. Exploration, normalization, and summaries of high density oligonucleotide array probe level data. Biostatistics. 4: 249–264. [online] http://biostatistics.oxfordjournals.org/.

39. Dai, M., P. Wang, A. D. Boyd, G. Kostov, B. Athey, E. G. Jones, W. E. Bunney, R. M. Myers, T. P. Speed, H. Akil, S. J. Watson, and F. Meng. 2005. Evolving gene/transcript definitions significantly alter the interpretation of GeneChip data. Nucleic Acids Res. 33: 1–9.

40. Robblee, M. M., C. C. Kim, J. P. Abate, M. Valdearcos, K. L. M. Sandlund, M. K. Shenoy, R. Volmer, T. Iwawaki, and S. K. Koliwad. 2016. Saturated Fatty Acids Engage an IRE1α-Dependent Pathway to Activate the NLRP3 Inflammasome in Myeloid Cells. Cell Rep. 14: 2611–2623. [online] http://dx.doi.org/10.1016/j.celrep.2016.02.053.

41. Dallinga-Thie, G. M., L. Yin, B. S. J. Davies, A. P. Beigneux, A. Bensadoun, P. Gin, J. D. Esko, L. G. Fong, S. G. Young, K. Melford, M. M. Weinstein, J. R. Bishop, and K. Estrada. 2008. Abnormal Patterns of Lipoprotein Lipase Release into the Plasma in GPIHBP1-deficient Mice. J. Biol. Chem. 283: 34511–34518.

42. Mandard, S., F. Zandbergen, S. T. Nguan, P. Escher, D. Patsouris, W. Koenig, R. Kleemann, A. Bakker, F. Veenman, W. Wahli, M. Müller, and S. Kersten. 2004. The direct peroxisome proliferator-activated receptor target fasting-induced adipose factor (FIAF/PGAR/ANGPTL4) is present in blood plasma as a truncated protein that is increased by fenofibrate treatment. J. Biol. Chem. 279: 34411–34420.

43. Robblee, M. M., C. C. Kim, J. P. Abate, M. Valdearcos, K. L. M. Sandlund, M. K. Shenoy, R. Volmer, T. Iwawaki, and S. K. Koliwad. 2016. Saturated Fatty Acids Engage an IRE1α-Dependent Pathway to Activate the NLRP3 Inflammasome in Myeloid Cells. Cell Rep. 1–13. [online] http://linkinghub.elsevier.com/retrieve/pii/S2211124716301747.

44. Kersten, S., S. Mandard, N. S. Tan, P. Escher, D. Metzger, P. Chambon, F. J. Gonzalez, B. Desvergne, and W. Wahli. 2000. Characterization of the fasting-induced adipose factor FIAF, a novel peroxisome proliferator-activated receptor target gene. J. Biol. Chem. 275: 28488–28493.

45. Doolittle, M. H., O. Ben-Zeev, J. Elovson, K. Martin, and Kirchgessner. 1990. The response of lipoprotein lipase to feeding and fasting. J. Biol. Chem. 265: 4570–4577.

46. Yoshida, K., T. Shimizugawa, M. Ono, and H. Furukawa. 2002. Angiopoietin-like protein 4 is a potent hyperlipidemia-inducing factor in mice and inhibitor of lipoprotein lipase. J. Lipid Res. 43: 1770–1772.

47. Georgiadi, A., Y. Wang, R. Stienstra, N. Tjeerdema, A. Janssen, A. Stalenhoef, J. A. Van Der Vliet, A. De Roos, J. T. Tamsma, J. W. a Smit, N. S. Tan, M. Müller, P. C. N. Rensen, and S. Kersten. 2013. Overexpression of angiopoietin-like protein 4 protects against atherosclerosis development. Arterioscler. Thromb. Vasc. Biol. 33: 1529–1537.

48. Aryal, B., N. Rotllan, E. Araldi, C. M. Ramírez, S. He, B. G. Chousterman, A. M. Fenn, A. Wanschel, J. Madrigal-Matute, N. Warrier, J. L. Martín-Ventura, F. K. Swirski, Y. Suárez, and C. Fernández-Hernando. 2016. ANGPTL4 deficiency in haematopoietic cells promotes monocyte expansion and atherosclerosis progression. Nat. Commun. 7.

49. Sukonina, V., A. Lookene, T. Olivecrona, and G. Olivecrona. 2006. Angiopoietin-like protein 4 converts lipoprotein lipase to inactive monomers and modulates lipase activity in adipose tissue. Pnas. 103: 17450–17455. [online] http://www.pnas.org/cgi/content/abstract/103/46/17450.

50. Cupp, M., A. Bensadoun, and K. Melford. 1987. Heparin decreases the degradation rate of lipoprotein lipase in adipocytes. J. Biol. Chem. 262: 6383–6388.

51. The response of lipoprotein lipase to feeding and fasting. Evidence for posttranslational regulation. 1990. J. Biol. Chem. 265: 4570–4577.

52. Koliwad, S. K., T. Kuo, L. E. Shipp, N. E. Gray, F. Backhed, A. Y. L. So, R. V. Farese, and J. C. Wang. 2009. Angiopoietin-like 4 (ANGPTL4, fasting-induced adipose factor) is a direct glucocorticoid receptor target and participates in glucocorticoid-regulated triglyceride metabolism. J. Biol. Chem. 284: 25593–25601.

53. Gray, N. E., L. N. Lam, K. Yang, A. Y. Zhou, S. Koliwad, and J. C. Wang. 2012. Angiopoietin-like 4 (Angptl4) protein is a physiological mediator of intracellular lipolysis in murine adipocytes. J. Biol. Chem. 287: 8444–8456.

54. Aryal, B., A. K. Singh, X. Zhang, L. Varela, N. Rotllan, L. Goedeke, B. Chaube, J. Camporez, D. F. Vatner, T. L. Horvath, G. I. Shulman, Y. Suárez, and C. Fernández-hernando. 2018. Absence of ANGPTL4 in adipose tissue improves glucose tolerance and attenuates atherogenesis. JCI Inisght. 3: 1–19.

55. Janssen, A. W. F., S. Katiraei, B. Bartosinska, D. Eberhard, and K. W. Van Dijk. 2018. Loss of angiopoietin-like 4 (ANGPTL4) in mice with diet-induced obesity uncouples visceral obesity from glucose intolerance partly via the gut microbiota. Diabetologia. 61: 1447–1458.

56. Davies, B. S. J. 2018. Can targeting ANGPTL proteins improve glucose tolerance ? Diabetologia. 61: 1277–1281.

57. Gusarova, V. et al. 2018. Genetic inactivation of ANGPTL4 improves glucose homeostasis and is associated with reduced risk of diabetes. Nat. Commun. 9: 1–11.

Supplemental Material

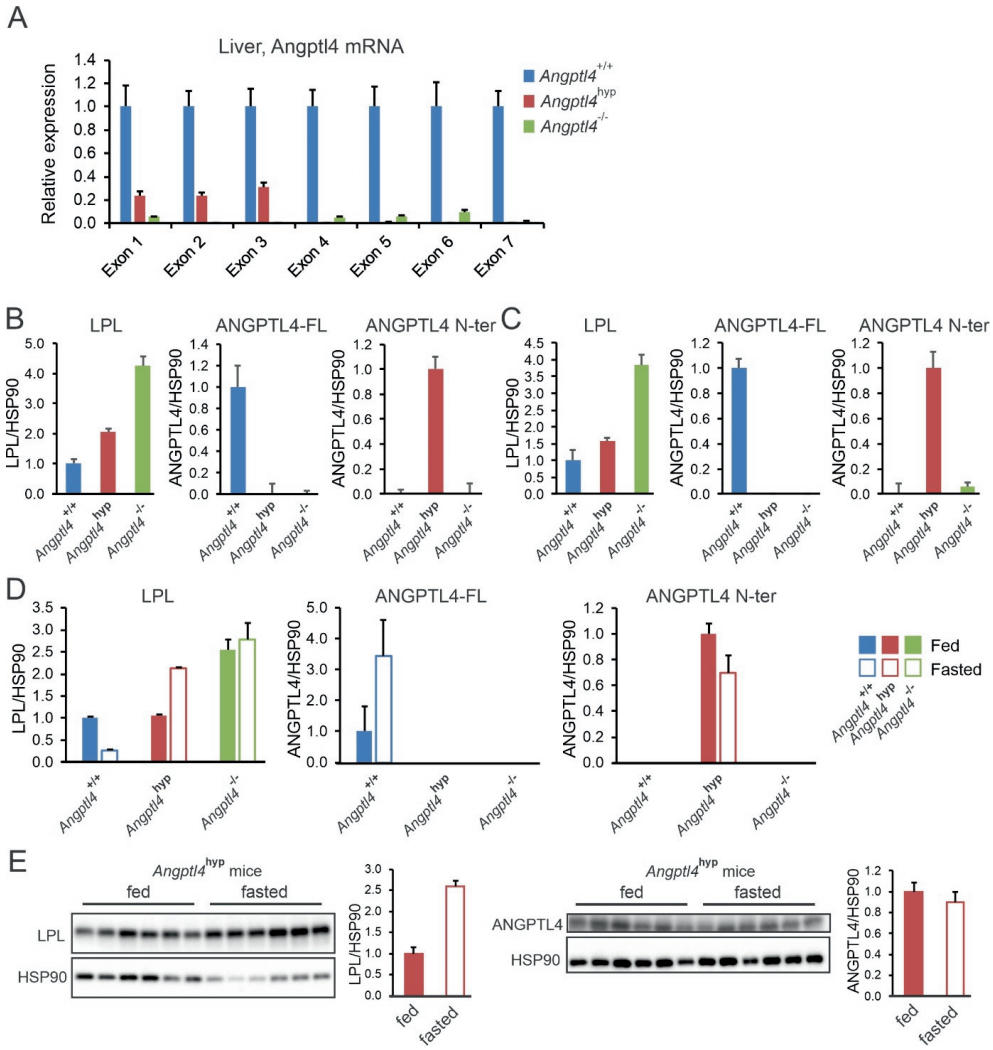

Supplemental Fig. 1. (A) Relative mRNA expression of all 7 exons of Angptl4 in the liver of *Angptl4*$^{-/-}$, *Angptl4*^{hyp} and wild-type mice. mRNA expression was normalized to *36b4*. N = 7 to 11 mice/group. Data are mean ± SEM. (B) Quantification of Western blots shown in figure 4E. (C) Quantification of Western blots shown in figure 4F. (D) Quantification of Western blots shown in figure 5C. Quantification of ANGPTL4 was based on antibody 742. (E) Western blot of LPL and N-terminal ANGPTL4 in adipose tissue of fed and fasted *Angptl4*^{hyp} mice. Quantification of Western blots is shown on the right. Data are mean ± SD.

Supplemental Table 1: Primer sequences used for qPCR

Genes	Forward primer	Reverse primer
m36B4	ATGGGTACAAGCGCGTCCTG	GCCTTGACCTTTTCAGTAAG
mAngptl4	GTTTGCAGACTCAGCTCAAGG	CCAAGAGGTCTATCTGGCTCTG
mHilpda	GCACGACCTGGTGTGACTGT	CCAGCACATAGAGGTTCAGCAT
mDdit3	CTGGAAGCCTGGTATGAGGAT	CAGGGTCAAGAGTAGTGAAGGT
mXbp1s	AAACAGAGTAGCAGCGCAGACTGC	GATCTCTAAAACTAGAGGCTTGGTG
mCxcl2	CCAACCACCAGGCTACAGG	GCGTCACACTCAAGCTCTG
mErn1	ACACCGACCACCGTATCTCA	CTCAGGATAATGGTAGCCATGTC
mPlin2	CTTGTGTCCTCCGCTTATGTC	GCAGAGGTCACGGTCTTCAC
mCxcl1	CTGGGATTCACCTCAAGAACATC	CAGGGTCAAGGCAAGCCTC
mCcr1	CTCATGCAGCATAGGAGGCTTAC	ATGGCATCACCAAAAATCCA
mPtgs2	TTCAACACACTCTATCACTGGC	AGAAGCGTTTGCGGTACTCAT
mCd14	CACACTCACTCAACTTTTCCT	GCTGAGATCAGTCCTCTCTCG
mGdf15	CTGGCAATGCCTGAACAACG	GGTCGGGACTTGGTTCTGAG
mAngtpl4 Exon1	CTTTGCATCCTGGGACGAGATG	GACAAGCGTTACCACAGGCAG
mAngtpl4 Exon2	GCTCAAGGCTCAAAACAGCAA	TGATAGGTATCTCTGCTGCTGG
mAngtpl4 Exon3	CCCACGCACCTAGACAATGG	TGGGAGTCAAGCCAATGAGC
mAngtpl4 Exon4	GGGACTGCCAGGAACTCTTC	AATGGTGGAGACCCCAGAGG
mAngtpl4 Exon5	GAGGCTGGACAGTGATTCAGAGA	GGGATCTCCGAAGCCATCCTT
mAngtpl4 Exon6	ACGGCCAATGAGCTGGG	GGGCAGGGAAAGGCCA
mAngtpl4 Exon7	CGCTACTATCCTCTGCAGGC	CCCTCGAGCCCATGTTTTCT
mSaa2	GCGAGCCTACACTGACATGA	TTTTCTCAGCAGCCCAGACT
mHp	GCTATGTGGAGCACTTGGTTC	CACCCATTGCTTCTCGTCGTT
mLcn2	TGGAAGAACCAAGGAGCTGT	GGTGGGGACAGAGAAGATGA
mOrm2	CAACATCACCATAGGCGACCC	ATTTCCTGCCGGTAATCAGGG

Supplemental Table 2: Overview of PCR reactions to determine transcribed mRNA in the *Angptl4* knockout-first mice (*Angptl4*^{hyp} mice).

Reaction	Forward primer	Reverse primer	Amplification
1	Angptl4 exon 1	Angptl4 exon 3	yes
2	Angptl4 exon 1	Angptl4 exon 5	no
3	Angptl4 exon 3	Angptl4 exon 3 fusion to Splice acceptor site	yes
4	Angptl4 exon 3	Splice acceptor site (end)	yes
5	Angptl4 exon 3 fusion to Splice acceptor site	ECMV IRES site (start)	yes
6	ECMV IRES site (start)	ECMV IRES site (testing predicted Stop)	yes
7	ECMV IRES site (start)	ECMV IRES site (mid)	yes
8	ECMV IRES site (start)	ECMV IRES site (end)	no
9	ECMV IRES site (start)	ECMV IRES site fusion to LacZ	no
10	ECMV IRES site fusion to LacZ	LacZ (1/4 of gene)	no
11	LacZ (2/4 of gene)	LacZ (2/4 of gene)	yes
12	LacZ (2/4 of gene)	LacZ (3/4 of gene)	yes

Supplemental Table 3: Overview of clinical outcomes in the 3 groups of mice fed a high fat diet

Clinical feature	Wild-type	*Angptl4*^{hyp}	*Angptl4*$^{-/-}$
Elevated SAA	No	Yes (attenuated)	Yes (pronounced)
Chylous ascites	No (0/7)	Yes (mild; 2/11)	Yes (pronounced; 7/8)
Touton giant cells	No (0/7)	Yes (10/11) Yes (7/8)	
Survival (20 weeks)	Yes (7/7)	Yes (11/11) No (2/8)	
Survival (36 weeks)	---	Yes (7/7)	---

6

Chapter 6

Butyrate but not beta-hydroxybutyrate impacts on cellular differentiation and whole genome expression *in vitro*

Philip M. M. Ruppert, Guido J. E. J. Hooiveld, Anja Zeigerer, Sander Kersten

Manuscript in preparation

Abstract

Intermittent fasting and caloric restriction-type interventions elicit a myriad of health benefits and are expected to provide clinical benefit for the prevention and treatment of obesity, type 2 and potentially cardiovascular disease and cancer. β-hydroxybutyrate (βOHB), levels of which increase to the low mM range during fasting, has been proposed as a potent signaling molecule mediating some of the beneficial effects of above-mentioned interventions. Here, we studied the capacity of βOHB to regulate differentiation of cells in vitro and screened for target genes in a panel of murine primary cells. We found that βOHB did not impact the differentiation process in C2C12 skeletal muscle cells and 3T3L1 adipocytes. Transcriptomics analysis revealed overall benign effects of βOHB on gene expression after 6h. βOHB did not consistently regulate genes and pathways in primary adipocytes, macrophages, myotubes and hepatocytes. The list of genes consistently regulated in at least 2 out of the 4 tested cell types is limited to Odc1, Stc1 (adipocytes & myotubes) and Inppl1 (macrophages and myotubes). In contrast, equimolar concentrations of the structurally related HDAC inhibitor Butyrate inhibited differentiation in C2C12 skeletal muscle cells and 3T3L1 adipocytes and induced dramatic and consistent gene expression changes in all primary cell types. Enrichr analysis corroborates an epigenetic mechanism of action for Butyrate. In conclusion, βOHB unlikely mediates beneficial effects of fasting via regulating gene expression or influencing cellular homeostatic processes such as differentiation. Additionally, in the tested cell primary cell types, βOHB's gene expression signature is disparate from the one of Butyrate suggesting that βOHB's HDAC inhibitory capacity may be negligible.

Keywords: β-hydroxybutyrate, HDAC inhibition, transcriptomics, butyrate

Introduction

Prevalence rates for obesity are spiraling out of control in many communities across the world. Inasmuch as obesity is a major risk factor for many chronic diseases, including type 2 diabetes, cardiovascular disease, and certain types of cancer [1], effective remedies to slow down the growth of obesity are direly needed. A common strategy that effectively promotes weight loss, at least in the short term, is caloric restriction, leading to an improvement in cardiometabolic risk profile. One of the more popular forms of caloric restriction is intermittent fasting, in which the normal abstinence of food consumption during the night is partly extended into the daytime [2]. In animal models, these dietary interventions increase median life-span, reduce body weight, mitigate inflammation, improve glucose homeostasis and insulin sensitivity, and delay the onset of diabetes, cardiovascular and neurological disease, as well as cancer. Similarly, human studies have shown that caloric restriction and intermittent fasting promote weight loss, reduce HbA1c and glucose levels, improve insulin sensitivity and blood lipid parameters, and reduce blood pressure [2]–[7].

Interestingly, it has been suggested that intermittent fasting may confer cardiometabolic health benefits independent of caloric restriction and concomitant weight loss. A number of mechanisms have been invoked in explaining the possible health benefits of intermittent fasting, including lower plasma insulin levels and higher levels of ketone bodies. The presence of ketone bodies in the blood is a characteristic feature of the fasted metabolic state. During the feeding-fasting transition, the body switches from glucose as a primary fuel source to the oxidation of fatty acids. In the liver, the high rates of fatty acid oxidation are accompanied by the synthesis of ketone bodies, which, as fasting progresses, become the dominant fuel for the brain [8]. The two main ketone bodies are β-hydroxybutyrate (βOHB) and acetoacetate (AcAc). Both compounds serve as sensitive biomarkers for the fasted state, increasing in combined concentration from less than 0.1 mM in the fed state to 5-7 mM when fasting for several weeks [8], [9].

In addition to serving as fuel in tissues such as the brain, heart, and skeletal muscle, recent research has unveiled that βOHB may also serve as a direct signaling molecule. By activating specific signaling pathways, βOHB may not only have an important regulatory role in the metabolic response to fasting but may also potentially mediate some of the beneficial health effects of fasting [2], [10]–[21]. Evidence has been presented that βOHB may regulate gene expression via epigenetic mechanisms. Shimazu *et al.* linked βOHB-mediated HDAC inhibition to protection against oxidative stress in kidney via the up-regulation of *FOXO3a*, *Catalase* and *MnSOD* [22]. While subsequent studies in neonatal hepatocytes, brain microvascular endothelial cells, and NB2a neuronal cells hinted at conservation of this pathway in different cell types [23], [24], other studies have since questioned the role of

βOHB as a potential physiological HDAC inhibitor [25], [26]. Interestingly, recent studies in hepatocytes, cortical neurons, myotubes and endothelial cells suggested that βOHB may serve as a novel substrate for a transcriptionally-activating histone modifications. This so called lysine β-hydroxy-butyrylation (kbhb) was found in proximity to fasting-relevant hepatic pathways, including amino acid catabolism, circadian rhythm, and PPAR signaling [26], and was found to regulate expression of BDNF [27] and hexokinase 2 [25]. How histones become β-hydroxybutyrylated remains unknown. Recent biochemical evidence suggests that SIRT3 facilitates the de-β-hydroxybutyrylation of histones [28]. While there is thus some evidence to suggest that βOHB may serve as a direct signaling molecule regulating genes, the potency and importance of βOHB as regulator of gene expression in various cell types is unclear.

In this work we aimed to further investigate the capacity of βOHB to regulate gene expression and thereby serve as a direct signaling molecule during the fasted state. To this end, we treated primary mouse adipocytes, macrophages, myotubes and hepatocytes with physiological concentrations of βOHB and unbiasedly assessed gene expression via RNA-seq. A direct comparison was made between the effects of βOHB and the colon-derived short-chain fatty acid butyrate. Butyrate is well known for its HDAC inhibitory activity and has a large structural resemblance to βOHB [29]. In contrast to butyrate, βOHB minimally impacted gene expression. Overall our data do not support the notion that βOHB is a powerful signaling molecule regulating gene expression.

Materials and methods

Materials

βOHB was (R)-(−)-3-Hydroxybutyric acid sodium salt from Sigma-Aldrich (#298360). Butyrate was Sodium butyrate from Sigma-Aldrich (#303410).

Differentiation experiments

3T3-L1 fibroblasts were maintained in DMEM supplemented with 10% newborn calf serum (NCS) and 1% penicillin/streptomycin (P/S) (all Lonza). Experiments were performed in six-well plates. For Oil red O stainings, cells were differentiated using the standard protocol. Two days post-confluence, cells were switched to DMEM supplemented with 10% fetal bovine serum (FBS), 1% P/S, 0.5 mM isobutylmethylxanthine, 1 µM dexamethasone, 5 µg/ml insulin for 2 days in the presence of either 8 mM βOHB or 8 mM Butyrate. After 2 days cells were switched to DMEM supplemented with 10% fetal bovine serum (FBS), 1% P/S, 5 µg/ml insulin and the tested compounds for another 2 days. Then cells were maintained in normal DMEM medium (2-3 days), in the presence of the tested compounds until the ORO stainings on day 10. For qPCR experiments cells were differentiated using the mild protocol, which allows for more sensitive assessment of compounds promoting the differentiation process at day 4 of differentiation [30]. Two days post-confluence, cells were switched to DMEM supplemented with 10% fetal bovine serum (FBS), 1% P/S, 0.5 mM isobutylmethylxanthine, 0.5 µM dexamethasone, 2 µg/ml insulin for 2 days, with the addition of either 1 µM Rosi, 8 mM βOHB or 8 mM Butyrate. After 2 days, the medium was changed to DMEM supplemented with 10% fetal bovine serum (FBS), 1% P/S, 2 µg/ml insulin and the tested compounds for another 2 days, before cells were harvested for RNA isolation.

C2C12 skeletal muscle cells were cultured in DMEM supplemented with 20% FBS (growth medium, GM) and induced to differentiate with DMEM supplemented with 2% horse serum (differentiation medium, DM) upon reaching confluence in the presence of either 5 mM βOHB or 5 mM Butyrate. DM was renewed every other day. Myotube formation was complete (visually) by day 5.

Isolation and differentiation of stromal vascular fraction

Inguinal white adipose tissue from 3-4 WT-C57Bl/6 male mice was collected and placed in Dulbecco's modified eagle's medium (DMEM; Lonza, Verviers, Belgium) supplemented with 1% Penicillin/Streptomycin (PS) and 1% bovine serum albumin (BSA; Sigma-Aldrich).

Material was minced finely with scissors and digested in collagenase-containing medium (DMEM with 3.2 mM $CaCl_2$, 1.5 mg/ml collagenase type II (C6885, Sigma-Aldrich), 10% FBS, 0.5% BSA, and 15 mM HEPES) for 1 h at 37°C, with occasional vortexing. Cells were filtered through a 100-µm cell strainer (Falcon). Subsequently, the cell suspension was centrifuged at 1600 rpm for 10 min and the pellet was resuspended in erythrocyte lysis buffer (155 mM NH_4Cl, 12 mM $NaHCO_3$, 0.1 mM EDTA). Upon incubation for 2 min at room temperature, cells were centrifuged at 1200 rpm for 5 min and the pelleted cells were resuspended in DMEM containing 10% fetal bovine serum (FBS) and 1% PS (DMEM/FBS/PS) and plated. Upon confluence, the cells were differentiated according to the protocol as described previously [31], [32]. Briefly, confluent SVFs were plated in 1:1 surface ratio, and differentiation was induced 2 days afterwards by switching to a differentiation induction cocktail (DMEM/FBS/PS, 0.5 mM isobutylmethylxanthine, 1 µM dexamethasone, 7 µg/ml insulin and 1 µM rosiglitazone) for 3 days. Subsequently, cells were maintained in DMEM/FBS/PS, and 7 µg/ml insulin for 3-6 days and switched to DMEM/FBS/PS for 3 days. Average rate of differentiation was at least 80% as determined by eye.

Isolation and differentiation of bone marrow derived monocytes

Bone marrow cells were isolated from femurs of WT-C57Bl/6 male mice following standard protocol and differentiated into macrophages (bone marrow-derived macrophages, BMDMs) in 6-8 days in DMEM/FBS/PS supplemented with 20% L929-conditioned medium (L929). After 6-8 days, non-adherent cells were removed, and adherent cells were washed and plated in 12-well plates in DMEM/FBS/PS + 10% L929. After 24 hours, medium was switched to 2% L929 in DMEM/FBS/PS overnight. Cells were treated the following day.

Isolation and differentiation of skeletal myotubes

Myoblasts from hindlimb muscle of WT-C57Bl/6 male mice were isolated as previously described [33]. In brief, the muscles were excised, washed in 1× PBS, minced thoroughly, and digested using 1.5 mL collagenase digestion buffer (500 U/ml or 4 mg/mL collagenase type II (C6885, Sigma-Aldrich), 1.5 U/ml or 5 mg/mL Dispase II (D4693, Sigma-Aldrich), and 2.5 mM CaCl2 in 1× PBS) at 37°C water bath for 1 h in a 50 ml tube, agitating the tube every 5 min. After digestion, the cell suspension containing small pieces of muscle tissue was diluted in proliferation medium (PM: Ham's F-10 Nutrient Mix (#31550023, Thermo Fisher Scientific) supplemented with 20% fetal calf serum, 10% HS, 0.5% sterile filtered chicken embryo extract (#092850145, MP Biomedicals), 2.5 ng/ml basic fibroblast growth factor (#PHG0367, Thermo Fisher Scientific), 1% gentamycin, and 1% PS), and the suspension was seeded onto matrigel-coated (0.9 mg/ml, #354234, Corning) T150 flasks at 20% surface

coverage. Cells were grown in 5% CO2 incubator at 37°C. Confluence was reached latest after 5 d in culture, upon which cells were trypsinized (0.25% trypsin), filtered with 70 µm filters, centrifuged at 300 g for 5 min, and then seeded on an uncoated T150 flask for 45 min to get rid of fibroblasts. Subsequently, myoblasts were seeded in PM at 150.000 cells/mL onto matrigel-coated 12-well plates cells. Upon reaching confluence, differentiation was induced by switching to differentiation medium (DM: Ham's F-10 Nutrient Mix supplemented with 5% horse serum (HS) and 1% PS). DM was replaced every other day. Myotubes fully differentiated by Day 5 of differentiation in DM. The medium was renewed every other day.

Isolation and differentiation of hepatocytes

Primary hepatocytes were isolated from C57BL/6NHsd male mice via collagenase perfusion as described previously [34]. Cells were plated onto collagen (0.9 mg/ml) coated 24-well plates at 200,000 cells/well in Williams E medium (PAN Biotech, Aidenbach, Germany), substituted with 10% FBS, 100 nM dexamethasone and penicillin/streptomycin and maintained at 37 °C in an atmosphere with 5% CO2. After four hours of attachment, cells were washed with phosphate buffer saline (PBS) and maintained in medium for the length of the experiment.

Treatments

Adipocytes and macrophages were treated for 6h with 5 mM βOHB or Butyrate, with PBS as control, in DMEM/FCS/PS. Myotubes were treated in DM. Hepatocytes were treated in Williams E medium. Cells were washed with PBS once and stored in -80 °C until RNA was isolated.

RNA isolation and sequencing

Total RNA from all cell culture samples was extracted using TRIzol reagent (Thermo Fisher Scientific, the Netherlands) and purified using the Qiagen RNeasy Mini kit (Qiagen, the Netherlands) according to manufacturer's instructions. RNA concentration was measured with a Nanodrop 1000 spectrometer and RNA integrity was determined using an Agilent 2100 Bioanalyzer with RNA 6000 microchips (Agilent Technologies, South Queensferry, UK). Library construction and RNA sequencing on BGISEQ-500 were conducted at Beijing Genomics Institute (BGI, Denmark) for pair-end 150bp runs. At BGI, Genomic DNA was removed with two digestions using Amplification grade DNAse I (Invitrogen, USA). The RNA was sheared and reverse transcribed using random primers to obtain cDNA, which was used

for library construction. The library quality was determined by using Bioanalyzer 2100 (Agilent Technologies, CA, USA). Then, the library was used for sequencing with the sequencing platform BGISEQ- 500 (BGI, Shenzhen, China). All the generated raw sequencing reads were filtered, by removing reads with adaptors, reads with more than 10% of unknown bases, and low quality reads. Clean reads were then obtained and stored as FASTQ format.

Normalized expression estimates were obtained from the raw intensity values applying the robust multi-array analysis preprocessing algorithm available in the Bioconductor library AffyPLM with default settings [35], [36]. Probe sets were defined according to Dai et al. [37]. In this method probes are assigned to Entrez IDs as a unique gene identifier. In this study, probes were reorganized based on the Entrez Gene database, build 37, version 1 (remapped CDF v22). The P values were calculated using an Intensity-Based Moderated T-statistic (IBMT) [38]. Genes were defined as significantly changed when $P < 0.001$. Geneset enrichment analysis (GSEA) was used to identify gene sets that were enriched among the TOP100 upregulated or downregulated genes [39]. Genes were ranked based on the IBMT-statistic and subsequently analyzed for over- or underrepresentation in predefined genesets derived from Gene Ontology, KEGG, National Cancer Institute, PFAM, Biocarta, Reactome and WikiPathways pathway databases. Only genesets consisting of more than 15 and fewer than 500 genes were taken into account. Statistical significance of GSEA results was determined using 1000 permutations.

Statistical analyses

Statistical analysis of the transcriptomics data was performed as described in the previous paragraph. Data are presented as mean ± SD. P-values < 0.05 were considered statistically significant.

Results

To solidify the concept of βOHB as a powerful signaling molecule influencing cellular homeostasis, we examined whether βOHB influences differentiation processes. Previously, we showed that butyrate, despite acting as a selective PPARγ agonist, inhibits adipogenesis in 3T3L1 cells [40]. Due to structural and possibly functional resemblance with butyrate, we hypothesized that βOHB might exert similar effects on the differentiation of 3T3-L1 cells. Compared to the control, 8 mM βOHB did not visibly affect differentiation, neither during the differentiation process (Day 4) nor terminally (Day 10; Figure 1A). By contrast and in line with previous studies, 1 μM rosiglitazone further stimulated the differentiation process (Day 4), whereas 8 mM butyrate markedly inhibited differentiation (Day 4 and 10; Figure 1A). Corroborating the visual assessment, rosiglitazone significantly induced expression of the adipogenic marker genes *Adipoq, Glut4* and *Fabp,* whereas butyrate significantly downregulated these genes. In line with the lack of effect on 3T3-L1 differentiation, βOHB did not alter the expression of these genes (Figure 1B).

Next we studied myogenesis. Butyrate was previously reported to inhibit myogenesis when present during the differentiation process [41]. To assess whether βOHB might influence myogenesis, we differentiated C2C12 myoblasts in the presence of 5 mM βOHB or 5 mM butyrate. In line with previous reports, butyrate inhibited the differentiation of myoblasts towards myotubes (Figure 1C) [41]. By contrast, βOHB did not visibly impact myotube formation (Figure 1C). Myogenesis is driven by muscle regulatory factors (MRFs) including *MyoG, MyoD* and *Myf5* [42], [43]. Supporting the lack of effect of βOHB on myogenesis, expression levels of all three MRFs were similar in βOHB and control-treated C2C12 cells at any time-point during the differentiation process (Figure 1D). This is in clear contrast to treatment with butyrate, which prevented upregulation of *MyoG* and *MyoD* and downregulated *Myf5* at all time-points, respectively. We also wondered whether βOHB instead of influencing the differentiation process, βOHB might affect the polarization of myotubes to either myosin heavy chain class I (MHCI) or class II (MHCII). Expression of *Myh3*, *Myh7* and *Myh8*, representing MHCI, were unchanged between βOHB and control treated myoblasts. Expression of *Myh1*, *Myh2* and *Myh4*, representing MHCII were also unchanged between βOHB and control, suggesting that βOHB does not impact the polarization of myotubes when present during the differentiation process.

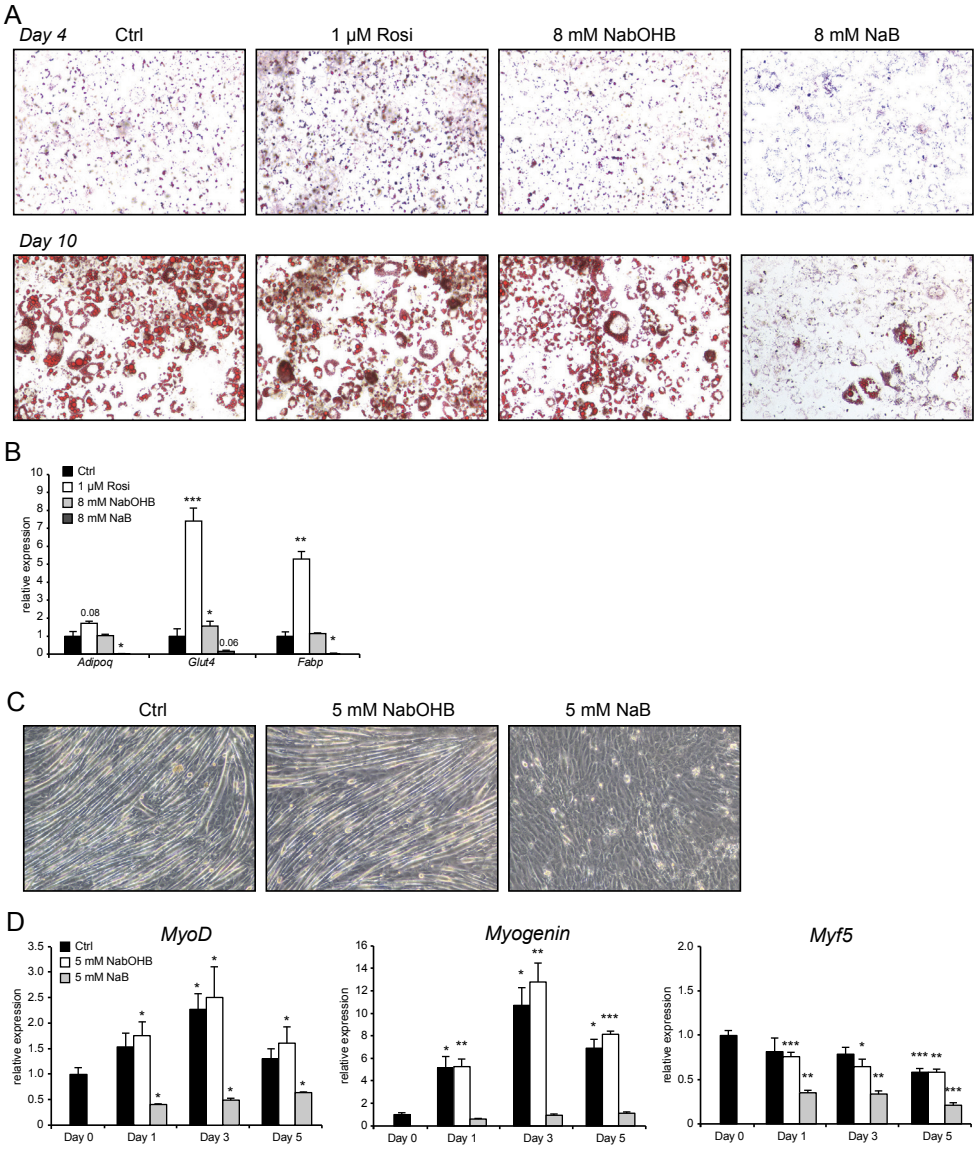
A
Day 4
Ctrl
1 µM Rosi
8 mM NabOHB
8 mM NaB
Day 10
B
Ctrl
1 µM Rosi
8 mM NabOHB
8 mM NaB
relative expression
0.08
0.06
Adipoq
Glut4
Fabp
C
Ctrl
5 mM NabOHB
5 mM NaB
D
MyoD
Myogenin
Myf5
Ctrl
5 mM NabOHB
5 mM NaB
relative expression
Day 0
Day 1
Day 3
Day 5

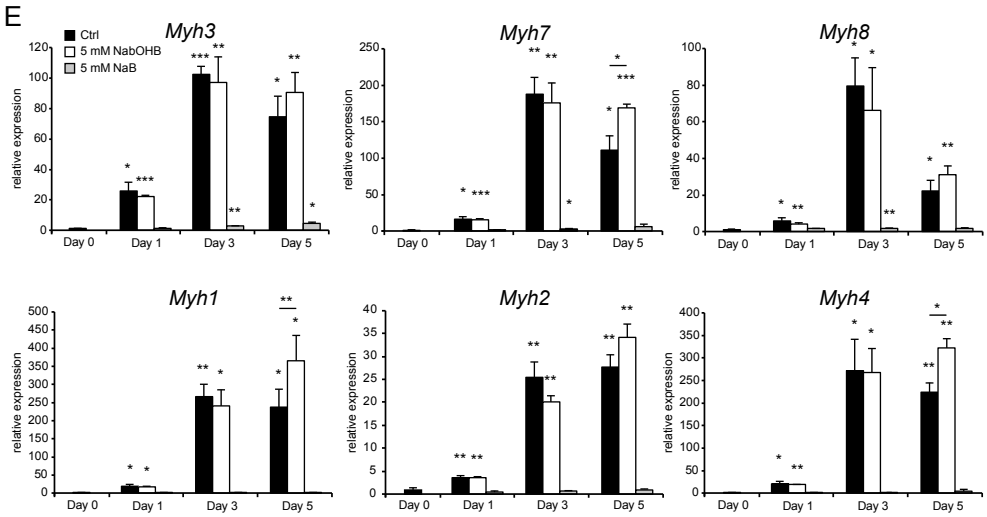

Figure 1: Differential effects of βOHB and Butyrate on the differentiation process of 3T3L1 adipocytes and C2C12 myotubes. (A) Representative Oil red O staining of 3T3-L1 adipocytes at day 4 of the standard differentiation protocol. (B) Expression of differentiation markers and PPARγ targets determined by qPCR at day 4 using the mild differentiation protocol in the presence of either 1 µM Rosi, 8 mM βOHB or 8 mM Butyrate. (C) Representative microscopic pictures of myotube formation after 5 days of differentiation in the presence of 5 mM βOHB or 5 mM Butyrate. (D) Gene expression of myocyte differentiation markers MyoD, Myogenin and Myf5 after differentiation. (E) Gene expression of myotube polarization markers for type I and type II muscle fibers. Error bars represent SD. Asterisks indicate significant differences according to Student's t test (* $p < 0.05$; ** $p < 0.01$; *** $p < 0.001$).

We reasoned that if βOHB has a signaling function, it would likely alter the expression of genes either directly or indirectly. Accordingly, we investigated the ability of βOHB to regulate gene expression in cells that have been suggested to be targeted by βOHB. Specifically, we collected primary mouse adipocytes, primary mouse bone-marrow derived macrophages, primary mouse myotubes, and primary mouse hepatocytes and performed RNA-sequencing after 6h treatment with either 5 mM βOHB and 5 mM butyrate.

The cells treated with butyrate showed an anti-conservative p-value distribution, suggesting that butyrate has a marked effect on gene expression in all cell types studied. Conversely, cells treated with βOHB showed a uniform or conservative p-value distribution (Figure 2B), suggesting that βOHB treatment minimally impacted gene expression in the various cells. To study the magnitude of gene regulation by βOHB and butyrate in the various primary cells, we performed Volcano plot analysis. Strikingly, the effect of βOHB on gene expression was very limited in all cell types, with only a limited number of genes reaching the statistical threshold of $p < 0.001$ (Figure 3A). In stark contrast, butyrate had a huge effect on gene expression in all primary cells tested (Figure 3A). Using $p < 0.001$ as statistical cut-off, βOHB significantly altered expression of 44, 38, 466 and 95 genes in adipocytes, macrophages, myocytes and hepatocytes, respectively. Of these genes 20, 13, 388 and 32 were significantly downregulated in the respective cell types (Figure 3B). Considering that not a single gene had a false discovery q value below 0.05, most of these genes likely represent false positives. By contrast, butyrate significantly changed expression of 7068, 7943, 6996 and 7158 genes in the respective cell types ($p < 0.001$), of which 50 – 52% were downregulated (Figure 3B). Collectively, these data suggest that βOHB minimally impacts gene expression in adipocytes, macrophages, myocytes and hepatocytes, whereas butyrate profoundly alters gene expression in these cell types.

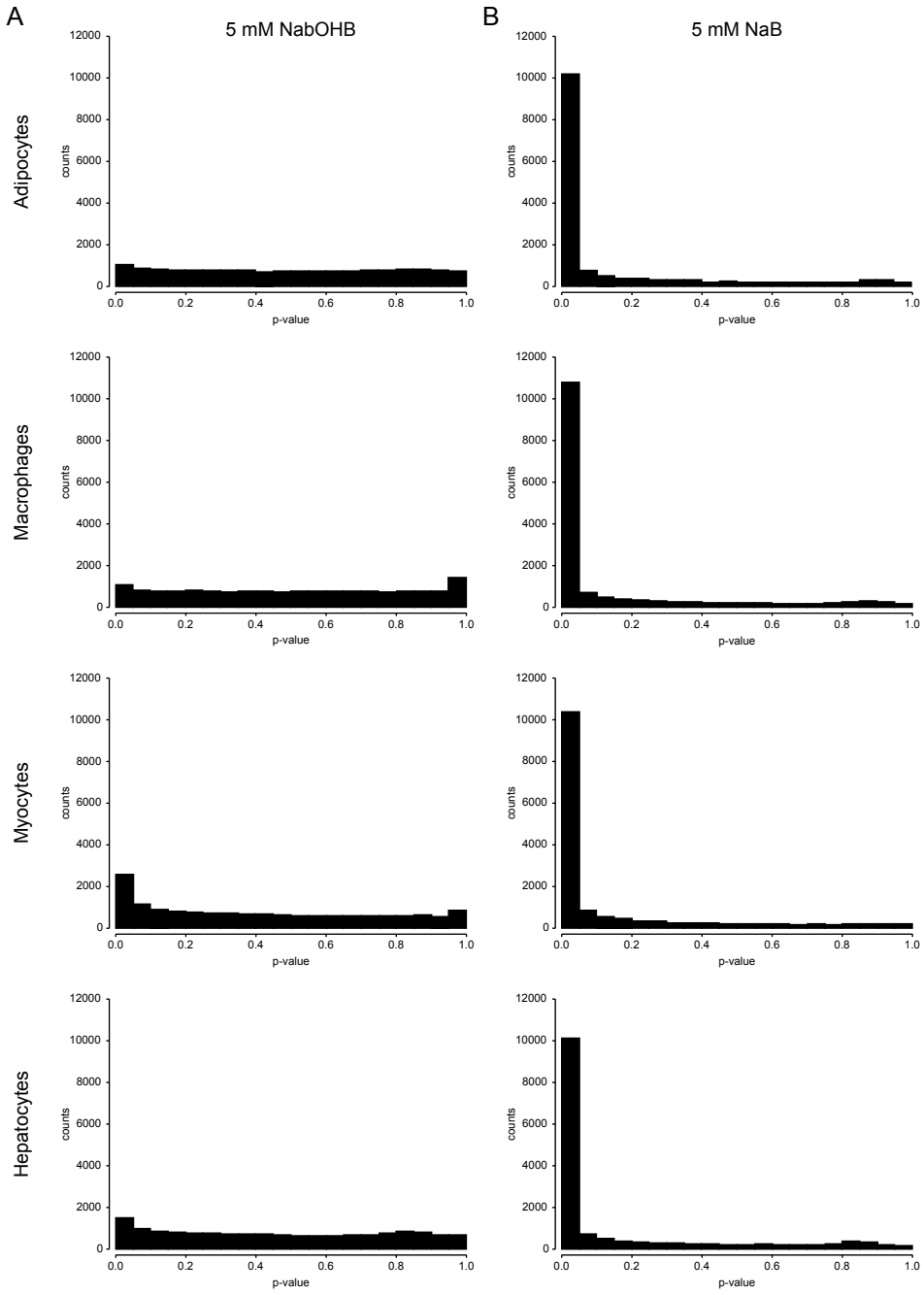

Figure 2: Raw p-value histograms. Histograms for butyrate (A) and βOHB treated cell types (B).

Next, in order to study the consistency of the response of each cell type to βOHB and butyrate, we performed hierarchical clustering and principle component analysis. Both analyses showed that the samples cluster by cell type first. However, within each cell type, the butyrate-treated samples cluster apart from the control and βOHB-samples (Figure 3C,D). Hierarchical biclustering of all significantly regulated genes per condition (from Figure 3B) further suggests similarity in the response to the treatment with butyrate irrespective of cell type. In comparison, the βOHB-induced expression changes are minor and show less clustering (Figure 3E). To assess the consistency in regulation of individual genes among the various cell types, we performed Venn diagram and heatmap analysis. Among all significantly regulated genes (from Figure 3B), only 3 genes were significantly regulated by βOHB in at least 2 of the tested cell types (Figure 4A). *Stc1* and *Inppl1* were significantly upregulated in adipocytes and myocytes or macrophages and myocytes, respectively. *Odc1* was significantly downregulated in adipocytes and myocytes (Figure 4B). By contrast, Venn diagrams for butyrate treated cells illustrate that most significantly regulated genes are shared in all cell types. Approx. 18% of all significantly upregulated genes are upregulated in every cell type. Vice versa, approx. 15% of all significantly downregulated genes are downregulated in every cell type (Figure 4A). Heatmaps of the TOP20 most significantly regulated genes in all 4 cell types after butyrate treatment indicate comparable signal log ratios (Figure 4B). Interestingly, the heatmaps for butyrate lists several genes related to histone metabolism (*H1f0, H1f2, H1f4, H1f3, Hcfc1, Phf2, Anp32b*). These analyses at the level of individual genes confirm that the effect of butyrate on gene expression is much more consistent and pronounced than the effect of βOHB.

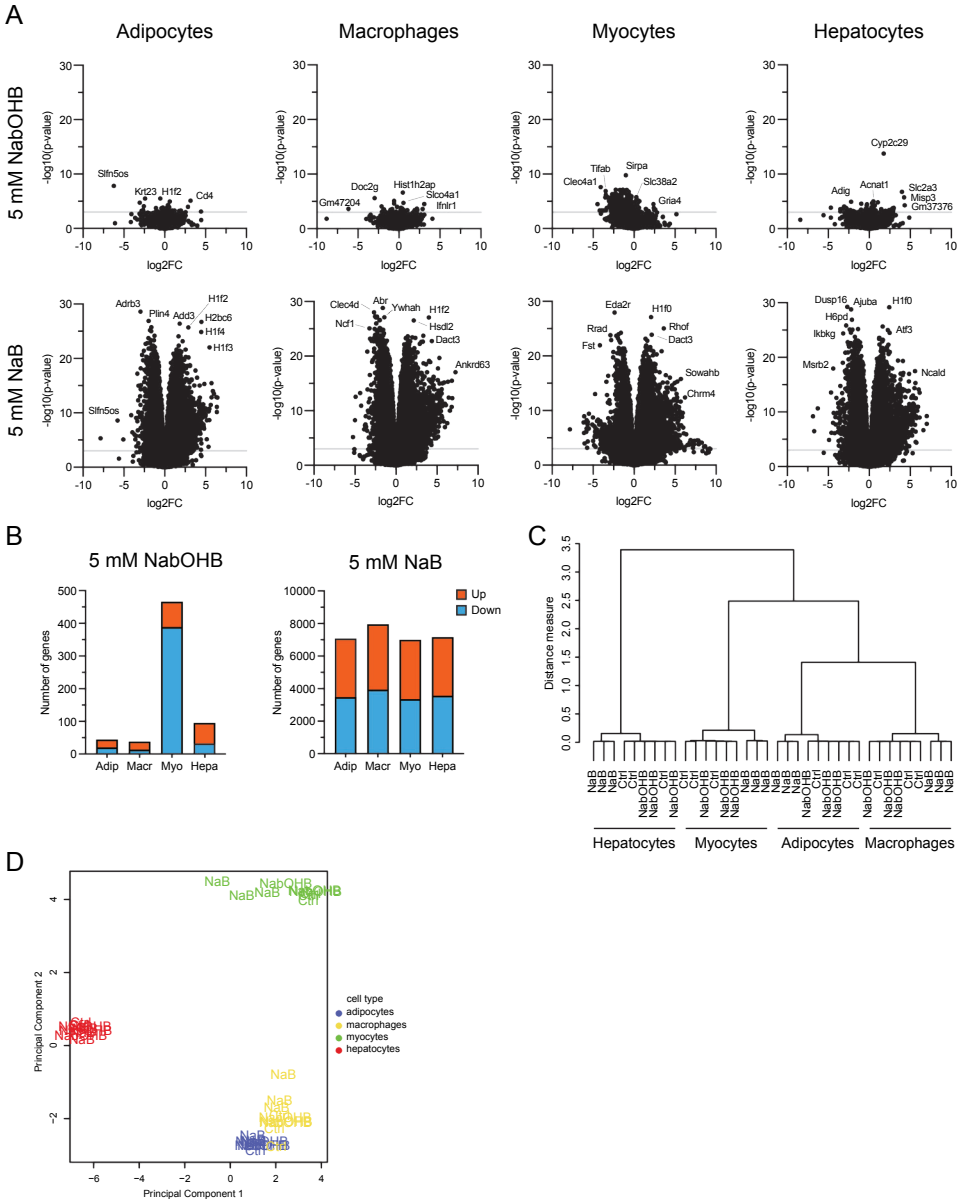
A
Adipocytes
Macrophages
Myocytes
Hepatocytes
5 mM NabOHB
5 mM NaB
-log10(p-value)
log2FC
Slfn5os
Krt23
H1f2
Cd4
Doc2g
Hist1h2ap
Slco4a1
Ifnlr1
Gm47204
Tifab
Sirpa
Cleo4a1
Slc38a2
Grta4
Cyp2c29
Adig
Acnat1
Slc2a3
Misp3
Gm37376
Adrb3
Plin4
Add3
H2bc6
H1f4
H1f3
Clec4d
Abr
Ywhah
Ncf1
Hsdl2
Dact3
Ankrd63
Eda2r
H1f0
Rrad
Rhof
Fst
Sowahb
Chrm4
Dusp16
Ajuba
H6pd
Ikbkg
Atf3
Msrb2
Ncald
B
5 mM NabOHB
5 mM NaB
Number of genes
Up
Down
Adip
Macr
Myo
Hepa
C
Distance measure
Hepatocytes
Myocytes
Adipocytes
Macrophages
D
Principal Component 1
Principal Component 2
cell type
adipocytes
macrophages
myocytes
hepatocytes

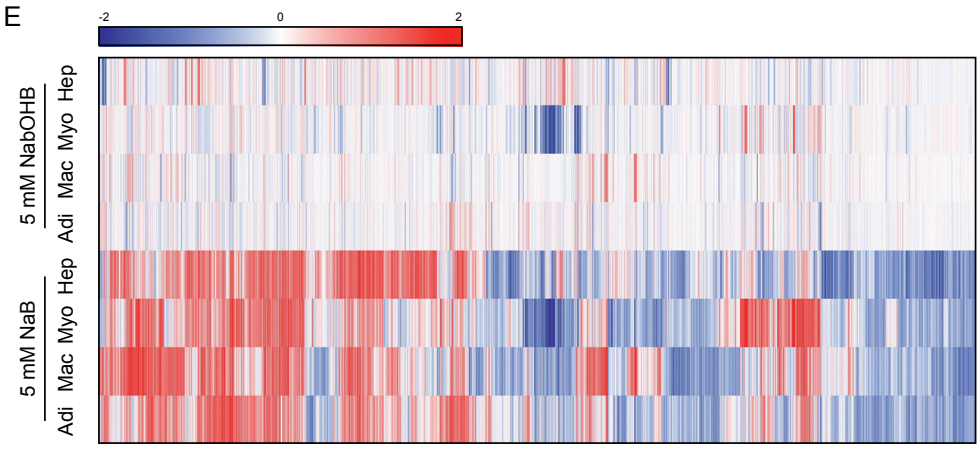

Figure 3: Disparate effects of βOHB and Butyrate on gene expression in primary adipocytes, macrophages, myotubes and hepatocytes. Volcano plots showing log2[fold-change] (x-axis) and the -10log of the raw p-value (y-axis) for every cell type treated with BOHB (A) and Butyrate. The grey line indicates p = 0.001. (B) Number of genes significantly ($p < 0.001$) altered by treatment with βOHB and Butyrate. Hierarchical clustering (C) and Principle component analysis (D) of βOHB and Butyrate treated samples. (E) Hierarchical biclustering of βOHB and Butyrate treated samples visualized in a heatmap. Clustered are significant differentially expressed genes based on pearson correlation with average linkage. Red indicates upregulated, blue indicates downregulated.

To gain more insight into the pathways differentially affected by βOHB and butyrate and to study which pathways are regulated consistently among the various cell types, we performed gene set enrichment analysis (GSEA). Specifically, we used the TOP100 up- and downregulated genes per cell type according to the T-statistic and expressed the normalized enrichment scores (NES) in heatmaps. In accordance with the limited and inconsistent effects of βOHB on gene expression, GSEA did not reveal any gene sets that were positively enriched in at least 2 cell types. Negatively enriched gene sets shared by at least 2 cell types were connected to transcriptional processes and include "MMU03010-RIBOSOME-KEGG", "MMU03030-DNA-REPLICATION-KEGG" and "MMU03040-SPLICEOSOME-KEGG" (Figure 4C). By contrast, butyrate treatment lead to the significant and consistent enrichment of various gene sets in almost all cell types. The top positively enriched gene sets include "MMU04070-PHOSPHATIDYLINOSITOL-SIGNALING-SYSTEM-KEGG" and "MMU00562-INOSITOL-PHOSPHATE-METABOLISM-KEGG" and various gene sets related to amino acids metabolism. The top negatively enriched gene sets also include the gene sets related to transcription (as listed above for βOHB), although the NES scores were substantially higher for the butyrate treatment. Another interesting negatively enriched gene set shared by 3 cell types is "MMU04350-TGF-BETA-SIGNALING-PATHWAY-KEGG" (Figure 4D). These analyses suggest that also at the level of pathways, the

transcriptional effect of butyrate is similar in the various cell types. By contrast, the effect of βOHB on the enrichment of gene sets is inconsistent between cell types and is limited to a few pathways related to transcriptional activity.

Lastly, to explore the possible underlying mechanisms for the observed gene expression effects for βOHB and butyrate, we submitted all differentially expressed genes of every cell type (from Figure 3B) to the Enrichment analysis tool Enrichr (https://amp.pharm.mssm.edu/Enrichr/). Enrichr starts with a list of differentially expressed genes and determines the enrichment of these genes on the basis of gene ontology or predefined pathways.[44], [45]. First, we compared our gene signatures to the "ENCODE Histone Modifications 2015" database. Our gene signatures after 5 mM butyrate treatment showed high overlap with gene signatures belonging to histone methylation and acetylation in various cells including myocyte and hepatocyte-related cell types. The lowest observed overlap was 1156/3076 (38%) genes changed associated to "H3K27ac liver mm9" in myocytes (Figure 4E). By comparison, the only significant overlap for 5 mM βOHB treated samples was seen for myocytes. This set of samples had a 3% overlap with gene signatures belonging to "H3K4me1 CH12.LX mm9" and "H3K4me1 MEL cell line mm9".

Additional comparisons of butyrate gene signatures to the "Drug Signature Database" (DSigDB) indicated overlap with gene signatures of treatments with various known HDAC inhibitors including Vorinostat, Trichostatin A and Valproic acid (Figure 4F). Lowest overlap was 39% (3248/8312) in myocytes for a gene set regulated by Valproic acid ("VALPROIC ACID CTD 00006977"). In contrast, gene signatures for the effect of 5 mM βOHB, again, overlapped minimally with existing gene sets in this database. The only HDAC inhibition-related overlap was seen for myocytes with "vorinostat HL60 DOWN" but overlap with genes belonging to this set was only 8% (Figure 4F). Taken together, these Enrichr analyses suggest that epigenetic regulation may be at least partly responsible for the effects of butyrate on gene expression. βOHB showed minimal overlap in the comparison to histone modification or drug signature datasets, not supporting HDAC inhibition as a relevant mechanism for the limited effects on gene expression.

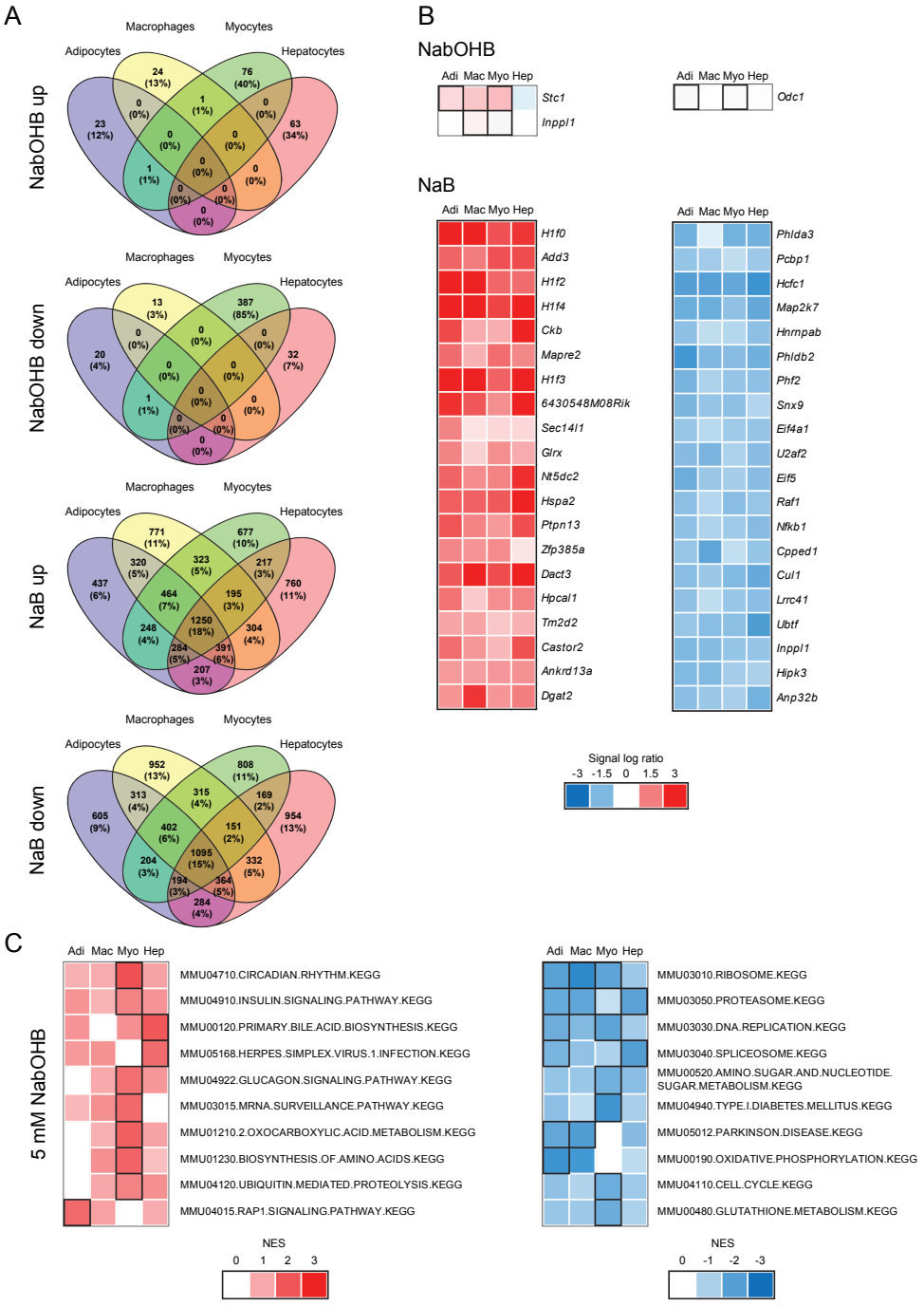
A
Macrophages
Myocytes
Adipocytes
Hepatocytes
NabOHB up
24 (13%)
76 (40%)
23 (12%)
63 (34%)
1 (1%)
NabOHB down
13 (3%)
387 (85%)
20 (4%)
32 (7%)
NaB up
771 (11%)
677 (10%)
320 (5%)
323 (5%)
217 (3%)
437 (6%)
760 (11%)
464 (7%)
195 (3%)
1250 (18%)
248 (4%)
304 (4%)
284 (5%)
391 (6%)
207 (3%)
NaB down
952 (13%)
808 (11%)
313 (4%)
315 (4%)
169 (2%)
605 (9%)
954 (13%)
402 (6%)
151 (2%)
1095 (15%)
204 (3%)
332 (5%)
194 (3%)
364 (5%)
284 (4%)
B
NabOHB
Adi Mac Myo Hep
Stc1
Inppl1
Odc1
NaB
H1f0
Add3
H1f2
H1f4
Ckb
Mapre2
H1f3
6430548M08Rik
Sec14l1
Glrx
Nt5dc2
Hspa2
Ptpn13
Zfp385a
Dact3
Hpcal1
Tm2d2
Castor2
Ankrd13a
Dgat2
Phlda3
Pcbp1
Hcfc1
Map2k7
Hnrnpab
Phldb2
Phf2
Snx9
Eif4a1
U2af2
Eif5
Raf1
Nfkb1
Cpped1
Cul1
Lrrc41
Ubtf
Inppl1
Hipk3
Anp32b
Signal log ratio
-3 -1.5 0 1.5 3
C
5 mM NabOHB
Adi Mac Myo Hep
MMU04710.CIRCADIAN.RHYTHM.KEGG
MMU04910.INSULIN.SIGNALING.PATHWAY.KEGG
MMU00120.PRIMARY.BILE.ACID.BIOSYNTHESIS.KEGG
MMU05168.HERPES.SIMPLEX.VIRUS.1.INFECTION.KEGG
MMU04922.GLUCAGON.SIGNALING.PATHWAY.KEGG
MMU03015.MRNA.SURVEILLANCE.PATHWAY.KEGG
MMU01210.2.OXOCARBOXYLIC.ACID.METABOLISM.KEGG
MMU01230.BIOSYNTHESIS.OF.AMINO.ACIDS.KEGG
MMU04120.UBIQUITIN.MEDIATED.PROTEOLYSIS.KEGG
MMU04015.RAP1.SIGNALING.PATHWAY.KEGG
NES
0 1 2 3
MMU03010.RIBOSOME.KEGG
MMU03050.PROTEASOME.KEGG
MMU03030.DNA.REPLICATION.KEGG
MMU03040.SPLICEOSOME.KEGG
MMU00520.AMINO.SUGAR.AND.NUCLEOTIDE.
SUGAR.METABOLISM.KEGG
MMU04940.TYPE.I.DIABETES.MELLITUS.KEGG
MMU05012.PARKINSON.DISEASE.KEGG
MMU00190.OXIDATIVE.PHOSPHORYLATION.KEGG
MMU04110.CELL.CYCLE.KEGG
MMU00480.GLUTATHIONE.METABOLISM.KEGG
NES
0 -1 -2 -3

D

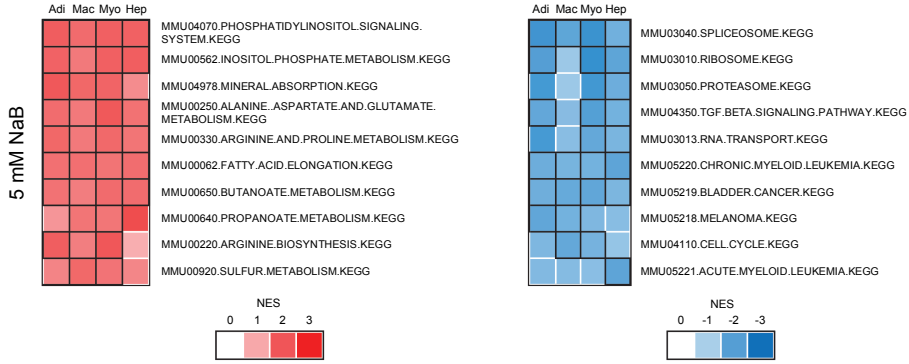

E

5 mM NaB

Term	Adipocytes			Macrophages			Myocytes			Hepatocytes			Average -log10 (adj. p-value)
	Overlap	Ratio	Adj. p-value	Overlap	Ratio	Adj. p-value	Overlap	Ratio	Adj. p-value	Overlap	Ratio	Adj. p-value	
H3K4me3 MEL cell line mm9	1796/4088	44%	3,87E-35	2094/4088	51%	2,26E-60	1640/4088	40%	4,22E-12	1890/4088	46%	2,35E-51	39
H3K4me3 CH12.LX mm9	1829/4143	44%	3,06E-37	2045/4143	49%	2,37E-43	1638/4143	40%	7,94E-10	1872/4143	45%	1,47E-42	33
H3ac myocyte mm9	925/2000	46%	2,87E-24	1053/2000	53%	4,22E-33	821/2000	41%	1,14E-07	958/2000	48%	4,47E-30	23
H3K4me3 C2C12 mm9	911/2000	46%	1,47E-21	1043/2000	52%	8,90E-31	789/2000	39%	1,40E-04	945/2000	47%	3,72E-27	20
H3K27ac heart mm9	1288/2941	44%	5,11E-23	1414/2941	48%	3,56E-22	1138/2941	39%	7,30E-05	1348/2941	46%	3,67E-32	20
H3K9ac MEL cell line mm9	894/2000	45%	2,22E-18	1051/2000	53%	1,09E-32	806/2000	40%	3,99E-06	935/2000	47%	6,25E-25	20
H3K27ac ES-E14 mm9	920/2000	46%	2,69E-23	1024/2000	51%	2,04E-26	815/2000	41%	4,79E-07	926/2000	46%	3,80E-23	19
H3K27ac liver mm9	1275/3076	41%	1,77E-13	1496/3076	49%	2,91E-26	1156/3076	38%	7,08E-03	1419/3076	46%	8,23E-36	19
H3K4me3 G1E mm9	1104/2531	44%	9,91E-19	1262/2531	50%	6,68E-27	1008/2531	40%	1,48E-06	1145/2531	45%	2,45E-24	18
H3ac C2C12 mm9	902/2000	45%	8,64E-20	1020/2000	51%	1,18E-25	806/2000	40%	3,66E-06	932/2000	47%	2,39E-24	18

5 mM NabOHB

Term	Adipocytes			Macrophages			Myocytes			Hepatocytes			Average -log10 (adj. p-value)
	Overlap	Ratio	Adj. p-value	Overlap	Ratio	Adj. p-value	Overlap	Ratio	Adj. p-value	Overlap	Ratio	Adj. p-value	
H3K4me1 CH12.LX mm9	6/3885	0%	1	10/3885	0%	1	133/3885	3%	4,19E-04	15/3885	0%	1	1
H3K4me1 MEL cell line mm9	3/4170	0%	1	7/4170	0%	1	136/4170	3%	2,13E-03	23/4170	1%	1	1
H3K27ac thymus mm9	4/2000	0%	1	2/2000	0%	1	62/2000	3%	1	8/2000	0%	1	0
H3K4me1 liver mm9	8/3706	0%	1	7/3706	0%	1	101/3706	3%	1	16/3706	0%	1	0
H3K27me3 MCF-7 hg19	1/989	0%	1	-	-	-	30/989	3%	1	3/989	0%	1	0
H3K36me3 MEL cell line mm9	4/3352	0%	1	3/3352	0%	1	89/3352	3%	1	11/3352	0%	1	0
H3K27me3 spleen mm9	10/2000	1%	1	3/2000	0%	1	43/2000	2%	1	12/2000	1%	1	0
H3K9me3 CD14-positive monocyte hg19	8/2000	0%	1	5/2000	0%	1	21/2000	1%	1	9/2000	0%	1	0
H3K4me3 spleen mm9	2/2000	0%	1	1/2000	0%	1	47/2000	2%	1	15/2000	1%	1	0
H3K4me3 kidney mm9	2/2000	0%	1	4/2000	0%	1	47/2000	2%	1	15/2000	1%	1	0

F

5 mM NaB

Term	Adipocytes			Macrophages			Myocytes			Hepatocytes			Average -log10 (adj. p-value)
	Overlap	Ratio	Adj. p-value	Overlap	Ratio	Adj. p-value	Overlap	Ratio	Adj. p-value	Overlap	Ratio	Adj. p-value	
7646-79-9 CTD 00000928	1467/3094	47%	9,60E-48	1612/3094	52%	1,43E-48	1328/3094	43%	7,25E-21	1487/3094	48%	1,21E-49	41
0175029-0000 PC3 DOWN	1557/3326	47%	2,35E-47	1632/3326	49%	2,71E-30	1409/3326	42%	7,98E-20	1548/3326	47%	9,58E-42	34
acetaminophen CTD 00005295	1811/4135	44%	1,02E-33	1988/4135	48%	1,17E-31	1689/4135	41%	1,49E-16	1906/4135	46%	4,73E-50	32
Copper sulfate CTD 00007279	2477/6016	41%	4,36E-27	2752/6016	46%	8,72E-28	2365/6016	39%	4,83E-15	2644/6016	44%	4,35E-52	30
vorinostat HL60 UP	417/727	57%	4,59E-32	443/727	61%	3,10E-29	393/727	54%	9,82E-24	419/727	58%	1,13E-31	28
trichostatin A PC3 DOWN	588/1133	52%	3,91E-29	655/1133	58%	1,62E-33	563/1133	50%	7,38E-23	591/1133	52%	1,09E-28	28
trichostatin A MCF7 UP	486/874	56%	6,19E-33	503/874	58%	2,43E-25	468/874	54%	5,43E-27	466/874	53%	4,66E-25	27
scriptaid PC3 DOWN	388/692	56%	3,57E-27	415/692	60%	1,43E-25	368/692	53%	7,56E-21	392/692	57%	1,37E-27	25
VALPROIC ACID CTD 00006977	3323/8312	40%	2,21E-28	3656/8312	44%	2,46E-23	3248/8312	39%	6,10E-22	3330/8312	40%	2,41E-24	24
2-Methylcholine CTD 00002006	793/1666	48%	1,42E-24	881/1666	53%	1,59E-27	723/1666	43%	9,17E-12	833/1666	50%	1,10E-32	23

5 mM NabOHB

5 mM bOHB	Adipocytes			Macrophages			Myocytes			Hepatocytes			Average -log10 (adj. p-value)
Term	Overlap	Ratio	Adj. p-value	Overlap	Ratio	Adj. p-value	Overlap	Ratio	Adj. p-value	Overlap	Ratio	Adj. p-value	
pergolide HL60 UP	-	-	-	-	-	-	33/312	11%	5,98E-10	-	-	-	9
dihydroergotamine HL60 UP	-	-	-	-	-	-	16/136	12%	2,79E-05	-	-	-	5
acacetin HL60 DOWN	-	-	-	-	-	-	10/54	19%	8,67E-05	-	-	-	4
Sodium dichromate CTD 00000827	1/208	0%	1	1/208	0%	1	28/208	13%	2,87E-10	-	-	-	3
tetryzoline HL60 UP	-	-	-	-	-	-	16/119	13%	5,39E-06	2/119	2%	1	3
methylergometrine HL60 UP	-	-	-	-	-	-	17/136	13%	5,47E-06	1/136	1%	1	3
tretinoin HL60 UP	2/241	1%	9,17E-01	-	-	-	26/241	11%	6,17E-08	2/241	1%	1	2
vorinostat HL60 DOWN	1/569	0%	1	1/569	0%	1	46/569	8%	4,31E-10	2/569	0%	1	2
mebendazole HL60 UP	1/346	0%	1	1/346	0%	1	33/346	10%	7,86E-09	2/346	1%	1	2
beta-D-allopyranose BOSS	1/97	1%	1	-	-	-	13/97	13%	8,88E-05	-	-	-	2

Figure 4: Disparate consistency of gene expression changes elicited by βOHB and Butyrate. (A) Venn diagrams showing overlap in significantly regulated genes between of βOHB and Butyrate regulates genes between cell types ($p < 0.001$). (B) Heatmaps showing genes that are significantly regulated in at least 2 cell types (βOHB) and in all 4 cell types (Butyrate). Genes with thick black border are significantly regulated ($p < 0.001$). In Butyrate-heatmaps all listed genes are significantly regulated and genes are sorted by significance. Top 10 up- and downregulated genesets in βOHB (C) and Butyrate-treated cells (D). Genesets were determined by geneset enrichment analysis (GSEA) based on t-values for the top 100 up- and downregulated genes and ranked according to averaged normalized enrichment score (NES). Pathways with thick black border are significantly enriched based on FDR q-value < 0.1. Differentially expressed genes (from Figure 3B) were submitted to Enrichr (https://amp.pharm.mssm.edu/Enrichr/) and compared to "ENCODE Histone Modifications 2015" (E) and "Drug Signature Database" (DSigDB) (F). TOP10 terms are shown sorted by descending average -log10 (adjusted p-value).

Discussion

In this paper we tested the potential of β-hydroxybutyrate (βOHB) to influence cellular differentiation and for the first time performed whole genome expression analysis in primary adipocytes, macrophages, myocytes and hepatocytes using βOHB side-by-side with the well-established HDAC inhibitor butyrate. At physiologically relevant concentrations of βOHB measured after fasting or ketogenic diet, βOHB did not impact differentiation of 3T3-L1 or C2C12 cells. Effects on gene expression elicited by βOHB were very small in comparison to butyrate and inconsistent between the primary cells studied. When using a statistical cut-off of 0.05 for false discovery q value, βOHB did not significantly influence the expression of any gene (not shown). The results from βOHB are in stark contrast to the consistent butyrate-mediated inhibition of differentiation in 3T3L1 and C2C12 cells, and the profound gene expression changes caused by butyrate in the various primary cells. Together, these data contradict the notion that βOHB serves as a potent signaling molecule during fasting via regulation of gene expression.

Interest in the beneficial effects of fasting has surged in the recent years. Illustrated by the sheer abundance of reviews and perspective papers on the potential benefits of βOHB (supplementation) (≥ 11 since 2014), βOHB is seen as one potential mediator of the fasting-related benefits [2], [10]–[21]. Common to all reviews is the prominent portrayal of βOHB as a potent HDAC inhibitor influencing gene expression, a notion originating from work by Shimazu *et al.* in kidney and HEK293 cells [22]. However, several authors have commented on the inability to reproduce changes in histone acetylation marks after incubating HEK293 cells with 20 mM βOHB [26], [27]. Instead, Xie *et al.* identified βOHB-derived lysine beta-hydroxybutyrylation (kbhb) as novel histone modification [26]. Recently, Chriett *et al.* revisited the assessment of βOHB's HDAC inhibitory activity and the accumulation of relevant histone marks, and also failed to reproduce the initial observations made by

Shimazu and coworkers. In addition, the authors reported a lack of HDAC inhibitory activity for βOHB in HMEC-1 human endothelial cells and L6 rat myotubes [25]. Like Shimazu *et al.*, Chriett *et al.* employed butyrate's powerful HDAC inhibitory effects as positive controls [22], [25]. Irrespective of the precise mechanism, epigenetic alterations ultimately require changes in gene expression to impact physiology. In our differentiation experiments, co-incubation with βOHB did not alter expression of key genes in the differentiation process of 3T3-L1 and C2C12 cells. Further unbiased assessment of whole genome expression in mouse primary adipocytes, mouse macrophages, myocytes and hepatocytes revealed that only 3 genes were significantly regulated in at least 2 of the tested primary cell types. Corroborating this finding, GSEA analysis using the top 100 up- and downregulated genes, irrespective of statistical significance, also revealed only limited overlap in βOHB regulated pathways between cell types. Overall, our study shows that the effect of βOHB on gene expression is minimal in controlled *in vitro* settings and lacks consistent regulation of specific target genes. These results do not support the notion that βOHB serves as an important signaling molecule regulating gene expression but do not exclude post-translational mechanisms or effects that may lay downstream of ATP generation.

In contrast to βOHB, the effects of butyrate on gene expression were prominent and displayed consistency between the tested primary cell lines and the differentiation experiments. A significant portion of genes were consistently regulated between cell types and the most highly enriched pathways were significantly enriched in most if not all cells. In line with butyrate's well-established effects on gene expression, pathways relevant to transcriptional activities were enriched as well. Additional analyses using Enrichr are in support of butyrate's prominent HDAC inhibitory action. Butyrate's effect on differentiation processes in 3T3-L1 and C2C12 cells is in line with previous research [40], [41] and may also be at least in part be explained by epigenetic mechanisms [46]. It should be noted, though, that the data presented here are not suitable to deduce potential physiological effects of butyrate and SCFA fermentation *in vivo*. Juxtaposing the supraphysiological concentration of 5 mM employed in this study are reports of 1 – 12 µM and 14 – 64 µM butyrate in the peripheral, respectively, central blood circulation measured in sudden death victims [47].

The main limitation of our study is the exclusive utilization of *in vitro* systems. We opted for this approach to allow for the identification of target genes that may be consistently regulated in more than one cell type in a controlled environment. While novel target genes would have to be replicated *in vivo*, this approach seemed more reasonable for this purpose compared to *in vivo* systems in which it is impossible to study the transcription regulation specifically attributable to βOHB. For example, the hepatic response to fasting is shaped by the FFA-PPARα axis, which regulates nearly every branch in lipid metabolism and is indispensable for the physiological adaptation to fasting [48], [49]. The increase of ketone body levels during fasting occurs concurrent with many other metabolic and hormonal

changes, including increased plasma fatty acids, cortisol, and glucagon levels, and decreased plasma insulin and leptin levels.

In conclusion, this work is the first to systematically assess the potential of the ketone body βOHB to influence gene expression in various primary cell types by RNA-sequencing. The lack of genes commonly regulated among cell types coupled to generally insignificant effects on gene expression contradict the notion that βOHB serves as a powerful signaling molecule regulating gene expression during the fasted state *in vivo.* In particular, by comparing βOHB to butyrate, we provide evidence against transcriptional mechanisms conferring the purported signaling effects in the first place. Our study does not rule out that βOHB confers signaling effects via other mechanisms secondary to oxidation or receptor activation, although such effects may be expected to indirectly lead to gene expression changes as well. Future research is necessary to delineate whether βOHB regulates gene expression in a tissue or context-specific manner. However, in comparison to other signaling axes regulating gene expression, such as the PPAR-system, stringent context- or tissue specific signaling effects by βOHB would equally dismiss the current portrayal of βOHB as the do-it-all-substrate during the fasted state.

References

[1] G. A. Bray, K. K. Kim, and J. P. H. Wilding, "Obesity: a chronic relapsing progressive disease process. A position statement of the World Obesity Federation," Obes. Rev., vol. 18, no. 7, pp. 715–723, Jul. 2017.

[2] A. Di Francesco, C. Di Germanio, M. Bernier, and R. de Cabo, "A time to fast.," Science, vol. 362, no. 6416, pp. 770–775, Nov. 2018.

[3] M. P. Mattson, V. D. Longo, and M. Harvie, "Impact of Intermittent Fasting on Health and Disease Processes," Ageing Res. Rev., vol. 39, pp. 46–58, Oct. 2016.

[4] V. D. Longo and S. Panda, "Fasting, Circadian Rhythms, and Time-Restricted Feeding in Healthy Lifespan," Cell Metab., vol. 23, no. 6, pp. 1048–1059, Jun. 2016.

[5] R. De Cabo and M. P. Mattson, "Effects of intermittent fasting on health, aging, and disease," New England Journal of Medicine, vol. 381, no. 26. Massachussetts Medical Society, pp. 2541–2551, 26-Dec-2019.

[6] S. Moon et al., "Beneficial effects of time-restricted eating on metabolic diseases: A systemic review and meta- analysis," Nutrients, vol. 12, no. 5. MDPI AG, 01-May-2020.

[7] K. Liu, B. Liu, and L. K. Heilbronn, "Intermittent fasting: what questions should we be asking?," Physiol. Behav., vol. 218, p. 112827, Feb. 2020.

[8] G. F. Cahill, "Fuel Metabolism in Starvation," Annu. Rev. Nutr., vol. 26, no. 1, pp. 1–22, 2006.

[9] Wildenhoff KE, Johansen JP, K. H, Yde H, and Sorensen NS, "Diurnal variations in the concentrations of blood acetoacetate and 3-hydroxybutyrate.," Acta Med Scand., vol. 195, no. 1–2, pp. 25–8, 1974.

[10] P. Rojas-Morales, E. Tapia, and J. Pedraza-Chaverri, "Beta-Hydroxybutyrate: A signaling metabolite in starvation response?," Cell. Signal., vol. 28, no. 8, pp. 917–923, Aug. 2016.

[11] R. L. Veech, "Ketone ester effects on metabolism and transcription," J. Lipid Res., vol. 55, no. 10, pp. 2004–2006, Oct. 2014.

[12] A. Dąbek, M. Wojtala, L. Pirola, and A. Balcerczyk, "Modulation of cellular biochemistry, epigenetics and metabolomics by ketone bodies. Implications of the ketogenic diet in the physiology of the organism and pathological states," Nutrients, vol. 12, no. 3. MDPI AG, 01-Mar-2020.

[13] B. J. Stubbs et al., "Investigating Ketone Bodies as Immunometabolic Countermeasures against Respiratory Viral Infections," Med, vol. 0, no. 0, Jul. 2020.

[14] P. Rojas-Morales, J. Pedraza-Chaverri, and E. Tapia, "Ketone bodies, stress response, and redox homeostasis," Redox Biology, vol. 29. Elsevier B.V., p. 101395, 01-Jan-2020.

[15] J. C. Newman and E. Verdin, "β-hydroxybutyrate: Much more than a metabolite," Diabetes Res. Clin. Pract., vol. 106, no. 2, pp. 173–181, 2014.

[16] L. B. Achanta and C. D. Rae, "β-Hydroxybutyrate in the Brain: One Molecule, Multiple Mechanisms," Neurochem. Res., vol. 42, no. 1, pp. 35–49, Jan. 2017.

[17] A. L. Hartman and J. M. Rho, "The new ketone alphabet soup: BHB, HCA, and HDAC," Epilepsy Currents, vol. 14, no. 6. pp. 355–357, 2014.

[18] J. C. Newman and E. Verdin, "β-Hydroxybutyrate: A Signaling Metabolite," Annu. Rev. Nutr., vol. 37, no. 1, pp. 51–76, 2017.

[19] R. L. Veech, B. Chance, Y. Kashiwaya, H. a Lardy, and G. F. Cahill, "Ketone bodies, potential therapeutic uses.," IUBMB Life, vol. 51, pp. 241–247, 2001.

[20] P. Puchalska and P. A. Crawford, "Multi-dimensional Roles of Ketone Bodies in Fuel Metabolism, Signaling, and Therapeutics," Cell Metab., vol. 25, no. 2, pp. 262–284, 2017.

[21] M. Maalouf, J. M. Rho, and M. P. Mattson, "The neuroprotective properties of calorie restriction, the ketogenic diet, and ketone bodies," Brain Res. Rev., vol. 59, no. 2, pp. 293–315, Mar. 2009.

[22] T. Shimazu et al., “Suppression of Oxidative Stress by -Hydroxybutyrate, an Endogenous Histone Deacetylase Inhibitor,” Science (80-.)., vol. 339, no. 6116, pp. 211–214, Jan. 2013.

[23] K. Tanegashima, Y. Sato-Miyata, M. Funakoshi, Y. Nishito, T. Aigaki, and T. Hara, “Epigenetic regulation of the glucose transporter gene Slc2a1 by β-hydroxybutyrate underlies preferential glucose supply to the brain of fasted mice,” Genes to Cells, vol. 22, no. 1, pp. 71–83, Jan. 2017.

[24] G. Rando et al., “Glucocorticoid receptor-PPARα axis in fetal mouse liver prepares neonates for milk lipid catabolism,” Elife, vol. 5, pp. 1–31, 2016.

[25] S. Chriett, A. Dąbek, M. Wojtala, H. Vidal, A. Balcerczyk, and L. Pirola, “Prominent action of butyrate over β-hydroxybutyrate as histone deacetylase inhibitor, transcriptional modulator and anti-inflammatory molecule,” Sci. Rep., vol. 9, no. 1, pp. 1–14, Dec. 2019.

[26] Z. Xie et al., “Metabolic Regulation of Gene Expression by Histone Lysine β-Hydroxybutyrylation,” Mol. Cell, vol. 62, no. 2, pp. 194–206, Apr. 2016.

[27] L. Chen, Z. Miao, and X. Xu, “β-hydroxybutyrate alleviates depressive behaviors in mice possibly by increasing the histone3-lysine9-β-hydroxybutyrylation,” Biochem. Biophys. Res. Commun., vol. 490, no. 2, pp. 117–122, Aug. 2017.

[28] X. Zhang et al., “Molecular basis for hierarchical histone de-β-hydroxybutyrylation by SIRT3,” Cell Discov., vol. 5, no. 1, Dec. 2019.

[29] E. P. M. Candido, R. Reeves, and J. R. Davie, “Sodium butyrate inhibits histone deacetylation in cultured cells,” Cell, vol. 14, no. 1, pp. 105–113, 1978.

[30] M. Scarsi et al., “Sulfonylureas and glinides exhibit peroxisome proliferator-activated receptor γ activity: A combined virtual screening and biological assay approach,” Mol. Pharmacol., vol. 71, no. 2, pp. 398–406, Feb. 2007.

[31] G. Ren, J. Y. Kim, and C. M. Smas, “Identification of RIFL, a novel adipocyte-enriched insulin target gene with a role in lipid metabolism,” Am. J. Physiol. - Endocrinol. Metab., vol. 303, no. 3, p. E334, Aug. 2012.

[32] F. Quagliarini et al., “Atypical angiopoietin-like protein that regulates ANGPTL3,” vol. 109, no. 48, pp. 19751–19756, Nov. 2012.

[33] A. Shahini et al., “Efficient and high yield isolation of myoblasts from skeletal muscle,” Stem Cell Res., vol. 30, pp. 122–129, Jul. 2018.

[34] S. Zellmer et al., “Transcription factors ETF, E2F, and SP-1 are involved in cytokine-independent proliferation of murine hepatocytes,” Hepatology, vol. 52, no. 6, pp. 2127–2136, 2010.

[35] B. M. Bolstad, R. A. Irizarry, M. Åstrand, and T. P. Speed, “A comparison of normalization methods for high density oligonucleotide array data based on variance and bias,” Bioinformatics, vol. 19, no. 2, pp. 185–193, 2003.

[36] R. A. Irizarry, “Summaries of Affymetrix GeneChip probe level data,” Nucleic Acids Res., vol. 31, no. 4, pp. 15e – 15, Feb. 2003.

[37] M. Dai et al., “Evolving gene/transcript definitions significantly alter the interpretation of GeneChip data,” Nucleic Acids Res., vol. 33, no. 20, pp. e175–e175, Nov. 2005.

[38] M. A. Sartor, C. R. Tomlinson, S. C. Wesselkamper, S. Sivaganesan, G. D. Leikauf, and M. Medvedovic, “Intensity-based hierarchical Bayes method improves testing for differentially expressed genes in microarray experiments,” BMC Bioinformatics, vol. 7, 2006.

[39] A. Subramanian et al., “Gene set enrichment analysis: A knowledge-based approach for interpreting genome-wide expression profiles,” Proc. Natl. Acad. Sci. U. S. A., vol. 102, no. 43, pp. 15545–15550, Oct. 2005.

[40] S. Alex et al., “Short-Chain Fatty Acids Stimulate Angiopoietin-Like 4 Synthesis in Human Colon Adenocarcinoma Cells by Activating Peroxisome Proliferator-Activated Receptor,” Mol. Cell. Biol., vol. 33, no. 7, pp. 1303–1316, 2013.

[41] S. Iezzi, G. Cossu, C. Nervi, V. Sartorelli, and P. L. Puri, “Stage-specific modulation of skeletal myogenesis by inhibitors of nuclear deacetylases,” Proc. Natl. Acad. Sci. U. S. A., vol. 99, no. 11, pp. 7757–7762, May 2002.

[42] M. Buckingham, “Skeletal muscle formation in vertebrates,” Current Opinion in Genetics and Development, vol. 11, no. 4. Elsevier Ltd, pp. 440–448, 01-Aug-2001.

[43] Y.-N. Jang and E. J. Baik, “JAK-STAT pathway and myogenic differentiation,” JAK-STAT, vol. 2, no. 2, p. e23282, Apr. 2013.

[44] E. Y. Chen et al., “Enrichr: Interactive and collaborative HTML5 gene list enrichment analysis tool,” BMC Bioinformatics, vol. 14, Apr. 2013.

[45] M. V. Kuleshov et al., “Enrichr: a comprehensive gene set enrichment analysis web server 2016 update,” Nucleic Acids Res., vol. 44, no. W1, pp. W90–W97, Jul. 2016.

[46] X. Deng, D. Z. Ewton, S. E. Mercer, and E. Friedman, “Mirk/dyrk1B decreases the nuclear accumulation of class II histone deacetylases during skeletal muscle differentiation,” J. Biol. Chem., vol. 280, no. 6, pp. 4894–4905, Feb. 2005.

[47] J. H. Cummings, E. W. Pomare, H. W. J. Branch, C. P. E. Naylor, and G. T. MacFarlane, “Short chain fatty acids in human large intestine, portal, hepatic and venous blood,” Gut, vol. 28, no. 10, pp. 1221–1227, 1987.

[48] S. Kersten, J. Seydoux, J. M. Peters, F. J. Gonzalez, B. Desvergne, and W. Wahli, “Peroxisome proliferator-activated receptor α mediates the adaptive response to fasting,” J. Clin. Invest., vol. 103, no. 11, pp. 1489–1498, 1999.

[49] S. Kersten, “Integrated physiology and systems biology of PPARα,” Mol. Metab., vol. 3, no. 4, pp. 354–371, Jul. 2014.

7

Chapter 7

General Discussion

Fasting elicits a multi-organ response that maintains physiological homeostasis of an organism despite constant energy requirements. An intricate network of evolutionarily conserved transcriptional, translational and post-translational regulatory mechanisms underlie this adaptive response and provide the basis for the survival of every fasting bout. Fasting, without starvation, leads to numerous salutary benefits on health in humans and animal models. The goal of this thesis was to characterize a number of transcriptional and translational regulatory mechanisms relevant to fasting, involving the transcription factors PPARα and CREB3L3, the LPL inhibitor ANGPTL4, and the ketone body β-hydroxybutyrate. In the context of basic animal and human physiology, further characterization of fasting-relevant mechanisms is expected to provide new avenues for clinical mitigation of metabolic diseases. The key findings of this thesis are:

- The transcription factors PPARα and CREB3L3 show great plasticity in regulating hepatic gene expression depending on nutritional status (**Chapter 2**).
- Fasting reduces LPL activity in human adipose tissue concomitant with an increase in ANGPTL4 gene expression and protein abundance (**Chapter 3**).
- ANGPTL4 promotes the intracellular degradation of LPL by members of the proprotein convertase subtilisin/kexin (PCSK) protein family in mouse adipocytes (**Chapter 4**).
- Mild whole body inactivation of ANGPTL4 in mice promotes to the development of mild inflammatory side-effects after high-fat feeding (**Chapter 5**).
- β-hydroxybutyrate (βOHB) does not appear to have pleiotropic effects on gene expression, questioning the notion that it mediates fasting-induced benefits via this mechanism (**Chapter 6**).

Control of the hepatic fasting response by PPARα and CREB3L3

One important level of control in the adaptation to fasting lies in the control of gene expression by transcription factors. Research has shown that PPARα is one particularly important transcription factor that governs the hepatic response to fasting [1]–[4]. Referred to as the "master regulator of lipid metabolism", it controls almost every branch of fatty acid metabolism as well as genes related to gluconeogenesis and glycogenolysis [5]. The pleiotropic effects of PPARα activation are being utilized clinically [6], [7]. Another important transcription factor which regulates hepatic gene expression during fasting is CREB3L3 [8]–[10]. Comparative transcriptomic analysis of livers from PPARα$^{-/-}$, CREB3L3$^{-/-}$ and double knockout mice after an overnight fast revealed that both transcription factors mostly regulate distinct genes and pathways and do so independently (**Chapter 2**). These data corroborate earlier studies that PPARα controls fatty acid metabolism from uptake to oxidation while CREB3L3 controls lipoprotein metabolism and secretion-associated pathways [5], [9], [11].

Another finding of this study is that under ketogenic diet feeding, in contrast to fasting, livers of CREB3L3$^{-/-}$ mice develop hepatomegaly, steatohepatitis and display a pro-inflammatory gene signature. This finding extends earlier reports of this phenotype by providing insights into the whole transcriptional response [12], [13]. Strikingly, this phenotype was completely dependent on PPARα. Studies that employed the synthetic PPARα-ligands Wy-14643 and Clofibrate illustrate that indeed hepatic PPARα activation drives the proliferation of hepatocytes resulting in hepatomegaly and steatohepatitis [14], [15]. In our study, contrasting the transcriptional profile of CREB3L3$^{-/-}$ livers to a publicly available dataset of a 5-day Wy-14643 treatment indeed showed great overlap, suggesting that the ablation of CREB3L3 results in selective activation of PPARα's mitogenic/proliferative effects. We suggest that, under conditions of ketogenic diet feeding, ablation of CREB3L3 may disrupt specific metabolic pathways resulting in the accumulation of intermediate fatty acid species. These specific fatty acids may differentially activate PPARα's mitogenic/proliferative effects. Fortunately, despite the striking phenotype, it is questionable whether these findings bear any relevance for the human situation, at least in part due to the fact that mitogenic effects have not been described for human PPARα *in vitro* [16].

One interesting point concerns the comparison between fasting and the ketogenic diet (KD). Originating from the Atkins diet, a typical KD comprises about ≤ 20 energy% from protein, ≥ 70 energy% from fat and ≤ 10 energy% from carbohydrate sources [17]. The reduction in carbohydrate consumption is thought to induce a "fasting-like" metabolic state via reduced insulin action which in turn promotes β-oxidation and ketogenesis [18]. Indeed, plasma parameters between fasting and ketogenic diet feeding are similar (**Chapter 2**). In

the recent years, this metabolic resemblance fueled scientific interest to understand whether fasting-like benefits can be mimicked with the ketogenic diet (**Chapter 1**). Of note, the ketogenic diet also (re-) gained popularity with many people in the *'health & fitness'* world advocating for various forms of KD (*cp. trends.google.com*).

The KD has a long history in the clinical mitigation of epilepsy, particularly in children [19]. Additionally, there are reports of beneficial effects on glycemic control in type 2 diabetics [20], [21], improved cognition during Alzheimer's [22] and general improvements in body composition coupled to weight loss [23], [24]. Reports about enhanced exercise performance when following KD appear unsubstantiated [24]–[27], as are claims about superior weight loss in comparison to calorie-matched low-fat diets [23], [28]. One underappreciated aspect in the current (public) discourse is the fact that KD elevates plasma LDL levels [23], [29], [30]. Given the well-established link between plasma LDL and atherosclerosis [31], [32], the lack of controlled RCT assessing long-term safety of KD in healthy individuals constitutes a major concern [33], [34]. While we did not address safety of the ketogenic diet in **Chapter 2**, our results indicate that fasting and ketogenic dieting impact metabolism in fundamentally distinct ways. It can be speculated that the severe phenotype of KD in CREB3L3$^{-/-}$ mice is related to the relatively high saturated fat content (37.5% of total calories), as unsaturated fatty acids did not activate PPARα's mitogenic effects in previous studies [35].

ANGPTL4 diverts triglycerides away from adipose tissue during fasting

Fasting initiates a switch in primary metabolic fuel sources from glucose to fatty acids and ketone bodies. This switch is accompanied by a reduction in plasma triglyceride (TG) and an increase in free fatty acid (FFA) levels from adipose tissue lipolysis. Since its discovery in 2000, extensive research efforts unveiled that ANGPTL4 – originally coined fasting induced adipose factor – inhibits LPL activity in mouse adipose tissue, preventing TG clearance and thereby futile cycling of free fatty acids in this tissue during the fasted state [36]–[38]. In the current model, ANGPTL4 expression and protein abundance are low in the fed state. Expression of the *Lpl* gene, which remains relatively stable between fed and fasted states, translates into LPL protein. Heparan sulfate proteoglycans (HSPGs) facilitate the localization of LPL on the plasma membrane of adipocytes from where LPL is transported to the vascular lumen by Glycosyl-phosphatidylinositol anchored high density lipoprotein binding protein 1 (GPIHBP1). Tethered to the endothelial surface, LPL binds to circulating VLDL and Chylomicron particles and hydrolyzes individual FFAs from enclosed TGs (Figure 1; Fed) [36]. In contrast to *Lpl*, adipose tissue *Angptl4* expression increases during fasting. ANGPTL4 protein promotes the unfolding and subsequent cleavage of LPL, as evident by the accumulation of N-terminal LPL cleavage products inside adipocytes [39] (**Chapter 4**). Augmented cleavage of LPL reduces the active LPL protein pool, and thereby LPL activity, along the secretory route and ultimately in the vascular lumen. As a result, TG clearance reduces in adipose tissue during fasting, sparing TGs to be hydrolyzed by LPL expressed in other tissues (Figure 1; Fasted). This model is supported by mouse models with genetically altered ANGPTL4 expression. Especially in the fasted state, Angptl4-transgenic mice display lower LPL activity and thus higher plasma TG levels compared to fasted WT mice [40]–[42]. Conversely, the fasting-induced decrease in adipose tissue LPL activity is abolished in *Angptl4*$^{-/-}$ mice leading to reduced plasma TG levels due to increased uptake of TG-derived fatty acids into adipose tissue [43], [44]. Stable *Lpl* transcription and slow LPL protein turnover, in conjunction with rapid induction or depression of Angptl4 mRNA based on feeding status, suggest that TG clearance by adipose tissue LPL is constitutively active yet sensitively and rapidly adjusted by ANGPTL4 in accordance with nutritional challenges such as fasting [43].

In **Chapter 3**, we validated this concept in humans. Previously, it was shown that LPL activity decreases in human adipose tissue during fasting [45], yet changes in corresponding protein levels had only been assessed cross-sectionally [46]. After a 26h fast in 23 volunteers we found that ANGPTL4 gene and protein expression were elevated in periumbilical subcutaneous adipose tissue. This coincided with a significant decrease in adipose tissue LPL activity in the absence of significant changes in LPL expression or protein levels. In analogy to the situation in mice, these data lead us to conclude that human ANGPTL4

inhibits adipose tissue LPL activity in the fasted state to spare TGs for other tissues as well (Figure 1; Fasted). In addition, our *in vitro* results suggest that reducing insulin and elevating FFA and cortisol levels jointly control *ANGPTL4* expression in adipocytes during fasting.

One intriguing question concerns the precise mechanism behind the ANGPTL4-mediated regulation of LPL activity in human adipocytes. Previous studies in mice showed that ANGPTL4 reduces the abundance of LPL protein in adipocytes (**Chapter 4**) [47]. In our human study we observed minimal changes in full length LPL protein abundance upon fasting and LPL cleavage products were generally non-detectable in tissues and primary cells. As discussed in **Chapter 3**, the benign non-significant changes in full length LPL protein abundance in the fasted state indicate that human ANGPTL4 does not regulate LPL activity by altering LPL protein abundance. Intriguingly, LPL protein abundance is also equal between wildtype and *Angptl4*$^{-/-}$ heart tissue and macrophages, indicating that the precise mechanism of action may be different between mouse tissues [47], [48] (**Chapter 5**). In future studies the question of how ANGPTL4 regulates LPL activity in human adipose tissue could be addressed by optimizing the LPL antibodies for the visualization of LPL cleavage products. Employing different LPL antibodies, we were able to confirm cleavage of LPL in adipose tissue (**Chapter 4**). However, in direct comparison to the Y-20 LPL antibody (employed in **Chapter 3**) those antibodies were inferior in visualizing full length LPL. Primary human adipocytes seem unsuitable for the study of LPL cleavage. None of the mentioned antibodies was able to detect LPL at the predicted size, and siANGPTL4 transfection experiments failed. Alternatively, an artificial expression system such as HEK293 cells could be employed to co-express (tagged) human ANGPTL4 and LPL. If it is possible to express properly folded LPL (as exemplified by Nimonkar *et al.*) [49], [50], western blots may be used to confirm the lack LPL cleavage induced by ANGPTL4. In conclusion, while we were able to confirm the functional importance of human ANGPTL4 for the regulation of LPL activity in adipose tissue during fasting, questions about the precise mechanism of action remain to be addressed in future studies.

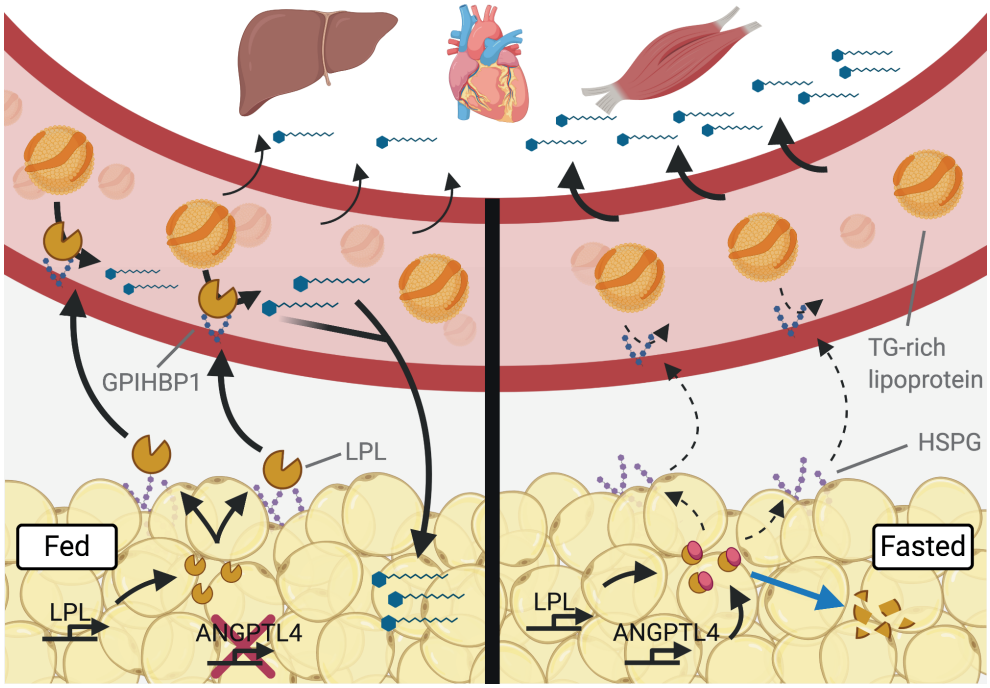

Figure 1: ANGPTL4 diverts TG away from the adipose tissue during fasting. During the fed state (left panel), expression of the LPL gene results in formation of LPL protein. HSPGs bind and display LPL on adipocytes. GPIHBP1 facilitates the transport of LPL through the interstitial space to the vascular lumen and tethers LPL to the endothelial surface. There, LPL binds to circulating VLDL and Chylomicron particles and hydrolyzes individual FFAs from enclosed TGs for uptake by adipose tissue. During fasting (right panel), expression of ANGPTL4 increases many-fold. ANGPTL4 protein interacts with LPL and reduces LPL activity, preventing clearance of TGs by adipose tissue. In mouse (blue arrow), ANGPTL4 promotes the cleavage of LPL in adipose tissue. Precisely how human ANGPTL4 regulates LPL activity in human adipose tissue is not known currently. Abbreviations: LPL Lipoprotein lipase, ANGPTL4 Angiopoietin-like 4; Heparan sulfate proteoglycans (HSPGs); Glycosyl-phosphatidylinositol anchored high density lipoprotein binding protein 1 (GPIHBP1).

The role of ANGPTL4 in non-adipose tissues during fasting

Suppressed TG clearance by adipose tissue during fasting suggests that non-adipose tissues account for the overall reduction in plasma TG levels (**Chapter 1**). Data from rats suggest that hepatic lipase activity declines during fasting, indicating that the liver unlikely accounts for the reduction in plasma TG levels [51]. Two tissues that show elevated LPL activity during fasting and might therefore be responsible for the reduction in plasma TGs are skeletal muscle and the heart [45], [52]–[54]. Besides adipose tissue, ANGPTL4 is also expressed in skeletal and heart muscle as well as liver, intestine and macrophages [38]. In a scenario where ANGPTL4 regulates adipose and non-adipose tissue TG distribution during feeding-fasting cycles, LPL activity and ANGPTL4 expression would require tissue-specific regulation in opposing fashion compared to adipose tissue.

Reciprocal regulation of LPL activity by ANGPTL4 between tissues has been described previously. A one-legged exercise study found that *ANGPTL4* expression increased in the non-exercising leg but did not change in exercising leg. Supported by a series of *in vitro* experiments, the authors concluded that elevated AMPK activity is preventing FFA-mediated induction of *ANGPTL4* in the exercising muscle, thereby facilitating local TG clearance to support ATP production during an exercise bout [55]. Similarly, during cold exposure, activation of AMPK was shown to selectively down-regulate *Angptl4* expression in brown adipose tissue, facilitating TG clearance to supply cold-induced non-shivering thermogenesis. Also here, *Angptl4* expression was reciprocally regulated and increased in white adipose tissue to prevent futile cycling of fatty acids [56]. Despite the fact that AMPK was previously shown to regulate LPL activity in heart tissue of fasted rats [54], a role for AMPK in regulating skeletal muscle LPL activity during fasting in humans is doubtful. Firstly, AMPK inhibits *Angptl4* in mouse myotubes, but reports that AMPK regulates *ANGPTL4* in human primary myotubes are inconsistent [55], [57]. Secondly, AMPK activity appears unchanged skeletal muscle during fasting [58]. Thirdly, the increase in skeletal muscle LPL activity during fasting, in fact, occurs in spite of augmented *ANGPTL4* expression in human and mice muscle [44], [57], [58]. The latter is also the case for heart muscle in rodents [44], [54].

One factor that may potentially underlie the reciprocal regulation of LPL activity in the face of unidirectional regulation of ANGPTL4 is their relative expression levels between tissues. Based on consensus expression data from '*humanproteinatlas',* adipose tissue expression of *LPL* is about 1.5x and 3x higher, yet adipose tissue *ANGPTL4* expression is 5x and 9x higher than in heart and skeletal muscle, respectively. At baseline, this results in a *LPL* to *ANGPTL4* transcript ratio of 3:1 in adipose tissue but merely 11:1 in heart and 9:1 in skeletal muscle. These transcript ratio's seem to match respective protein abundances at least in mouse tissues [47]. Together with the observation that only adipose tissue shows elevated VLDL

clearance in fasted *Angptl4*$^{-/-}$ mice [44], these data suggest that ANGPTL4 inhibitory capacity in non-adipose tissues is low irrespective of nutritional status. Consequently, one may speculate that LPL activity in heart and muscle tissue is subject to a greater degree of regulation by GPIHBP1 and the apolipoproteins C1, C2, C3 and A5 and may thus appear elevated despite increased *ANGPTL4* expression. Interestingly, *ANGPTL4* is only 2-3x-fold induced in muscle during fasting, yet induction levels observed to divert TGs away from non-exercising muscle reached 5x-fold [55], [58] (**Chapter 3**). Whether these differences in *ANGPTL4* induction levels are reflective of a tipping point for ANGPTL4-mediated inhibition of LPL activity (as seen in non-exercising muscle) requires further study.

Another factor relates to the time-point of measuring *ANGPTL4* expression. Most fasting studies investigate the effects of fasting at a single time-point [57], [59] (**Chapter 3**), yet as outlined in **Chapter 1**, the adaptation to fasting is a continuous process. In this regard, Ruge *et al.* observed an increase in skeletal muscle LPL activity only after 30h of fasting, while the fasting-mediated induction of *ANGPTL4* observed in various non-adipose tissues peak at 4h of fasting in mice and humans [45], [58]. In addition, a recent mouse study showed that plasma TG levels reduce significantly within 2h of food withdrawal and plateau thereafter [60]. This observation makes it conceivable that, in mice, the peaking of *Angptl4* expression after 4h of fasting may in fact act to limit further reducing of plasma TG levels. Consequentially, the switch from plasma TGs to FFA's directly released form adipose tissue as primary sources for FFA's would occur very rapidly upon commencing of the fast. If this hypothesis holds true in the humans remains to be seen. One approach to better understand the role of ANGPTL4 in non-adipose tissues during fasting, would be to characterize LPL activity per tissue over time during fasting, in conjunction with ANGPTL4 mRNA and protein levels and actual FFA uptake. Collectively, these data illustrate that albeit induced, the role of ANGPTL4 in regulating LPL activity in non-adipose tissues during fasting is currently unclear.

Local vs endocrine role for ANGPTL4

Another contributing factor to the apparent mismatch between ANGPTL4 expression and LPL activity in skeletal muscle and heart during fasting could be related to the location where ANGPTL4 inhibits LPL. Based on a previous finding from our group that ANGPTL4 ablation impacts LPL protein levels inside of mouse adipocytes [47], in **Chapter 4** of this thesis we extended these findings by identifying the proprotein convertase family member PCSK3 as a factor involved in the intracellular degradation pathway of LPL. Specifically, we

showed that knockdown and pharmacological inhibition of PCSK3 prevents the appearance of N-terminal LPL cleavage products in various adipocyte models *in vitro* and that this ablated differences in LPL abundances between *Angptl4*$^{-/-}$ and wildtype adipocytes. Considering the characterization of a PCSK-cleavage site within LPL, we propose a model in which ANGPTL4 promotes the unfolding of LPL, which in turn renders it more susceptible to cleavage by PCSK3 (Figure 2). LPL cleavage products may be cleared via lysosomal degradation. Of note, recent studies on the structure and binding between ANGPTL4 and LPL unveiled that LPL can be active as a monomer in addition to a homodimer [50], [61].

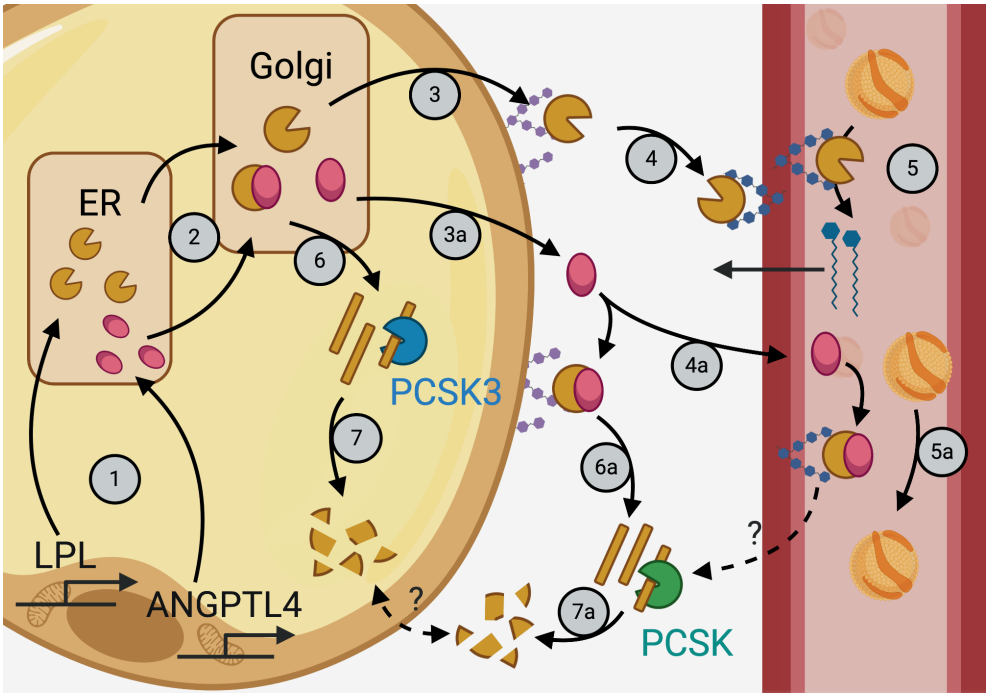

Figure 2: ANGPTL4 promotes degradation of LPL via PCSK3 inside adipocytes. Expression of *Lpl* (1) results in the formation of LPL protein. LPL matures along the secretory route (2,3) and is secreted with the help of HSPGs. GPIHBP1 facilitates the transport of LPL through the interstitial space and the display of LPL in the vascular lumen. There, LPL hydrolyses TG-rich lipoproteins to release FFAs (5), which subsequently are available for uptake by adipocytes. Expression of *Angptl4* (1), results in the translation of ANGPTL4 protein. ANGPTL4 likely also matures along the secretory route (2). In the Golgi, ANGPTL4 binds LPL which promotes the unfolding of LPL (6). This renders LPL more susceptible to cleavage by PCSK3 and subsequent degradation (7). Alternatively, it is possible that ANGPTL4 and LPL are secreted from adipocytes separately (3a/4a) and either interact on the cell surface or in the vascular lumen. To the effect of lowered LPL activity and omission of TG hydrolysis from TG-rich lipoproteins (5a), ANGPTL4 may promote the unfolding of LPL extracellularly (6a). Subsequently, extracellular PCSKs may facilitate the degradation of LPL (7a). Abbreviations: LPL Lipoprotein lipase, ANGPTL4 Angiopoietin-like 4; Proprotein convertase furin/PCSK3 (PCSK3); for HSPGs, GPIHBP1 and TG-rich lipoproteins see Figure 1.

On the other hand, LPL mediated triglyceride clearance occurs on the endothelial lumen (Figure 2) [62]. Indeed multiple studies employing recombinant ANGPTL4 or anti-ANGPTL4 antibodies *in vitro* and *in vivo* support the notion that secreted ANGPTL4 regulates LPL activity on the vascular endothelium and potentially also in the subendothelial space [40], [63]–[66]. In line, plasma ANGPTL4 levels are subject to physiological regulation, as shown after 24h of fasting (**Chapter 3**), or after an exercise bout [55], [57]. Therefore, LPL inhibition in any specific tissue does not need to be confined to the local expression of ANGPTL4 but can also be mediated by ANGPTL4 originating from other tissues. The local versus endocrine function of ANGPTL4 likely depends on several factors that also include the basal expression levels of *ANGPTL4* and *LPL* (see previous section). The rise in plasma ANGPTL4 levels during exercise concomitant with the stark upregulation of *ANGPTL4* in skeletal muscle led to the initial hypothesis that skeletal muscle contributes to the circulating ANGPTL4 pool during exercise [55]. However, in line with the much higher ANGPTL4:LPL expression ratio in the liver, this notion had been refuted by Ingerslev *et al.* who instead showed that the hepato-splanchnic bed drove the elevated plasma ANGPTL4 levels during exercise [57]. This hypothesis corroborates the observation that the liver expresses primarily a truncated form of ANGPTL4, which is the main form present in the circulation [67]. Expression levels of ANGPTL4 are drastically induced in the liver during fasting [44], which makes it conceivable that ANGPTL4 originating from the liver mediates LPL inhibition in the circulation. However, while tissue-specific knockout experiments amply documented that ANGPTL4 in white and brown adipose tissue [68], [69] and heart [70] impacts plasma TG levels, corresponding data from liver is still lacking. Two recent pre-prints addressed the role of ANGPTL4 in liver using liver-specific knockout animals. Strikingly, while one manuscript reports a clear reduction of plasma TG levels by hepatocyte-specific ANGPTL4 deficiency, the other manuscript reports no effect [71], [72]. Taken together, the current body of evidence suggests that ANGPTL4 inhibits LPL both locally and in the circulation.

To further understand to what extent the various tissues contribute to circulating ANGPTL4 levels, it would be of great interest to measure circulating ANGPTL4 levels in tissue-specific knockout models under various physiological conditions. However, the study of murine ANGPTL4 is currently severely hindered by the lack of sensitive antibodies. One alternative could be the selective deletion of amino acids 1 – 25, comprising the signal sequence of ANGPTL4 [73]. Trapping ANGPTL4 inside tissues, in either tissue-specific or global fashion could shed light on the general or tissue-specific importance of local vs circulatory ANGPTL4 for the regulation of plasma TG levels.

Targeting ANGPTL4 for the mitigation of hypertriglyceridemia

Hypertriglyceridemia is an independent risk factor for the development of cardiovascular disease, the leading cause of death worldwide [74], [75]. ANGPTL4 is a physiological regulator of plasma TG levels by inhibiting LPL activity in mice and humans. Ample preclinical studies documented that targeting ANGPTL4 by various means powerfully modulates plasma TG levels [40]–[42], [44], [64], [76]. Reinforcing clinical interest, human genetic studies identified that carriers of the inactivating E40K mutation in the *ANGPTL4* gene have reduced plasma TG concentrations alongside a reduced risk for developing cardiovascular disease [66], [77]. Beyond studying efficacy, in particular one pre-clinical study from our group explored the safety of targeting ANGPTL4 by feeding mice a high saturated fat diet (HFD) [78]. Strikingly, complete whole body ablation of ANGPTL4, after 20 weeks of HFD, led to ultimately lethal side effects that included the development of lipid-laden Touton giant cells in the mesentery, fibrinopurulent peritonitis, chylous ascites and elevation of acute-phase proteins in plasma [78]. These observations impede with the putative clinical benefit of targeting ANGPTL4 in humans. In order to expand on the clinical relevance of ANGPTL4, in **Chapter 5**, we employed whole body ANGPTL4-hypomorphic mice. Characterized by partial expression of the N-terminal LPL-inhibiting domain, in conjunction with complete ablation of the C-terminal ANGPTL4 domain, these hypomorphic mice allowed for the study of a milder form of genetic ANGPTL4 ablation. ANGPTL4-hypomorphic mice showed similar reductions in plasma triglyceride levels as the whole body ANGPTL4$^{-/-}$ mice, both after fasting and 20 weeks of HFD. Interestingly, after 20 weeks of HFD, the hypomorphic mice developed less severe side-effects compared to the complete ANGPTL4 knockout mice. Only 12% of hypomorphic mice developed chylous ascites, compared to 80% in the knockout group. Acute inflammation was significantly lower and delayed in the ANGPTL4-hypomorphic mice as well. While reports of any lifestyle related side-effects in individuals with inactivating variants of ANGPTL4 (E40K) are currently lacking [66], our findings in **Chapter 5** suggest that potential side effects of targeting ANGPTL4 *in vivo* are dependent on the degree of ablation. Partial instead of complete ablation of ANGPTL4 could be one suitable strategy to lower plasma TG, if diet-dependent side-effects can be omitted completely. The approximately 50% reduction in N-terminal ANGPTL4 did produce side-effects albeit less severe, suggesting that ablation of ANGPTL4 to omit side effects completely might need to be lower.

Another finding of our work in **Chapter 5** is that partial ablation of ANGPTL4 did not mitigate Touton giant cell formation in mesenteric lymph nodes in comparison to complete ANGPTL4 knockout animals. In about 90% of mice in both groups foam cells were present. This finding suggests that Touton giant cell formation is uncoupled from the deleterious systemic side effects, a conclusion further supported by an earlier study from our group in which feeding

Angptl4$^{-/-}$ mice a high trans-fat diet resulted in Touton giant cell formation in the absence of systemic inflammation [42]. Nevertheless, the protective effect of ANGPTL4 on macrophages cannot be dismissed. In line with our finding that also endogenously produced ANGPTL4 protects macrophages from the pro-inflammatory effects subsequent to excessive saturated fat uptake *in vitro* (**Chapter 5**), alteration of ANGPTL4 expression *in vivo* impacts on macrophage-driven atherosclerosis development. ApoE*3-Leiden mice backcrossed with ANGPTL4-transgenic mice developed reduced plaque sizes alongside reduced macrophage numbers following a Western type diet [79]. Conversely, deletion of ANGPTL4 in haematopoietic stem cells exacerbated atherosclerosis development and vascular inflammation [80]. These studies illustrate that the best approach to harness clinical benefit from targeting ANGPTL4 could be one that targets selected tissues. Adipose tissue has arguably the highest capacity to store lipids and could be one suitable target. Indeed recent studies show that adipose tissue-specific inactivation of ANGPTL4 potently reduces plasma TGs, yet the authors did not screen for underlying inflammation (SAA, haptoglobin) that had been identified in earlier studies or tested a longer intervention period [68], [69]. As mentioned, studies that selectively target ANGPTL4 in liver are underway [71], [72]. Overall, among its family members, ANGPTL4 shows the greatest capacity to modulate plasma TG levels and hence associated cardiovascular disease risk [81]. Despite this fact, the clinical development of drugs targeting ANGPTL4 has been slowed down by unfavorable outcomes in mentioned pre-clinical studies. By contrast, pre-clinical studies focused on ANGPTL3 did not report side-effects which promoted the clinical development of drugs candidates. Antibody-based approaches are currently in phase 3 clinical trials (*clinicaltrials.gov*).

The signaling roles of β-hydroxybutyrate

The metabolic state of ketosis, elicited by various fasting and caloric-restriction protocols as well as by carbohydrate-restricted ketogenic diets (KD), is associated with numerous health benefits (**Chapter 1**) [82]. In **Chapter 6** we tested the notion that β-hydroxybutyrate (βOHB), as a metabolite specifically present during ketosis, drives some of these salutary health effects by serving as a powerful signaling molecule on top of providing a source for ATP [82]–[94]. Specifically, we focused on its effect on gene expression in the context of proposed HDAC inhibitory action [95]–[98]. Strikingly, RNA-sequencing in primary adipocytes, macrophages, myotubes and hepatocytes after 6h treatment with 5 mM βOHB revealed limited effects on gene expression, which displayed little consistency between the tested cell types. In addition, the overlap with Butyrate, a potent HDAC inhibitor was

limited, while Butyrate's effect among the different cell types was consistent. This finding suggests that βOHB has little effect on gene expression via epigenetic or other mechanisms and corroborates a recent study that illustrated that also βOHB's effect on histone acetylation dwarfs in comparison to the effects elicited by Butyrate [95], [99].

Our findings do not exclude the possibility that βOHB impacts cellular metabolism beyond serving as a substrate for oxidative phosphorylation, including the epigenetic control of gene expression via HDAC inhibition (as discussed in **Chapter 6**). In the recent years, various novel histone residues have been identified which are thought to modulate the electrostatic interactions between DNA and histones, resulting in gene expression changes, just as the classical acetylation and methylation histone marks [100]. These novel histone marks include propionylation, crotonylation and β-hydroxybutyrylation (kbhb), among others [101]. In light of our findings, one interesting consideration regards the biological relevance of the recently discovered β-hydroxybutyrylation (kbhb) modification of histone lysine residues. While refuting βOHB's HDAC inhibitor activity in HEK293 cells and documenting its absence in endothelial cells and myotubes, Chriett *et al.* confirmed the βOHB-induced appearance of kbhb histone marks [99]. Xie *et al.* first discovered this new histone mark as H3K4bhb, H3K9bhb, H3K18bhb and H4K8bhb, which dose-dependently accumulated when treating HEK293 cells with 2-10 mM βOHB. Subsequently, 11 kbhb bearing histone sites were identified *in vivo* in mice livers. After 48h of fasting kbhb marks were elevated between 4-40x fold [102]. Using comparative analysis of Chip-seq and RNA-seq data, fasting-induced kbhb marks were found in the proximity of genes belonging to pathways of amino acid catabolism, redox balance, circadian rhythm, PPAR, and oxidative phosphorylation. Interestingly, no kbhb marks were associated with repressed pathways leading the authors to conclude that the novel histone kbhb mark is indicative of active gene expression [102]. A second study by Chen *et al.* found that concentrations of up to 20 mM βOHB dose-dependently increase the abundance of kbhb histone marks in primary neurons. Three week i.p. injections of 300 mg/kg βOHB as well as treatment of primary neurons with 10 mM βOHB were then shown to rescue spatial restraint stress or dexamethasone-induced reductions in BDNF protein levels, respectively [103]. Recently, a third report associated augmented histone kbhb modifications with increased *Adipoq* expression in 3T3L1 adipocytes treated with 10 mM βOHB [104].

Importantly, all three studies correlate the appearance of kbhb histone marks with alterations in gene expression but do not formerly show that kbhb marks are required or are facilitating these effects. What is more, Chriett *et al.* observed the accumulation of histone kbhb marks after treatment with Butyrate and other established HDAC inhibitors [99]. Since gene expression changes were observed in conjunction with histone acetylation induced by these compounds, the latter finding may suggest that kbhb marks are not specific to βOHB exposure but possibly byproducts of general metabolism of 4C substrates

[99]. In addition, investigating kbhb accumulation *in vivo* after complex metabolic challenges such as fasting requires considerate experimental design. The dramatic metabolic and hormonal changes that are governing the fasting response (**Chapter 1**) could potentially overpower benign effects elicited by βOHB. One obvious example is the importance of the FFA-PPARα axis in regulating the hepatic response to fasting (**Chapter 2**). Likewise, caution is required when weighing the conclusions from the copious *in vitro* experiments that utilize βOHB concentrations ≥ 10 mM, while sometimes displaying miniscule effects [95], [96], [102]–[106]. In humans, these concentrations are only seen during the pathological state of ketoacidosis, a potentially fatal condition marked by very high plasma glucose and ketone body levels. Despite these initial findings, the biological relevance of histone kbhb marks is not well established yet. Interestingly, Liu *et al.* recently identified kbhb marks on the tumor suppressor p53, indicating that β-hydroxybutyrylation marks may not be confined to histone proteins [105]. Generally, epigenetic effects for βOHB are conceivable on the basis that (1) ketolysis results in acetyl-CoA which serves as a substrate for epigenetic acetylation reactions and (2) that oxidation of βOHB, in relation to other substrates such as glucose, favorably affects NAD^+ levels, which serve as cofactors for a group of Class III deacylases called Sirtuins [100]. Future studies need to establish functional relevance of proposed mechanisms of action for βOHB.

Multiple alternative explanations exist why our *in vitro* screen might have missed βOHB's significant effects on gene expression. Besides the fact that we opted for an *in vitro* approach, one possible explanation for the benign gene expression effects in our work relates to the lack of the appropriate fasting-environment in which βOHB would naturally be present. Several reports exist that illustrate the importance of the proper context. In a study to explore the regulation of hepatic lipid metabolism in newborns, Rando *et al.* discovered that the PPARα-mediated induction of the hepatokines *Fgf21* and *Angptl4* is controlled by HDAC3. Indeed treatment of primary hepatocytes from fetal origin with Butyrate, βOHB or Trichostatin A in conjunction with Wy-14643 induced expression of *Fgf21,* whereas Wy-14643, βOHB or Butyrate in isolation had no effect [97]. After birth, expression of both genes naturally increased in neonates compared to their expression in fetuses, suggesting that the epigenetic remodeling is required once upon birth, presumably to aid digestion of milk lipids. Lending further support to the notion that βOHB's signaling effects may be context-dependent, βOHB's GPR109a-mediated anti-inflammatory effects appear only conferred in conjunction with LPS or TNFα stimulation [107]–[111]. By contrast, there are reports that βOHB exerts pro-inflammatory in HMEC-1 and cattle hepatocytes and proliferative effects on various cancer cell lines [98], [99], [112]. Therefore, beyond mechanisms, future studies are also required to precisely define in which contexts βOHB is relevant and whether its effects are always beneficial.

Our results do not formerly exclude that βOHB may exert signaling effects influencing gene expression, via HDAC inhibition or other mechanisms. However, in light of context-specific and contradicting evidence on mechanisms and beneficial effects, the current literature does not support the portrayal of βOHB acting as a pleiotropic signaling molecule. In this context, in particular a recent perspective paper postulating nutritionally or exogenously induced ketosis as a remedy for viral infections (including COVID19) appears like wild speculation [86]. It is conceivable that βOHB serves as a niche-signaling molecule fine-tuning specific metabolic responses, however future studies need to be carefully controlled for mechanisms. To justify the designation "signaling molecule" it is furthermore important that future mechanistic studies adequately control for effects that may lay downstream of supplementing ATP. To uncover the potential signaling functions of βOHB *in vivo*, future studies may utilize models with defective ketolysis. Ideally, ketolysis would be targeted in a tissue-specific manner, since fasting-induced hepatic steatosis in whole body *Bdh1*$^{-/-}$ mice might facilitate off-target effects [113].

Conclusion

In this thesis we characterized a number of transcriptional and translational regulatory mechanisms relevant to fasting. Depending on nutritional status the transcription factors PPARα and CREB3L3 show great plasticity in regulating hepatic gene expression (**Chapter 2**). Furthermore, we were able to confirm the functional importance of human ANGPTL4 for the regulation of LPL activity in adipose tissue during fasting (**Chapter 3**). The role of ANGPTL4 in regulating LPL activity in non-adipose tissues during fasting is currently unclear. In contrast to mouse adipose tissue, where PCSK3 is involved in the degradation of LPL cleavage products, the precise mechanisms of LPL cleavage in human adipocytes remains to be addressed in future studies (**Chapter 4**). Current evidence on the potential whole body targeting of ANGPTL4 to correct dyslipidemia is unfavorable yet future studies will have to address the efficacy and safety of tissue-targeted approaches (**Chapter 5**). Lastly, our results in **Chapter 6** in the context of currently available literature do not support the current portrayal of βOHB acting as a pleiotropic signaling molecule. Future research should focus on further defining in which circumstances and via which mechanisms βOHB displays robust signaling effects.

References

[1] T. Hashimoto, W. S. Cook, C. Qi, A. V. Yeldandi, J. K. Reddy, and M. S. Rao, "Defect in peroxisome proliferator-activated receptor α-inducible fatty acid oxidation determines the severity of hepatic steatosis in response to fasting," J. Biol. Chem., vol. 275, no. 37, pp. 28918–28928, Sep. 2000.

[2] S. Kersten, J. Seydoux, J. M. Peters, F. J. Gonzalez, B. Desvergne, and W. Wahli, "Peroxisome proliferator-activated receptor α mediates the adaptive response to fasting," J. Clin. Invest., vol. 103, no. 11, pp. 1489–1498, 1999.

[3] T. C. Leone, C. J. Weinheimer, and D. P. Kelly, "A critical role for the peroxisome proliferator-activated receptor α (PPARα) in the cellular fasting response: The PPARα-null mouse as a model of fatty acid oxidation disorders," Proc. Natl. Acad. Sci. U. S. A., vol. 96, no. 13, pp. 7473–7478, Jun. 1999.

[4] M. C. Sugden, K. Bulmer, G. F. Gibbons, B. L. Knight, and M. J. Holness, "Peroxisome-proliferator-activated receptor-α (PPARα) deficiency leads to dysregulation of hepatic lipid and carbohydrate metabolism by fatty acids and insulin," Biochem. J., vol. 364, no. 2, pp. 361–368, Jun. 2002.

[5] S. Kersten, "Integrated physiology and systems biology of PPARα," Mol. Metab., vol. 3, no. 4, pp. 354–371, Jul. 2014.

[6] L. Han, W. J. Shen, S. Bittner, F. B. Kraemer, and S. Azhar, "PPARs: Regulators of metabolism and as therapeutic targets in cardiovascular disease. Part I: PPAR-α," Future Cardiology, vol. 13, no. 3. Future Medicine Ltd., pp. 259–278, 01-May-2017.

[7] S. Kersten and R. Stienstra, "The role and regulation of the peroxisome proliferator activated receptor alpha in human liver," Biochimie, vol. 136, pp. 75–84, 2017.

[8] A. H. Lee, "The role of CREB-H transcription factor in triglyceride metabolism," Curr. Opin. Lipidol., vol. 23, no. 2, pp. 141–146, Apr. 2012.

[9] Y. Nakagawa and H. Shimano, "CREBH regulates systemic glucose and lipid metabolism," Int. J. Mol. Sci., vol. 19, no. 5, pp. 1–15, 2018.

[10] H. Danno et al., "The liver-enriched transcription factor CREBH is nutritionally regulated and activated by fatty acids and PPARα," Biochem. Biophys. Res. Commun., vol. 391, no. 2, pp. 1222–1227, Jan. 2010.

[11] H. A. Khan and C. E. Margulies, "The role of mammalian Creb3-like transcription factors in response to nutrients," Frontiers in Genetics, vol. 10, no. JUN. Frontiers Media S.A., p. 591, 2019.

[12] J. G. Park et al., "CREBH-FGF21 axis improves hepatic steatosis by suppressing adipose tissue lipolysis," Sci. Rep., vol. 6, no. May, pp. 1–13, 2016.

[13] Y. Nakagawa et al., "CREB3L3 controls fatty acid oxidation and ketogenesis in synergy with PPARα," Sci. Rep., vol. 6, no. 1, p. 39182, Dec. 2016.

[14] S. S. Lee et al., "Targeted disruption of the alpha isoform of the peroxisome proliferator-activated receptor gene in mice results in abolishment of the pleiotropic effects of peroxisome proliferators.," Mol. Cell. Biol., vol. 15, no. 6, pp. 3012–3022, Jun. 1995.

[15] C. N. Brocker, J. Yue, D. Kim, A. Qu, J. A. Bonzo, and F. J. Gonzalez, "Hepatocyte-specific PPARA expression exclusively promotes agonist-induced cell proliferation without influence from nonparenchymal cells," Am. J. Physiol. - Gastrointest. Liver Physiol., vol. 312, no. 3, pp. G283–G299, Mar. 2017.

[16] B. J. Blaauboer et al., "The effect of beclobric acid and clofibric acid on peroxisomal β-oxidation and peroxisome proliferation in primary cultures of rat, monkey and human hepatocytes," Biochem. Pharmacol., vol. 40, no. 3, pp. 521–528, Aug. 1990.

[17] E. H. Kossoff and J. L. Dorward, "The modified Atkins diet," in Epilepsia, 2008, vol. 49, no. SUPPL. 8, pp. 37–41.

[18] W. Pogozelski, N. Arpaia, and S. Priore, "The metabolic effects of low carbohydrate diets and incorporation into a Biochemistry Course," Biochem. Mol. Biol. Educ., vol. 32, no. 2, pp. 91–100, 2005.

[19] K. J. Martin-McGill, R. Bresnahan, R. G. Levy, and P. N. Cooper, “Ketogenic diets for drug-resistant epilepsy,” Cochrane Database Syst. Rev., vol. 6, Jun. 2020.

[20] Y. J. Choi, S.-M. Jeon, and S. Shin, “Impact of a Ketogenic Diet on Metabolic Parameters in Patients with Obesity or Overweight and with or without Type 2 Diabetes: A Meta-Analysis of Randomized Controlled Trials,” Nutrients, vol. 12, no. 7, p. 2005, Jul. 2020.

[21] N. H. Bhanpuri et al., “Cardiovascular disease risk factor responses to a type 2 diabetes care model including nutritional ketosis induced by sustained carbohydrate restriction at 1 year: An open label, non-randomized, controlled study,” Cardiovasc. Diabetol., vol. 17, no. 1, May 2018.

[22] M. G. Grammatikopoulou et al., “To Keto or Not to Keto? A Systematic Review of Randomized Controlled Trials Assessing the Effects of Ketogenic Therapy on Alzheimer Disease,” Adv. Nutr., Jun. 2020.

[23] N. B. Bueno et al., “Very-low-carbohydrate ketogenic diet v. low-fat diet for long-term weight loss: a meta-analysis of randomised controlled trials.,” Br. J. Nutr., vol. 110, no. 7, pp. 1178–87, 2013.

[24] S. Vargas-Molina et al., “Effects of a ketogenic diet on body composition and strength in trained women,” J. Int. Soc. Sports Nutr., vol. 17, no. 1, Apr. 2020.

[25] P. J. M. M. Pinckaers, T. A. Churchward-Venne, D. Bailey, and L. J. C. C. van Loon, “Ketone Bodies and Exercise Performance: The Next Magic Bullet or Merely Hype?,” Sport. Med., vol. 47, no. 3, pp. 383–391, Mar. 2016.

[26] P. J. Cox and K. Clarke, “Acute nutritional ketosis: implications for exercise performance and metabolism.,” Extrem. Physiol. Med., vol. 3, p. 17, 2014.

[27] C. P. Bailey and E. Hennessy, “A review of the ketogenic diet for endurance athletes: Performance enhancer or placebo effect?,” Journal of the International Society of Sports Nutrition, vol. 17, no. 1. BioMed Central Ltd., 22-Jun-2020.

[28] K. D. Hall et al., “Energy expenditure and body composition changes after an isocaloric ketogenic diet in overweight and obese men,” Am. J. Clin. Nutr., vol. 104, no. 2, pp. 324–333, Aug. 2016.

[29] A. J. Nordmann et al., “Effects of low-carbohydrate vs low-fat diets on weight loss and cardiovascular risk factors: A meta-analysis of randomized controlled trials,” Archives of Internal Medicine, vol. 166, no. 3. Arch Intern Med, pp. 285–293, 13-Feb-2006.

[30] E. Fechner, E. T. H. C. Smeets, P. Schrauwen, and R. P. Mensink, “The effects of different degrees of carbohydrate restriction and carbohydrate replacement on cardiometabolic risk markers in humans—a systematic review and meta-analysis,” Nutrients, vol. 12, no. 4. MDPI AG, 01-Apr-2020.

[31] J. Borén et al., “Low-density lipoproteins cause atherosclerotic cardiovascular disease: pathophysiological, genetic, and therapeutic insights: a consensus statement from the European Atherosclerosis Society Consensus Panel Translational medicine,” Eur. Heart J., vol. 41, 2020.

[32] B. A. Ference et al., “Low-density lipoproteins cause atherosclerotic cardiovascular disease. 1. Evidence from genetic, epidemiologic, and clinical studies. A consensus statement from the European Atherosclerosis Society Consensus Panel,” Eur. Heart J., vol. 38, pp. 2459–2472, 2017.

[33] B. O’neill and P. Raggi, “Clinical and scientific debates on atherosclerosis The ketogenic diet: Pros and cons,” Atherosclerosis, vol. 292, pp. 119–126, 2019.

[34] W. Dafoe and G. T. Gyenes, “Comments on ‘The ketogenic diet: Pros and cons,’” Atherosclerosis, vol. 296. Elsevier Ireland Ltd, p. 1, 01-Mar-2020.

[35] L. M. Sanderson et al., “Effect of synthetic dietary triglycerides: A novel research paradigm for nutrigenomics,” PLoS One, vol. 3, no. 2, Feb. 2008.

[36] W. Dijk and S. Kersten, “Regulation of lipid metabolism by angiopoietin-like proteins,” Curr. Opin. Lipidol., vol. 27, no. 3, pp. 249–256, Jun. 2016.

[37] R. Zhang, “The ANGPTL3-4-8 model, a molecular mechanism for triglyceride trafficking,” Open Biol., vol. 6, no. 4, p. 150272, 2016.

[38] W. Dijk and S. Kersten, “Regulation of lipoprotein lipase by Angptl4,” Trends Endocrinol. Metab., vol. 25, no. 3, pp. 146–155, Mar. 2014.

[39] W. Dijk, P. M. M. Ruppert, L. J. Oost, and S. Kersten, “Angiopoietin-like 4 promotes the intracellular cleavage of lipoprotein lipase by PCSK3/furin in adipocytes,” J. Biol. Chem., vol. 1, no. 3, p. jbc.RA118.002426, 2018.

[40] A. Köster et al., “Transgenic angiopoietin-like (Angptl)4 overexpression and targeted disruption of Angptl4 and Angptl3: Regulation of triglyceride metabolism,” Endocrinology, vol. 146, no. 11, pp. 4943–4950, 2005.

[41] L. Lichtenstein et al., “Angptl4 Upregulates Cholesterol Synthesis in Liver via Inhibition of LPL- and HL-Dependent Hepatic Cholesterol Uptake,” Arterioscler. Thromb. Vasc. Biol., vol. 27, no. 11, pp. 2420–2427, Nov. 2007.

[42] S. Mandard et al., “The fasting-induced adipose factor/angiopoietin-like protein 4 is physically associated with lipoproteins and governs plasma lipid levels and adiposity,” J. Biol. Chem., vol. 281, no. 2, pp. 934–944, Jan. 2006.

[43] O. Kroupa et al., “Linking nutritional regulation of Angptl4, Gpihbp1, and Lmf1 to lipoprotein lipase activity in rodent adipose tissue.,” BMC Physiol., vol. 12, p. 13, 2012.

[44] E. M. Cushing, X. Chi, K. L. Sylvers, S. K. Shetty, M. J. Potthoff, and B. S. J. Davies, “Angiopoietin-like 4 directs uptake of dietary fat away from adipose during fasting.,” Mol. Metab., vol. 6, no. 8, pp. 809–818, 2017.

[45] T. Ruge, M. Svensson, J. W. Eriksson, and G. Olivecrona, “Tissue-specific regulation of lipoprotein lipase in humans: effects of fasting,” Eur. J. Clin. Invest., vol. 35, no. 3, pp. 194–200, Mar. 2005.

[46] W. Dijk, S. Schutte, E. O. Aarts, I. M. C. Janssen, L. Afman, and S. Kersten, “Regulation of angiopoietin-like 4 and lipoprotein lipase in human adipose tissue,” J. Clin. Lipidol., vol. 12, no. 3, pp. 773–783, 2018.

[47] W. Dijk, A. P. Beigneux, M. Larsson, A. Bensadoun, S. G. Young, and S. Kersten, “Angiopoietin-like 4 (ANGPTL4) promotes intracellular degradation of lipoprotein lipase in adipocytes.,” J. Lipid Res., vol. 7, no. 11, pp. 956–963, 2016.

[48] A.-B. Oteng et al., “Characterization of ANGPTL4 function in macrophages and adipocytes using Angptl4 -knockout and Angptl4 -hypomorphic mice,” J. Lipid Res., vol. 60, no. 10, pp. 1741–1754, Oct. 2019.

[49] A. V Nimonkar et al., “A lipoprotein lipase --GPI-anchored high density lipoprotein binding protein 1 fusion lowers triglycerides in mice: implications for managing familial chylomicronemia syndrome,” J. Biol. Chem., p. jbc.RA119.011079, Oct. 2019.

[50] R. Arora et al., “Structure of lipoprotein lipase in complex with GPIHBP1,” Proc. Natl. Acad. Sci. U. S. A., vol. 116, no. 21, pp. 10360–10365, 2019.

[51] J. Peinado-Onsurbe, J. Julve, X. Galan, M. Llobera, and I. Ramírez, “Effect of fasting on hepatic lipase activity in the liver of developing rats,” Biol. Neonate, vol. 77, no. 2, pp. 131–138, Feb. 2000.

[52] A. M. Bak et al., “Prolonged fasting-induced metabolic signatures in human skeletal muscle of lean and obese men,” PLoS One, vol. 13, no. 9, pp. 1–19, 2018.

[53] J. D. Browning, J. Baxter, S. Satapati, and S. C. Burgess, “The effect of short-term fasting on liver and skeletal muscle lipid, glucose, and energy metabolism in healthy women and men,” J. Lipid Res., vol. 53, no. 3, pp. 577–586, Mar. 2012.

[54] D. An, T. Pulinilkunnil, D. Qi, S. Ghosh, A. Abrahani, and B. Rodrigues, “The metabolic ‘switch’ AMPK regulates cardiac heparin-releasable lipoprotein lipase,” Am. J. Physiol. Metab., vol. 288, no. 1, pp. E246–E253, Jan. 2005.

[55] M. Catoire et al., “Fatty acid-inducible ANGPTL4 governs lipid metabolic response to exercise.,” Proc. Natl. Acad. Sci. U. S. A., vol. 111, no. 11, pp. E1043-52, 2014.

[56] W. Dijk et al., “ANGPTL4 mediates shuttling of lipid fuel to brown adipose tissue during sustained cold exposure,” Elife, vol. 4, no. OCTOBER2015, Oct. 2015.

[57] B. Ingerslev et al., “Angiopoietin-like protein 4 is an exercise-induced hepatokine in humans, regulated by glucagon and cAMP,” Mol. Metab., vol. 6, no. 10, pp. 1286–1295, Oct. 2017.

[58] M. A. Wijngaarden et al., “Regulation of skeletal muscle energy/nutrient-sensing pathways during metabolic adaptation to fasting in healthy humans,” Am. J. Physiol. Metab., vol. 307, no. 10, pp. E885–E895, Nov. 2014.

[59] H. Pilegaard, B. Saltin, and P. D. Neufer, “Effect of short-term fasting and refeeding on transcriptional regulation of metabolic genes in human skeletal muscle,” Diabetes, vol. 52, no. 3, pp. 657–662, Mar. 2003.

[60] D. Carper, M. Coué, C. Laurens, D. Langin, and C. Moro, “Reappraisal of the optimal fasting time for insulin tolerance tests in mice,” Mol. Metab., p. 101058, Jul. 2020.

[61] A. P. Beigneux et al., “Lipoprotein lipase is active as a monomer,” Proc. Natl. Acad. Sci. U. S. A., vol. 116, no. 13, pp. 6319–6328, 2019.

[62] J. R. Mead, S. A. Irvine, and D. P. Ramji, “Lipoprotein lipase: Structure, function, regulation, and role in disease,” J. Mol. Med., vol. 80, no. 12, pp. 753–769, 2002.

[63] E. Makoveichuk et al., “Inactivation of lipoprotein lipase occurs on the surface of THP-1 macrophages where oligomers of angiopoietin-like protein 4 are formed,” Biochem. Biophys. Res. Commun., vol. 425, no. 2, pp. 138–143, Aug. 2012.

[64] K. Yoshida, T. Shimizugawa, M. Ono, and H. Furukawa, “Angiopoietin-like protein 4 is a potent hyperlipidemia-inducing factor in mice and inhibitor of lipoprotein lipase,” J. Lipid Res., vol. 43, no. 11, pp. 1770–1772, Nov. 2002.

[65] U. Desai et al., “Lipid-lowering effects of anti-angiopoietin-like 4 antibody recapitulate the lipid phenotype found in angiopoietin-like 4 knockout mice,” Proc. Natl. Acad. Sci. U. S. A., vol. 104, no. 28, pp. 11766–11771, Jul. 2007.

[66] F. E. Dewey et al., “Inactivating Variants in ANGPTL4 and Risk of Coronary Artery Disease.,” N. Engl. J. Med., vol. 374, no. 12, pp. 1123–33, Mar. 2016.

[67] S. Mandard et al., “The direct peroxisome proliferator-activated receptor target fasting-induced adipose factor (FIAF/PGAR/ANGPTL4) is present in blood plasma as a truncated protein that is increased by fenofibrate treatment,” J. Biol. Chem., vol. 279, no. 33, pp. 34411–34420, Aug. 2004.

[68] B. Aryal et al., “Absence of ANGPTL4 in adipose tissue improves glucose tolerance and attenuates atherogenesis.,” JCI insight, vol. 3, no. 6, Mar. 2018.

[69] A. K. Singh et al., “Brown adipose tissue derived ANGPTL4 controls glucose and lipid metabolism and regulates thermogenesis,” Mol. Metab., vol. 11, pp. 59–69, May 2018.

[70] X. Yu et al., “Inhibition of cardiac lipoprotein utilization by transgenic overexpression of Angptl4 in the heart,” Proc. Natl. Acad. Sci. U. S. A., vol. 102, no. 5, pp. 1767–1772, Feb. 2005.

[71] K. M. Spitler, S. K. Shetty, E. M. Cushing, K. L. Sylvers-Davie, and B. S. J. Davies, “ANGPTL4 from adipose, but not liver, is responsible for regulating plasma triglyceride partitioning,” bioRxiv, p. 2020.06.02.106815, Jan. 2020.

[72] A. K. Singh et al., “Liver-specific suppression of ANGPTL4 improves obesity-associated diabetes and mitigates atherosclerosis in mice,” bioRxiv, p. 2020.06.02.130922, Jan. 2020.

[73] C. Carbone et al., “Angiopoietin-like proteins in angiogenesis, inflammation and cancer,” International Journal of Molecular Sciences, vol. 19, no. 2. MDPI AG, p. 431, 01-Feb-2018.

[74] P. B. Sandesara, S. S. Virani, S. Fazio, and M. D. Shapiro, “The Forgotten Lipids: Triglycerides, Remnant Cholesterol, and Atherosclerotic Cardiovascular Disease Risk,” Endocr. Rev., vol. 40, no. 2, pp. 537–557, Apr. 2019.

[75] A. Onat, I. Sari, M. Yazici, G. Can, G. Hergenç, and G. Ş. Avci, “Plasma triglycerides, an independent predictor of cardiovascular disease in men: A prospective study based on a population with prevalent metabolic syndrome,” Int. J. Cardiol., vol. 108, no. 1, pp. 89–95, Mar. 2006.

[76] V. et al Gusarova et al., “Genetic inactivation of ANGPTL4 improves glucose homeostasis and is associated with reduced risk of diabetes,” Nat. Commun., vol. 9, no. 1, pp. 1–11, 2018.

[77] K. Abid et al., “ANGPTL4 variants E40K and T266M are associated with lower fasting triglyceride levels and predicts cardiovascular disease risk in type 2 diabetic Tunisian population,” Lipids Health Dis., vol. 15, no. 1, 2016.

[78] L. Lichtenstein et al., “Angptl4 protects against severe proinflammatory effects of saturated fat by inhibiting fatty acid uptake into mesenteric lymph node macrophages,” Cell Metab., vol. 12, no. 6, pp. 580–592, Dec. 2010.

[79] A. Georgiadi et al., “Overexpression of Angiopoietin-Like Protein 4 Protects Against Atherosclerosis Development,” Arterioscler. Thromb. Vasc. Biol., vol. 33, no. 7, pp. 1529–1537, Jul. 2013.

[80] B. Aryal et al., “ANGPTL4 deficiency in haematopoietic cells promotes monocyte expansion and atherosclerosis progression,” Nat. Commun., vol. 7, 2016.

[81] S. Kersten, “New insights into angiopoietin-like proteins in lipid metabolism and cardiovascular disease risk,” Curr. Opin. Lipidol., p. 1, Mar. 2019.

[82] A. Di Francesco, C. Di Germanio, M. Bernier, and R. de Cabo, “A time to fast.,” Science, vol. 362, no. 6416, pp. 770–775, Nov. 2018.

[83] P. Rojas-Morales, E. Tapia, and J. Pedraza-Chaverri, “Beta-Hydroxybutyrate: A signaling metabolite in starvation response?,” Cell. Signal., vol. 28, no. 8, pp. 917–923, Aug. 2016.

[84] R. L. Veech, “Ketone ester effects on metabolism and transcription,” J. Lipid Res., vol. 55, no. 10, pp. 2004–2006, Oct. 2014.

[85] A. Dąbek, M. Wojtala, L. Pirola, and A. Balcerczyk, “Modulation of cellular biochemistry, epigenetics and metabolomics by ketone bodies. Implications of the ketogenic diet in the physiology of the organism and pathological states,” Nutrients, vol. 12, no. 3. MDPI AG, 01-Mar-2020.

[86] B. J. Stubbs et al., “Investigating Ketone Bodies as Immunometabolic Countermeasures against Respiratory Viral Infections,” Med, vol. 0, no. 0, Jul. 2020.

[87] P. Rojas-Morales, J. Pedraza-Chaverri, and E. Tapia, “Ketone bodies, stress response, and redox homeostasis,” Redox Biology, vol. 29. Elsevier B.V., p. 101395, 01-Jan-2020.

[88] J. C. Newman and E. Verdin, “β-hydroxybutyrate: Much more than a metabolite,” Diabetes Res. Clin. Pract., vol. 106, no. 2, pp. 173–181, 2014.

[89] L. B. Achanta and C. D. Rae, “β-Hydroxybutyrate in the Brain: One Molecule, Multiple Mechanisms,” Neurochem. Res., vol. 42, no. 1, pp. 35–49, Jan. 2017.

[90] A. L. Hartman and J. M. Rho, “The new ketone alphabet soup: BHB, HCA, and HDAC,” Epilepsy Currents, vol. 14, no. 6. pp. 355–357, 2014.

[91] J. C. Newman and E. Verdin, “β-Hydroxybutyrate: A Signaling Metabolite,” Annu. Rev. Nutr., vol. 37, no. 1, pp. 51–76, 2017.

[92] R. L. Veech, B. Chance, Y. Kashiwaya, H. a Lardy, and G. F. Cahill, “Ketone bodies, potential therapeutic uses.,” IUBMB Life, vol. 51, pp. 241–247, 2001.

[93] P. Puchalska and P. A. Crawford, “Multi-dimensional Roles of Ketone Bodies in Fuel Metabolism, Signaling, and Therapeutics,” Cell Metab., vol. 25, no. 2, pp. 262–284, 2017.

[94] M. Maalouf, J. M. Rho, and M. P. Mattson, “The neuroprotective properties of calorie restriction, the ketogenic diet, and ketone bodies,” Brain Res. Rev., vol. 59, no. 2, pp. 293–315, Mar. 2009.

[95] T. Shimazu et al., “Suppression of Oxidative Stress by -Hydroxybutyrate, an Endogenous Histone Deacetylase Inhibitor,” Science (80-.)., vol. 339, no. 6116, pp. 211–214, Jan. 2013.

[96] K. Tanegashima, Y. Sato-Miyata, M. Funakoshi, Y. Nishito, T. Aigaki, and T. Hara, “Epigenetic regulation of the glucose transporter gene Slc2a1 by β-hydroxybutyrate underlies preferential glucose supply to the brain of fasted mice,” Genes to Cells, vol. 22, no. 1, pp. 71–83, Jan. 2017.

[97] G. Rando et al., “Glucocorticoid receptor-PPARα axis in fetal mouse liver prepares neonates for milk lipid catabolism,” Elife, vol. 5, pp. 1–31, 2016.

[98] C.-K. Huang et al., “Adipocytes promote malignant growth of breast tumours with monocarboxylate transporter 2 expression via β-hydroxybutyrate,” Nat. Commun., vol. 8, p. 14706, 2017.

[99] S. Chriett, A. Dąbek, M. Wojtala, H. Vidal, A. Balcerczyk, and L. Pirola, “Prominent action of butyrate over β-hydroxybutyrate as histone deacetylase inhibitor, transcriptional modulator and anti-inflammatory molecule,” Sci. Rep., vol. 9, no. 1, pp. 1–14, Dec. 2019.

[100] H. Bin Ruan and P. A. Crawford, “Ketone bodies as epigenetic modifiers,” Current Opinion in Clinical Nutrition and Metabolic Care, vol. 21, no. 4. Lippincott Williams and Wilkins, pp. 260–266, 01-Jul-2018.

[101] B. R. Sabari, D. Zhang, C. D. Allis, and Y. Zhao, “Metabolic regulation of gene expression through histone acylations,” Nature Reviews Molecular Cell Biology, vol. 18, no. 2. Nature Publishing Group, pp. 90–101, 01-Feb-2017.

[102] Z. Xie et al., “Metabolic Regulation of Gene Expression by Histone Lysine β-Hydroxybutyrylation,” Mol. Cell, vol. 62, no. 2, pp. 194–206, Apr. 2016.

[103] L. Chen, Z. Miao, and X. Xu, “β-hydroxybutyrate alleviates depressive behaviors in mice possibly by increasing the histone3-lysine9-β-hydroxybutyrylation,” Biochem. Biophys. Res. Commun., vol. 490, no. 2, pp. 117–122, Aug. 2017.

[104] S. Nishitani, A. Fukuhara, J. Shin, Y. Okuno, M. Otsuki, and I. Shimomura, “Metabolomic and microarray analyses of adipose tissue of dapagliflozin-treated mice, and effects of 3-hydroxybutyrate on induction of adiponectin in adipocytes,” Sci. Rep., vol. 8, no. 1, pp. 1–11, Dec. 2018.

[105] K. Liu et al., “p53 β-hydroxybutyrylation attenuates p53 activity,” Cell Death Dis., vol. 10, no. 3, p. 243, Mar. 2019.

[106] D. Mikami et al., “β-Hydroxybutyrate enhances the cytotoxic effect of cisplatin via the inhibition of HDAC/survivin axis in human hepatocellular carcinoma cells,” J. Pharmacol. Sci., vol. 142, no. 1, pp. 1–8, Jan. 2020.

[107] K. Zandi-Nejad et al., “The role of HCA2 (GPR109A) in regulating macrophage function,” FASEB J., vol. 27, no. 11, pp. 4366–4374, Nov. 2013.

[108] M. Rahman et al., “The β-hydroxybutyrate receptor HCA2 activates a neuroprotective subset of macrophages.,” Nat. Commun., vol. 5, no. May, p. 3944, May 2014.

[109] S. P. Fu et al., “BHBA suppresses LPS-induced inflammation in BV-2 cells by inhibiting NF- B activation,” Mediators Inflamm., vol. 2014, 2014.

[110] S.-P. Fu et al., “Anti-inflammatory effects of BHBA in both in vivo and in vitro Parkinson’s disease models are mediated by GPR109A-dependent mechanisms,” J. Neuroinflammation, vol. 12, no. 1, p. 9, 2015.

[111] S.-P. Fu et al., “β-Hydroxybutyric Acid Inhibits Growth Hormone-Releasing Hormone Synthesis and Secretion Through the GPR109A/Extracellular Signal-Regulated 1/2 Signalling Pathway in the Hypothalamus,” J. Neuroendocrinol., vol. 27, no. 3, pp. 212–222, Mar. 2015.

[112] X. Shi et al., “β-Hydroxybutyrate Activates the NF-κB Signaling Pathway to Promote the Expression of Pro-Inflammatory Factors in Calf Hepatocytes,” Cell. Physiol. Biochem., vol. 33, no. 4, pp. 920–932, 2014.

[113] H. Otsuka et al., “Deficiency of 3-hydroxybutyrate dehydrogenase (BDH1) in mice causes low ketone body levels and fatty liver during fasting,” J. Inherit. Metab. Dis., p. jimd.12243, Apr. 2020.

Summary

Abstaining from food intake, i.e. fasting, elicits a multi-organ response that maintains the physiological homeostasis of an organism despite a constant requirement for energy. This distinguishes it from the fed state in which the organism maintains homeostasis utilizing ingested nutrients. An intricate network of evolutionarily conserved transcriptional, translational and post-translational regulatory mechanisms underlie the adaptive transition from the fed to the fasted state and provide the basis for the survival of every fasting bout. In recent years, numerous studies documented the salutary health benefits the various fasting protocols elicit in human and animal models. The regulatory mechanisms that facilitate the feeding-fasting transition are incompletely understood. Hence, the goal of this thesis was to characterize a number of transcriptional and translational regulatory mechanisms relevant to fasting. Their uncovering and understanding in the context of basic animal and human physiology is expected to provide new avenues for clinical mitigation of metabolic diseases.

Chapter 1 summarizes the benefits of fasting and describes the feeding-fasting transition. Intermittent fasting (IF), time-restricted feeding (TRF), alternate-day fasting (ADF) and periodic fasting (PF) are the main fasting regimes that are currently being researched. In humans and animal models these regimes normalize HbA1c and glucose levels, improve insulin sensitivity and blood lipid parameters, reduce blood pressure and induce weight loss. In animal models there is evidence for the extension of life span and the mitigation of disease in experimental models for diabetes, cardiovascular disease, neurological disease and cancer.

Key metabolic organs to understand feeding-fasting cycles are the liver, muscle tissue, adipose tissue and the brain. The fed state commences with the ingestion of a meal. Insulin is a key hormone that signals the ‘fed’ state due to its numerous central functions in nutrient uptake and storage. It triggers the uptake of glucose into liver, adipose and muscle tissue, and its utilization to produce ATP via glycolysis. The oxidation of FFA for ATP is generally low in most tissues when Insulin levels are high. In the fed state, the adipose tissue remains the principal tissue for the clearance and storage of FFA in the form of TG inside of lipid droplets. The brain mostly metabolized glucose. The body transitions from the fed to the fasted state when the last meal is fully digested and absorbed. In the first phase, hepatic glycogenolysis and gluconeogenesis are augmented and jointly maintain blood glucose levels. Together with other gluconeogenic substrates like lactate, amino acids are readily liberated upon fasting to maintain blood glucose levels – at the expense of muscle mass. However, uncontrolled catabolism of muscle mass is expected to impede with the long-term survival of the fasting individual. Hence with the extension of the fast from several hours into days, a second vital priority becomes to reduce the reliance on glucose for the generation of ATP. In the second phase plasma amino acid levels and urinary excretion decline, while the body reduces total glucose production. Governed by a dramatic hormonal

switch from insulin and leptin to glucagon, cortisol and epinephrine the organism increases rates of β-oxidation for the production of ATP to substitute glucose as a substrate. Activation of adipose tissue lipolysis causes levels of free fatty acids (FFA) and glycerol to increase after 24h of fasting. Additionally, TCA cycle intermediates such as oxaloacetate are utilized to maintain basal levels of gluconeogenesis, resulting in a reduction in hepatic TCA cycle activity. As a result, FFA's released from the adipose tissue accumulate in the liver and condense into to the ketone bodies acetoacetate (AcAc) and β-hydroxybutyrate (βOHB). Ketone bodies can rise up to 8 mM and, in addition to FFA, are increasingly oxidized by most tissues, including the brain which can derive up to 2/3rd of its energy requirements from ketone body oxidation after several weeks of fasting. The maximal duration of the fast depends on the quantity of endogenous energy. It is estimated that a 70 kg man with 15 kg of adipose tissue could a survive a 70-90 day fast, based on a basal energy expenditure of 1800 kcal/day.

Peroxisome Proliferator-Activated receptor α (PPARα) and cAMP-Responsive Element Binding Protein 3-Like 3 (CREB3L3) are transcription factors governing lipid metabolism in the liver. In **Chapter 2** of this thesis, we investigated the interrelationship of the transcription factors PPARα and CREB3L3 in regulating the adaptive response of the liver to feeding-fasting cycles. Male wild-type, PPARα–/–, CREB3L3–/– and combined PPARα/CREB3L3–/– mice were subjected to a 16-hour fast or 4 days of ketogenic diet feeding and whole genome expression analysis was performed on liver samples. The results indicate great plasticity in the degree of synergism and co-dependence between both transcription factors that was dependent on nutritional status. Under conditions of overnight fasting, the effects of PPARα ablation and CREB3L3 ablation on plasma triglyceride, plasma β-hydroxybutyrate, and hepatic gene expression were largely disparate, and showed only limited interdependence. Gene and pathway analysis underscored the importance of CREB3L3 in regulating (apo)lipoprotein metabolism, and of PPARα as master regulator of intracellular lipid metabolism. By contrast, a strong interaction between PPARα and CREB3L3 ablation was observed during ketogenic diet feeding. Loss of CREB3L3 reduced expression of PPARα and its target genes involved in fatty acid oxidation and ketogenesis. In stark contrast, the hepatoproliferative function of PPARα was markedly activated by loss of CREB3L3. Overall, these data indicate that CREB3L3 ablation uncouples the hepatoproliferative and lipid metabolic effects of PPARα. Except for the shared regulation of a very limited number of genes, the roles of PPARα and CREB3L3 in hepatic lipid metabolism are clearly distinct and are highly dependent on dietary status.

Lipoprotein lipase (LPL), a ubiquitously expressed enzyme, is responsible for the hydrolysis of plasma triglycerides on the endothelial lumen to accommodate tissue specific requirements for fatty acids. One protein that increases in abundance during the fasted state and regulates the clearance of triglycerides is Angiopoietin-like 4 (ANGPTL4). In

Chapter 3 of this thesis we performed a 24h fasting study to investigate the mechanistic control of adipose tissue LPL activity by ANGPTL4 in humans. Our results indicate that ANGPTL4 levels in human adipose tissue are increased by fasting, likely via increased plasma cortisol and free fatty acids, and decreased plasma insulin, resulting in decreased LPL activity. We conclude that ANGPTL4 levels in human adipose tissue are increased by fasting, resulting in decreased LPL activity. This likely serves to direct TG away from adipose tissue and prevent futile cycling of fatty acids in the fasted state.

In **Chapter 4** we examined the mechanism of how ANGPTL4 regulates LPL activity. Previous research indicated that ANGPTL4 regulates LPL activity by cleavage. Treatment of different mouse adipocytes with the PCSK-inhibitor Dec-RVKR-CMK markedly decreased LPL cleavage, indicating that LPL is cleaved by PCSKs. Silencing of *Pcsk3/furin* significantly decreased LPL cleavage in cell culture medium and lysates of adipocytes. Remarkably, PCSK-mediated cleavage of LPL in adipocytes was diminished by *Angptl4* silencing and was decreased in adipocytes and adipose tissue of Angptl4–/– mice. Differences in LPL cleavage between Angptl4–/– and wild-type mice were abrogated by treatment with Dec-RVKR-CMK. Induction of ANGPTL4 in adipose tissue during fasting enhanced PCSK-mediated LPL cleavage, concurrent with decreased LPL activity, in wild-type but not Angptl4–/– mice. In adipocytes levels of N-terminal LPL were markedly higher in wild-type compared to Angptl4–/– adipocytes, suggesting an intracellular mode of action for the stimulation of PCSK-mediated LPL cleavage by ANGPTL4. We conclude that ANGPTL4 promotes PCSK-mediated intracellular cleavage of LPL in adipocytes, likely contributing to regulation of LPL in adipose tissue.

ANGPTL4 impacts plasma TG levels via the regulation of LPL activity. This renders ANGPTL4 an attractive target for correcting dyslipidemia. However, whole body ANGPTL4 inactivation in mice fed a high fat diet causes chylous ascites, an acute-phase response, and mesenteric lymphadenopathy. In **Chapter 5**, the mechanisms underlying the adverse effect of whole-body inactivation of ANGPTL4 are studied using Angptl4-hypomorphic and Angptl4–/– mice. Angptl4-hypomorphic mice with partial expression of truncated N-terminal ANGPTL4 exhibited reduced fasting plasma triglyceride, cholesterol, and non-esterified fatty acid levels, strongly resembling Angptl4$^{-/-}$ mice. However, during high fat feeding, Angptl4-hypomorphic mice showed markedly delayed and attenuated elevation in plasma serum amyloid A and much milder chylous ascites than Angptl4$^{-/-}$ mice, despite similar abundance of lipid-laden giant cells in mesenteric lymph nodes. Compared with the absence of ANGPTL4, low levels of N-terminal ANGPTL4 mitigate the development of chylous ascites and an acute-phase response in mice. However, since side-effects were still observed, whole body inactivation of ANGPTL4 may not be suitable as a clinical strategy for correcting dyslipidemia.

Intermittent fasting and caloric restriction-type interventions elicit a myriad of health benefits and are expected to provide clinical benefit for the prevention and treatment of obesity, type 2 and potentially cardiovascular disease and cancer. β-hydroxybutyrate (βOHB), levels of which increase to the low mM range during fasting, has been proposed as a potent signaling molecule mediating some of the beneficial effects of fasting interventions. **Chapter 6** explores whether the ketone body β-hydroxybutyrate (βOHB) influences differentiation *in vitro* and regulates genes expression in several primary cell types. We found that βOHB did not impact the differentiation process in C2C12 skeletal muscle cells and 3T3-L1 adipocytes. Transcriptomics analysis revealed overall benign effects of βOHB on gene expression after 6h. βOHB did not consistently regulate genes and pathways in primary adipocytes, macrophages, myotubes and hepatocytes. In contrast, equimolar concentrations of the structurally related HDAC inhibitor butyrate prevented differentiation in C2C12 skeletal muscle cells and 3T3-L1 adipocytes and induced dramatic and consistent gene expression changes in all cell types. Our results suggest that βOHB unlikely mediates the beneficial effects of fasting via regulating gene expression or influencing cellular homeostatic processes such as differentiation. Additionally, in the tested primary cell types, βOHB's gene expression signature is disparate from the one of butyrate suggesting that βOHB's HDAC inhibitory capacity may be negligible.

In conclusion, in this thesis we characterized a number of transcriptional and translational regulatory mechanisms relevant to fasting. Depending on nutritional status the hepatic transcription factors PPARα and CREB3L3 show great plasticity in regulating gene expression in the liver (**Chapter 2**). Furthermore, we were able to confirm the functional importance of human ANGPTL4 for the regulation of LPL activity in adipose tissue during fasting (**Chapter 3**). The role of ANGPTL4 in regulating LPL activity in non-adipose tissues during fasting is currently unclear. In contrast to mouse adipose tissue, where PCSK3 is involved in the degradation of LPL cleavage products, the precise mechanisms of LPL cleavage in human adipocytes remains to be addressed in future studies (**Chapter 4**). Current evidence on the potential whole body targeting of ANGPTL4 to correct dyslipidemia is unfavorable yet future studies will have to address the efficacy and safety of tissue-targeted approaches (**Chapter 5**). Lastly, our results in **Chapter 6** in the context of currently available literature do not support the current portrayal of βOHB acting as a pleiotropic signaling molecule. Future research should focus on further defining in which circumstances and via which mechanisms βOHB displays robust signaling effects.

Acknowledgements

The most read pages of every thesis. Chances are you should probably read Chapters 1-7 first ;-).

Egocentric bias leaves us to overestimate our own contribution to everything we're involved in. While this may be a useful delusion that keeps us invested, it is far from reality. Attitude and work ethic are important, but how far we actually come is also determined by chance. An important factor are the people we meet:

Before arriving in Wageningen several people have been instrumental to my development. During high school it was my biology teacher **Ms Rudloff** who was always willing to stay a little longer in class to satisfy all my questions. I remember you calling me "scattered professor" several times, a trait I'm still displaying today (yet I think I've gotten better at it). Thank you for all the extra attention. I think it has been paying off. Furthermore, there are **Wolfgang, Frank, Ralf, Chris** and **Stefanie**, a.k.a. the NonWoTecc team. Thanks to all of you for welcoming me so openly and trusting me that I could contribute to building our company with mere 19 years of age. I've taken so much experience and confidence out of this period. Special thanks to **Wolfgang** for the countless fun hours in the clean room and passing so much of your technical knowledge on to me.

No other person had a bigger impact on me in the recent years than Prof. Dr. Sander Kersten. **Sander** thanks for everything. You've passed on knowledge, were always available for discussions explanations and late night emails, listened to personal issues when needed, taught me what solid research looks like and pushed me to deliver even in times I didn't feel like. You're coming close to the ideal supervisor and if there is one thing I will miss it's the exposure to your breath of knowledge and experience (I won't miss your jokes, sorry). Thanks for the good times! I will stay in touch.

Montse you're one of the coolest women I know. You're always spreading your positive vibes by laughing and helping everyone. And while taking care of your own PhD you've even "produced" two babies! Your counseling helped me keep my sanity many times and it was a blessing having someone around who understood sarcasm. I'm happy to call you a friend and thanks for being my paranymph!

Antwi, you've been very instrumental to my development. We discussed our projects and explained issues we didn't understand to each other almost daily. Indeed, I think we could have swapped projects easily. I too remember fondly our evenings playing FIFA or watching Champions League, but especially the times I kicked your ass on the soccer field. ;-) I cherish the good times working beside you and I'm happy to have acted as your paranymph during one of the coolest defenses in history! Just like you've been explaining me your current

muricholic acid story last night, I'm looking forward to many more discussions. Thank you my friend!

Danny, it was a difficult start for you in the lab. Yet you've worked so hard, improved so fast and skillfully entertained everyone with your charming attitude; that was truly impressive. Thank you for so many nice moments and your amazing cooking skills! I wish you best success with the time you have left in your PhD. I'm sure you'll do well and I'm looking forward to reading your papers. Thank you for being my paranymph!

Certainly, the biggest kudos go to our technicians: **Mieke, Shohreh, Karin, Jenny, Mechteld, Marlies and Carolien** who keep things running in Helix and **Bert, Wilma and René** who take care of all our animals at the CKP. You all are the backbone of our lab and none of our work would be possible without you. You are taking care of all the big and small things behind the scenes from breeding our mice, ordering, cell culture, qPCR, histology to sample storage, safety and general organization. Thank you for all the technical, emotional and other last-minute support you have been offering me. You are the heroes of the lab!

Further, thank you **Mieke** for the continuous and enjoyable efforts to setup a lab soap opera with me starring as the male actor. I'm happy I could get around being in this spotlight and we were able to setup the very successful "bier en friet" outings instead. This brought a little more social interaction in for everyone! Thank you also to my "Bro" **Shohreh** for the good chats over coffee or food. I've always wanted to play a trick on you and give you salty cookies to balance your sugar addiction. I'll keep this for another time ;-).

Thanks to my office mates **Roland, Juri, Pim, Mara** and **Rieneke** for the nice time, interesting talks and discussing science!

Lisa S., Merel and **Xanthe**, it was great to have you guys as colleagues. We've had many interesting discussions and you always assisted if you could. Thanks for also significantly awakening the atmosphere in the lab. I wish you loads of luck with the rest of your PhD and success with future plans.

Anouk, Charlotte, Tessa, Benthe and **Miranda** thanks for being so nice colleagues. Good luck finishing up your PhDs and success with future plans!

Pol thanks for the good times during the PhD tour, watching premier league and visiting so many stadiums. Special thanks for awesome challenge to play squash against you (and loosing almost every game).

Past members of the lab: **Aafke, Wieneke, Lily, Sophie, Diederik** and **Rogier** you were good examples in the time we shared as colleagues. Thanks for the times that you helped out with advice or in the lab. Special thanks to **Aafke** for introducing me to the group and supervising me during my MSc thesis. I wish you successes in your current job positions.

Guido, Mark and **Rinke** thank you for an enormous amount of questions and new perspectives, sharing knowledge, helping with some analysis and random entertaining talks as well as entertaining through impeccable style (Rinke)!

Wilma, Lydia, Jocelijn, Klaske and **Michiel**, thank you for creating a stimulating atmosphere at work, your nice questions, suggestions and feedbacks on my work during the Thursday morning group meetings. I wish you successes with your projects.

A big thanks also goes to the students I was able to supervise during the past 4 years. **Francesca, Lisa S., Xiaochen, Lisa P., Noa, Gaelle** it was a pleasure working with you. I learned a lot about myself when guiding you for your projects and you've been very valuable help for my projects. I wish you all the best for your next steps. I hope they are successful, just as your thesis' have been!

Furthermore, I want to thank **Cátia** and her crazy dog **Flôr**. Your soothing love in the past year made possible so much more. Thank you! ♡ It's such a blessing to enjoy the time we spent now in your natural habitat ;-D.

Lastly to my parents **Barbara** and **Stephan Ruppert**: Ohne eure Liebe wäre meine Reise überhaupt nicht gestartet. Danke für all die liebevolle Zuneigung in den vergangenen 30 Jahren. Uns hat es nie an irgendwas gefehlt. Ich liebe euch. To my siblings **Hendrik** and **Johanna**, extended family and friends thank you for continued interest and support.

Thank you all for creating such a stimulating environment to learn in!

Philip

To my Wageningen friends

The finalization of my PhD also marks the end my era here in Wageningen. For 6 years I have lived in and lived through an incredible number of places and experiences – with the best bunch of friends. On my very first day in school I met **Eleni, Konstantina** and **Bella.** It was impossible not to become friends with you. You had such a unique and infectious positive energy; you were literally redefining how to enjoy life while attending to duties. We spent almost every free minute together and beyond providing me with "love & onions" at 4 a.m. when I hadn't eaten for a whole day due to my ACT deadline, we enjoyed amazing

trips to Tripoli, Athens, Kats and Paris. Obviously, in **Lukas** and **Yann** (and later **Léo**), we had just the perfect (musical) company! It broke my heart to see you return to Greece after what felt like a life-time of 5 months.

Next, I lived in the wildly international jungle of Waterhouse (>10 nationalities, > 40 people). A truly cultural experience that saved a lot of money for traveling! To my kopeles **Lukina, Dian & Blanca, Hristo, Chris** and **Lucas** and my malakas **John, Serko** and **Lazare (TT)** and all the other people who came and went: The time we shared is unforgettable, but our stories are best told in person. The miniculture parties we had under the willow tree were by far the best in town yet the level of confusion was very high! Special thanks to our Shaman **Hristo** for inventing the device that protected all our brain waves. I'm looking forward to seeing all of you again soon! I'm also grateful to **Iris Z**. for having taken off several of my rough edges in very short amount of time. You held me accountable and I've benefitted from it. In Droevendaal **Lukas** introduced me to 89 where we lived with **Guidone**, **Tommaso** and **Tita**. Boi are Italians fun! "5 people discussing how 1 is doing the job" is just the perfect description for how free but engaged you're going about your day. Thank you for becoming such good friends, listening to all the struggles, providing always the right groove and most importantly (haha), feeding me. Italian food is just the best! I hope we can reunite in Elba soon and that there is much to come.

Next, it was a bliss living with you **Giorgos, Milos, Vera, Marco, Thomas, Fiona, Jordi** in 95. Jordi's paella or other shared meals (mostly cooked by Thomas), life and Giorgos-storytelling was always so much fun that I had regular cramps from laughing. I've taken a lot of positive energy from living with you. **Theo, Leonardo** and **Spyros** thanks for the good times, Theo-music and Inis-sessions until late in the morning! The 93+95 combo was the ideal distraction from all the PhD work for the core time of my PhD. Thanks guys! Thanks also to **Paula, Maria & Harold, Adri & Angel, Berta & Giulio, Ainoah, Silvia, Oriana** and **Fede** for many other amazing memories, whether it was Kats, Girona, Florence, your wedding in Cuba or just good talks, parties and other blissful moments we shared. I hope to see many of you again soon!

Towards the end of my PhD I was seeking more tranquility and moved towards the city center. Big thanks to **Tobi, Floor, Maaike, Iris** and **Mekdi** for the freedom and support you showed towards me in the final stages of my PhD. I have been withdrawing myself more and more towards the end, but you knew it was because I had to finish this book here!

Wageningen has transformed my life and I'm lucky and grateful to have crossed paths with everyone of you here.

About the author

Philip Ruppert was born on March 19th, 1988 in Cologne, Germany. Between 1994 and 2007 he received his elementary and secondary school education in Cologne. Philip was always most interested in subjects of science, particularly biology and chemistry. He successfully completed this stage with the German high school diploma "Abitur" in the summer of 2007. Yet fed up with top-down schooling, Philip sought practical working experience next and thus joined the recently founded start-up NonWoTecc Medical GmbH, Cologne in late 2007. In 2½ years, he was able to support the growth of the company from 5 to about 25 employees by assisting in (the development of) production and product, quality control and management, storage and IT-infrastructure while simultaneously undergoing vocational training to become Germany's first production-technologist in 2010. Encouraged by these successes, Philip eventually started his bachelor studies in Applied Biology at the University of Applied Sciences Bonn-Rhein-Sieg. During these studies he had been selected for a DAAD PROMOS studentship, which facilitates a yearly exchange with the University of Aberdeen, Scotland. In the summer of 2012 he relocated to Aberdeen to join the final honors year of the Human biology program in Aberdeen. In 2013, Philip successfully completed these studies with a Double degree in Applied and Human biology from both universities. After a short stint at the LBMCC, Luxembourg, he followed his passion and studied Molecular Biology with a focus on Nutrition at Wageningen University, the Netherlands in early 2014. He performed his Master thesis research on the gene regulatory effects of the butyrate at the Nutrition, Metabolism and Genomics Group at Wageningen University. For his internship, Philip joined the pharmaceutical company Grünenthal GmbH in Aachen, Germany. This work focused on the development of an NK-cell immunoassay for the screening of potential drug targets. After completion of his Master's degree in June 2016, Philip joined the Nutrition, Metabolism and Genomics Group again as a PhD candidate under the supervision of Sander Kersten. Described in this thesis, his PhD research focused on various regulatory mechanisms relevant to the feeding-fasting transition. After completion, Philip will join the new lab of James Mitchell at the ETH Zurich as a post-doctoral researcher focusing on amino acid metabolism during fasting.

List of publications

This thesis

Dijk W*, **Ruppert PMM***, Oost LJ, Kersten S. Angiopoietin-like 4 promotes the intracellular cleavage of lipoprotein lipase by PCSK3/furin in adipocytes. J Biol Chem. 2018;1(3):jbc.RA118.002426.

Ruppert PMM, Park J-G, Xu X, Hur KY, Lee A-H, Kersten S. Transcriptional profiling of PPARα−/− and CREB3L3−/− livers reveals disparate regulation of hepatoproliferative and metabolic functions of PPARα. BMC Genomics. 2019 Dec 11;20(1):199.

Ruppert PMM*, Michielsen CCJR*, Hazebroek EJ, Pirayesh A, Olivecrona G, Afman LA, Kersten S. Fasting induces ANGPTL4 and reduces LPL activity in human adipose tissue. Mol Metab. 2020 Jun 3;101033.

Oteng A-B*, **Ruppert PMM***, Boutens L, Dijk W, van Dierendonck XAMH, Olivecrona G, Stienstra R, Kersten S. Characterization of ANGPTL4 function in macrophages and adipocytes using Angptl4 -knockout and Angptl4 -hypomorphic mice. J Lipid Res. 2019 Oct;60(10):1741–54.

Ruppert, PMM, Hooiveld, GJEJ, Kersten, S, Prominent effects of butyrate over beta-hydroxybutyrate on cellular differentiation and whole genome expression in vitro. *Manuscript in preparation.*

* equal contribution

Others

Defour M, Dijk W, **Ruppert PMM**, Nascimento EBM, Schrauwen P, Kersten S. The Peroxisome Proliferator-Activated Receptor α is dispensable for cold-induced adipose tissue browning in mice. Mol Metab. 2018;10.

van den Berg R, Kooijman S, Noordam R, Ramkisoensing A, Abreu-Vieira G, Tambyrajah LL, Dijk W, **Ruppert PMM**, Mol IM, Kramar B, Caputo R, Puig LS, de Ruiter EM, Kroon J, Hoekstra M, van der Sluis RJ, Meijer OC, Willems van Dijk K, van Kerkhof LWM, Christodoulides C, Karpe F, Gerhart-Hines Z, Kersten S, Meijer JH, Coomans CP, van Heemst D, Biermasz NR, Rensen PCN. A Diurnal Rhythm in Brown Adipose Tissue Causes Rapid Clearance and Combustion of Plasma Lipids at Wakening. Cell Rep. 2018;22(13).

Kuipers EN, Held NM, In Het Panhuis W, Modder M, **Ruppert PMM**, Kersten S, Kooijman S, Guigas B, Houtkooper RH, Rensen PCN, Boon MR. A single day of high-fat diet feeding induces lipid accumulation and insulin resistance in brown adipose tissue in mice. Am J Physiol Endocrinol Metab. 2019 Nov 1;**317**(5):E820–30.

Ruppert PMM, Kersten S. A lipase fusion feasts on fat. Vol. 295, Journal of Biological Chemistry. American Society for Biochemistry and Molecular Biology Inc.; p. 2913–4.

Overview of completed training activities

Discipline specific activities

Courses & Meetings

- CVON-Energise (Leiden, the Netherlands, 2016)
- CVON-Energise (Wageningen, the Netherlands, 2016)
- Healthy & sustainable diets: synergies and trade-offs, VLAG (Wageningen, the Netherlands, 2017)
- CVON-Energise, Young talent forum (Utrecht, the Netherlands, 2017)
- CVON-Energise (Maastricht, the Netherlands, 2017)
- Energy metabolism & body composition in nutrition and health research, VLAG (Wageningen, the Netherlands, 2018)
- CVON-Energise (Leiden, the Netherlands, 2018) – poster presentation
- CVON-Energise (Leiden, the Netherlands, 2018) – oral presentation
- CVON-Energise, Young talent forum (Wageningen, the Netherlands, 2018)
- CVON-Energise (Wageningen, the Netherlands, 2019) – oral presentation
- CVON-Energise (Amsterdam, the Netherlands, 2019) – oral presentation

Conferences

- Annual Dutch Diabetes Research Meeting, NVDO (Oosterbeek, the Netherlands, 2016)
- Annual Dutch Diabetes Research Meeting, NVDO (Oosterbeek, the Netherlands, 2017)
- XX Lipid Meeting, eventlab (Leipzig, Germany, 2017)
- Nederlandse Lipoproteinen Club, NLC (Amsterdam, the Netherlands, 2018) – oral presentation
- 41st European Lipoprotein Club, EAS (Tutzing, Germany, 2018) – oral presentation
- Nuclear Receptor Research Network, NR2N (Eindhoven, the Netherlands, 2018) – oral presentation

- 87th EAS congress, EAS (Maastricht, the Netherlands, 2019) – poster presentation
- EAS 2019 satellite symposium, MINT (Maastricht, the Netherlands, 2019)
- Kern Lipid Conference (Vail, Colorado, USA, 2019) – poster presentation

Training

- Training period at Institute of Diabetes and Cancer (IDC), Helmholtz Zentrum München (Munich, Germany, 2019)

General courses

- VLAG PhD week, VLAG (Baarlo, the Netherlands, 2016)
- Brain Training & Brain Training Follow-up, WGS (Wageningen, the Netherlands, 2017)
- PhD Carousel, VLAG (Wageningen, the Netherlands, 2017)
- Philosophy and Ethics of Food Science and Technology, VLAG (Wageningen, the Netherlands, 2017)
- Competence Assessment, WGS (Wageningen, the Netherlands, 2017)
- Project and Time Management, WGS (Wageningen, the Netherlands, 2017)
- Reviewing a Scientific Paper, WGS (Wageningen, the Netherlands, 2018)
- Introduction to R, VLAG (Wageningen, the Netherlands, 2018)
- Applied Statistics, VLAG (Wageningen, the Netherlands, 2018)
- Laboratory Animal Science, VLAG (Wageningen, the Netherlands, 2019)

Optional courses/activities

- Preparation of research proposal (Wageningen, the Netherlands, 2016)
- NMG lab meetings, including organization (Wageningen, the Netherlands, 2016-2020)
- PhD study tour to United Kingdom, including organization (2017)
- Supervision of BSc/MSc students (Wageningen, the Netherlands, 2016-2020)

The research contained in this thesis was financially supported by 'ENERGISE' (CVON2014-02) and the Graduate School VLAG (Advanced studies in Food Technology, Agrobiotechnology, Nutrition and Health Sciences).

I gratefully acknowledge the financial support by Wageningen University and the Graduate School VLAG for the printing and publishing of this thesis.

Cover: Vera van Beek (proefschriftmaken)

Layout: Philip Ruppert; Vera van Beek (proefschriftmaken)

Printed by: Digiforce || proefschriftmaken.nl